PROCEEDINGS OF THE "FOURTH INTERNATIONAL CONFERENCE OF FMR1 PREMUTATION: BASIC MECHANISMS, CLINICAL INVOLVEMENT AND THERAPY"

EDITED BY: Cecilia Giulivi, Laia Rodriguez-Revenga, Karen Usdin, Rob Willemsen and Renate K. Hukema

PUBLISHED IN: Frontiers in Molecular Biosciences, Frontiers in Genetics, Frontiers in Pediatrics and Frontiers in Cell and Developmental Biology

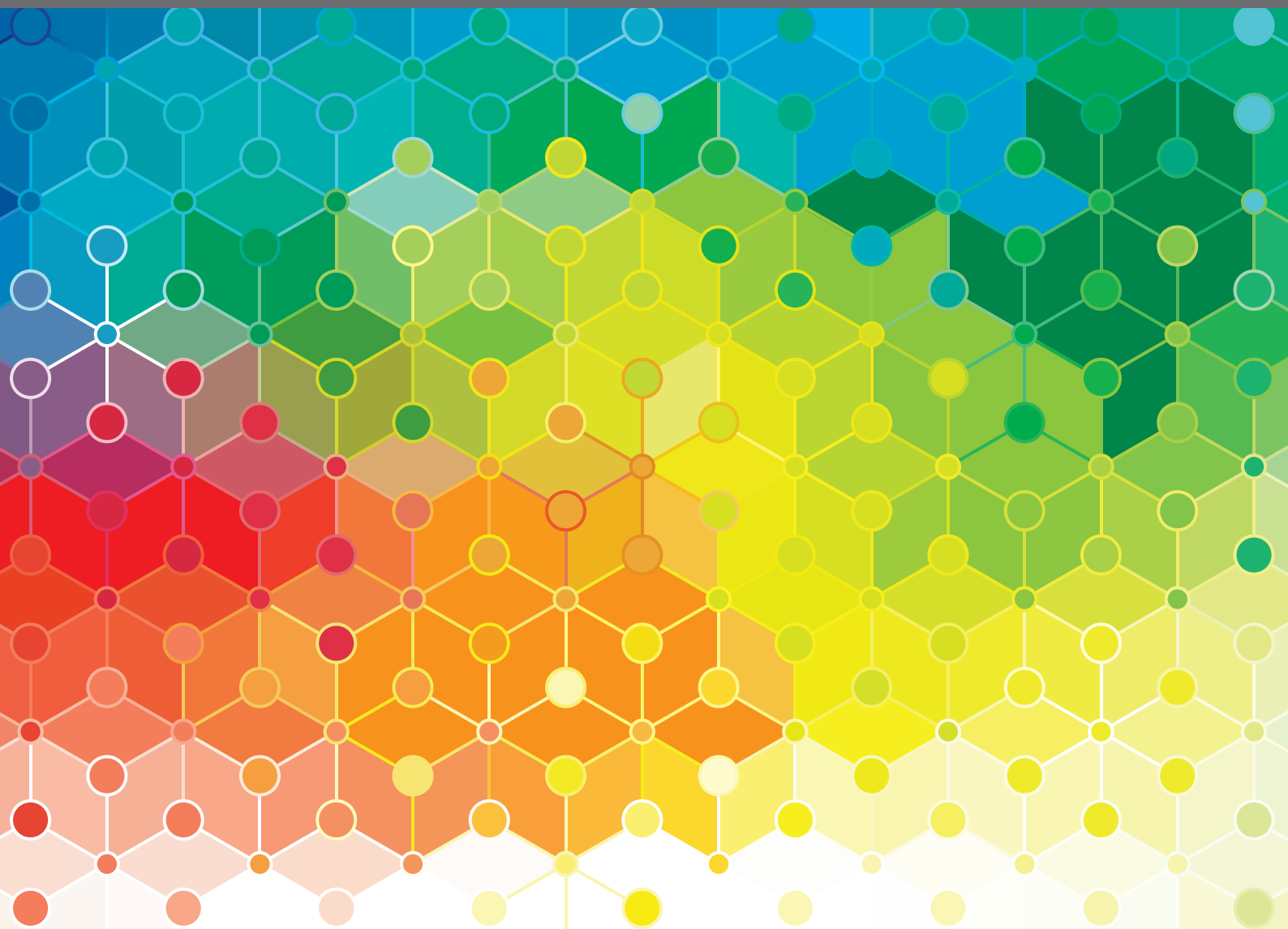

frontiers Research Topics

frontiers

ISSN 1664-8714
ISBN 978-2-88966-919-6
DOI 10.3389/978-2-88966-919-6

About Frontiers

Frontiers is more than just an open-access publisher of scholarly articles: it is a pioneering approach to the world of academia, radically improving the way scholarly research is managed. The grand vision of Frontiers is a world where all people have an equal opportunity to seek, share and generate knowledge. Frontiers provides immediate and permanent online open access to all its publications, but this alone is not enough to realize our grand goals.

Frontiers Journal Series

The Frontiers Journal Series is a multi-tier and interdisciplinary set of open-access, online journals, promising a paradigm shift from the current review, selection and dissemination processes in academic publishing. All Frontiers journals are driven by researchers for researchers; therefore, they constitute a service to the scholarly community. At the same time, the Frontiers Journal Series operates on a revolutionary invention, the tiered publishing system, initially addressing specific communities of scholars, and gradually climbing up to broader public understanding, thus serving the interests of the lay society, too.

Dedication to Quality

Each Frontiers article is a landmark of the highest quality, thanks to genuinely collaborative interactions between authors and review editors, who include some of the world's best academicians. Research must be certified by peers before entering a stream of knowledge that may eventually reach the public - and shape society; therefore, Frontiers only applies the most rigorous and unbiased reviews.
Frontiers revolutionizes research publishing by freely delivering the most outstanding research, evaluated with no bias from both the academic and social point of view. By applying the most advanced information technologies, Frontiers is catapulting scholarly publishing into a new generation.

What are Frontiers Research Topics?

Frontiers Research Topics are very popular trademarks of the Frontiers Journals Series: they are collections of at least ten articles, all centered on a particular subject. With their unique mix of varied contributions from Original Research to Review Articles, Frontiers Research Topics unify the most influential researchers, the latest key findings and historical advances in a hot research area! Find out more on how to host your own Frontiers Research Topic or contribute to one as an author by contacting the Frontiers Editorial Office: frontiersin.org/about/contact

PROCEEDINGS OF THE "FOURTH INTERNATIONAL CONFERENCE OF FMR1 PREMUTATION: BASIC MECHANISMS, CLINICAL INVOLVEMENT AND THERAPY"

Topic Editors:
Cecilia Giulivi, University of California, Davis, United States
Laia Rodriguez-Revenga, Hospital Clínic de Barcelona, Spain
Karen Usdin, National Institutes of Health (NIH) Bethesda, United States
Rob Willemsen, Erasmus Medical Center Rotterdam, Netherlands
Renate K. Hukema, Rotterdam University of Applied Sciences, Netherlands

Citation: Giulivi, C., Rodriguez-Revenga, L., Usdin, K., Willemsen, R., Hukema, R. K., eds. (2021). Proceedings of the "Fourth International Conference of FMR1 Premutation: Basic Mechanisms, Clinical Involvement and Therapy". Lausanne: Frontiers Media SA. doi: 10.3389/978-2-88966-919-6

Table of Contents

frontiers in Molecular Biosciences

EDITORIAL
published: 27 April 2021
doi: 10.3389/fmolb.2021.671875

Editorial: Proceedings of the "Fourth International Conference of the *FMR1* Premutation: Basic Mechanisms, Clinical Involvement and Therapy"

Karen Usdin[1], *Laia Rodriguez-Revenga*[2], *Rob Willemsen*[3], *Renate Hukema*[3] and *Cecilia Giulivi*[4,5]*

[1] Gene Structure and Disease Section, Laboratory of Cell and Molecular Biology, National Institute of Diabetes, Digestive and Kidney Diseases, National Institutes of Health, Bethesda, MD, United States, [2] Biochemistry and Molecular Genetics Department, Hospital Clinic of Barcelona and CIBER of Rare Diseases (CIBERER), Instituto de Salud Carlos III, Barcelona, Spain, [3] Department of Clinical Genetics, Erasmus MC, Rotterdam, Netherlands, [4] Department of Molecular Biosciences, School of Veterinary Medicine, University of California, Davis, Davis, CA, United States, [5] The MIND Institute, University of California, Davis Medical Center, Sacramento, CA, United States

Keywords: ***FMR1*** **premutation, triplet nucleotide repeats, AGG interruptions, FXTAS, FXPOI, mouse model, mitochondrial dysfunction**

Editorial on the Research Topic

Proceedings of the "Fourth International Conference of *FMR1* Premutation: Basic Mechanisms, Clinical Involvement and Therapy"

Edited and reviewed by:
Luigi Michele Pavone, University of Naples Federico II, Italy

***Correspondence:**
Cecilia Giulivi
cgiulivi@ucdavis.edu

Specialty section:
This article was submitted to Cellular Biochemistry, a section of the journal Frontiers in Molecular Biosciences

Received: *24 February 2021*
Accepted: *29 March 2021*
Published: *27 April 2021*

Citation:
Usdin K, Rodriguez-Revenga L, Willemsen R, Hukema R and Giulivi C (2021) Editorial: Proceedings of the "Fourth International Conference of the FMR1 Premutation: Basic Mechanisms, Clinical Involvement and Therapy". Front. Mol. Biosci. 8:671875. doi: 10.3389/fmolb.2021.671875

Fragile X mental retardation 1 (*FMR1*) is an X-linked gene with a hypervariable CGG repeat tract in its 5′ UTR. Alleles with 55–200 CGG repeats are known as premutation alleles (Kogan et al., 2008). Alleles with >200 repeats, known as full mutation alleles, are responsible for Fragile X syndrome, the most common inherited form of intellectual disability and autism spectrum disorder (Verkerk et al., 1991; Yu et al., 1991). The repeat tract in premutation alleles expands on intergenerational transmission to produce larger premutation or full mutation alleles. However, the mechanism responsible for this expansion is largely unknown. Premutation alleles, once thought to be asymptomatic, are now known to confer risk of developing Fragile X-associated tremor/ataxia syndrome (FXTAS), a neurodegenerative disorder (Jacquemont et al., 2003; Grigsby et al., 2006) and a form of ovarian dysfunction known as Fragile X-associated primary ovarian insufficiency (Sherman, 2000; Wittenberger et al., 2007). Premutation carriers can also have other symptoms including fibromyalgia, chronic fatigue, and sleep problems that are referred to collectively as the Fragile X-Associated Neuropsychiatric Disorders (Hagerman et al., 2018). The molecular basis of the pathology seen in premutation carriers is still the subject of much debate (Glineburg et al., 2018).

This special collection of *Frontiers in Cell and Developmental Biology* contains contributions from leading groups in this field that were presented at the 4th International Conference of the *FMR1* Premutation held in Rotterdam on September 25–27, 2019 organized by Drs. Renate Hukema and Rob Willemsen. This collection covers recent advances in basic and clinical research into the underlying mutation and pathology associated with the *FMR1* premutation.

MECHANISMS OF EXPANSION AND DISEASE PATHOLOGY

Gazy et al. showed that embryonic stem cells from *FMR1* premutation mice (Entezam et al., 2007) recapitulate expansion in a dish, thus providing the first cell model that can be used to

study expansion mechanisms. As in cells from human premutation carriers, these cells show mitochondrial abnormalities (Napoli et al., 2016), an *FMR1*-associated R-loop (Groh et al., 2014; Loomis et al., 2014; Kumari and Usdin, 2016) and elevated *Fmr1* transcription (Tassone et al., 2000). Interestingly, increased transcription was sensitive to O_2 tensions. Since these cells can be readily gene-edited, they may help expedite studies of the expansion mechanism as well as premutation pathology.

One model for premutation pathology proposes that RAN translation from premutation alleles produces toxic proteins including FMRpolyGlycine (FMRpolyG), that are responsible both for disease pathology and the intranuclear neuronal inclusions that are a hallmark of FXTAS (Krans et al., 2019). Two papers in this issue address the issue of the role of FMRpolyG. Haify et al. describes an inducible mouse model of FXTAS containing the 5' UTR of the human *FMR1* gene with 103 CGG repeats cloned downstream of a dox-inducible *CamKII*-α promoter. This allowed the regulated expression of FMRpolyG by doxycycline. However, after 12 weeks of FMRpolyG induction no evidence of a behavioral phenotype was seen despite the presence of many intranuclear inclusions throughout the brain. Thus, neither inclusions nor the expression of FMRpolyG *per se* are sufficient to cause neurological problems, at least in young adult mice.

Holm et al. describe the analysis of the cerebral cortex proteome in individuals with FXTAS. Significant differences from the normal proteome were observed including decreased tenascin-C (TNC) and increased levels of the small ubiquitin-like modifier 1/2 (SUMO1/2). FMRpolyG, which has only been identified in trace amounts in studies of FXTAS inclusions (Ma et al., 2019), was not identified in either FXTAS or control brains. Interestingly, in contrast to many other neurodegenerative diseases, the proteome of end-stage FXTAS provides no evidence for a strong inflammation-mediated degenerative response.

CLINICAL INVOLVEMENT IN *FMR1* PREMUTATION CARRIERS

Johnson et al. report on the recommendations of the European Fragile X Network, made in consultation with other stakeholders at the meeting, that the term Fragile X Premutation Associated Conditions (FXPAC) be used to encompass all conditions related to the premutation. This recommendation was made in part to avoid stigmatization of carriers and to facilitate patient evaluation and treatment.

Two papers address metabolic alterations in premutation carriers. Cao et al. review the altered metabolites identified in previous studies of plasma from premutation carriers and the cerebella of FXTAS mice. Napoli et al. address the metabolic footprint of plasma from female carriers using a combined multi-omics approach. Down-regulation of RNA and mRNA metabolism, protein translation, carbon and protein metabolism and the unfolded protein response, and up-regulation of glycolysis and the antioxidant response were observed. Some changes were linked to decreased protein translation, but others seemed to be secondary to oxidative stress.

Finally, Tassanakijpanich et al. discuss rarely appreciated cardiovascular problems in premutation carriers and possible contributing mechanisms including RNA toxicity and mild FMRP deficiency. The review underscores cardiac arrhythmia, autonomic dysfunction, and hypertension as problems that clinicians need to be aware of in this population.

MOTOR AND NEUROCOGNITIVE PROFILE OF *FMR1* PREMUTATION CARRIERS

Although FXTAS is more prevalent and severe in males than females, specific sex differences have not been well-documented. In this section, Loesch et al. report a 2-fold faster progression in males than in females in key measures of tremor and ataxia, while psychiatric symptoms only progressed in females. They postulate the existence of neuroprotective effects beyond the presence of one normal *FMR1* allele in female carriers, specifically affecting cerebellar circuitry.

Winston et al. describe patterns of visual attention in premutation carriers, parents of individuals with autism spectrum disorders, and typically developing controls. Their results demonstrate a visual attention profile that appears strongly associated with the premutation in women and that thus may constitute a meaningful biomarker. Mailick et al. compared the response to parenting stress in mothers with "low zone" (LZ; ≤25 CGGs) alleles to mothers whose repeats were in the normal range. LZ mothers who had children with disabilities had greater limitations in executive functioning, depression, anxiety, daily health symptoms, and balance, than LZ mothers of non-disabled children. In contrast, mothers with normal-range CGG repeats did not differ based on stress exposure consistent with greater resilience.

ANALYSIS OF CGG REPEAT ALLELES

Villate et al. report the analysis of 87 maternal transmissions of alleles with 45–65 repeats and variable numbers of AGG interruptions. Their results confirm the protective effect of AGGs reported previously (Nolin et al., 2013). The authors suggest that assessment of the risk of unstable transmissions should be based on the presence or absence of AGG interruptions and not on the classical cutoffs that define different *FMR1* alleles. Rodrigues et al. described a new approach for evaluating normal *FMR1* alleles that includes the contribution from the AGG interspersion pattern of each allele. The outcome, a numerical parameter named "*allelic score,*" describes the allelic complexity of the *FMR1* gene and provides an additional tool to evaluate pathogenicity and expansion risk.

CONCLUDING REMARKS AND FUTURE DIRECTIONS

The studies published in this special collection demonstrate just how far our understanding of the pathogenic mechanisms, disease diagnosis and management of affected individuals has come in the few years since the 3rd International Meeting on the *FMR1* Premutation. However, these studies also highlight the work that still needs to be done to improve our understanding and treatment of these disorders. Hopefully, some of these issues will be addressed at the 5th iteration of this conference scheduled for New Zealand in March 2022.

AUTHOR CONTRIBUTIONS

All authors listed have made a substantial, direct and intellectual contribution to the work, and approved it for publication.

REFERENCES

Entezam, A., Biacsi, R., Orrison, B., Saha, T., Hoffman, G. E., Grabczyk, E., et al. (2007). Regional FMRP deficits and large repeat expansions into the full mutation range in a new Fragile X premutation mouse model. *Gene* 395, 125–134. doi: 10.1016/j.gene.2007.02.026

Glineburg, M. R., Todd, P. K., Charlet-Berguerand, N., and Sellier, C. (2018). Repeat-associated non-AUG (RAN) translation and other molecular mechanisms in Fragile X Tremor Ataxia Syndrome. *Brain Res.* 1693, 43–54. doi: 10.1016/j.brainres.2018.02.006

Grigsby, J., Brega, A. G., Jacquemont, S., Loesch, D. Z., Leehey, M. A., Goodrich, G. K., et al. (2006). Impairment in the cognitive functioning of men with fragile X-associated tremor/ataxia syndrome (FXTAS). *J. Neurol. Sci.* 248, 227–233. doi: 10.1016/j.jns.2006.05.016

Groh, M., Lufino, M. M., Wade-Martins, R., and Gromak, N. (2014). R-loops associated with triplet repeat expansions promote gene silencing in Friedreich ataxia and fragile X syndrome. *PLoS Genet.* 10:e1004318. doi: 10.1371/journal.pgen.1004318

Hagerman, R. J., Protic, D., Rajaratnam, A., Salcedo-Arellano, M. J., Aydin, E. Y., and Schneider, A. (2018). Fragile X-Associated Neuropsychiatric Disorders (FXAND). *Front. Psychiatry* 9:564. doi: 10.3389/fpsyt.2018.00564

Jacquemont, S., Hagerman, R. J., Leehey, M., Grigsby, J., Zhang, L., Brunberg, J. A., et al. (2003). Fragile X premutation tremor/ataxia syndrome: molecular, clinical, and neuroimaging correlates. *Am. J. Hum. Genet.* 72, 869–878. doi: 10.1086/374321

Kogan, C. S., Turk, J., Hagerman, R. J., and Cornish, K. M. (2008). Impact of the Fragile X mental retardation 1 (FMR1) gene premutation on neuropsychiatric functioning in adult males without fragile X-associated Tremor/Ataxia syndrome: a controlled study. *Am. J. Med. Genet. B Neuropsychiatr. Genet.* 147B, 859–872. doi: 10.1002/ajmg.b.30685

Krans, A., Skariah, G., Zhang, Y., Bayly, B., and Todd, P. K. (2019). Neuropathology of RAN translation proteins in fragile X-associated tremor/ataxia syndrome. *Acta Neuropathol. Commun.* 7:152. doi: 10.1186/s40478-019-0782-7

Kumari, D., and Usdin, K. (2016). Sustained expression of FMR1 mRNA from reactivated fragile X syndrome alleles after treatment with small molecules that prevent trimethylation of H3K27. *Hum. Mol. Genet.* 25, 3689–3698. doi: 10.1093/hmg/ddw215

Loomis, E. W., Sanz, L. A., Chedin, F., and Hagerman, P. J. (2014). Transcription-associated R-loop formation across the human FMR1 CGG-repeat region. *PLoS Genet.* 10:e1004294. doi: 10.1371/journal.pgen.1004294

Ma, L., Herren, A. W., Espinal, G., Randol, J., Mclaughlin, B., Martinez-Cerdeno, V., et al. (2019). Composition of the intranuclear inclusions of fragile X-associated Tremor/Ataxia Syndrome. *Acta Neuropathol. Commun.* 7:143. doi: 10.1186/s40478-019-0796-1

Napoli, E., Song, G., Wong, S., Hagerman, R., and Giulivi, C. (2016). Altered bioenergetics in primary dermal fibroblasts from adult carriers of the FMR1 premutation before the onset of the neurodegenerative disease fragile X-associated tremor/ataxia syndrome. *Cerebellum* 15, 552–564. doi: 10.1007/s12311-016-0779-8

Nolin, S. L., Sah, S., Glicksman, A., Sherman, S. L., Allen, E., Berry-Kravis, E., et al. (2013). Fragile X AGG analysis provides new risk predictions for 45-69 repeat alleles. *Am. J. Med. Genet. A* 161A, 771–778. doi: 10.1002/ajmg.a.35833

Sherman, S. L. (2000). Premature ovarian failure in the fragile X syndrome. *Am. J. Med. Genet.* 97, 189–194. doi: 10.1002/1096-8628(200023)97:3andlt;189::AID-AJMG1036andgt;3.0.CO;2-J

Tassone, F., Hagerman, R. J., Taylor, A. K., Gane, L. W., Godfrey, T. E., and Hagerman, P. J. (2000). Elevated levels of FMR1 mRNA in carrier males: a new mechanism of involvement in the fragile-X syndrome. *Am. J. Hum. Genet.* 66, 6–15. doi: 10.1086/302720

Verkerk, A. J., Pieretti, M., Sutcliffe, J. S., Fu, Y. H., Kuhl, D. P., Pizzuti, A., et al. (1991). Identification of a gene (FMR-1) containing a CGG repeat coincident with a breakpoint cluster region exhibiting length variation in fragile X syndrome. *Cell* 65, 905–914. doi: 10.1016/0092-8674(91)90397-H

Wittenberger, M. D., Hagerman, R. J., Sherman, S. L., Mcconkie-Rosell, A., Welt, C. K., Rebar, R. W., et al. (2007). The FMR1 premutation and reproduction. *Fertil. Steril.* 87, 456–465. doi: 10.1016/j.fertnstert.2006.09.004

Yu, S., Pritchard, M., Kremer, E., Lynch, M., Nancarrow, J., Baker, E., et al. (1991). Fragile X genotype characterized by an unstable region of DNA. *Science* 252, 1179–1181. doi: 10.1126/science.252.5009.1179

Conflict of Interest: The authors declare that the research was conducted in the absence of any commercial or financial relationships that could be construed as a potential conflict of interest.

frontiers in Pediatrics

ORIGINAL RESEARCH
published: 14 May 2020
doi: 10.3389/fped.2020.00223

FMR1 Low Zone CGG Repeats: Phenotypic Associations in the Context of Parenting Stress

Marsha R. Mailick[1], Jinkuk Hong[1], Leann Smith DaWalt[1], Jan S. Greenberg[1], Arezoo Movaghar[1], Mei Wang Baker[2], Paul J. Rathouz[3] and Murray H. Brilliant[1,4]*

[1] Waisman Center, University of Wisconsin-Madison, Madison, WI, United States, [2] Wisconsin State Laboratory of Hygiene, Madison, WI, United States, [3] Dell Medical School at the University of Texas at Austin, Austin, TX, United States, [4] Marshfield Clinic Research Institute, Marshfield, WI, United States

The *FMR1* gene on the X chromosome has varying numbers of CGG repeats. The modal number is 30, and expansion to >200 results in fragile X syndrome, but the copy number extends down to 6. Past research suggests that individuals whose CGGs are in the "low zone" (LZ; defined here as ≤ 25 CGGs) may be more environmentally-reactive than those with normal range repeats (26–40 CGGs)—a gene x environment interaction. Using a population-based DNA biobank, in our primary analysis we compared 96 mothers with LZ CGG repeats on both alleles to 280 mothers who had CGG repeats in the normal range. Secondarily, we conducted parallel analyses on fathers. We investigated how parents in these two CGG repeat categories differentially responded to stress, defined as parenting a child with disabilities. Significant gene x environment interactions indicated that LZ mothers who had children with disabilities had greater limitations (in executive functioning, depression, anxiety, daily health symptoms, and balance) than LZ mothers whose children did not have disabilities. In contrast, mothers with normal-range CGG repeats did not differ based on stress exposure. For fathers, a similar pattern was evident for one phenotype only (hand tremors). Although on average LZ CGGs are not associated with compromised functioning, the average masks differential response to the environment.

Keywords: *FMR1* CGG repeats, gene x environment interactions, stressful parenting, trinucleotide repeat disorders, low zone genotype-phenotype associations

OPEN ACCESS

Edited by:
Renate K. Hukema, Erasmus Medical Center, Netherlands

Reviewed by:
Chiara Di Resta, Vita-Salute San Raffaele University, Italy
Fan Jin, Zhejiang University, China

****Correspondence:***
Marsha R. Mailick
mailick@waisman.wisc.edu

Specialty section:
This article was submitted to Genetic Disorders, a section of the journal Frontiers in Pediatrics

Received: *24 February 2020*
Accepted: *14 April 2020*
Published: *14 May 2020*

Citation:
Mailick MR, Hong J, DaWalt LS, Greenberg JS, Movaghar A, Baker MW, Rathouz PJ and Brilliant MH (2020) FMR1 Low Zone CGG Repeats: Phenotypic Associations in the Context of Parenting Stress. Front. Pediatr. 8:223. doi: 10.3389/fped.2020.00223

INTRODUCTION

The *FMR1* gene on the X chromosome encodes the fragile X mental retardation protein (FMRP), an RNA-binding protein that regulates the expression of hundreds of genes and plays a key role in brain development and function (1, 2). In the 5′ untranslated region of the *FMR1* mRNA, there are varying numbers of CGG trinucleotide repeats. The modal number of CGG repeats in the human population is around 30, whereas expansion above 200 CGG repeats leads to fragile X syndrome (FXS). CGG repeats between 55 and 200 are classified as "premutation," because individuals with CGGs in this range are at increased risk for having children with full mutation FXS, and may also be at higher risk themselves for motor, reproductive, and mental health symptoms (3–5). Those in the "gray zone" (variously defined as 45–54 or 41–54 CGG repeats) are at risk for repeat instability and expansion when passed to subsequent generations, and there is emerging evidence that a small sub-group of those in the gray zone may have elevated risks of motor (6, 7) and reproductive (8) symptoms.

The focus of this study is on *FMR1* CGG repeats *below the gray zone*, considered normal by the American College of Medical Genetics and Genomics [ACMG; (9)]. Even in the putative normal range, the number of *FMR1* CGG repeats in the human population is highly polymorphic (10, 11) and the reported copy number extends down to 6 CGGs (10, 12–14).

Given this level of polymorphism, much may be learned by exploring phenotypic associations of low copy numbers of CGG repeats within *FMR1*.

GENOTYPE-PHENOTYPE ASSOCIATIONS

Several previous reports probed genotype-phenotype associations across the full *FMR1* CGG repeat range (below the FXS level of 200+ CGG repeats). These reports suggest that the phenotypes associated with both lower than normal and expanded numbers of repeats might be *symmetrical*. Chen et al. (13) transfected synthetic human *FMR1* promoter sequences into cell lines, and showed that there was reduced protein translation at both low and high numbers of CGG repeats compared to 30 CGGs. Nagamani et al. (15), in case reports, showed that duplication and deletion of *FMR1* can lead to overlapping clinical neurodevelopmental phenotypes. Ramocki and Zoghbi (16) argued that there is a need for tight neuronal homeostatic control mechanisms for normal cognition and behavior, and that imbalances in homeostatic controls in multiple genes, including *FMR1*, might be responsible for neurodevelopmental and neuropsychiatric disorders. Together these reports suggest that both low and high numbers of CGG repeats in *FMR1* result in similar neurodevelopmental phenotypes.

Motivated by this suggestion of symmetry in the phenotypes associated with both low and expanded copy numbers of *FMR1* CGG repeats, our group previously used representative population survey data from the Wisconsin Longitudinal Study (WLS) to examine genotype-phenotype associations in a birth cohort of aging adults (n = 6,747; mean age = 71) who had CGG repeats ranging from 8 to 134. Using this data, we explored the interaction between the number of CGG repeats and stress exposure, defined as parenting an adult son or daughter who had mental health problems or developmental disabilities (17). Among parents of adults with such disabilities, having CGG repeats either in the low or expanded range was associated with *worse* health and functional limitations than having average numbers of CGG repeats. In contrast, among those who did not have children with such disabilities, having CGG repeats either in the low or expanded range was associated with *better* health and functional outcomes than those having average numbers of CGG repeats.

This pattern of gene by environment interactions was interpreted to be consistent with "differential susceptibility" (18, 19) or the "flip-flop phenomenon" (20, 21). Both of these conceptualizations, though drawing from different research literatures, hypothesize that people with certain genotypes are more reactive to the environment—both positive and negative environments—whereas those who have other genotypes are less environmentally-reactive.

THE PRESENT STUDY

Given contemporary concerns about reproducibility of genetic results (22), there is a need to verify novel findings. The present study aimed to both replicate and also to extend our prior WLS research using data from a completely independent population. As the present study drew from a population nearly three times larger than the WLS sample, we were able to design this new analysis to control for the influence of factors that might otherwise confound the effect of low numbers of CGG repeats.

Specifically, although our past WLS research did not separately analyze data from men and women, we were able to do so in the present study. This was particularly advantageous given our focus on stressful parenting, as research has shown that family caregiving often has greater impacts on mothers than fathers [e.g., (23–28)]. We further restricted our sample of mothers in the present analysis to those who were homozygous for CGG repeats, which we defined as having both alleles within the low range of the CGG distribution or both alleles within the normal range of CGG repeats (see below for definitions of low and normal-range CGGs). In contrast, in our previous WLS research on CGG effects and stressful parenting, we included both homozygous and heterozygous women. Additionally, the population studied in our prior WLS research was based on members of a single birth cohort and their siblings. The members of that birth cohort were age 71 at the time the relevant data were collected. In contrast, the participants in the present study ranged in age from 28 to over 90, making it possible to explore here how age may interact with stressful parenting and CGG effects. However, unlike the WLS research, the present study was not able to investigate the effect of CGG *expansions* because there were no women (out of 11,526) who were homozygous in the premutation range and very few men with premutation alleles (n = 27 out 8,463).

The major hypothesis of this study is that, for women, having low vs. normal numbers of CGG repeats in *FMR1* interacts with stress exposure to predict divergent profiles in specific cognitive, mental health, and physical health phenotypes. The focus on these phenotypes was motivated by prior reports of symmetry in low and expanded copy numbers of CGG repeats in *FMR1* vs. modal copy numbers; all of these phenotypes have been shown to be associated with expanded numbers of CGG repeats [e.g., (5)]. The specific phenotypes include executive functioning, depressive symptoms, anxiety symptoms, daily health symptoms, problems with balance, hand tremors, and for women age at menopause and severity of menopause symptoms. We hypothesized that there would be a significant interaction between stressful parenting status and CGG repeat category, such that among mothers in the low zone, those whose children have disabilities will have *poorer* outcomes for these phenotypes than those whose children are not disabled, whereas among mothers with normal-range CGGs, those who have children with disabilities will not differ from those whose children are not disabled. Our major focus is on mothers because, as noted, the findings of past research showed greater evidence for parenting stress effects for mothers than for fathers. However,

we also explored whether these same patterns would be evident for fathers.

As a follow-up analysis, for those phenotypes for which the predicted gene x environment interaction effects are found to be significant, we explore age effects. We pursue this exploratory analysis because exposure to parenting stress likely varies throughout the parent's life course. Although parenting is a lifelong role, and parenting adult children with disabilities remains stressful even after the children reach adulthood (29), the intensity of parenting is greatest in its early years. Therefore, here we explore whether the hypothesized gene x environment interaction differs by parental age.

METHODS

Population

The study sample was drawn from the population-based Marshfield Clinic Personalized Medicine Research Project (PRMP). Starting in 2002, PMRP enrolled ∼20,000 individuals (40% of the eligible population of the Marshfield Epidemiologic Study Area, a 19-zipcode region centered geographically around Marshfield Wisconsin and an additional 9-zipcode area in northern Wisconsin) who consented to share their DNA and participate in research (30). The participants were diverse in age, with birth years ranging from pre-1922 to 1991. The overwhelming majority of PMRP members are White non-Hispanic (98.4%). This research was approved by the Institutional Review Boards of the Marshfield Clinic Research Institute and the University of Wisconsin-Madison. All participants provided written informed consent prior to their inclusion in the study.

Definition of Low and Normal-Range CGG Repeats

Precisely defining the categories that constitute the *FMR1* CGG repeat range is challenging due to both scientific and technical factors. The published guidelines provided by the American College of Medical Genetics and Genomics for defining normal and mutation categories in *FMR1* (9) note that the borders of the various categories are approximate. "Each definition may change with increased empirical data and research" (p. 578), and there is an acceptable margin of error of several CGG repeats at the borders of the categories.

In our earlier descriptive study using the WLS (31), we defined the "low zone" statistically (≤23 CGGs, which was 2 SDs below the mean of the WLS distribution). We adopted this approach for that descriptive study because extant research did not offer a biological or clinical basis to differentiate normal-range from low numbers of CGG repeats. However, one study (32) defined low numbers of CGGs as ≤25 repeats. Recognizing the margin of error described by the ACMG, we adopted the more inclusive definition of the low zone for the present analysis (i.e., ≤25 repeats).

Definition of normal-range CGGs also has varied in past research. Weghofer et al. (32) defined the normal range narrowly as 26 to 34 CGGs. The ACMG defines normal as any number of CGGs below the gray zone, i.e., <45 CGGs. Some researchers have defined normal as <41 CGGs based on the downward extension of the gray zone to 41 CGG (7, 33–35), referred to in Maenner et al. (36) as the "expanded gray zone." Therefore, for the present research, we defined the normal range as 26 to 40 CGG repeats (i.e., beginning one CGG repeat above the upper bound of the low zone and ending one CGG repeat below the lower bound of the expanded gray zone).

Data

Figure 1 portrays the study workflow, including genetic screening of the population, selection of participants who met inclusion criteria, data collection, and statistical analysis. We show separate workflows for females and males because of the added step of needing to identify females who were homozygous within the low zone or the normal-range.

Using procedures described previously (36, 37), 19,989 DNA samples from PRMP participants were assayed for *FMR1* CGG repeat length, of which 11,526 were samples from females and 8,463 were samples from males. We identified 188 females who had low zone CGG repeats on both alleles, and 895 males with CGG repeats in the low zone. We randomly selected 873 controls with normal-range CGG repeats (504 homozygous females and 369 males). The number of randomly selected normal-range females and males was based on a power analysis designed to yield 80–90% power to detect small (0.2–0.4) Cohen's D phenotypic effect sizes between groups (38).

As part of a larger study, questionnaires were sent to these 1956 men and women, of whom 360 were subsequently found to be deceased, in long-term care, or had an undeliverable address at the time of the questionnaire survey ($n = 115$ females and 245 males). Of the remaining potential participants, 78.5% of the females and 73.0% of the males completed and returned questionnaires. The questionnaires encompassed a broad range of demographic and phenotypic data, including measures of cognitive functioning, mental health and physical health (described below). Also measured were characteristics of participants' children, including child disabilities, the variable that was used in the identification of stressful parenting status. (Note that when we refer to the children of these parents, we are referring to sons and daughters of any age, including adult children).

An additional inclusion criterion for the present analysis was parental status, since a primary focus of the present study is on exposure to stressful parenting. Thus, the present analytic sample included 96 mothers who were homozygous for CGG repeats within the low zone (≤25 repeats) and 280 mothers who were homozygous for CGG repeats in the normal range (26–40 repeats), for a total analytic sample size of 376 mothers. The analytic sample also included 400 fathers in the low zone and 182 who had normal-range CGG repeats. None of the participants were aware of their *FMR1* status (per IRB stipulation).

Definition of Stressful Parenting

Parents reported whether any of their biological children had a developmental (e.g., ADD/ADHD, learning disability, autism spectrum disorder) or a mental health (e.g., anxiety/depression, bipolar disorder, alcohol/drug problems) condition, and if so they

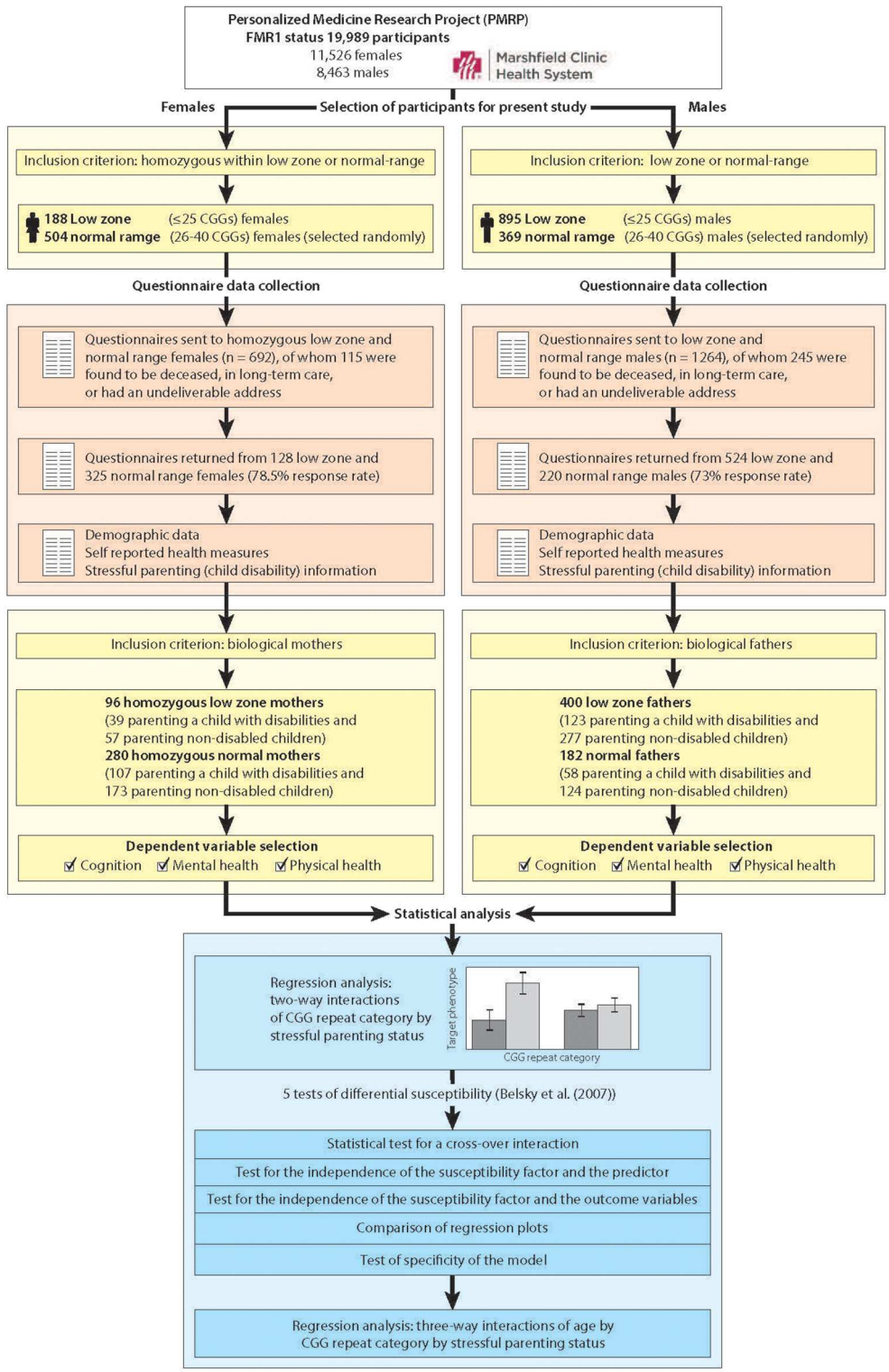

FIGURE 1 | Workflow overview of selection of participants, data collection, and statistical analysis.

were included in the "stressful parenting" group. The comparison group consisted of parents who did not report that any of their children had a developmental or mental health condition.

To confirm that having a child with disabilities is a valid indicator of stressful parenting, we compared parents who had a child with a disability and parents who did not have any

children with disabilities with respect to objective and subjective indicators of parenting stress. For the *objective measure*, we calculated the number of negative life events that parents reported were experienced by their children during the past year, derived from Abidin's (39) Life Stress Scale of the Parenting Stress Index. Parents of children with disabilities reported that their children experienced significantly more negative life events during the past year than parents of children who did not have disabilities ($F = 10.05$, $p < 0.01$ and $F = 13.10$, $p < 0.001$ for mothers and fathers, respectively). For the *subjective measure*, we used the Parenting Stress Scale (40), a self-report 18-item measure with previously established reliability and validity. In the present study, parents of children with disabilities reported significantly higher levels of parenting stress than parents whose children did not have disabilities ($F = 39.8$, $p < 0.001$, and $F = 33.8$, $p < 0.001$ for mothers and fathers, respectively).

These descriptive comparisons confirm that the two parenting groups—those who had a child with disabilities and those whose children did not have disabilities—differed in parenting stress, objectively and subjectively measured. Notably, there were no significant differences in these stress markers between parents with CGGs in the low zone and those with normal-range CGGs.

Phenotypic Measures

Cognition

To measure cognitive functioning, we administered the BRIEF-A [Behavior Rating Inventory of Executive Functioning—Adult Version, (41)], a standardized self-report measure that captures an adult's executive functions or self-regulation in the everyday environment. The BRIEF-A includes 75 items within nine non-overlapping theoretically and empirically derived clinical scales: Inhibit, Self-Monitor, Plan/Organize, Shift, Initiate, Task Monitor, Emotional Control, Working Memory, and Organization of Materials. Together, they constitute the BRIEF-A Global Executive Composite (GEC), which was the measure analyzed for the present study. For the normative sample (41), T-scores were normalized to have a mean of 50 and standard deviation of 10, and in the present sample, the mean was 50.5 with a standard deviation of 10.4. About 10 percent of the present sample (10.5% of mothers and 10.4% of fathers) had a T-score of 65 or higher, the suggested cutoff for clinically significant executive dysfunction. For the normative sample, Cronbach's alpha = 0.96. For the present sample, Cronbach's alpha was also 0.96 for both the mother sample and father samples.

Mental Health

Mental health was measured by two standardized self-report measures. Depressive symptoms were assessed by the Center for Epidemiological Studies-Depression Scale [CES-D; (42)]. For each of 20 depression symptoms, the respondent was asked to indicate how many days in the past week the symptom was experienced (0 = less than 1 day to 3 = 5 to 7 days). Examples of items included "I was bothered by things that usually don't bother me," "I had trouble keeping my mind on what I was doing," "I was depressed," "I felt that everything I did was an effort." The total score is the sum of the ratings for the 20 items, ranging from 0 to 60. Radloff (42) reported Cronbach's alpha to be 0.84–0.85. For the current analytic mother sample, Cronbach's alpha = 0.90, the mean was 8.9 (s.d. = 8.9), and 17% of the sample had scores 16 or higher, the cutoff for the clinical depression. For fathers, Cronbach's alpha = 0.86, the mean was 6.9 (s.d. = 7.3), and 10% of the sample had scores 16 or higher.

Anxiety was measured by the POMS (Profile of Mood States) Tension-Anxiety scale (43), which is a summary score of 9 items asking the degree to which respondents felt each of the following emotional states during the past week: tense, shaky, on edge, panicky, relaxed, uneasy, restless, nervous, and anxious (the positive item was reverse coded). Items were rated on a 5-point scale (0 = not at all to 4 = extremely) and summed, with the total score ranging from 0 to 36. In an adult sample, Cronbach's alpha was reported to be 0.89 (44). For the current analytic mother sample, Cronbach's alpha was also = 0.89. The sample mean of the Tension-Anxiety scale was 6.0 (s.d. = 5.7). For fathers, Cronbach's alpha = 0.84, and the mean was 4.9 (s.d. = 4.5).

Physical Health

Physical health was assessed by three indicators: a count of daily health symptoms, two items reflecting FXTAS-type motor symptoms, and two items reflecting FXPOI-type reproductive symptoms. To measure daily physical health symptoms, we used an adapted version of Larsen and Kasimatis' (45) physical symptom checklist, consisting of 27 health symptoms. For each symptom, the respondents indicated whether they experienced the symptom during the past 24 hours, and if affirmative, they reported the degree of the severity on a 10 point scale, 1 = very mild to 10 = very severe. The list included symptoms such as headache, backache, fatigue, joint pain, sore throat, cold/flu, nausea, and diarrhea. For the present measure, only symptoms with severity ratings of 4 or higher were selected, and the summary score was calculated by counting the number of symptoms that met this criterion. We selected the cut-off severity rating of 4 or higher because the average rating of symptoms (of those who reported any symptoms) was 3.6. Thus, a rating of 4 or higher represented the more severe range of the rating scale. For mothers, the average number of health symptoms above a severity rating of 4 was 2.2 (s.d. = 2.7), ranging from 0 to 17. For fathers, the average number of health symptoms above a severity rating of 4 was 1.6 (s.d. = 2.5), ranging from 0 to 15.

Two items were used to measure motor functioning; "Have you had any problems with your balance" and "Do you have tremor (shakiness) of your hands?" with a binary response, 0 = absent, 1 = present. About a quarter of the mothers (23.9%) and one-fifth of fathers (19.4%) reported having problems with balance, and just under one-tenth of the sample members (9.6% of mothers 8.8% of fathers) reported having hand tremors.

For mothers, two variables were used to measure reproductive phenotypes: the severity of menopausal symptoms and age at menopause. The severity of menopausal symptoms was measured for those who were peri-menopausal, menopausal, or post-menopausal ($n = 307$) using a summary score of 6 items rating the severity of menopausal symptoms (0 = not at all to 3 = a lot): hot flushes/flashes, depression, sleep disturbance, bone pains, night sweats, and other symptoms. For the current analytic mother sample, Cronbach's alpha = 0.72, and the

mean was 5.6 (s.d. = 3.7) with scores ranging from 0 to 18. Mothers who were post-menopausal (n = 145) reported their age at last menstrual period (mean = 50.4, s.d. = 5.3), ranging from 37 to 60.

Statistical Analysis

The data for mothers and fathers were analyzed separately. To test the hypothesis of gene x environment interactions, we estimated regression models with indicator variables for CGG repeat category (low zone vs. normal-range CGGs) and for stressful parenting status (parenting a child with disabilities vs. parenting non-disabled children) as the key predictors. The key variable of interest was the interaction of CGG repeat category by stressful parenting status. Model 1 is the main effects model, including two control variables (parental age and number of biological children) as well as variables for CGG repeat category and stressful parenting category. In Model 2, the interaction between CGG repeat category and stressful parenting category is added. If this interaction is non-significant, Model 1 results are interpreted.

In PMRP, it was possible for several members of a family to volunteer for and be included in the research. Although the number of such family members who met criteria for the present study was small, nevertheless to account for the potential dependency of observations, we used the Generalized Estimating Equation with the exchangeable correlation structure (GEE) (46) approach to regression modeling, and report regression coefficients with robust standard errors based on clustering at the level of family. The use of robust standard errors also protects against bias in inferences due to heteroskedasticity.

Next we tested for differential susceptibility by following the steps outlined in Belsky et al. (18). Step 1 involves a statistical test for a cross-over interaction. Step 2 involves testing the independence of the susceptibility factor (low zone vs. normal-range CGG repeats in the present study) and the predictor (stressful parenting status). Step 3 involves testing the independence of the susceptibility factor and the outcome variables. Step 4 involves comparison of the regression plot with prototypical displays in Figure 1 in Belsky et al. (18). Step 5 involves replacing the susceptibility factors and outcomes with different susceptibility factors and outcomes to test the specificity of the model. For Step 5, we demonstrated the specificity of the model with other outcomes. However, we did not have access to a different susceptibility factor within the PMRP population, so we could only partially test Step 5.

Finally, in exploratory analyses, given the large age range of mothers and fathers in the present sample, we probed whether variation in parental age further conditioned the variability in parenting effects. To do so, for those dependent variables that met the criteria for differential susceptibility, we examined the three-way interaction of gene (low zone vs. normal range) by environment (parenting a child with disabilities vs. parenting non-disabled children) by age (measured continuously). Because few members of the present sample were over the age of 85, for this step in the analysis the age variable was top-coded at 85.

RESULTS FOR MOTHERS

Descriptive Findings

There were no significant differences between the mothers who had children with disabilities and those who did not with respect to CGG repeat number on either the shorter or longer allele. Consistent with population estimates (47, 48), more than a third of the mothers in the present sample (n = 146, 38.8%) had at least one child with the range of disabilities included here (see **Table 1** for a listing of these diagnoses). Mothers in the low zone and mothers with normal-range CGGs did not differ in their likelihood of having children with disabilities (40.6 vs. 38.2%, respectively), nor did they differ in the specific diagnosis of their child. As shown in **Table 1**, the most common conditions affecting the children in both CGG groups were anxiety/depression (n = 58) and ADD/ADHD (n = 35). Very few had a child with severe conditions such as schizophrenia or autism spectrum disorder.

Table 2 presents the characteristics of mothers divided into four groups based on CGG repeat category and stressful parenting. The four groups did not differ with respect to level of education, current marital status, current employment status, or household income. About half of the mothers had at least some post-high school education and were currently employed. The average household income was ∼$55,000. Nearly one-quarter (23.6%) had annual household incomes of $30,000 or less, reflecting the economic diversity of the participants in the present study (data not shown).

However, there were significant differences with respect to maternal age and number of biological children. Mothers in the low zone were significantly younger on average than mothers with normal-range CGGs (55.5 vs. 59.4 years of age) and had a significantly greater number of biological children (3.2 vs. 2.9,

TABLE 1 | Developmental or mental health conditions of mothers' biological children.

Condition	Frequency	Percentage (%)
None	230	61.17%
Anxiety/depression	58	15.43%
ADHD	35	9.31%
Autism spectrum disorders	13	3.46%
Developmental disabilities[a]	12	3.19%
Seizures	7	1.86%
Learning disabilities	5	1.33%
Alcohol/drug problems	5	1.33%
Bipolar disorder	5	1.33%
Schizophrenia	3	0.01%
Other[b]	3	0.01%
Total	376	100.0%

[a] *Including cerebral palsy, Down syndrome, intellectual disabilities, Tourette syndrome.*
[b] *Including sensory loss, mild mental health conditions.*
Some mothers in the present study had more than one child with a developmental or mental health condition. The conditions of the children within each family were independently reviewed by three experienced raters (authors LSD, MM, JH) and the condition determined to be most severe was reported here in this table.

TABLE 2 | Demographic characteristics of mothers by CGG category and stressful parenting status.

	Low zone		Normal-range		
	Children without disabilities ($n = 57$)	Children with disabilities ($n = 39$)	Children without disabilities ($n = 173$)	Children with disabilities ($n = 107$)	Total ($n = 376$)
Age	55.9 (18.1) [29, 91]	53.8 (16.0) [30, 98]	60.0 (16.4) [28, 95]	58.6 (14.0) [29, 91]	58.3 (16.1) [28, 98]
Some post-high school education	53.5%	56.4%	52.3%	61.7%	55.6%
Currently married	80.3%	59.0%	74.2%	72.6%	73.1%
Household income	$58K	$52K	$54K	$55K	$54K
Currently employed	58.9%	66.7%	53.4%	56.0%	56.4%
Number of biological children	3.1 (1.6) [1,7]	2.9 (1.3) [1,6]	2.8 (1.5) [1,8]	2.8 (1.4) [1,8]	2.9 (1.5) [1,8]

on average). Notably, both of these variables had large ranges (maternal age ranged from ∼30 to over 90 years of age in each group, and the number of biological children ranged from one to eight). Therefore, in all analyses, maternal age and number of biological children were statistically controlled.

Multivariate Findings

Table 3 presents the results of the regression models that tested whether CGG repeat category interacted with stressful parenting status with respect to the outcome variables. The significant interaction effects are graphically displayed in **Figure 2**, and the means are included in **Figure 3**.

Cognition

There was a significant CGG repeat category by stressful parenting status interaction effect for executive functioning, as hypothesized. Mothers in the low zone who had children with disabilities had significantly greater limitations in executive functioning than mothers in the low zone whose children did not have disabilities, whereas mothers with normal range CGG repeats did not differ significantly based on stressful parenting status.

Mental Health

There was a consistent pattern of interaction effects across both measures of mental health, supporting our hypothesis. Mothers in the low zone who had children with disabilities had significantly greater depressive and anxiety symptoms than low zone mothers whose children did not have disabilities. Similar to the results for executive functioning limitations, mothers with normal-range CGGs did not differ significantly in depressive or anxiety symptoms based on stressful parenting status.

Physical Health

Of the measures of physical health, the CGG repeat category by stressful parenting interaction was significant for the number of daily health symptoms and problems with balance. Mothers in the low zone who had children with disabilities had significantly more daily health symptoms and were more likely to have problems with balance than low zone mothers whose children were non-disabled. However, mothers with normal-range CGG repeats did not differ significantly based on stressful parenting status.

For hand tremors, severity of menopausal symptoms, and age at menopause, the interactions between CGG repeat category by stressful parenting status were not significant. However, there were significant main effects for both CGG repeat category and for stressful parenting status for severity of menopausal symptoms such that mothers in the low zone had less severe symptoms than those in the normal range, and mothers who experienced stressful parenting had more severe symptoms than those whose children did not have disabilities. Finally, there were no main effects of either CGG repeat category or stressful parenting status for hand tremor or age at menopause.

Differential Susceptibility Analyses

We next tested the differential susceptibility hypothesis for those phenotypes for which there were significant CGG repeat category x stressful parenting status by following the five steps proposed by Belsky et al. (18). The first step is to demonstrate that there is a genuine interaction between the susceptibility factor (low zone vs. normal-range CGGs) and the predictor to show that the regression lines of the predictor for each subgroup of the susceptibility factor crossed each other. In **Table 3**, we showed that there were statistically significant interactions between CGG repeat category and stressful parenting status for five dependent variables. Graphic depiction of the interactions showed that the regression lines for low zone CGGs and normal-range CGGs crossed each other for these variables (see **Figure 3A**).

Specifically, it is not just that the effects of stressful parenting are stronger in the low zone CGG group vs. the normal-range CGG group; rather, they are weak or non-existent in the normal-range group.

The second step in establishing differential susceptibility is to demonstrate the independence of the susceptibility factor and the predictor. The partial correlation between CGG repeat category and stressful parenting status, net of maternal age and the number of children, was not significant ($r = 0.017$, $p = 0.744$), supporting differential susceptibility.

TABLE 3 | GEE (Generalized Estimating Equations linear unless noted as logistic) models predicting phenotypes by stressful parenting and CGG repeat categories: mothers[a].

	Executive functioning (BRIEF-A)		Depressive symptoms (CES-D)		Anxiety (POMS)	
	Model 1	**Model 2**	**Model 1**	**Model 2**	**Model 1**	**Model 2**
Maternal age	0.09 (0.04)**	0.09 (0.04)**	−0.08 (0.03)**	−0.08 (0.03)**	−0.08 (0.02)***	−0.08 (0.02)***
Number of biological children	0.38 (0.41)	0.39 (0.40)	0.11 (0.31)	0.13 (0.30)	0.26 (0.18)	0.27 (0.18)
CGG repeat categories (low zone CGGs = 1)	−0.79 (1.24)	−3.46 (1.40)*	−1.05 (1.06)	−3.67 (1.00)***	−0.59 (0.66)	−2.02 (0.62)**
Stressful parenting (parenting children with disabilities = 1)	1.96 (1.10)+	0.33 (1.26)	3.21 (0.97)**	1.55 (1.06)	1.85 (0.63)**	0.94 (0.71)
LZ x SP	–	6.54 (2.54)*	–	6.51 (2.37)**	–	3.55 (1.49)*
	Number of daily health symptoms		**Problems with balance (logistic)**		**Hand tremor (logistic)**	
	Model 1	**Model 2**	**Model 1**	**Model 2**	**Model 1**	**Model 2**
Maternal age	−0.00 (0.01)	−0.00 (0.01)	0.06 (0.01)***	0.06 (0.01)***	0.02 (0.01)+	0.02 (0.01)+
Number of biological children	0.04 (0.11)	0.05 (0.11)	−0.04 (0.10)	−0.03 (0.11)	0.07 (0.11)	0.08 (0.11)
CGG repeat categories (low zone CGGs = 1)	−0.14 (0.31)	−0.72 (0.36)*	0.08 (0.32)	−0.65 (0.45)	−0.51 (0.48)	−1.35 (0.76)
Stressful parenting (parenting children with disabilities = 1)	0.80 (0.29)**	0.43 (0.33)	0.29 (0.27)	−0.07 (0.30)	−0.18 (0.38)	−0.53 (0.44)
LZ x SP	–	1.43 (0.65)*	–	1.57 (0.63)*	–	1.81 (0.99)+
	Age at menopause		**Severity of menopausal symptoms**			
	Model 1	**Model 2**	**Model 1**	**Model 2**		
Maternal age	0.05 (0.05)	0.05 (0.05)	−0.03 (0.02)	−0.03 (0.02)		
Number of biological children	−0.24 (0.40)	−0.23 (0.39)	−0.15 (0.16)	−0.15 (0.16)		
CGG Repeat categories (low zone CGGs = 1)	−0.49 (1.1)	−0.97 (1.3)	−1.22 (0.47)*	−0.92 (0.64)		
Stressful parenting (Parenting children with disabilities = 1)	1.63 (0.88)+	1.39 (0.97)	1.06 (0.46)*	1.20 (0.54)*		
LZ x SP	–	1.10 (2.22)	–	−0.66 (0.95)		

*+p <0.10, *p < 0.05, **p < 0.01, ***p < 0.001.*

[a] *Unstandardized regression coefficients are presented with standard errors in parenthesis.*

The third step in establishing differential susceptibility is to demonstrate the independence of the susceptibility factor and each outcome. Partial correlations between the CGG repeat category and each outcome, net of covariates, were not statistically significant (correlations ranging from 0.011 to 0.043 with the smallest *p*-value being 0.312), again supporting differential susceptibility.

The fourth test is to compare the regression plots with the prototypical graphs depicted in Figure 1 in the Belsky et al. (18) paper. Not only do the regression lines need to cross each other, it is required that the regression line for the susceptible subgroup (in this study, low zone CGGs) should be significantly different from zero and significantly different from that of the non-susceptible subgroup (normal-range CGGs), and further that the regression line of the non-susceptible group should not be significantly different from zero. Graphs shown in **Figure 3A** are consistent with the fourth criterion for differential susceptibility.

The fifth step is to test the specificity of the model by demonstrating that the current model is not replicated using other susceptibility factors and other outcomes. Regarding specificity of effects for other susceptibility factors, we were not able to test this criterion since there was no other available genetic

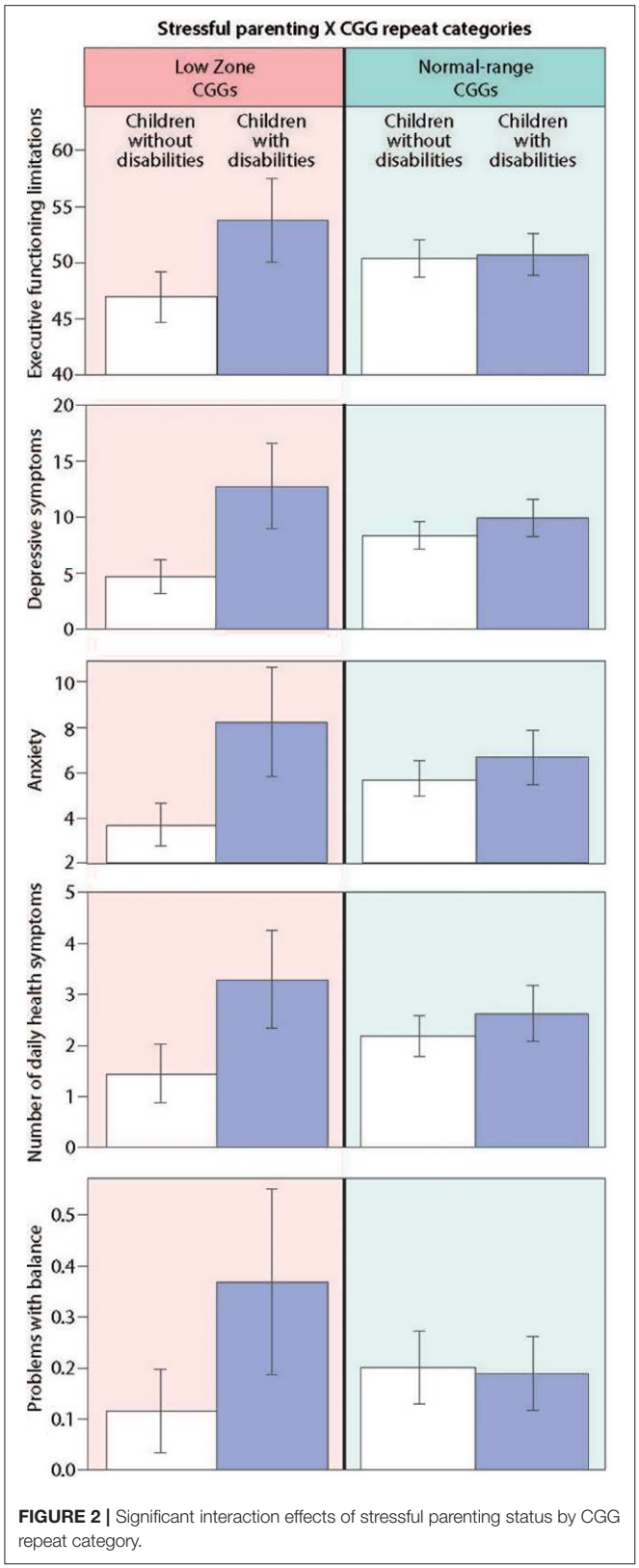

FIGURE 2 | Significant interaction effects of stressful parenting status by CGG repeat category.

information in the current data set. Regarding effects for other outcomes, we already showed that the interactions between CGG repeat category and stressful parenting status were not significant for hand tremor, age at menopause, and severity of menopausal symptoms (see **Table 3** and **Figure 3B**).

Exploring How Age Interacts With Differential Susceptibility

The wide age range of the present study participants offered the possibility of exploring whether the differential susceptibility effects detected above were stable across the mothers' life course or were more pronounced at certain stages of life. To do so, we expanded the regression models for the five outcomes where differential susceptibility had been established (i.e., executive functioning, depressive symptoms, anxiety, number of daily health symptoms, and problems with balance). These expanded regression models included all two-way interactions of the main effect variables, as well as the three-way interaction of CGG repeat category by stressful parenting by maternal age. A significant three-way interaction would suggest that differential susceptibility varied by maternal age.

The three-way interaction for executive functioning was not statistically significant; the differential susceptibility effect was similar in mothers of all ages. However, for the other four outcomes where differential susceptibility was established, maternal age was found to be a potentially important factor. Specifically, the three-way interaction effect approached statistical significance for depressive symptoms [$b = -0.30$ (0.16), $p = 0.056$], anxiety [$b = -0.20$ (0.11), $p = 0.062$], number of health symptoms [$b = -0.10$ (0.05), $p = 0.062$], and was statistically significant for problems with balance [$b = -0.10$ (0.05), $p < 0.05$]. **Figure 4** presents graphs of these findings, plotting raw data (tables depicting the full models are available from the authors). As shown in the left panel of **Figure 4**, for mothers with low zone CGG repeats, the patterns indicate that the differential susceptibility effect was most prominent when mothers were in their 30s and 40s. At these ages, mothers in the low zone who had children with disabilities had high levels of depressive symptoms, anxiety, daily health symptoms, and problems with balance, while mothers in the low zone whose children were non-disabled had the much lower levels of these conditions. In contrast, as shown in the right panel of **Figure 4**, mothers in the normal range (both those who had children with disabilities and those who did not) were similar across all ages. For problems with balance, in addition to the higher level for low zone mothers at younger ages, all four groups had greater difficulties with balance at later ages.

RESULTS FOR FATHERS

We conducted parallel analyses for the sample of low zone and normal-range fathers as reported above for mothers, which we report briefly here given our primary focus on mothers (all tables presenting results for fathers are available from the authors). Nearly one-third of fathers in the present sample ($n = 181$, 31.1%) had at least one child with disabilities. Fathers in the low zone and fathers with normal-range CGGs

A

		Executive functioning limitaions	Depressive symptoms	Anxiety	Number of daily health symptoms	Problems with balance
	Plots of significant interactions	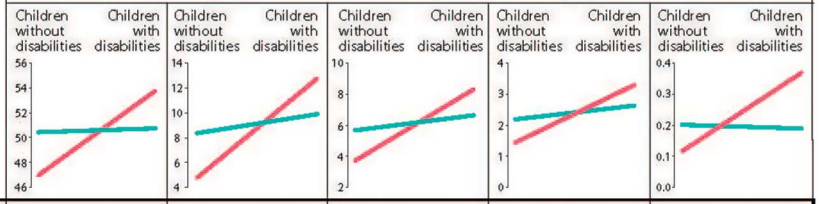				
Low Zone CGGs	Children without disabilities (n = 57)	47.4 (8.8)	5.3 (6.1)	4.1 (3.8)	1.4 (2.1)	0.16 (0.37)
	Children with disabilities (n = 39)	53.3 (11.4)	13.2 (12.8)	8.6 (8.1)	3.2 (3.2)	0.33 (0.48)
	Regression coefficient	6.87 (2.20)**	8.05 (2.11)***	4.49 (1.31)***	1.86 (0.56)***	1.49 (0.57)**
Normal-range CGGs	Children without disabilities (n = 173)	50.6 (10.8)	8.4 (8.2)	5.7 (5.1)	2.1 (2.6)	0.27 (0.44)
	Children with disabilities (n = 107)	50.8 (9.8)	9.9 (8.8)	6.6 (6.0)	2.6 (2.8)	0.23 (0.42)
	Regression coefficient	0.33 (1.26)	1.54 (1.05)	0.94 (0.71)	0.44 (0.35)	−0.08 (0.31)

B

		Hand tremor	Age at menopause	Severity of menopausal symptoms
	Plots of non-significant interactions	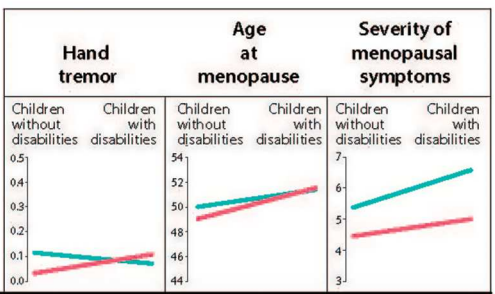		
Low Zone CGGs	Children without disabilities (n = 57)	0.03 (0.19)	49.1 (4.8) (n=17)	4.3 (0.3) (n=30)
	Children with disabilities (n = 39)	0.10 (0.31)	51.4 (6.6) (n=14)	5.1 (3.0) (n=27)
	Regression coefficient	1.28 (0.90)	2.49 (2.0)	0.54 (0.79)
Normal-range CGGs	Children without disabilities (n = 173)	0.13 (0.34)	50.0 (5.4) (n=75)	5.3 (3.6) (n=127)
	Children with disabilities (n = 107)	0.07 (0.26)	51.4 (4.6) (n=39)	6.6 (4.0) (n=80)
	Regression coefficient	−0.53 (0.44)	1.39 (0.97)	1.20 (0.54)*

FIGURE 3 | Test of differential susceptibility for mothers. **(A)** Outcomes with differential susceptibility established. **(B)** Outcomes with differential susceptibility not established. *$p < 0.05$, **$p < 0.01$, ***$p < 0.001$.[a] Unadjusted means are present with standard deviations in parenthesis. Unstandardized regression coefficients are presented with standard errors in parenthesis.

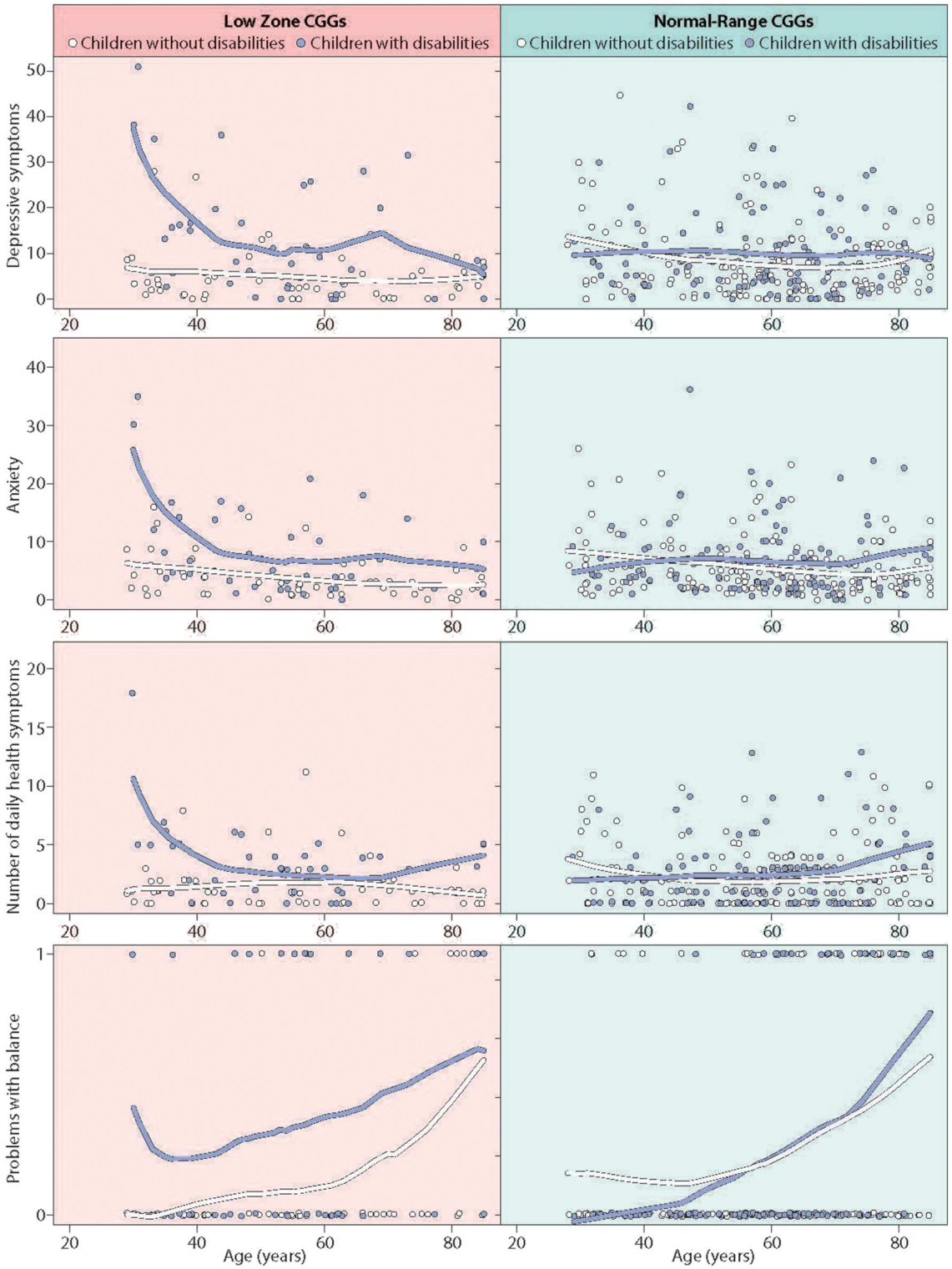

FIGURE 4 | Significant three-way interaction effects of age by stressful parenting status by CGG repeat category.

did not differ in their likelihood of having children with disabilities (30.1 vs. 31.9%, respectively), nor did they differ in the specific condition of their child. Similar to the mothers in the present sample, the most common conditions affecting the children in both CGG groups were anxiety/depression (n = 60) and ADD/ADHD (n = 36), while very few had a

child with severe disabilities such as schizophrenia or autism spectrum disorder.

We conducted regression analyses that tested whether for fathers, CGG repeat category interacted with stressful parenting status with respect to the outcome variables. The regression models paralleled those conducted for mothers, and included executive functioning, depressive symptoms, anxiety symptoms, number of daily health symptoms, problems with balance, and hand tremors. Only one interaction effect was statistically significant, namely for hand tremors. Fathers in the low zone who had children with disabilities were significantly more likely to have hand tremors than those whose children with not disabled, whereas there was no such difference among fathers who had normal-range CGG repeats. Follow-up analyses indicated that this interaction effect met all criteria for differential susceptibility. However, the three-way interaction (age x CGG repeat category x stressful parenting status) was not significant.

For the other five outcome variables, there were no main effects indicating a different phenotypic pattern for fathers in the low zone and fathers with normal-range CGGs. Two main effects for stressful parenting reached statistical significance, namely number of daily health symptoms and problems with balance; fathers whose children had disabilities had a greater number of health symptoms and were more likely to have problems with balance than fathers whose children were all non-disabled. Older age was associated greater executive functioning deficits, anxiety, and problems with balance.

DISCUSSION

Parenting is one of the most salient and gratifying roles of adulthood and parenting a child with disabilities is surprisingly common. In the U.S., ∼10% of children have ADHD (48), and there are nearly as high rates of depression or anxiety [8.4%; (47)]. Lifetime rates of these disorders are higher, consistent with the patterns observed in the present study. Studies of the impact of parenting children with disabilities report high levels of parenting stress, particularly for mothers, as well as significant heterogeneity in the degree to which parents of individuals with disabilities experience negative outcomes (23, 28, 49). In the present study, we show that variability in *FMR1* CGG repeats might be one reason why some mothers are more vulnerable in the context of parenting children with disabilities and why others may be more resilient. Specifically, in the present cohort, mothers in the low zone had greater vulnerability to stressful parenting with respect to executive functioning limitations, depressive and anxiety symptoms, health symptoms, and problems with balance. However, not all phenotypes were similarly affected; the differential susceptibility effect was not evident for age at menopause, menopausal symptoms, or hand tremors.

For mothers, this study extends our past research findings in which individuals were found to differ in their susceptibility to both positive and negative aspects of the family environment, depending on whether they have low vs. average numbers of *FMR1* CGG repeats (17). In both studies, those with low numbers of CGG repeats were more reactive to environmental stress than those with average numbers of CGG repeats; low zone mothers who had children with disabilities were more vulnerable than those whose children were non-disabled. In contrast, those with average repeat numbers were more resilient, as they did not vary in health and mental health based on the disability status of their children.

However, with the exception of hand tremors, this pattern was not evident for fathers in the present study, suggesting a more pronounced gene x environment interaction effect for mothers than for fathers. This is consistent with past research that has reported greater effects of family caregiving for mothers than for fathers (see Hayes & Watson). It is possible that different types of stress may be more salient for fathers, a possibility warranting investigation in future research.

Although these results converge with those obtained in our previous investigation using an independent population, the specific phenotypes that showed the pattern of differential susceptibility were not identical in the two studies, and these differences may be due to the inclusion of both mothers and fathers in the prior WLS study as well as to the ages of the respective study participants. In our previous WLS research, in which participants clustered tightly around 71 years of age, differential susceptibility was evident for limitations in everyday memory, number of physical health symptoms, and limitations in physical functioning, but not for depressive symptoms or anxiety. In the present research, where the participants were nearly 15 years younger on average and ranged from early adulthood to old age, a somewhat different profile of vulnerability emerged, particularly with regards to mental health.

Furthermore, in the present study, we found that it was in the earlier years of parenting (during the 30s and 40s) that mothers' differential susceptibility for depression and anxiety was most pronounced, whereas after around age 50 the groups no longer diverged. Since the participants in the WLS study were in their early 70s, it was not possible to examine differential susceptibility effects for mental health in the vulnerable age category in that study. Thus, this apparent inconsistency between the two studies may be a function of age differences between the respective participants. Although there were other methodological differences between the two studies that could have contributed to these differences in the specific phenotypes that were implicated, the overall pattern of differential susceptibility in those with low zone CGG repeats was evident in both studies.

Furthermore, in both investigations, the phenotypic characteristics of those with average numbers of CGG repeats did not differ based on whether or not they had chronic exposure to stressful parenting—this is the profile characteristic of non-susceptible genotypes. Many previous studies have noted that are substantial individual differences and great heterogeneity in response to the stress of parenting children with disabilities, with some parents manifesting profiles of resilience and others profiles of vulnerability [see (23), for a meta-analysis]. While multiple factors may contribute to this heterogeneity, our research suggests that genetics (in this case, variation in the *FMR1* gene) may be one individual difference factor.

A similar pattern of results (although with different susceptibility genes) has been shown for other aspects of the family environment. For example, Brummett et al. (50) compared women with the s/s allele of the serotonin transporter polymorphism and those with the l/l allele, and further divided the groups by whether they were caregivers for a relative with Alzheimer's or were non-caregivers. The study found that women having the s/s allele who were caregivers for a relative with Alzheimer's disease had higher levels of depressive symptoms, whereas those women with the s/s allele who were not caregivers had substantially *lower* levels of depressive symptoms than those with the l/l allele. The s/s allele conferred susceptibility to variation in the family environment. In contrast, those with the l/l allele had similar levels of depression whether caring for a relative with Alzheimer's or not. In another example, Fortuna et al. (51) compared mothers with the 7-repeat allele of DRD4-III and those without the 7-repeat, and further divided the groups into those whose infants were premature and those with full-term infants. The results showed that mothers with the 7-repeat allele manifested less sensitive parenting if their infants were preterm, but manifested more sensitive parenting if their infants were born full-term. However, those who did not carry the 7-repeat allele of DRD4-III did not differ in parenting sensitivity based on the risk level of their infants. In both of these examples, as in the present study, exposure to stressful vs. non-stressful family environments was associated with behavioral and psychological differences in genetically susceptible women, but not among women who were in the genetically non-susceptible categories for the gene under investigation.

Limitations, Strengths, and Next Steps

The present study is limited by the use of an overwhelmingly white sample (over 90% white non-Hispanic) with measures based on responses to survey questions. Future research that includes more diverse sample members would strengthen the conclusions reported here. Details about the timing of the onset of the child's disability or the severity of the child's symptoms are not available, which would further aid interpretation of study findings. An additional limitation is the use of cross-sectional data, particularly in the investigation of age-related differences. There are likely selection effects with respect to both differential rates of survey participation and mortality among the oldest members of the PMRP population. It is also possible that there is confounding of other environmental or genetic effects that impact both the parent's health outcomes and children's risk of developmental or mental health disabilities.

Along with these limitations there are a number of study strengths, including drawing the study participants from a population-based sample and the high response rate (over 75% of eligible participants). This extension of our prior WLS research was possible due to the availability of *FMR1* CGG repeat data across the full population range, as well as measures of many of the same phenotypes. The present study's wide age range enabled extension of the past work into investigation of age effects.

Future research should probe the mechanisms that could account for the differential susceptibility observed here. Chen et al.'s (13) finding that translation is less efficient at lower numbers of CGG repeats in *FMR1* may offer a clue that can be pursued in future research, as inefficiency in translation might potentiate responses to environmental effects. Translational efficiency and/or localization of specific mRNAs are molecular mechanisms that may underlie these differences. Future studies are needed to unveil the impact of CGG repeat number of *FMR1* on neuronal function and plasticity, and to uncover the link between CGG repeat number and the genes that drive susceptibility to stress.

CONCLUSIONS

Parenting a child with disabilities is a prevalent source of chronic stress, particularly for mothers, with substantial heterogeneity in the associated health impacts. Variation in *FMR1* CGG repeats may partially explain individual differences in resilience and vulnerability to stressful parenting. The results of the present investigation could be useful in predicting the parenting stress response in individuals with varying genotypes, and in offering resources and supports to reduce and manage high levels of stress emanating from having a child with disabilities.

Currently, there is consensus that reproducibility of results is critical to biomedical research. The largely convergent findings across two independent populations using different study designs lends credence to the idea that low numbers of CGG repeats in the *FMR1* gene may be one source of susceptibility to both the positive and negative impacts of the family environment. Studies of human populations are challenged to identify sources of individual differences, and the confluence of genetic and environmental factors provides a fruitful avenue.

DATA AVAILABILITY STATEMENT

The datasets generated for this study will not be made publicly available. The terms of the IRB protocol prohibit public sharing of the data sets. Requests to access the datasets should be directed to Marsha R. Mailick, marsha.mailick@wisc.edu.

AUTHOR CONTRIBUTIONS

MM, JH, and PR designed the study. JH carried out the statistical analysis. MHB provided the DNA samples. MWB carried out the assays. MM wrote the manuscript and all other authors JH, LD, JG, AM, MWB, PR, and MHB contributed to and approved the manuscript.

FUNDING

This study was supported in part by a core grant to the Waisman Center from the National Institute of Child Health and Human Development (U54 HD090256). Additional funding was provided by NICHD R01 HD082110 and the Centers for Disease Control and Prevention, National Center for Birth Defects and Developmental Disorders through the Association for University Centers on Disability (U01DD00023).

PR was supported by NHGRI U01HG8701 (eMERGE), NCATS UL1TR000427 (ICTR).

ACKNOWLEDGMENTS

The authors would like to acknowledge all of the participants in this study who so generously provided data. We are grateful to Elizabeth Berry-Kravis, MD, Ph.D., Anita Bhattacharyya, Ph.D., Paul Hagerman, MD, Ph.D., and Xinyu Zhao, Ph.D. for their scientific advice and consultation. We also would like to thank Terrie Kitchner (Marshfield Clinic Research Institute) and Renee Makuch (Waisman Center) for coordinating the data collection, and Bryan Kim for assistance with manuscript preparation. We are grateful to H. Adam Steinberg who created the figures and workflow.

REFERENCES

1. Ascano M Jr, Mukherjee N, Bandaru P, Miller JB, Nusbaum JD, Corcoran DL, et al. FMR1 targets distinct mRNA sequence elements to regulate protein expression. *Nature.* (2012) 492:382–6. doi: 10.1038/nature11737
2. Darnell JC, Van Driesche SJ, Zhang C, Hung KY, Mele A, Fraser CE, et al. FMRP stalls ribosomal translocation on mRNAs linked to synaptic function and autism. *Cell.* (2011) 146:247–61. doi: 10.1016/j.cell.2011.06.013
3. Hagerman R, Hagerman P. Advances in clinical and molecular understanding of the FMR1 premutation and fragile X-associated tremor/ataxia syndrome. *Lancet Neurol.* (2013) 12:786–98. doi: 10.1016/S1474-4422(13)70125-X
4. Movaghar A, Page D, Brilliant M, Baker MW, Greenberg J, Hong J, et al. Data-driven phenotype discovery of FMR1 premutation carriers in a population-based sample. *Sci Adv.* (2019) 5:eaaw7195. doi: 10.1126/sciadv.aaw7195
5. Wheeler AC, Bailey DB Jr, Berry-Kravis E, Greenberg J, Losh M, Mailick M, et al. Associated features in females with an FMR1 premutation. *J Neurodev Disord.* (2014) 6:30. doi: 10.1186/1866-1955-6-30
6. Hall D, Tassone F, Klepitskaya O, Leehey M. Fragile X-associated tremor ataxia syndrome in FMR1 gray zone allele carriers. *Mov Disord.* (2012) 27:297–301. doi: 10.1002/mds.24021
7. Hall DA. In the gray zone in the fragile X gene: what are the key unanswered clinical and biological questions? *Tremor Other Hyperkinet Mov.* (2014) 4:208. doi: 10.7916/D8NG4NP3
8. Bretherick KL, Fluker MR, Robinson WP. FMR1 repeat sizes in the gray zone and high end of the normal range are associated with premature ovarian failure. *Hum Genet.* (2005) 117:376–82. doi: 10.1007/s00439-005-1326-8
9. Monaghan KG, Lyon E, Spector EB. ACMG standards and guidelines for fragile X testing: a revision to the disease-specific supplements to the standards and guidelines for clinical genetics laboratories of the American College of Medical Genetics and Genomics. *Genet Med.* (2013) 15:575–86. doi: 10.1038/gim.2013.61
10. Fu Y-H, Kuhl DPA, Pizzuti A, Pieretti M, Sutcliffe JS, Richards S, et al. Variation of the CGG repeat at the fragile X site results in genetic instability: resolution of the Sherman paradox. *Cell.* (1991) 67:1047–58. doi: 10.1016/0092-8674(91)90283-5
11. Eichler EE, Hammond HA, Macpherson JN, Ward PA, Nelson DL. Population survey of the human FMR1 CGG repeat substructure suggests biased polarity for the loss of AGG interruptions. *Hum Mol Genet.* (1995) 4:2199–208. doi: 10.1093/hmg/4.12.2199
12. Brown WT, Houck GE Jr, Jeziorowska A, Levinson FN, Ding X, Dobkin C, et al. Rapid fragile X carrier screening and prenatal diagnosis using a nonradioactive PCR test. *JAMA.* (1993) 270:1569–75. doi: 10.1001/jama.1993.03510130075034
13. Chen L-S, Tassone F, Sahota P, Hagerman PJ. The (CGG)n repeat element within the 5′ untranslated region of the FMR1 message provides both positive and negative cis effects on *in vivo* translation of a downstream reporter. *Hum Mol Genet.* (2003) 12:3067–74. doi: 10.1093/hmg/ddg331
14. Snow K, Doud LK, Hagerman R, Pergolizzi RG, Erster SH, Thibodeau SN. Analysis of a CGG sequence at the FMR-1 locus in fragile X families and in the general population. *Am J Hum Genet.* (1993) 53:1217–28.
15. Nagamani SCS, Erez A, Probst FJ, Bader P, Evans P, Baker LA, et al. Small genomic rearrangements involving FMR1 support the importance of its gene dosage for normal neurocognitive function. *Neurogenetics.* (2012) 13:333–9. doi: 10.1007/s10048-012-0340-y
16. Ramocki MB, Zoghbi HY. Failure of neuronal homeostasis results in common neuropsychiatric phenotypes. *Nature.* (2008) 455:912–8. doi: 10.1038/nature07457
17. Mailick MR, Hong J, Greenberg J, Dawalt LS, Baker MW, Rathouz PJ. FMR1 genotype interacts with parenting stress to shape health and functional abilities in older age. *Am J Med Genet Part B Neuropsychiatr Genet.* (2017) 174:399–412. doi: 10.1002/ajmg.b.32529
18. Belsky J, Bakermans-Kranenburg MJ, van IJzendoorn MH. For better and for worse: differential susceptibility to environmental influences. *Curr Dir Psychol Sci.* (2007) 16:300–4. doi: 10.1111/j.1467-8721.2007.00525.x
19. Belsky J, Pluess M. Beyond diathesis stress: differential susceptibility to environmental influences. *Psychol Bull.* (2009) 135:885–908. doi: 10.1037/a0017376
20. Hunter JE, Leslie M, Novak G, Hamilton D, Shubeck L, Charen K, et al. Depression and anxiety symptoms among women who carry the FMR1 premutation: impact of raising a child with fragile X syndrome is moderated by CRHR1 polymorphsims. *Am J Med Genet Part B Neuropsychiatr Genet.* (2012) 159:549–59. doi: 10.1002/ajmg.b.32061
21. Lin P-I, Vance JM, Pericak-Vance MA, Martin ER. No gene is an island: the flip-flop phenomenon. *Am J Hum Genet.* (2007) 80:531–8. doi: 10.1086/512133
22. Chanock SJ, Manolio T, Boehnke M, Boerwinkle E, Hunter DJ, Thomas G, et al. Replicating genotype-phenotype associations. *Nature.* (2007) 447:655–60. doi: 10.1038/447655a
23. Hayes SA, Watson SL. The impact of parenting stress: a meta-analysis of studies comparing the experience of parenting stress in parents of children with and without autism spectrum disorder. *J Autism Dev Disord.* (2013) 43:629–42. doi: 10.1007/s10803-012-1604-y
24. Herring S, Gray K, Taffe J, Tonge B, Sweeney D, Einfeld S. Behaviour and emotional problems in toddlers with pervasive developmental disorders and developmental delay: associations with parental mental health and family functioning. *J Intellect Disabil Res.* (2006) 50:874–82. doi: 10.1111/j.1365-2788.2006.00904.x
25. Pinquart M, Sörensen S. Gender differences in caregiver stressors, social resources, and health: an updated meta-analysis. *J Gerontol Ser B Psychol Sci.* (2006) 61:33–45. doi: 10.1093/geronb/61.1.p33
26. Seltzer MM, Floyd F, Song J, Greenberg J, Hong J. Midlife and aging parents of adults with intellectual and developmental disabilities: impacts of lifelong parenting. *Am J Intellect Dev Disabil.* (2011) 116:479–99. doi: 10.1352/1944-7558-116.6.479
27. Song J, Mailick MR, Greenberg JS, Ryff CD, Lachman ME. Cognitive aging in parents of children with disabilities. *Jf Gerontol Ser B Psychol Sci Soc Sci.* (2016) 71:821–30. doi: 10.1093/geronb/gbv015
28. Wiener J, Biondic D, Grimbos T, Herbert M. Parenting stress of parents of adolescents with attention-deficit hyperactivity disorder. *J Abnorm Child Psychol.* (2016) 44:561–74. doi: 10.1007/s10802-015-0050-7
29. Namkung EH, Greenberg JS, Mailick MR, Floyd FJ. Lifelong parenting of adults with developmental disabilities: growth trends over 20 years in midlife and later life. *Am J Intellect Dev Disabil.* (2018) 123:228–40. doi: 10.1352/1944-7558-123.3.228
30. McCarty CA, Wilke RA, Giampietro PF, Wesbrook SD, Caldwell MD. Marshfield Clinic Personalized Medicine Research Project (PMRP): design, methods and recruitment for a large population-based biobank. *Pers Med.* (2005) 2:49–79. doi: 10.1517/17410541.2.1.49

31. Mailick MR, Hong J, Rathouz P, Baker MW, Greenberg JS, Smith L, et al. Low-normal FMR1 CGG repeat length: phenotypic associations. *Front Genet.* (2014) 5:309. doi: 10.3389/fgene.2014.00309
32. Weghofer A, Tea M-K, Barad DH, Kim A, Singer CF, Wagner K, et al. BRCA1/2 mutations appear embryo-lethal unless rescued by low (CGG n<26) FMR1 sub-genotypes: explanation for the "BRCA paradox"? *PLoS ONE.* (2012) 7:e44753. doi: 10.1371/journal.pone.0044753
33. Berry-Kravis E, Goetz CG, Leehey MA, Hagerman RJ, Zhang L, Li L, et al. Neuropathic features in fragile X premutation carriers. *Am J Med Genet Part A.* (2007) 143A:19–26. doi: 10.1002/ajmg.a.31559
34. Hall DA, Bennett DA, Filley CM, Shah RC, Kluger B, Ouyang B, et al. Fragile X gene expansions are not associated with dementia. *Neurobiol Aging.* (2014) 35:2637–8. doi: 10.1016/j.neurobiolaging.2014.04.027
35. Loesch DZ, Bui QM, Huggins RM, Mitchell RJ, Hagerman RJ, Tassone F. Transcript levels of the intermediate size or grey zone fragile X mental retardation 1 alleles are raised, and correlate with the number of CGG repeats. *J Med Genet.* (2007) 44:200–4. doi: 10.1136/jmg.2006.043950
36. Maenner MJ, Baker MW, Broman KW, Tian J, Barnes JK, Atkins A, et al. FMR1 CGG expansions: prevalence and sex ratios. *Am J Med Genet Part B Neuropsychiatr Genet.* (2013) 162:466–73. doi: 10.1002/ajmg.b.32176
37. Seltzer MM, Baker MW, Hong J, Maenner M, Greenberg J, Mandel D. Prevalence of CGG expansions of the FMR1 gene in a US population-based sample. *Am J Med Genet Part B Neuropsychiatr Genet.* (2012) 159:589–97. doi: 10.1002/ajmg.b.32065
38. Cohen J. *Statistical Power Analysis for the Behavioral Sciences.* 2nd ed. Hillsdale, NJ: Lawrence Erlbaum Associates (1988).
39. Abidin RR. *Parenting Stress Index.* 2nd ed. Charlottesville, VA: Pediatric Psychology Press (1986).
40. Berry JO, Jones WH. The parental stress scale: initial psychometric evidence. *J Soc Pers Relat.* (1995) 12:463–72. doi: 10.1177/0265407595123009
41. Roth RM, Isquith PK, Gioia GA. *BRIEF-A: Behavior Rating Inventory of Executive Function - Adult Version: Professional Manual.* Lutz, FL: Psychological Assessment Resources (2005).
42. Radloff LS. The CES-D Scale: a self-report depression scale for research in the general population. *Appl Psychol Meas.* (1977) 1:385–401. doi: 10.1177/014662167700100306
43. McNair DM, Lorr M, Droppleman LF. *Manual for the Profile of Mood States.* San Diego, CA: Educational and Industrial Testing Service (1971).
44. Watson D, Weber K, Assenheimer JS, Clark LA, Strauss ME, McCormick RA. Testing a tripartite model: I. Evaluating the convergent and discriminant validity of anxiety and depression symptom scales. *J Abnorm Psychol.* (1995) 104:3.
45. Larsen RJ, Kasimatis M. Day-to-day physical symptoms: individual differences in the occurrence, duration, and emotional concomitants of minor daily illnesses. *J Pers.* (1991) 59:387–423. doi: 10.1111/j.1467-6494.1991.tb00254.x
46. Diggle PJ, Heagerty P, Liang K-Y, Zeger SL. *Analysis of Longitudinal Data.* 2nd ed. Oxford: Oxford University Press (2013).
47. Bitsko RH, Holbrook JR, Ghandour RM, Blumberg SJ, Visser SN, Perou R, et al. Epidemiology and impact of healthcare provider diagnosed anxiety and depression among US children. *J Dev Behav Pediatr.* (2018) 39:395–403. doi: 10.1097/DBP.0000000000000571
48. Danielson ML, Bitsko RH, Ghandour RM, Holbrook JR, Kogan MD, Blumberg SJ. Prevalence of parent-reported ADHD diagnosis and associated treatment among U.S. children and adolescents, 2016. *J Clini Child Adolesc Psychol.* (2018) 47:199–212. doi: 10.1080/15374416.2017.1417860
49. Barroso NE, Mendez L, Graziano PA, Bagner DM. Parenting stress through the lens of different clinical groups: a systematic review & meta-analysis. *J Abnorm Child Psychol.* (2018) 46:449–61. doi: 10.1007/s10802-017-0313-6
50. Brummett BH, Boyle SH, Siegler IC, Kuhn CM, Ashley-Koch A, Jonassaint CR, et al. Effects of environmental stress and gender on associations among symptoms of depression and the serotonin transporter gene linked polymorphic region (5-HTTLPR). *Behav Genet.* (2008) 38:34–43. doi: 10.1007/s10519-007-9172-1
51. Fortuna K, van IJzendoorn MH, Mankuta D, Kaitz M, Avinun R, Ebstein RP, et al. Differential genetic susceptibility to child risk at birth in predicting observed maternal behavior. *PLoS ONE.* (2011) 6:e19765. doi: 10.1371/journal.pone.0019765

Conflict of Interest: MM is the Chair of the Scientific Advisory Board of the John Merck Fund.

The remaining authors declare that the research was conducted in the absence of any commercial or financial relationships that could be construed as a potential conflict of interest.

frontiers in Pediatrics

PERSPECTIVE
published: 27 May 2020
doi: 10.3389/fped.2020.00266

Fragile X Premutation Associated Conditions (FXPAC)

Kirsten Johnson[1]*, *Jonathan Herring*[2] and *Jörg Richstein*[3]

[1] The Fragile X Society, Great Dunmow, United Kingdom, [2] Faculty of Law, University of Oxford, Oxford, United Kingdom, [3] Interessengemeinschaft Fragiles-X e.V, Rostock, Germany

The European Fragile X Network (EFXN) proposes that Fragile X Premutation Associated Conditions (FXPAC) be adopted as a universal term covering any condition linked to the Fragile X premutation. To date, there has not been an umbrella term assigned to issues associated with the FMR1 premutation, though several defined conditions which affect some premutation carriers, namely Fragile X-associated Primary Ovarian Insufficiency (FXPOI) and Fragile X-associated Tremor/Ataxia Syndrome (FXTAS), are now commonly accepted. An overarching term covering all FX premutation conditions will help doctors in determining how the premutation might be affecting their patient; and encourage researchers to explore the interrelationships of the various conditions affecting premutation carriers. Further, there are ongoing discoveries about physical and psychological issues faced by premutation carriers, and a new term helps encompass all of these burgeoning developments.

Keywords: Fragile X, premutation, FXTAS, FXPOI, FXPAC

OPEN ACCESS

Edited by:
Renate K. Hukema,
Erasmus Medical Center, Netherlands

Reviewed by:
Randi Jenssen Hagerman,
University of California, Davis, United States
Avinash Vijay Dharmadhikari,
Columbia University, United States

***Correspondence:**
Kirsten Johnson
kirsten@fragilex.org.uk

Specialty section:
This article was submitted to Genetic Disorders, a section of the journal Frontiers in Pediatrics

Received: *27 February 2020*
Accepted: *28 April 2020*
Published: *27 May 2020*

Citation:
Johnson K, Herring J and Richstein J (2020) Fragile X Premutation Associated Conditions (FXPAC). Front. Pediatr. 8:266. doi: 10.3389/fped.2020.00266

Fragile X Syndrome (FXS) is the most common form of inherited learning difficulty (1) and has been estimated to affect one in every 2,500–7,000 males and one in 2,500–11,000 females (2). Those with FXS typically have an expanded CGG repeat of over 200 in the 5′ untranslated region of FMR1 at Xq27.3. The general population have an average of 30 CGG repeats; those who have between 55 and 200 repeats are deemed to have the premutation (3). The precise presentation of the conditions varies. Most males with FXS have intellectual disability and behavior features including anxiety, attention deficit and symptoms of being on the autism spectrum. The symptoms for females with FXS range from mild to severe, and include learning difficulties, social skills and communication challenges, and mental health issues (4). For females who are less affected, whilst their difficulties are more subtle, they as a result face all the challenges associated with that of hidden disability.

Initial research into FXS assumed that the only significance for being a carrier was that their children might inherit the gene. However, it is now clear that the health issues for carriers go beyond the impact on the progeny.

Research is ongoing into the conditions which affect Fragile X premutation carriers. Established conditions associated with the premutation include Fragile X-associated Tremor/Ataxia Syndrome (FXTAS) (5) and Fragile X-associated Primary Ovarian Insufficiency (FXPOI) (6). FXTAS is a late-onset neurodegenerative condition with symptoms typically displaying after the age of fifty and worsening with age. It presents more commonly in men, with around 40% of male premutation carriers developing FXTAS and 16% of females. Characteristic symptoms include intention tremor, as well as difficulty with coordination and balance (ataxia), although not everyone with FXTAS evidences both features. Diagnosis is made based upon a combination of clinical and radiological examinations (7).

FXPOI is seen in around 20% of women with the *FMR1* premutation. Indeed, the Fragile X premutation is the most frequent single gene cause of primary ovarian insufficiency (8). FXPOI is characterized by reduced indicators of ovarian function (such as unpredictable or absent menses) and an impaired ovarian response. On average, the age of menopause is five years younger in women with the Fragile X premutation than the general population (9).

Research has shown people who are premutation carriers experience some mental and physical health symptoms at higher rates than in the general population (10). These are not encompassed by FXTAS or FXPOI. These additional impacts of being a carrier have been identified through studies with people who are aware that they are Fragile X premutation carriers (typically with a child with Fragile X Syndrome); and, more recently, in research which involved looking at the health records of a large sample of people in the general population, some of whom were premutation carriers (11). In 2018, the term Fragile X-associated Neuropsychiatric Disorders (FXAND) has been suggested to cover a range of neuropsychiatric and physical conditions associated with the Fragile X premutation. Neuropsychiatric conditions are said to affect approximately half of premutation carriers. Anxiety and depression are the most common issues seen in adults, though researchers have argued that physical problems such as chronic pain and autoimmune difficulties can heighten neuropsychiatric issues (12).

It is clear that we are only beginning to understand the wider significance of being a Fragile X premutation carrier and further research is needed to understand all the possible consequences. This is necessary to ensure there is effective recognition, understanding, and support for all people with the Fragile X premutation.

The European Fragile X Network (EFXN), at their meeting in Rotterdam, The Netherlands, on 29 September 2019, had a symposium on recent research on conditions which affect Fragile X premutation carriers. EFXN represents 17 family organizations across 16 countries in Europe, and consists of volunteers who advocate on behalf of those with Fragile X and associated conditions. Many of these volunteers carry the Fragile X premutation and are therefore directly affected by any terminology used.

There has been dismay over the past year at the suggested term Fragile X-associated Neuropsychiatric Disorder (FXAND). This term includes both physical and psychiatric symptoms under one umbrella (12). Many females carrying the premutation testified to the stigma they felt when labeled with having a "disorder."

In their discussions, EFXN members identified several concerns:

- The term FXAND (Fragile X-associated Neuropsychiatric Disorder), by including auto-immune conditions and neuropsychiatric conditions under a single term, was not well-defined. It grouped together a wide variety of conditions. The term seemed to the EFXN representatives to be used as a "catch all" to refer to conditions that were not covered by FXTAS and FXPOI. While it might be helpful to have a term that referred to all conditions that might impact a carrier or a term that referred to a tightly defined set of conditions, FXAND as defined in the 2018 article was neither of these.
- The inclusion of the word disorder in the term FXAND was seen as stigmatizing of the premutation carrier. The conditions that fall under the current term FXAND are various, including social phobia, sensitivity to external stimuli, and depression. At the meeting, such characteristics were not seen as disorders but a common part of the human condition for many**.** The term disorder portrayed the impact of being a carrier in a necessarily poor light and could induce social or professional exclusion. Many premutation carriers are high-functioning with university degrees and established careers. They do not regard themselves as "disordered." Using "condition" rather than "disorder" would be much preferred by the EFXN as it is broader language and keeps open a discussion about the desirability of the state.

After much debate, both on the day and then later in consultation with researchers, particularly those who were advisors to the Fragile X groups, it was decided to propose the umbrella term Fragile X Premutation Associated Conditions (FXPAC). This refers to all conditions affecting the premutation carrier. FXPAC does not replace FXTAS or FXPOI, rather FXTAS and FXPOI are specific examples of FXPAC. Further, FXAND should be replaced with two terms: Fragile X-associated Neuropsychiatric Conditions (FXANC); and Fragile X Various Associated Conditions (FXVAC), to cover other physical conditions that are not neuropsychiatric in nature. These suggestions are motivated by three main reasons.

First, the term FXPAC is a helpful overarching term to describe all conditions that might be associated with being a premutation carrier. We are still learning what all these conditions are and how they interrelate with each other and can interact. By having one label for them all researchers can be encouraged to explore their relationship further.

Second, the EFXN representatives found the term FXAND as being a confusing collection of physical and psychiatric conditions. The symptoms associated with FXPAC will include those linked to FXTAS and FXPOI. The neuropathology of FXTAS is well-established (13) and the clinical symptoms clearly differentiated (14, 15). FXPOI also has neat diagnostic indicators for clinical diagnosis (16). Recent research has looked at the clustering of symptoms in 355 females with the premutation (17). Though research is ongoing, the following symptoms (in addition to those associated with FXTAS or FXPOI) have been found to occur in higher rates in people with the Fragile X premutation:

- Anxiety, and anxiety disorders
- Low mood and depression
- Elevated traits related to autism, such as differences in the processing of social information and use of social (pragmatic) language. Of note, this refers to subtle characteristics that occur to varying degrees in the general population rather than symptoms of autism, *per se*. Although, in a small number of individuals a diagnosis of autism might be appropriate.

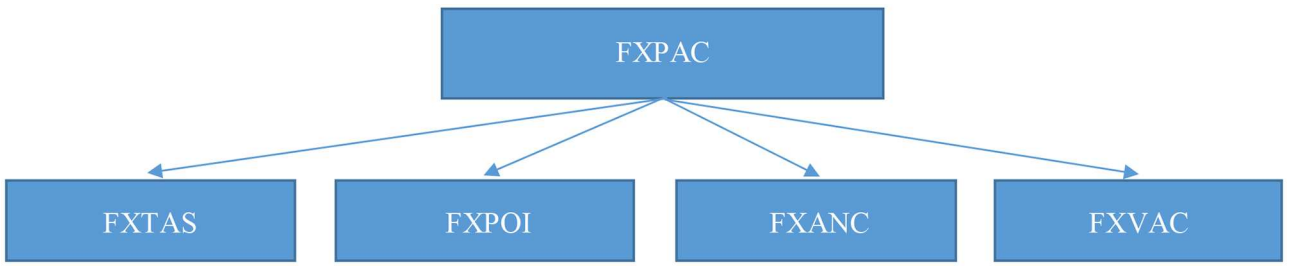

FIGURE 1 | FXPAC, Fragile X Premutation Associated Conditions; FXTAS, Fragile X-associated Tremor/Ataxia Syndrome; FXPOI, Fragile X-associated Primary Ovarian Insufficiency; FXANC, Fragile X-associated Neuropsychiatric Conditions; FXVAC, Fragile X Various Associated Conditions.

- Physical health symptoms such as chronic fatigue, chronic pain, fibromyalgia, autoimmune disorders, and sleep problems have also been identified at higher rates in people with the Fragile X premutation.

It is not helpful to have FXAND cover such a broad range of conditions. The proposed term FXANC would be narrower and be limited to neuropsychiatric conditions. FXVAC can be used for other physical conditions. The new terms FXANC and FXVAC would have more clearly defined boundaries and meanings than the "catch all" term of FXAND.

Third, the proposed terminology avoids the label "disorder." The European premutation carriers felt strong that the word condition is a more accurate and less stigmatizing word to use for these conditions. We do recognize that in some countries the term disorder has benefits in strengthening arguments that treatment for it should be funded under health insurance. However, these financial considerations must be weighed against the stigma facing those with the condition. Further, it is hard to believe that the label used will impact on whether an insurance policy covers a particular condition or not.

EFXN, therefore, proposes Fragile X Premutation Associated Conditions (FXPAC) to be an overarching term to cover issues relating to being a carrier. Under that general heading, specific conditions will be:

- FXTAS (Fragile X-associated Tremor/Ataxia Syndrome)
- FXPOI (Fragile X-associated Primary Ovarian Insufficiency)
- FXANC (Fragile X-associated Neuropsychiatric Conditions), replacing the word "disorder" in FXAND, with "conditions";
- FXVAC (Fragile X Various Associated Conditions) for any other non-psychiatric conditions (such as auto-immune conditions, chronic fatigue, fibromyalgia, etc.) which should not be included in FXANC but referred to as FXVAC (**Figure 1**).

Further research might define these terms more precisely and/or add to them. Also, the inter-relation between the various FXPAC conditions is not understood, with some carriers seemingly being unaffected, and others having a combination of conditions affecting them.

The European Fragile X Network hopes that researchers and clinicians will adopt FXPAC when generally referring to conditions that may affect premutation carriers. Having a unified term FXPAC gives a doctor, when helping someone with the premutation, a starting point for looking at the array of conditions which may or may not affect a particular premutation carrier. Further, it will encourage researchers to explore the interactions between these conditions.

It is important to highlight that many of the FXPAC symptoms are also common in the general population. However, the emerging research suggests that people with the premutation may be at higher risk of some of the symptoms. In addition, for many, these traits may present in subtle ways that do not affect day-to-day life. Though, a proportion of people who are Fragile X premutation carriers will experience symptoms to the extent it has a negative impact for them. Being a carrier does not mean that these symptoms are inevitable, and treatment should be sought for these symptoms as for anyone in the general population.

In conclusion, there is a need for a term which encompasses conditions affecting Fragile X premutation carriers. The EFXN, covering a population of over 500 million people throughout Europe, has worked together to come up with new terminology. FXPAC (Fragile X Premutation Associated Conditions) has been proposed to describe the wide range of symptoms which may affect premutation carriers. This has been welcomed by European researchers and clinicians.

FXPAC will aid researchers who wish to explore the many ways the premutation affects carriers, allowing for the fact we do not yet understand how these may be interlinked. FXPAC will help carriers who experience a range of conditions and wish to have a medical diagnosis. FXPAC will be a one-stop shop for doctors who need to explore the various conditions which may affect their patient. The network of European Fragile X family organizations very much hopes these ideas will be widely adopted outside Europe and around the world.

AUTHOR'S NOTE

Information on the work of the European Fragile X Network may be found at www.fragilex.eu. This is a group of charitable organizations who support families and those affected by Fragile X across Europe.

AUTHOR CONTRIBUTIONS

This article was drafted by KJ, revised by JH, with additional contributions from JR.

FUNDING

This article was written on behalf of the European Fragile X Network, a group of charities representing families and those affected by Fragile X and the Fragile X premutation.

ACKNOWLEDGMENTS

The authors are grateful for the support of all the organizations and their representatives which are part of the European Fragile X Network; and for the support of European researchers and clinicians in refining these ideas. Particular thanks to Dr. Becky Hardiman, CEO of the Fragile X Society, UK, for her support in developing the idea of FXPAC and for her help with this article.

REFERENCES

1. Hagerman PJ. The fragile X prevalence paradox. *J Med Genet.* (2008) 45:498–9. doi: 10.1136/jmg.2008.059055
2. Hunter J, Rivero-Arias O, Angelov A, Kim E, Fotheringham I, Leal J. Epidemiology of fragile X syndrome: a systematic review and meta-analysis. *Am J Med Genet Part A*. (2014) 164:1648–58. doi: 10.1002/ajmg.a.36511
3. Fu YH, Kuhl DPA, Pizzuti A, Pieretti M, Sutcliffe JS, Richards S, et al. Variation of the CGG repeat at the fragile X site results in genetic instability: resolution of the Sherman paradox. *Cell.* (1991) 67:1047–58. doi: 10.1016/0092-8674(91)90283-5
4. Bartholomay KL, Lee CH, Bruno JL, Lightbody AA, Reiss AL. Closing the gender gap in fragile X syndrome: review of females with fragile X syndrome and preliminary research findings. *Brain Sci.* (2019) 9:11. doi: 10.3390/brainsci9010011
5. Leehey MA, Hall DA, Liu Y, Hagerman RJ. Clinical neurological phenotype of FXTAS. In: F. Tassone, D. Hall, editors. *FXTAS, FXPOI, and Other Premutation Disorders*. Cham: Springer (2016). p. 1–221. doi: 10.1007/978-3-319-33898-9_1
6. Allen EG, Glicksman A, Tortora N, Charen K, He W, Amin A, et al. FXPOI: pattern of AGG interruptions does not show an association with age at amenorrhea among women with a premutation. *Front Genet*. (2018) 9:292. doi: 10.3389/fgene.2018.00292
7. Berry-Kravis E, Abrams L, Coffey SM, Hall DA, Greco C, Gane LW, et al. Fragile X-associated tremor/ataxia syndrome: clinical features, genetics, and testing guidelines. *Movem Dis.* (2007) 22:2018–30. doi: 10.1002/mds.21493
8. Sherman SL. Premature ovarian failure in the Fragile X syndrome. *Am J Med Genet.* (2000) 97:189–94. doi: 10.1002/1096-8628(200023)97:3<189::AID-AJMG1036>3.0.CO;2-J
9. Allen EG, Grus WE, Narayan S, Espinel W, Sherman SL. Approaches to identify genetic variants that influence the risk for onset of fragile X-associated primary ovarian insufficiency (FXPOI): a preliminary study. *Front Genet*. (2014) 5:260. doi: 10.3389/fgene.2014.00260
10. Wheeler AC, Bailey DB Jr, Berry-Kravis E, Greenberg J, Losh M, Mailick M, et al. Associated features in females with an *FMR1* premutation. *J Neurodevelop Dis.* (2014) 6:30. doi: 10.1186/1866-1955-6-30
11. Movaghar A, Page D, Brilliant M, Baker MW, Greenberg J, Hong J, et al. Data-driven phenotype discovery of *FMR1* premutation carriers in a population-based sample. *Sci Adv.* (2019) 5:eaaw7195. doi: 10.1126/sciadv.aaw7195
12. Hagerman R, Protic D, Rajaratnam A, Salcedo-Arellano MJ, Aydin EY, Schneider A. Fragile X-associated neuropsychiatric disorders (FXAND). *Front Psychol.* (2018) 9:564. doi: 10.3389/fpsyt.2018.00564
13. Greco CM, Berman RF, Martin RM, Tassone F, Schwartz PH, Chang A, et al. Neuropathology of fragile X-associated tremor/ataxia syndrome (FXTAS). *Brain.* (2006) 129:243–55. doi: 10.1093/brain/awh683
14. Juncos JL, Lazarus JT, Graves-Allen E, Shubeck L, Rusin M, Novak G, et al. New clinical findings in the fragile X-associated tremor ataxia syndrome (FXTAS). *Neurogenetics.* (2011) 12:123–35. doi: 10.1007/s10048-010-0270-5
15. Hall DA, Leehey MA, Berry-Kravis E, Hagerman RJ. Treatment and management of FXTAS. In: F. Tassone, D. Hall, editors. *FXTAS, FXPOI, and Other Premutation Disorders*. Cham: Springer (2016). p. 181–97. doi: 10.1007/978-3-319-33898-9_9
16. Sherman SL, Allen EG, Spencer JB, Nelson LM. Clinical manifestation and management of FXPOI. In: F. Tassone, D. Hall, editors. *FXTAS, FXPOI, and Other Premutation Disorders*. Cham: Springer (2016). p. 199–224. doi: 10.1007/978-3-319-33898-9_10
17. Allen EG, Charen K, Hipp HS, Shubeck L, Amin A, He W, et al. Clustering of comorbid conditions among women who carry an FMR1 premutation. *Genet Med.* (2020) 22:758–66. doi: 10.1038/s41436-019-0733-5

Conflict of Interest: The authors declare that the research was conducted in the absence of any commercial or financial relationships that could be construed as a potential conflict of interest.

frontiers in Cell and Developmental Biology

ORIGINAL RESEARCH
published: 30 June 2020
doi: 10.3389/fcell.2020.00482

CGG Repeat Expansion, and Elevated *Fmr1* Transcription and Mitochondrial Copy Number in a New Fragile X PM Mouse Embryonic Stem Cell Model

*Inbal Gazy[1,2], Carson J. Miller[1], Geum-Yi Kim[1] and Karen Usdin[1]**

[1] *Laboratory of Cell and Molecular Biology, NIDDK, National Institutes of Health, Bethesda, MD, United States,*
[2] *KwaZulu-Natal Research Innovation and Sequencing Platform (KRISP), College of Health Sciences, University of KwaZulu-Natal, Durban, South Africa*

OPEN ACCESS

Edited by:
Konstantinos Zarbalis, University of California, Davis, United States

Reviewed by:
Peter Kennedy Todd, University of Michigan, United States
Michael Ryan Hunsaker, The University of Utah, United States
Elisabetta Tabolacci, Catholic University of the Sacred Heart, Rome, Italy
Nicolas Charlet-Berguerand, Institut National de la Santé et de la Recherche Médicale (INSERM), France
Eleonora Napoli, University of California, Davis, United States

***Correspondence:**
Karen Usdin
karenu@nih.gov;
ku@helix.nih.gov

Specialty section:
This article was submitted to Cellular Biochemistry, a section of the journal Frontiers in Cell and Developmental Biology

Received: *29 January 2020*
Accepted: *22 May 2020*
Published: *30 June 2020*

Citation:
Gazy I, Miller CJ, Kim G-Y and Usdin K (2020) CGG Repeat Expansion, and Elevated Fmr1 Transcription and Mitochondrial Copy Number in a New Fragile X PM Mouse Embryonic Stem Cell Model. Front. Cell Dev. Biol. 8:482. doi: 10.3389/fcell.2020.00482

The Fragile-X related disorders (FXDs) are Repeat Expansion Diseases (REDs) that result from expansion of a CGG-repeat tract located at the 5′ end of the *FMR1* gene. While expansion affects transmission risk and can also affect disease risk and severity, the underlying molecular mechanism responsible is unknown. Despite the fact that expanded alleles can be seen both in humans and mouse models *in vivo*, existing patient-derived cells do not show significant repeat expansions even after extended periods in culture. In order to develop a good tissue culture model for studying expansions we tested whether mouse embryonic stem cells (mESCs) carrying an expanded CGG repeat tract in the endogenous *Fmr1* gene are permissive for expansion. We show here that these mESCs have a very high frequency of expansion that allows changes in the repeat number to be seen within a matter of days. CRISPR-Cas9 gene editing of these cells suggests that this may be due in part to the fact that non-homologous end-joining (NHEJ), which is able to protect against expansions in some cell types, is not effective in mESCs. CRISPR-Cas9 gene editing also shows that these expansions are MSH2-dependent, consistent with those seen *in vivo*. While comparable human Genome Wide Association (GWA) studies are not available for the FXDs, such studies have implicated MSH2 in expansion in other REDs. The shared unusual requirement for MSH2 for this type of microsatellite instability suggests that this new cell-based system is relevant for understanding the mechanism responsible for this peculiar type of mutation in humans. The high frequency of expansions and the ease of gene editing these cells should expedite the identification of factors that affect expansion risk. Additionally, we found that, as with cells from human premutation (PM) carriers, these cell lines have elevated mitochondrial copy numbers and *Fmr1* hyperexpression, that we show here is O_2-sensitive. Thus, this new stem cell model should facilitate studies of both repeat expansion and the consequences of expansion during early embryonic development.

Keywords: repeat expansion, Fragile X syndrome, Fragile X-related disorders, premutation, mouse embryonic stem cells, mitochondrial abnormalities, *Fmr1* hyperexpression

INTRODUCTION

The Fragile X-related disorders (FXDs), are members of the Repeat Expansion Disorders (REDs), a group of 35+ human diseases that arise due to an expansion or increase in the length of a disease-specific microsatellite. The microsatellite responsible for the FXDs is a CGG repeat tract located in the 5′ untranslated region (UTR) of the X-linked *FMR1* gene. Premutation (PM) alleles contain 55–200 repeats and carriers of such alleles are at risk of developing Fragile X-associated tremor/ataxia syndrome (FXTAS), a late-onset neurodegenerative disorder, and Fragile X-associated primary ovarian insufficiency (FXPOI), a cause of early menopause and infertility of women carriers before the age of 40 (Mila et al., 2018). In addition to the risk of FXTAS and FXPOI, women carrying a PM allele are at risk of transmitting a much larger full mutation (FM) allele to their children. Such alleles contain more than 200 repeats and give rise to a third disorder, Fragile X syndrome, the leading cause of inherited intellectual disability and autism spectrum disorder (ASD; Crawford et al., 2001).

Expansions into the PM range result in elevated *FMR1* transcript levels (Tassone et al., 2000). However, this increase in transcript levels does not result in increased production of FMRP, the protein product of *FMR1*. In fact, FMRP levels are reduced in PM cells due to impaired translation of transcripts with large numbers of CGG repeats (Kenneson et al., 2001). PM pathology results from the deleterious consequences of the PM transcripts (Renoux and Todd, 2012) that are likely to be exacerbated by the elevated levels of the expanded CGG-repeat containing *FMR1* transcript. While expansions have important consequences for disease pathology in humans, the underlying mechanism responsible for the expansion mutation is still largely unclear, as is the timing of the expansion from a PM to a FM allele.

Unlike other REDs where patient derived cell-culture models show a progressive increase in repeat number over time in culture (Cannella et al., 2009; Du et al., 2012, 2013), expansion in differentiated cells from human FX PM carriers, induced pluripotent stem cells (iPSC) derived from these cells, or human embryonic stem cells (hESCs) carrying large unmethylated alleles, either does not occur or occurs extremely rarely (Brykczynska et al., 2016; Zhou et al., 2016). Furthermore, expansion in a PM knock-in (KI) mouse model (Entezam et al., 2007) is known to be very cell type specific (Lokanga et al., 2013; Zhao and Usdin, 2018; Gazy et al., 2019). Thus, in order to develop a good tissue culture model for repeat expansion that could be used to expedite studies of the expansion mechanism, we needed to identify a cell type permissive for this mutation that can be readily cultured for long periods. Work with PM mice suggested that expansions occur at a high frequency in the early embryo (Lokanga et al., 2014; Zhao et al., 2016). Since expansions are not seen in hESCs (Zhou et al., 2016), a cell type that is thought to resemble the more developmentally advanced primed EpiSCs rather than naïve ESCs (Smith, 2017), we hypothesized that high frequency expansions in the early embryo may be limited to cells more reminiscent of earlier stages in embryonic development. Given that mouse embryonic stem cells (mESCs) have the characteristics of more naïve ESCs (Smith, 2017), it was possible that mESCs generated from PM mice would show expansions that occur at high enough frequency to allow the expansion process to be studied *in vitro*. We show here that indeed this is the case, with expansions occurring in most cells in the mESC population as often as twice a week depending on the repeat number. This very high mutation rate has implications for the mechanism involved. It also allows factors that affect this mutation rate to be readily examined. The PM mESC lines also display cellular changes that resemble those found in cells of human PM carriers. Thus, these mESCs can serve as a useful model to facilitate our understanding both of the expansion mechanism and its consequences.

MATERIALS AND METHODS

Generation of mESCs Lines

The C57BL/6 *Fmr1* FX KI (knock-in) mice were described previously (Entezam et al., 2007). Mice were maintained in accordance with the guidelines of the NIDDK Animal Care and Use Committee and with the Guide for the Care and Use of Laboratory Animals (NIH publication no. 85–23, revised 1996). Embryos were isolated from superovulated $Fmr1^{WT/KI}$ females mated with $Fmr1^{WT}$ males. Preimplantation embryos were obtained by flushing the uterine horns with M2 medium (GSM-5120, MTI-GlobalStem, Rockville, MD, United States) at post coitum day 3.5. Embryos were first washed with M2, then a 1:1 mixture of M2 and KSOM medium (GSM-5140, MTI-GlobalStem), and finally with KSOM. Embryos were then plated separately in 0.1% gelatin (ES-006-B, MilliporeSigma, St. Louis, MO, United States) coated wells pre-equilibrated with KSOM medium. Most embryos hatched from the zona pellucida 1–2 days after plating, at which point media was exchanged to N2B27 medium supplemented with 2i [3 μM CHIR99021 (S2924, Selleckchem, Houston, TX, United States), 1 μM PD0325901 (S1036, Selleckchem)], and LIF (1000 unit/ml; ESG1107, MilliporeSigma; hereafter referred to as N2B27 2i/LIF medium; Nichols and Ying, 2006; Ying et al., 2008). The embryos were grown for ∼7 days with daily medium changes until the emergence of ES-cell colonies. The cells were then trypsinized (TrypLE^{TM} Select, Thermo Fisher Scientific, Waltham, MA, United States) and transferred to new wells containing N2B27 2i/LIF supplemented with 10 ng/ml BMP-4 (314-BP-010, R&D Systems, Minneapolis, MN, United States). Once these cultures were ready for passaging, cells were replated and 1 day after plating the medium was replaced with N2B27 2i/LIF lacking BMP-4. For routine propagation, cells were maintained on 0.1% gelatin coated wells in N2B27 2i/LIF media (Nichols and Ying, 2006; Ying et al., 2008) with daily media changes and passaged 1:3–1:6 every 2–3 days. Evaluation of pluripotency markers was carried out using standard immunofluorence protocols. Briefly, cells were fixed in 4% PFA, permeabilized, and blocked with 0.3% Triton X-100, 10% normal goat serum in PBS prior to immunostaining. Details of primary antibodies used are provided in **Supplementary Table S4**. Primary antibodies were detected with appropriate

secondary antibodies labeled with Alexa-Fluor 555 (Thermo Fisher Scientific). Images were acquired using EVOS FL Microscope (Thermo Fisher Scientific).

Generation of *Msh2*$^{-/-}$, *Lig4*$^{-/-}$, and *Pkrdc*$^{-/-}$ mESCs

For each gene to be edited 2 guide RNAs (gRNAs) were used in conjunction with a single-stranded oligonucleotide (ssODN) and CRISPR-Cas9 to generate null lines. The gRNAs and ssODNs are listed in **Supplementary Table S1**. The relevant DNAs encoding the appropriate gRNAs were cloned into a modified pX459 V2.0 [a gift from Feng Zhang (Addgene plasmid # 62988; http://n2t.net/addgene:62988; and RRID:Addgene_62988; (Ran et al., 2013)] with each gRNA expressed under a human U6 promoter and containing a downstream gRNA scaffold. Transfection of a mESC line containing ∼170 repeats was carried out using Lipofectamine® LTX reagent with PLUS™ reagent (15338030, Thermo Fisher Scientific) following the manufacturer's protocol. Control lines were obtained by mock transfections without a gRNA construct. To mitigate potential off-target effects we used multiple independently derived cell lines for these experiments. Three micrograms of the gRNAs/Cas9 expressing plasmids, 1 μg ssODN, and 4 μl PLUS™ reagent were mixed into 250 μl OPTI-MEM (Thermo Fisher Scientific) and incubated for 5 min at room temperature. 12 μl of Lipofectamine LTX reagent was diluted into 240 μl of OPTI-MEM and combined with the DNA:PLUS™ mixture and incubated for 30 min at room temperature. Two hundred thousand mESC cells were suspended in 1 ml N2B27 2i/LIF and mixed with the DNA:PLUS™:Lipofectamine LTX mixture and plated onto a well of a 6-well plate. Cells were incubated with the transfection mix for 4–6 h at 37°C. Transfected cells were collected, pelleted and resuspended in fresh media and plated in a 60 mm dish. 24 h post transfection, cells were selected with puromycin (1 μg/ml) for 24 h, then grown for 4–5 more days. Single colonies were picked and plated in a 24-well plate. DNA was isolated from established clones and analyzed using PCR amplification and sequencing of either the PCR products directly or cloned products. The primers used are listed in **Supplementary Table S2**. The sequences of the relevant alleles in the mutant lines chosen for further analysis are shown in **Supplementary Figure S2**. All mutations involved large deletions. The loss of protein expression in these lines was then verified using western blots of total proteins extracted from these cells using standard procedures (**Supplementary Figure S3**). No significant differences were noted in the growth rates of any of these cell lines. For the evaluation of the effects of the mutations on repeat instability we picked control and mutant cell lines that were match for repeat number. The repeat number of the cell lines is shown in the relevant figures. For all experiments, cells were used at early passage numbers to minimize any potential selection artifacts.

Analysis of Repeat Expansions

Control and mutant cell lines matched for repeat number were grown in culture for the indicated number of days. Cells were passaged every third day by treatment with TrypLE™ Select according to the supplier's instructions, followed by inactivation by growth medium containing 15% ES qualified FBS (Sigma-Aldrich, St. Louis, MO, United States). The cell suspension was replated ∼1:6 into 0.1% gelatin coated wells for further propagation while DNA was made from the remaining cells. DNA isolation was carried out by resuspending cells in lysis buffer (10 mM Tris–HCl pH 7.5, 400 mM NaCl, 100 mM EDTA pH 8.0, and 0.6% SDS) with 0.58 mg/ml proteinase K solution (Thermo Fisher Scientific), and incubating the cell suspension at 55°C overnight before the addition of 1.25 M NaCl. The resultant precipitate was pelleted by centrifugation and equal volume of 100% ethanol was added to supernatant. DNA was pelleted and dissolved in TE. All genotyping PCRs were carried out using KAPA2G Fast HotStart Genotyping Mix (KK5621, KAPA Biosystems, Wilmington, MA, United States) according to the manufacturer's instructions. *Fmr1* PM allele genotyping and repeat number evaluation was performed on bulk DNA using a fluorescent PCR assay with a FAM-labeled FraxM4 and unlabeled FraxM5 primer pair (**Supplementary Table S2**). PCR was carried out using the KAPA2G Fast HotStart Genotyping Mix supplemented with 2.5 M betaine (Sigma-Aldrich), 2% DMSO (americanBIO, Natick, MA, United States), and 0.12 mM dGTP and dCTP (Thermo Scientific), and PCR parameters: 95°C for 10 min, 35 × (95°C for 15 s, 65°C for 15 s, and 72°C for 30 s), 72°C for 10 min. Small pool PCR (SP-PCR) was carried out on diluted DNA using nested PCR. The first round of PCR was carried out using FraxC and FraxF primer pair (**Supplementary Table S2**). PCR was carried out using the KAPA2G Fast HotStart Genotyping Mix supplemented with 2.5 M betaine (Sigma-Aldrich), 2% DMSO, and PCR parameters: 95°C for 10 min, 30 × (95°C for 15 s, 65°C for 15 s, and 72°C for 30 s), 72°C for 10 min. One microliter of this PCR mix was used in second round of PCR with FAM-labeled FraxM4 and FraxM5 primer pair (**Supplementary Table S2**). PCR was carried out using the KAPA2G Fast HotStart Genotyping Mix supplemented with 2.5 M betaine (Sigma-Aldrich, St. Louis, MO, United States), 2% DMSO and 0.12 mM dGTP and dCTP (Thermo scientific, Waltham, MA, United States), and PCR parameters: 95°C for 5 min, 30 × (95°C for 15 s, 65°C for 15 s, and 72°C for 30 s), 72°C for 10 min. Repeat PCR reactions were resolved by capillary electrophoresis on an ABI Genetic Analyzer (Roy J Carver Biotechnology Center, University of Illinois, Urbana, IL, United States). The resultant fsa file was then displayed using a custom R script that is available upon request (Hayward et al., 2016).

RNA Isolation and Quantitative RT–PCR (qRT-PCR)

RNA was isolated from cell lines with 8 repeats wild-type (WT) and from lines with ∼170 repeats (PM) using TRIzol™ reagent, treated with DNase and reverse transcribed with SuperScript IV VILO Master Mix with ezDNase Enzyme (all from Thermo Fisher Scientific). Transcript levels were determined by qPCR

of the resultant cDNA using the TaqMan assays listed in **Supplementary Table S3**. Since an examination of GEO Datasets[1] of RNA-seq data from neurons in *Fmr1* WT and KO mice [(Korb et al., 2017): GSE81803]; [(Ding et al., 2020): GSE114015]; and microarray data comparing gene expression differences in the blood of human carriers of normal and PM alleles [(Mateu-Huertas et al., 2014): GSE48873] showed no significant difference in β-actin levels, β-actin was used for normalization.

DNA-RNA Immunoprecipitation (DRIP) Assay

DNA-RNA immunoprecipitation assays were performed on cells containing either 8 repeats (WT) or ∼170 repeats (PM) as described previously (Kumari and Usdin, 2016) with slight modifications. For each DNA sample, three DRIP assays were performed: a no antibody control and assays with S9.6 antibody either without or with RNAse H pretreatment. A total of 25 μg DNA was either mock digested or digested with 1.7 units of RNAse H (M0297S, New England Biolabs, Ipswich, MA, United States) per 1 μg DNA in 100 μl final volume at 37°C for 6 h. Three hundred microliters of ChIP dilution buffer (167 mM NaCl, 0.01% SDS, 1.1% Triton X-100, 1.2 mM EDTA, and 16.7 mM Tris, pH 8.0) was added to each sample and the samples were then sonicated using the medium setting on the Bioruptor sonication system (Diagenode, Denville, NJ, United States) with cycles of 30 s on/30 s off for 10 min. To 350 μl of the sonicated DNA, 650 μl of ChIP dilution buffer supplemented with protease inhibitor cocktail (P8340-5ML, Sigma-Aldrich) was added and mixed. An aliquot (1%) was saved as input sample. The sonicated DNA was then precleared with 50 μl of Protein A agarose beads/Salmon sperm DNA slurry (16–157, EMD MilliporeSigma) for 1 h on a rotator at 4°C. The precleared supernatant was incubated with or without 5 μg S9.6 antibody (MABE1095, EMD MilliporeSigma) overnight on a rotator at 4°C. The sample was then incubated with 60 μl of the Protein A agarose beads/salmon sperm DNA slurry for 1 h on a rotator at 4°C to collect the immune complexes. The material was washed with low-salt washing buffer (150 mM NaCl, 0.1% SDS, 1% Triton X-100, 2 mM EDTA, and 20 mM Tris–HCl, pH 8.0) followed by high-salt washing buffer (500 mM NaCl, 0.1% SDS, 1% Triton X-100, 2 mM EDTA, and 20 mM Tris–HCl, pH 8.0), LiCl immune complex wash buffer [0.25 M LiCl, 1% IGEPAL CA630, 1% deoxycholic acid (sodium salt), 1 mM EDTA, 10 mM Tris, pH 8.0], and finally washed twice with TE buffer. The immunoprecipitated material was then eluted from the beads using elution buffer (1% SDS and 0.1 M $NaHCO_3$). The input and DRIP samples were treated with phenol/chloroform and precipitated overnight at −20°C with 120 mM sodium acetate and ethanol. After washing with 70% ethanol, the samples were resuspended in 50 μl 0.1X TE, pH 8.0. Real-time PCR was carried out using the PowerUp™ SYBR® Green Master Mix (A25778, Thermo Fisher Scientific) and a StepOnePlus Real-Time PCR system (Thermo Fisher Scientific). β-*actin* was used as a positive control (Skourti-Stathaki et al., 2019). The primer sequences are provided in **Supplementary Table S2**.

[1]https://www.ncbi.nlm.nih.gov/gds

Evaluation of Mitochondrial DNA Copy Number

The relative mitochondrial DNA (mtDNA) copy number was measured in cell lines containing either 8 repeats (WT) or ∼170 repeats (PM) using real-time PCR to determine the levels of a mitochondrial gene, *COXI*, relative to a nuclear gene, *GAPDH*, using the primer pairs shown in **Supplementary Table S2**. The relative mtDNA copy number was calculated using the $2^{-\Delta\Delta Ct}$ method. Primer sequences are provided in **Supplementary Table S2**.

Western Blotting

Cell pellets from cells with either 8 repeats WT or ∼170 repeats PM were collected in RIPA buffer (150 mM NaCl, 1.0% NP-40, 0.5% DOC, 0.1% SDS, 50 mm Tris pH 8.0, and protease inhibitor cocktail) and sonicated at 40% power 5 times 10 s on/10 s off using a Branson 250 Sonifier. Proteins (30–50 μg) were separated on polyacrylamide gels (Thermo Fisher Scientific) and transferred onto nitrocellulose membrane (Bio-Rad Laboratories, Hercules, CA, United States). Primary antibodies used are listed in **Supplementary Table S4**. Images were taken with ChemiDoc imaging system (Bio-Rad Laboratories).

Statistical Analysis

Statistical analysis of the SP-PCR data was carried out using the Mann-Whitney *U* test[2]. Other comparisons were based on Student's *t* test using an unpaired, two-tailed distribution.

RESULTS

mESCs With an Expanded CGG Tract in the *Fmr1* Gene Show a High Frequency of MSH2-Dependent Repeat Expansions *in vitro*

We derived male mESC lines from pre-implantation embryos of $Fmr1^{WT/KI}$ females carrying different numbers of repeats, as described in the section "Materials and Methods." Lines containing 130, 182, and 292 repeats were initially chosen for further study. We included a line with an allele in the FM range since mice with FM sized alleles do not become methylated (Entezam et al., 2007). Thus, the allele with 292 repeats should still be capable of expansion in a permissive cell type. The derived KI mESC lines displayed similar morphology and expressed pluripotency factors at the same levels as WT control lines carrying the normal murine *Fmr1* allele (**Supplementary Figures S1A,B**).

Repeat PCR analysis of the smallest cell line tested, one having 130 repeats, showed an initial PCR profile that had a left-skew, a characteristic we have previously shown to be associated with alleles that do not expand *in vivo* [(**Figure 1A**; Zhao et al., 2019)]. These cell lines show no significant increase in repeat number after 52 days in culture and no change in the skewness of the PCR profile. In contrast, lines with larger

[2]http://vassarstats.net/

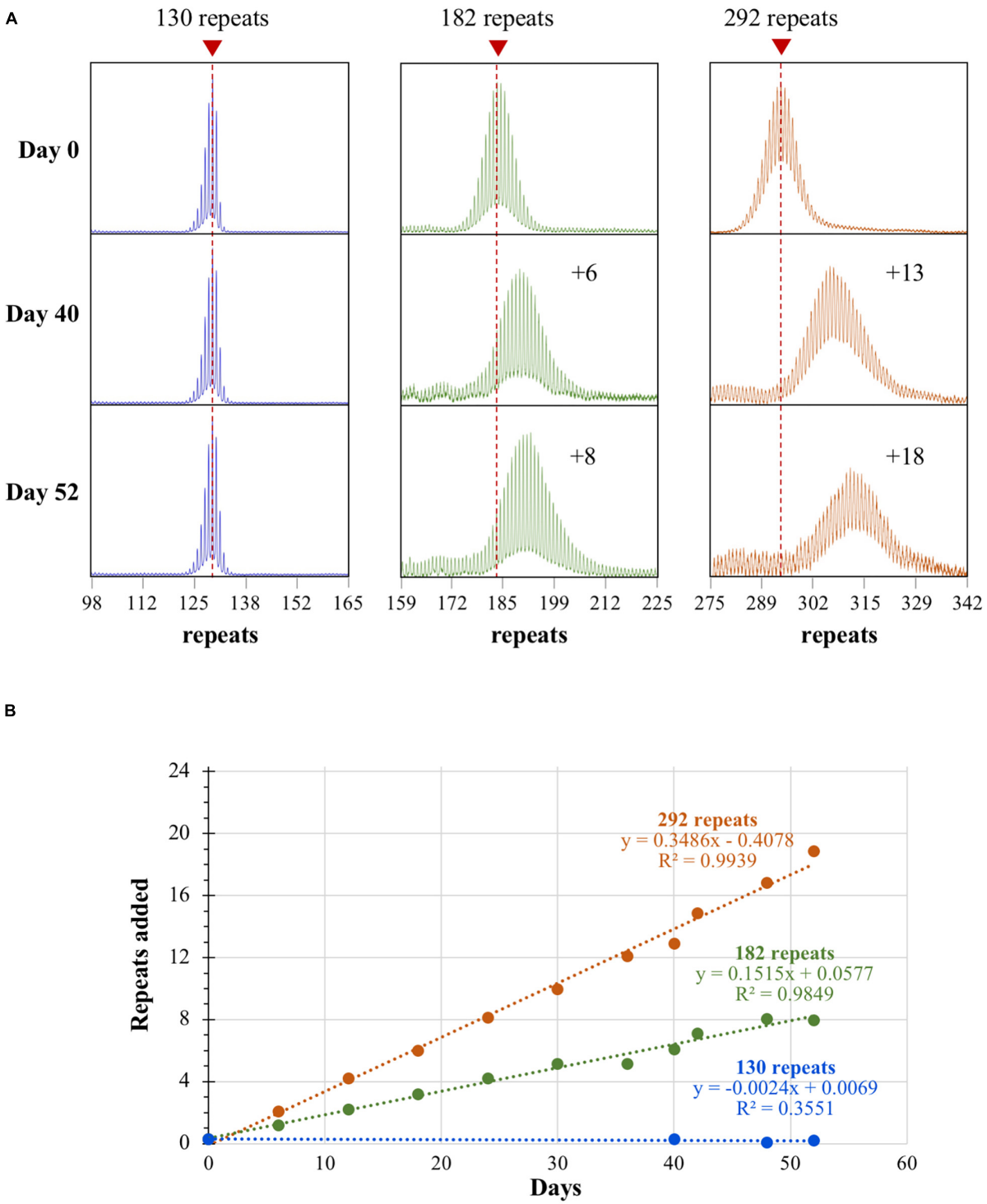

FIGURE 1 | Repeat expansion in mESCs with different numbers of CGG repeats. **(A)** Repeat PCR profiles for cell lines with 130, 182, and 292 repeats after 0, 40, and 52 days in culture. Dashed lines represent the initial allele size at day 0. **(B)** Graph showing the change in repeat number over time for the 3 mESC lines shown in **(A)**.

alleles start off, even at very low passage number, with a more normal allele distribution profile (**Figure 1A**). They also show a steady increase in the average repeat number over time such that the whole population of alleles shifts in an apparently synchronous fashion. The net effect being that the 182 repeat line gains on average 8 repeats over a 52-day period whilst the 292

repeat line gains 18 repeats (**Figure 1A**). Thus, mESCs indeed show frequent, length-dependent expansions. The failure to see expansion in the 130 repeat line is consistent with observations from mice and likely reflects a much slower expansion rate than is seen in the cell lines with larger repeat tracts. The repeat PCR profile for both cell lines containing larger repeat tracts is similar to what is seen in somatic cells from human PM carriers (Zhao et al., 2019) and in iPSCs from individuals with myotonic dystrophy type 1, another RED that shows large, maternally transmitted intergenerational expansions (Du et al., 2013). Computer simulations that are consistent with this sort of expansion profile require a high frequency of expansion events that add only 1–2 repeats with each event (Mollersen et al., 2010). Frequent sampling from the same mESC culture over time that is possible with the mESCs confirms this interpretation. These cells show sequential expansion events, each involving a gain of a single repeat, as can be seen in the line with 182 repeats, with an average of 1 repeat gained every ∼6 days which occurs in the bulk of cells in the population (**Figure 1B**). By way of comparison, a gain of an average of 8 repeats is seen in the brains of 6-month-old mice with a similar repeat number (Zhao and Usdin, unpublished observations). This corresponds to a ∼3.5-fold higher rate of expansion in mESCs. Thus, while most expansions are small, they can be so frequent in certain cell types such as mESCs that large alleles could readily arise over time from the cumulative effect of multiple high frequency expansion events.

Bulk PCR tends to bias the analysis toward the most common alleles. As a result, contractions and expansions that generate unique allele sizes are difficult to discern. In addition, the major peak in the bulk PCR profile represents a mixture of PCR stutter (resulting from strand-slippage during the PCR reaction across the repeats) and true peaks from multiple alleles. SP-PCR performed on single alleles can give a better representation of the true allele distribution. We therefore carried out SP-PCR on an mESC line carrying a mid-size PM allele (175 repeats) at day 0 (representing passage 10 after derivation) and day 24. As can be seen in **Figure 2**, SP-PCR demonstrates a strong shift in the distribution of alleles toward larger sizes at day 24, with the modal repeat number being 8 repeats larger than the modal repeat

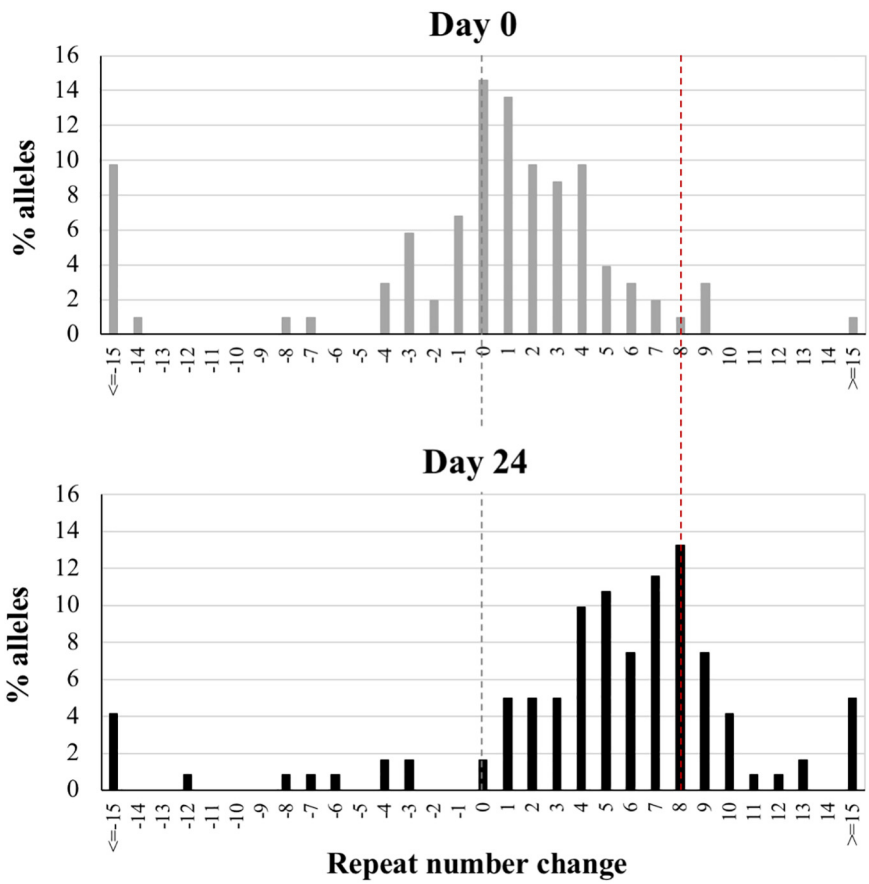

FIGURE 2 | Small pool PCR analysis of PM cell line showing the change in the distribution of alleles with time. Nested PCR on diluted DNA from a cell line carrying 175 repeats was performed at day 0 and day 24. The nested PCR results in a ∼3 repeat decrease in the average PCR product relative to the bulk DNA because of the bias generated by strand-slippage during the PCR reactions. Thus, the distributions were corrected accordingly and the major allele at day 0 was set at 0 with the remaining alleles shown as the change in repeat number relative to this allele. The black dotted line reflects the major allele in the starting population and the red dotted line the major allele in the sample at 24 days. More than 100 alleles were examined for each sample.

number at day 0. This is associated with a significant change in the distribution of allele sizes as assessed by the Mann-Whitney *U* test ($p < 0.0001$). The allele distributions seen in these cells are very similar to the distributions seen in the tissues of mice with a similar number of repeats (Zhao et al., 2016). Thus, both small expansions and large expansions occur in the PM mESCs, with small expansions predominating.

Large contractions are also seen, although at lower frequency. In some cases, cells containing specific contracted alleles tend to become more prominent over time. This likely reflects the difficulty associated with replication of long CGG-repeat tracts (Voineagu et al., 2008) resulting in a selective advantage for cells containing smaller alleles.

MSH2, a DNA mismatch repair protein, is essential for expansions in the FX KI mouse model (Lokanga et al., 2014), and Genome Wide Association (GWA) studies have implicated MSH2-containing complexes in the expansion process in other REDs (Bettencourt et al., 2016; Morales et al., 2016; Moss et al., 2017; Flower et al., 2019). Using CRISPR-Cas9-mediated gene disruption, we generated *Msh2* knockout PM mESC lines (**Supplementary Figures S2A**, **S3A**) and tested them in culture with size matched $Msh2^{+/+}$ mESC lines. As can be seen in **Figure 3**, at day 0 $Msh2^{-/-}$ cells show an allele profile with left-skew characteristic of cells that do not expand [(**Figure 1A** and (Zhao et al., 2019)]. After growth for 24 days, no repeats were added to the PM allele in these cells and no change in the profile skewness was observed. In contrast, $Msh2^{+/+}$ cells show a more normal distribution of allele sizes and show clear evidence of expansion by day 24. This can be visualized clearly by comparing an overlay of the bulk PCR profiles from day 0 and day 24 for each cell line. The $Msh2^{+/+}$ cells show a clear shift in the allele distribution, while the PCR profiles from $Msh2^{-/-}$ cells are indistinguishable (**Figure 3B**). Thus, our data demonstrate that the PM mESC lines show CGG repeat expansion that has an MSH2-dependence and similar dynamics to those observed in mice and humans. This, together with their high expansion frequency, suggest that these PM mESCs are a useful system for studying expansion in the FXDs.

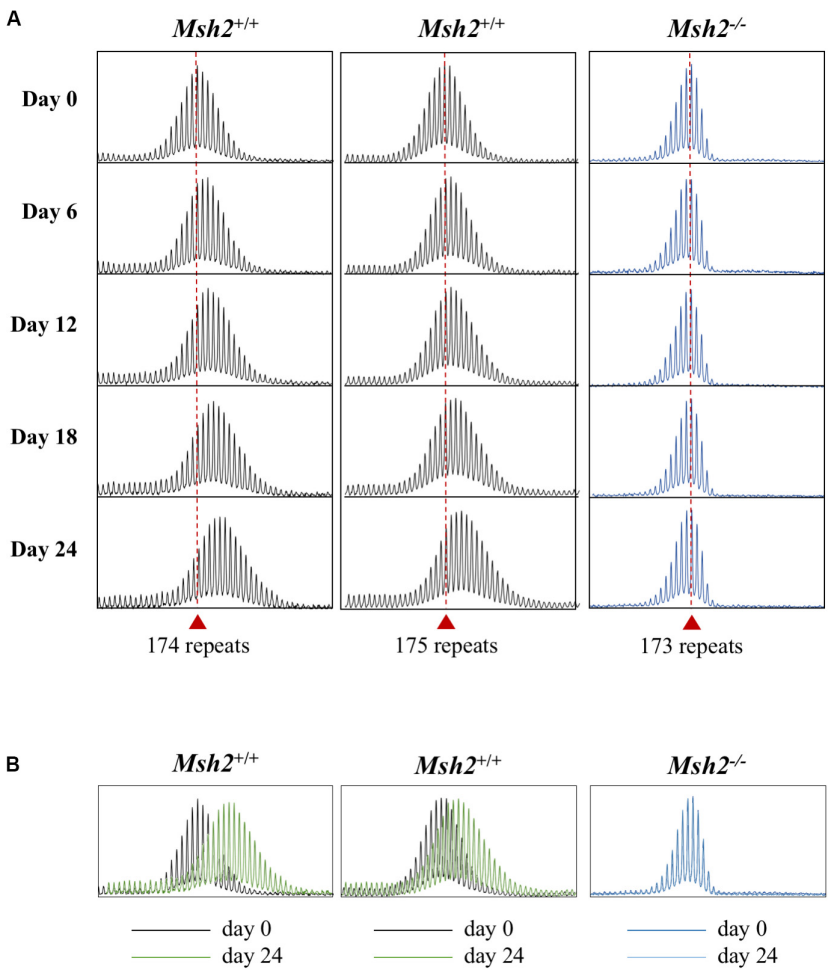

FIGURE 3 | Effect of the loss of MSH2 on repeat expansion in mESCs. **(A)** Representative repeat PCR profiles of the 2 $Msh2^{+/+}$ and 1 $Msh2^{-/-}$ lines with 173–175 repeats grown in culture for the indicated times. Dashed lines represent the initial allele at day 0. At least 2 mESC lines were tested for each genotype with similar results being obtained for each line. **(B)** Overlays of the day 0 and day 24 scans for each of the cell lines.

We had previously shown that in liver LIG4, a DNA ligase essential for non-homologous end-joining (NHEJ), a form of double-strand break repair, protects against expansion (Gazy et al., 2019). We were unable to examine the contribution of LIG4 to embryonic expansion in these animals since the absence of LIG4 results in early embryonic lethality due to defective neurogenesis (Barnes et al., 1998). To investigate the role of NHEJ in embryonic cells we were now able to generate PM mESCs lines deficient for *Lig4* and *Prkdc,* which encodes the catalytic subunit of DNA-PK, another important NHEJ protein (**Supplementary Figures S2B,C**, **S3B**), as these lines are both viable. While loss of LIG4 in mouse livers results in a significant increase in expansions, the loss of LIG4, or DNA-PK resulted in expansions that were indistinguishable from those seen in WT cells (**Figure 4**). This is consistent with the fact that NHEJ is known to be less active in stem cells than in differentiated cells (Tichy et al., 2010). Thus, NHEJ has little, if any, protective effect against repeat expansion in the early embryo and this may account, at least in part, for the large number of expansions seen in these cells.

Fmr1 mRNA Levels Are Elevated in PM mESCs

FMR1 transcription is elevated in cells isolated from PM human carriers (Tassone et al., 2000) and in various tissues isolated from PM mice (Lokanga et al., 2013). To assess whether the same is true for mESCs, we measured *Fmr1* transcript levels in WT and PM mESCs with ∼170 repeats. It should be noted that mouse WT alleles only have 8 repeats, whilst most normal *FMR1* alleles in humans have ∼30 repeats. Whilst data from human studies suggest that alleles of different sizes within the normal range have similar transcript levels (Tassone et al., 2000), it is possible that any differences observed between the behavior of WT and PM alleles in these experiments, as well as those described in subsequent sections, might be larger than that expected in humans. However, we found only a 1.9-fold higher level of *Fmr1* mRNA in the PM lines compared to WT lines (**Figure 5A**). While significant, this difference is smaller than the typical differences seen in tissues of these animals as well as in human PM cells. Since cells in culture are typically grown at atmospheric O_2 levels and the physiological O_2 level in tissues and cells is much lower, between 1–9% depending on the tissue (Mas-Bargues et al., 2019), we tested the transcript levels after growth in 3% O_2. Under those conditions the *Fmr1* mRNA in WT cells increased modestly, while the transcript in PM mESCs showed a larger increase, resulting in transcript levels that were 2.7-fold higher than in WT mESCs (**Figure 5A**). This suggests a heretofore unappreciated role of O_2 tension in the regulation of the PM alleles. Note that neither the levels of the pluripotency markers Nanog, Oct4, Sox2, and Rex1 nor the repeat size were affected by O_2 concentrations (**Supplementary Figure S1**). Despite the elevated level of *Fmr1* mRNA in the PM cells, western blots showed sharply reduced FMRP levels in these cells (**Figure 5B**) comparable to previous observations in mice brain (Entezam et al., 2007) and human cells (Kenneson et al., 2001).

The 5′ End of the Mouse *Fmr1* Gene Also Forms a Stable R-Loop in mESCs

R-loops form on the 5′ end of the human *FMR1* gene where they have been shown to be enriched on expanded alleles compared

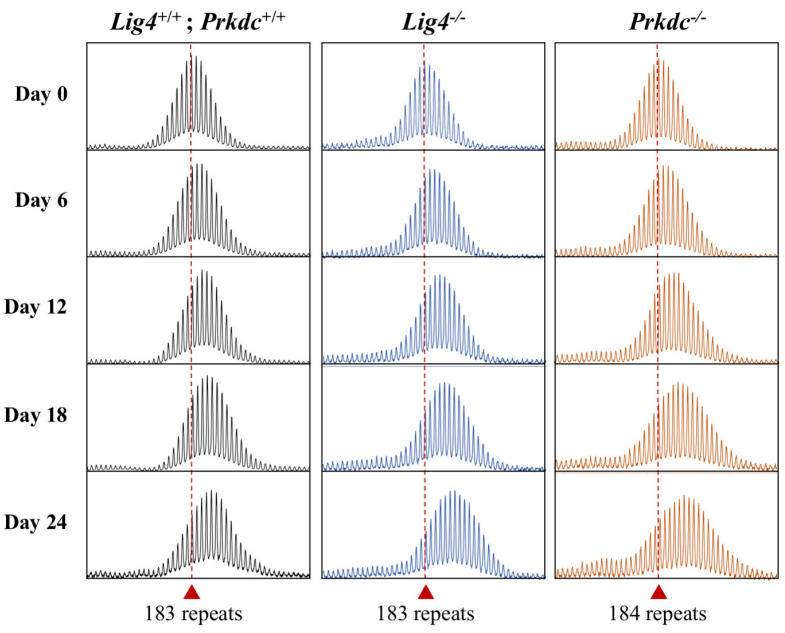

FIGURE 4 | Effect of the loss of NHEJ proteins on repeat expansion in mESCs. Representative repeat PCR profiles of *Lig4*$^{+/+}$; *Prkdc*$^{+/+}$, *Lig4*$^{-/-}$, and *Prkdc*$^{-/-}$ mESCs with 183–184 repeats that were grown in culture for the indicated times. Dashed lines represent the initial repeat size at day 0. At least 2 mESC lines were tested for each genotype with similar results being obtained for each line.

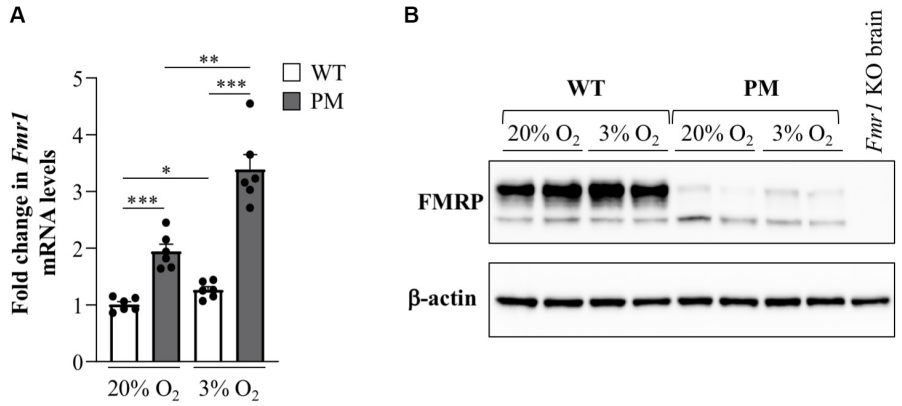

FIGURE 5 | *Fmr1* expression in FX PM mESCs. **(A)** Quantitative reverse-transcription-PCR analysis of *Fmr1* expression in WT and PM lines cultured at 20% or 3% O_2 using β-*actin* for normalization. Values are relative to the average expression of the WT lines cultured at 20% O_2. Results are from 3 mESC lines for each condition and represented as mean ± SEM. $n = 6$; $^*p < 0.01$; $^{**}p < 0.001$; and $^{***}p \leq 0.00001$. **(B)** Western blot analysis of FMRP expression in 2 WT and 2 PM lines cultured at 20% or 3% O_2.

to normal controls (Groh et al., 2014; Loomis et al., 2014; Kumari and Usdin, 2016; Abu Diab et al., 2018). Using DNA:RNA immunoprecipitation (DRIP) with an antibody (S9.6) that recognizes DNA:RNA hybrids (Boguslawski et al., 1986), we tested whether the *Fmr1* transcript also forms an R-loop in mESCs. We found that R-loops indeed form on the mouse *Fmr1* locus in both WT and PM mESCs (**Figure 6**). However, as in humans, R-loop levels in the PM cells were 5- and 2.7-fold higher than in WT in the promoter and exon 1 regions, respectively, (**Figure 6B**). Thus, these cells may be useful for understanding the factors that promote R-loop formation as well as some of its downstream consequences.

The PM mESCs Also Show Elevated Mitochondrial Copy Numbers

We assessed the mtDNA copy number in WT and PM mESCs grown at atmospheric and physiological O_2 concentrations. PM mESCs showed significantly elevated mtDNA copy numbers compared to the WT at both O_2 concentrations (**Figure 7A**). This was associated with a similar increase in expression of transcripts for three mitochondrially encoded genes, *Atp6*, *Cox3,* and *Nd3* (**Figures 7B–D**). Since elevated mtDNA copy number can be a response to increased oxidative stress (Malik and Czajka, 2013), it suggests that the mESCs may also be useful for studying the molecular basis of the mitochondrial changes and oxidative stress seen in PM carriers and PM mouse models (Ross-Inta et al., 2010; Conca Dioguardi et al., 2016; Napoli et al., 2016; Alvarez-Mora et al., 2017; Gohel et al., 2019).

DISCUSSION

Here we report the establishment of FX KI mESC lines that show a high frequency of progressive CGG repeat expansions in tissue culture. These expansions resemble those seen in the blood and saliva of human PM carriers in that all the repeat PCR profiles are consistent with a high frequency of expansions most of which involve the addition of 1–2 repeats [**Figures 1–3** and (Zhao et al., 2019)]. Expansions in the mESCs also show a dependence on MSH2 (**Figure 3**) consistent with data from GWA studies that implicate MMR in the REDs (Bettencourt et al., 2016; Morales et al., 2016; Moss et al., 2017; Flower et al., 2019). The fact that in the 182 and 292 repeat lines expansion occurs in most cells in the population every few days (**Figure 1B**) indicates that the underlying trigger for expansion must be very common. It has been suggested that the repair of 8-oxoguanine generated by oxidative stress is this trigger (Kovtun et al., 2007). However, given that the total number of oxidative hits to DNA is thought to be of the order of 10^4–10^5 per cell per day in mammals (Ames et al., 1993), this would require the CGG-repeat tract in the mouse *Fmr1* locus to be orders of magnitude more prone to oxidative damage than the rest of the genome. Thus, it may be that oxidative damage is not the only trigger for expansions in the FXDs.

While most of the expansions we observe in these cell lines are small, their frequency makes it plausible for the large expansions, characteristic of the intergenerational transmission of FX alleles, to arise over time in the oocyte/embryo by the cumulative effect of these small expansions with or without a contribution from the rarer large expansions that are also seen (**Figure 2**). It is noteworthy that expansions are not seen in FX hESC lines, cells that correspond to a slightly later developmental stage than mESCs (Smith, 2017), nor human iPSC lines (Zhou et al., 2016), although expansions are seen in iPSCs from patients with Friedreich ataxia and Myotonic Dystrophy (Du et al., 2012, 2013). This suggests that very specific conditions are required for expansion at the FX locus that go beyond the simple requirement for genetic factors like MSH2 that are expressed at high levels in both ESCs and iPSCs (Du et al., 2012). Interestingly, the heart is an organ that does not show post-natal expansions in mice; however, the repeat PCR profiles in the heart suggest a very small number of pre-natal expansion events (Zhao et al., 2019). It is thus tempting to speculate that expansions occur in the early blastocyst, cease early on in the developing embryo and resume

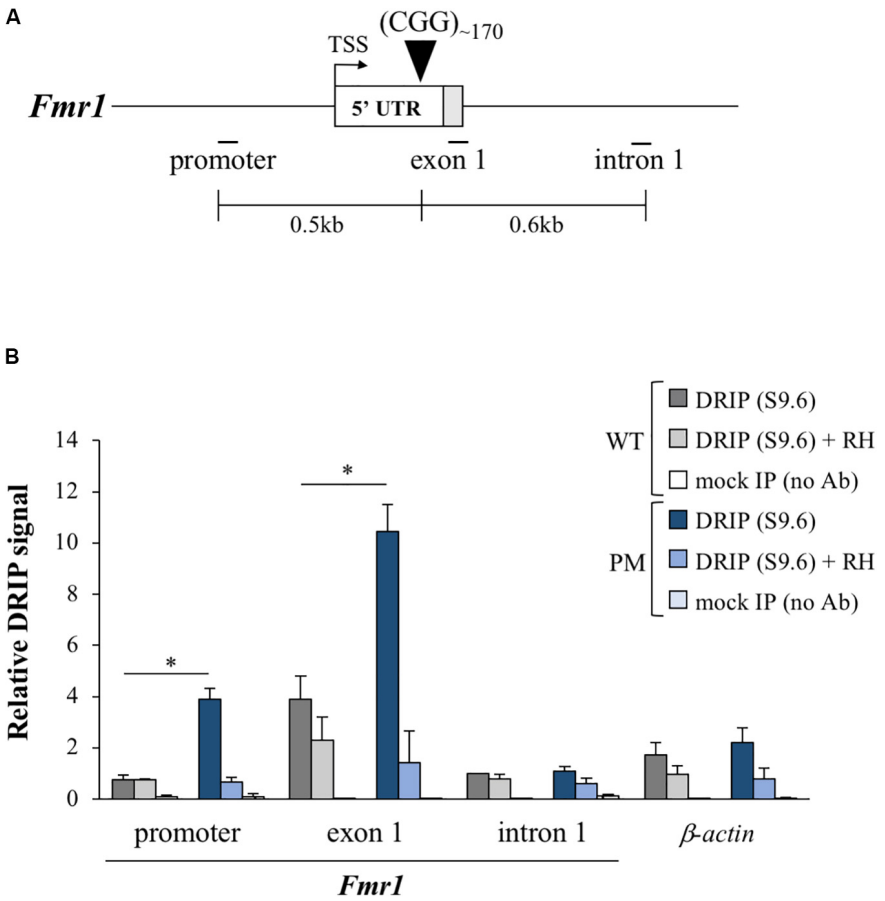

FIGURE 6 | R-loop formation in the FX PM mESCs. **(A)** Diagram of the *Fmr1* gene 5′ region showing the relative positions of the qPCR amplicons used in DNA:RNA immunoprecipitation (DRIP) experiments. White box is exon 1 5′ UTR and gray the coding sequence (CDS). TSS is the transcriptional start site. Numbers indicate the distances from the CGG repeats. **(B)** R-loop enrichment in the *Fmr1* locus and β-actin (positive control gene; Skourti-Stathaki et al., 2019) was determined by DRIP analysis in 3 WT and 3 PM lines cultured at 3% O_2. Pretreatment with RNase H (RH) was used as a control for the pull down. Values are relative to intron 1 in WT cells and displayed as mean ± SEM. *$p < 0.01$.

later in development only in expansion-prone tissues. Given that mESCs can be differentiated into different cell lineages, it should be possible to use these cells to test this hypothesis.

The fact that a significant number of expansions can be seen over weeks or even days in culture, means that these cells can be used to study some aspects of the expansion mechanism much more efficiently than is possible *in vivo*. An added advantage of these cells is that they consist of a single cell type, thus avoiding the problem of multiple cell types with different propensities to expand that is a confounding factor in different organs *in vivo* (Gazy et al., 2019; Zhao et al., 2020). Given the ease of gene editing in these cell lines, genetic factors that contribute to expansion risk can be rapidly identified. Furthermore, the presence of R-loops on the expanded CGG repeat region in the mESCs (**Figure 6**) is consistent with the hypothesis that R-loops play a role in repeat expansion (Schmidt and Pearson, 2016), an observation that can also be readily tested in these cells. However, not all factors that affect the extent of expansion may be apparent in these cells. For example, we show here that while the NHEJ protein LIG4 protects against expansion in mouse hepatocytes (Gazy et al., 2019), loss of LIG4 has little, if any effect in the mESCs. This is consistent with the idea that the extent of expansion that is seen in any particular cell type represents the balance between factors that promote expansion and those factors that protect against them. Thus, while factors that are required for expansion would be seen in all cells that expand including mESCs, factors that play a non-essential role in expansion or protect against expansion may not always be apparent in this cell type.

In addition to exhibiting repeat expansion, the PM mESCs also recapitulate the hyperexpression of the expanded *Fmr1* allele seen in mice and humans (**Figure 5**). Interestingly, we found that hyperexpression in these cells is exacerbated by growth at the low O_2 concentrations that prevail *in vivo*. In this regard, it may be of interest that a number of proteins, including Egr-1 and Purα that bind CGG-DNA repeats (Cao et al., 1993; Weber et al., 2016), increase transcriptional activation of their target genes in response to reduced O_2 tensions (Bae et al., 1999; Kong et al., 2007). We speculate that increased binding of such proteins to the long repeat tracts on PM alleles may contribute to *Fmr1* hyperexpression. In addition, R-loop formation has

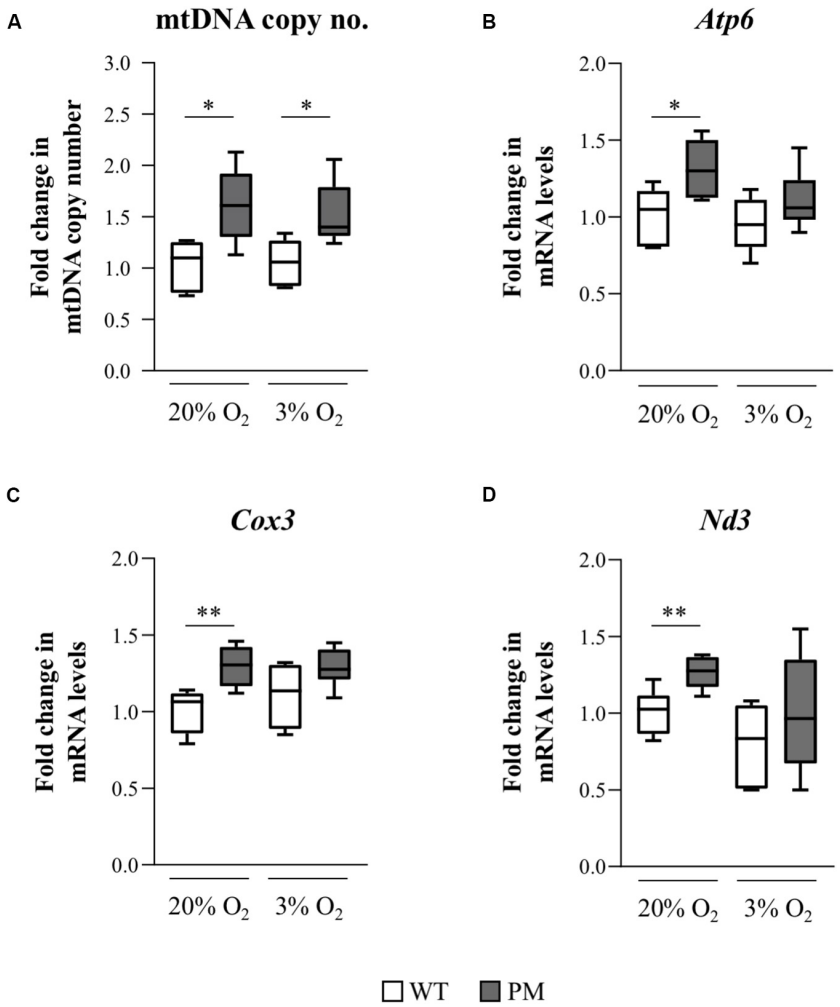

FIGURE 7 | Mitochondrial DNA copy number and mitochondrial gene expression in FX PM mESCs. **(A)** mtDNA copy number was measured using qPCR to determine levels of a mitochondrial gene, *COXI,* relative to a nuclear gene, *GAPDH*, in 3 WT and 3 PM lines cultured at 20% or 3% O_2. Values are relative to the average value of WT cells cultured at 20% O_2 and displayed as mean ± SEM. $n = 5$; $^*p < 0.03$. **(B–D)** Quantitative reverse-transcription-PCR analysis for the expression of the mitochondrial-encoded genes *Atp6* **(B)**, *Cox3* **(C)**, and *Nd3* **(D)** in 3 WT and 3 PM lines cultured at 20% or 3% O_2 using β-actin for normalization. Values are relative to the average expression of the WT lines cultured at 20% O_2 and shown as mean ± SEM. $n = 6$; $^*p < 0.02$; and $^{**}p \leq 0.006$.

been suggested to promote gene expression by recruitment of activating chromatin modifiers. Thus, the mESC model may provide a simple system for testing these hypotheses.

In addition to the increase in *Fmr1* transcript levels and decrease in FMRP protein levels, an increase in mtDNA copy number and elevated transcripts from mitochondrially encoded genes was also observed (**Figure 7**). Mitochondrial dysfunction is thought to contribute to the pathology seen in human PM carriers where both increases and decreases in mtDNA copy number and mitochondrial activity have been reported (Ross-Inta et al., 2010; Napoli et al., 2016; Song et al., 2016; Loesch et al., 2017; Alvarez-Mora et al., 2019). The occurrence of both increased and decreased mtDNA copy numbers are not necessarily inconsistent. While an initial increase in mtDNA copy number is thought to reflect an adaptive response to mitochondrial dysfunction and the associated increased cellular stress (Lee et al., 2000; Malik and Czajka, 2013), over time the increased mtDNA copy number exacerbates chronic oxidative stress and mitochondrial damage and results ultimately in a reduction in the number of mitochondria (Lee et al., 2000; Malik and Czajka, 2013). Interestingly, in another RED, Huntington disease, a neurodegenerative condition that is associated with oxidative stress, a biphasic pattern of mtDNA copy number variation is seen, with increased copy numbers being seen prior to disease onset and decreased copy numbers thereafter (Petersen et al., 2014). Thus, the PM mESCs might represent early stages of response to cellular damage, preceding the decline in mtDNA copy number observed in some human PM brains (Alvarez-Mora et al., 2019). It is noteworthy that mitochondrial abnormalities are also seen in *Fmr1* knockout mice which do not express FMRP (D'Antoni et al., 2019; Shen et al., 2019). Hence, it remains

to be seen whether the mitochondrial changes we observe are related to the expression of the PM allele, the deficiency of FMRP (**Figure 5**), or a combination of the two.

Current models for repeat-induced pathology in PM carriers include repeat-mediated sequestration of important CGG-binding proteins and toxic protein production by repeat-associated non-AUG (RAN) translation (Glineburg et al., 2018). Since these mESCs contain the endogenous murine stop codon situated immediately upstream of the repeats in exon 1 of the *Fmr1* gene, they do not produce high levels of FMRPolyG, the major product of RAN translation seen in humans (Todd et al., 2013). Thus, the mESCs we have derived can serve as a useful *in vitro* model system not only for modeling repeat expansion but also for studying the cellular abnormalities associated with the PM that may be independent of FMRPolyG.

DATA AVAILABILITY STATEMENT

All datasets generated for this study are included in the article/**Supplementary Material**.

ETHICS STATEMENT

The animal study was reviewed and approved by NIDDK Animal Care and Use Committee.

AUTHOR CONTRIBUTIONS

IG and KU conceived the original idea and planned the experiments. IG, CM, and G-YK carried out the experiments. IG and KU wrote the manuscript with support from CM and G-YK. All authors contributed to the article and approved the submitted version.

FUNDING

The work described in this manuscript was funded by a grant from the Intramural Program of the NIDDK to KU (DK057808).

ACKNOWLEDGMENTS

We would like to acknowledge all the hard work done by the staff who takes care of our mice and without whom this work would not have been possible. Thank you also to all the Usdin lab members for ideas and support.

SUPPLEMENTARY MATERIAL

The Supplementary Material for this article can be found online at: https://www.frontiersin.org/articles/10.3389/fcell.2020.00482/full#supplementary-material

REFERENCES

Abu Diab, M., Mor-Shaked, H., Cohen, E., Cohen-Hadad, Y., Ram, O., Epsztejn-Litman, S., et al. (2018). The G-rich repeats in FMR1 and C9orf72 loci are hotspots for local unpairing of DNA. *Genetics* 210, 1239–1252. doi: 10.1534/genetics.118.301672

Alvarez-Mora, M. I., Podlesniy, P., Gelpi, E., Hukema, R., Madrigal, I., Pagonabarraga, J., et al. (2019). Fragile X-associated tremor/ataxia syndrome: regional decrease of mitochondrial DNA copy number relates to clinical manifestations. *Genes Brain Behav.* 18:e12565. doi: 10.1111/gbb.12565

Alvarez-Mora, M. I., Rodriguez-Revenga, L., Madrigal, I., Guitart-Mampel, M., Garrabou, G., and Mila, M. (2017). Impaired mitochondrial function and dynamics in the pathogenesis of FXTAS. *Mol. Neurobiol.* 54, 6896–6902. doi: 10.1007/s12035-016-0194-7

Ames, B. N., Shigenaga, M. K., and Hagen, T. M. (1993). Oxidants, antioxidants, and the degenerative diseases of aging. *Proc. Natl. Acad. Sci. U.S.A.* 90, 7915–7922. doi: 10.1073/pnas.90.17.7915

Bae, S. K., Bae, M. H., Ahn, M. Y., Son, M. J., Lee, Y. M., Bae, M. K., et al. (1999). Egr-1 mediates transcriptional activation of IGF-II gene in response to hypoxia. *Cancer Res.* 59, 5989–5994.

Barnes, D. E., Stamp, G., Rosewell, I., Denzel, A., and Lindahl, T. (1998). Targeted disruption of the gene encoding DNA ligase IV leads to lethality in embryonic mice. *Curr. Biol.* 8, 1395–1398. doi: 10.1016/s0960-9822(98)00021-9

Bettencourt, C., Hensman-Moss, D., Flower, M., Wiethoff, S., Brice, A., Goizet, C., et al. (2016). DNA repair pathways underlie a common genetic mechanism modulating onset in polyglutamine diseases. *Ann. Neurol.* 79, 983–990. doi: 10.1002/ana.24656

Boguslawski, S. J., Smith, D. E., Michalak, M. A., Mickelson, K. E., Yehle, C. O., Patterson, W. L., et al. (1986). Characterization of monoclonal antibody to DNA.RNA and its application to immunodetection of hybrids. *J. Immunol. Methods* 89, 123–130. doi: 10.1016/0022-1759(86)90040-2

Brykczynska, U., Pecho-Vrieseling, E., Thiemeyer, A., Klein, J., Fruh, I., Doll, T., et al. (2016). CGG repeat-induced FMR1 silencing depends on the expansion size in human iPSCs and neurons carrying unmethylated full mutations. *Stem Cell Rep.* 7, 1059–1071. doi: 10.1016/j.stemcr.2016.10.004

Cannella, M., Maglione, V., Martino, T., Ragona, G., Frati, L., Li, G. M., et al. (2009). DNA instability in replicating Huntington's disease lymphoblasts. *BMC Med. Genet.* 10:11. doi: 10.1186/1471-2350-10-11

Cao, X., Mahendran, R., Guy, G. R., and Tan, Y. H. (1993). Detection and characterization of cellular EGR-1 binding to its recognition site. *J. Biol. Chem.* 268, 16949–16957.

Conca Dioguardi, C., Uslu, B., Haynes, M., Kurus, M., Gul, M., Miao, D. Q., et al. (2016). Granulosa cell and oocyte mitochondrial abnormalities in a mouse model of fragile X primary ovarian insufficiency. *Mol. Hum. Reprod.* 22, 384–396. doi: 10.1093/molehr/gaw023

Crawford, D. C., Acuna, J. M., and Sherman, S. L. (2001). FMR1 and the fragile X syndrome: human genome epidemiology review. *Genet. Med.* 3, 359–371. doi: 10.1097/00125817-200109000-00006

D'Antoni, S., De Bari, L., Valenti, D., Borro, M., Bonaccorso, C. M., Simmaco, M., et al. (2019). Aberrant mitochondrial bioenergetics in the cerebral cortex of the Fmr1 knockout mouse model of fragile X syndrome. *Biol. Chem.* 401, 497–503. doi: 10.1515/hsz-2019-0221

Ding, Q., Sethna, F., Wu, X. T., Miao, Z., Chen, P., Zhang, Y., et al. (2020). Transcriptome signature analysis repurposes trifluoperazine for the treatment of fragile X syndrome in mouse model. *Commun. Biol.* 3:127.

Du, J., Campau, E., Soragni, E., Jespersen, C., and Gottesfeld, J. M. (2013). Length-dependent CTG.CAG triplet-repeat expansion in myotonic dystrophy patient-derived induced pluripotent stem cells. *Hum. Mol. Genet.* 22, 5276–5287. doi: 10.1093/hmg/ddt386

Du, J., Campau, E., Soragni, E., Ku, S., Puckett, J. W., Dervan, P. B., et al. (2012). Role of mismatch repair enzymes in GAA.TTC triplet-repeat expansion in Friedreich ataxia induced pluripotent stem cells. *J. Biol. Chem.* 287, 29861–29872. doi: 10.1074/jbc.m112.391961

Entezam, A., Biacsi, R., Orrison, B., Saha, T., Hoffman, G. E., Grabczyk, E., et al. (2007). Regional FMRP deficits and large repeat expansions into the full mutation range in a new Fragile X premutation mouse model. *Gene* 395, 125–134. doi: 10.1016/j.gene.2007.02.026

Flower, M., Lomeikaite, V., Ciosi, M., Cumming, S., Morales, F., Lo, K., et al. (2019). MSH3 modifies somatic instability and disease severity in Huntington's and myotonic dystrophy type 1. *Brain* 142, 1876–1886.

Gazy, I., Hayward, B., Potapova, S., Zhao, X., and Usdin, K. (2019). Double-strand break repair plays a role in repeat instability in a fragile X mouse model. *DNA Repair* 74, 63–69. doi: 10.1016/j.dnarep.2018.12.004

Glineburg, M. R., Todd, P. K., Charlet-Berguerand, N., and Sellier, C. (2018). Repeat-associated non-AUG (RAN) translation and other molecular mechanisms in Fragile X Tremor Ataxia Syndrome. *Brain Res.* 1693, 43–54. doi: 10.1016/j.brainres.2018.02.006

Gohel, D., Sripada, L., Prajapati, P., Singh, K., Roy, M., Kotadia, D., et al. (2019). FMRpolyG alters mitochondrial transcripts level and respiratory chain complex assembly in Fragile X associated tremor/ataxia syndrome [FXTAS]. *Biochim. Biophys. Acta Mol. Basis Dis.* 1865, 1379–1388. doi: 10.1016/j.bbadis.2019.02.010

Groh, M., Lufino, M. M., Wade-Martins, R., and Gromak, N. (2014). R-loops associated with triplet repeat expansions promote gene silencing in Friedreich ataxia and fragile X syndrome. *PLoS Genet.* 10:e1004318. doi: 10.1371/journal.pgen.1004318

Hayward, B. E., Zhou, Y., Kumari, D., and Usdin, K. (2016). A set of assays for the comprehensive analysis of FMR1 alleles in the fragile X-related disorders. *J. Mol. Diagn.* 18, 762–774. doi: 10.1016/j.jmoldx.2016.06.001

Kenneson, A., Zhang, F., Hagedorn, C. H., and Warren, S. T. (2001). Reduced FMRP and increased FMR1 transcription is proportionally associated with CGG repeat number in intermediate-length and premutation carriers. *Hum. Mol. Genet.* 10, 1449–1454. doi: 10.1093/hmg/10.14.1449

Kong, T., Scully, M., Shelley, C. S., and Colgan, S. P. (2007). Identification of Pur alpha as a new hypoxia response factor responsible for coordinated induction of the beta 2 integrin family. *J. Immunol.* 179, 1934–1941. doi: 10.4049/jimmunol.179.3.1934

Korb, E., Herre, M., Zucker-Scharff, I., Gresack, J., Allis, C. D., and Darnell, R. B. (2017). Excess translation of epigenetic regulators contributes to fragile X syndrome and is alleviated by Brd4 inhibition. *Cell* 170, 1209–1223.e20. doi: 10.1016/j.cell.2017.07.033

Kovtun, I. V., Liu, Y., Bjoras, M., Klungland, A., Wilson, S. H., and Mcmurray, C. T. (2007). OGG1 initiates age-dependent CAG trinucleotide expansion in somatic cells. *Nature* 447, 447–452. doi: 10.1038/nature05778

Kumari, D., and Usdin, K. (2016). Sustained expression of FMR1 mRNA from reactivated fragile X syndrome alleles after treatment with small molecules that prevent trimethylation of H3K27. *Hum. Mol. Genet.* 25, 3689–3698. doi: 10.1093/hmg/ddw215

Lee, H. C., Yin, P. H., Lu, C. Y., Chi, C. W., and Wei, Y. H. (2000). Increase of mitochondria and mitochondrial DNA in response to oxidative stress in human cells. *Biochem. J.* 348(Pt 2), 425–432. doi: 10.1042/bj3480425

Loesch, D. Z., Annesley, S. J., Trost, N., Bui, M. Q., Lay, S. T., Storey, E., et al. (2017). Novel blood biomarkers are associated with white matter lesions in fragile X- associated tremor/ataxia syndrome. *Neurodegener. Dis.* 17, 22–30. doi: 10.1159/000446803

Lokanga, R. A., Entezam, A., Kumari, D., Yudkin, D., Qin, M., Smith, C. B., et al. (2013). Somatic expansion in mouse and human carriers of fragile X premutation alleles. *Hum. Mutat.* 34, 157–166. doi: 10.1002/humu.22177

Lokanga, R. A., Zhao, X. N., and Usdin, K. (2014). The mismatch repair protein MSH2 is rate limiting for repeat expansion in a fragile X premutation mouse model. *Hum. Mutat.* 35, 129–136. doi: 10.1002/humu.22464

Loomis, E. W., Sanz, L. A., Chedin, F., and Hagerman, P. J. (2014). Transcription-associated R-loop formation across the human FMR1 CGG-repeat region. *PLoS Genet.* 10:e1004294. doi: 10.1371/journal.pgen.1004294

Malik, A. N., and Czajka, A. (2013). Is mitochondrial DNA content a potential biomarker of mitochondrial dysfunction? *Mitochondrion* 13, 481–492. doi: 10.1016/j.mito.2012.10.011

Mas-Bargues, C., Sanz-Ros, J., Roman-Dominguez, A., Ingles, M., Gimeno-Mallench, L., El Alami, M., et al. (2019). Relevance of oxygen concentration in stem cell culture for regenerative medicine. *Int. J. Mol. Sci.* 20:1195. doi: 10.3390/ijms20051195

Mateu-Huertas, E., Rodriguez-Revenga, L., Alvarez-Mora, M. I., Madrigal, I., Willemsen, R., Mila, M., et al. (2014). Blood expression profiles of fragile X premutation carriers identify candidate genes involved in neurodegenerative and infertility phenotypes. *Neurobiol. Dis.* 65, 43–54. doi: 10.1016/j.nbd.2013.12.020

Mila, M., Alvarez-Mora, M. I., Madrigal, I., and Rodriguez-Revenga, L. (2018). Fragile X syndrome: an overview and update of the FMR1 gene. *Clin. Genet.* 93, 197–205. doi: 10.1111/cge.13075

Mollersen, L., Rowe, A. D., Larsen, E., Rognes, T., and Klungland, A. (2010). Continuous and periodic expansion of CAG repeats in Huntington's disease R6/1 mice. *PLoS Genet.* 6:e1001242. doi: 10.1371/journal.pgen.1001242

Morales, F., Vasquez, M., Santamaria, C., Cuenca, P., Corrales, E., and Monckton, D. G. (2016). A polymorphism in the *MSH3* mismatch repair gene is associated with the levels of somatic instability of the expanded CTG repeat in the blood DNA of myotonic dystrophy type 1 patients. *DNA Repair* 40, 57–66. doi: 10.1016/j.dnarep.2016.01.001

Moss, D. J. H., Pardinas, A. F., Langbehn, D., Lo, K., Leavitt, B. R., Roos, R., et al. (2017). Identification of genetic variants associated with Huntington's disease progression: a genome-wide association study. *Lancet Neurol.* 16, 701–711.

Napoli, E., Song, G., Wong, S., Hagerman, R., and Giulivi, C. (2016). Altered bioenergetics in primary dermal fibroblasts from adult carriers of the FMR1 premutation before the onset of the neurodegenerative disease fragile X-associated tremor/ataxia syndrome. *Cerebellum* 15, 552–564. doi: 10.1007/s12311-016-0779-8

Nichols, J., and Ying, Q. L. (2006). Derivation and propagation of embryonic stem cells in serum- and feeder-free culture. *Methods Mol. Biol.* 329, 91–98. doi: 10.1385/1-59745-037-5:91

Petersen, M. H., Budtz-Jorgensen, E., Sorensen, S. A., Nielsen, J. E., Hjermind, L. E., Vinther-Jensen, T., et al. (2014). Reduction in mitochondrial DNA copy number in peripheral leukocytes after onset of Huntington's disease. *Mitochondrion* 17, 14–21. doi: 10.1016/j.mito.2014.05.001

Ran, F. A., Hsu, P. D., Wright, J., Agarwala, V., Scott, D. A., and Zhang, F. (2013). Genome engineering using the CRISPR-Cas9 system. *Nat. Protoc.* 8, 2281–2308.

Renoux, A. J., and Todd, P. K. (2012). Neurodegeneration the RNA way. *Prog. Neurobiol.* 97, 173–189. doi: 10.1016/j.pneurobio.2011.10.006

Ross-Inta, C., Omanska-Klusek, A., Wong, S., Barrow, C., Garcia-Arocena, D., Iwahashi, C., et al. (2010). Evidence of mitochondrial dysfunction in fragile X-associated tremor/ataxia syndrome. *Biochem. J.* 429, 545–552.

Schmidt, M. H. M., and Pearson, C. E. (2016). Disease-associated repeat instability and mismatch repair. *DNA Repair* 38, 117–126. doi: 10.1016/j.dnarep.2015.11.008

Shen, M., Wang, F., Li, M., Sah, N., Stockton, M. E., Tidei, J. J., et al. (2019). Reduced mitochondrial fusion and Huntingtin levels contribute to impaired dendritic maturation and behavioral deficits in Fmr1-mutant mice. *Nat. Neurosci.* 22, 386–400. doi: 10.1038/s41593-019-0338-y

Skourti-Stathaki, K., Torlai Triglia, E., Warburton, M., Voigt, P., Bird, A., and Pombo, A. (2019). R-loops enhance polycomb repression at a subset of developmental regulator genes. *Mol. Cell* 73, 930–945.

Smith, A. (2017). Formative pluripotency: the executive phase in a developmental continuum. *Development* 144, 365–373. doi: 10.1242/dev.142679

Song, G., Napoli, E., Wong, S., Hagerman, R., Liu, S., Tassone, F., et al. (2016). Altered redox mitochondrial biology in the neurodegenerative disorder fragile X-tremor/ataxia syndrome: use of antioxidants in precision medicine. *Mol. Med.* 22, 548–559. doi: 10.2119/molmed.2016.00122

Tassone, F., Hagerman, R. J., Taylor, A. K., Gane, L. W., Godfrey, T. E., and Hagerman, P. J. (2000). Elevated levels of *FMR1* mRNA in carrier males: a new mechanism of involvement in the fragile-X syndrome. *Am. J. Hum. Genet.* 66, 6–15. doi: 10.1086/302720

Tichy, E. D., Pillai, R., Deng, L., Liang, L., Tischfield, J., Schwemberger, S. J., et al. (2010). Mouse embryonic stem cells, but not somatic cells, predominantly use homologous recombination to repair double-strand DNA breaks. *Stem Cells Dev.* 19, 1699–1711. doi: 10.1089/scd.2010.0058

Todd, P. K., Oh, S. Y., Krans, A., He, F., Sellier, C., Frazer, M., et al. (2013). CGG repeat-associated translation mediates neurodegeneration in fragile X tremor ataxia syndrome. *Neuron* 78, 440–455. doi: 10.1016/j.neuron.2013.03.026

Voineagu, I., Narayanan, V., Lobachev, K. S., and Mirkin, S. M. (2008). Replication stalling at unstable inverted repeats: interplay between DNA hairpins and fork stabilizing proteins. *Proc. Natl. Acad. Sci. U S A* 105, 9936–9941. doi: 10.1073/pnas.0804510105

Weber, J., Bao, H., Hartlmuller, C., Wang, Z., Windhager, A., Janowski, R., et al. (2016). Structural basis of nucleic-acid recognition and double-strand unwinding by the essential neuronal protein Pur-alpha. *eLife* 5:e11297.

Ying, Q. L., Wray, J., Nichols, J., Batlle-Morera, L., Doble, B., Woodgett, J., et al. (2008). The ground state of embryonic stem cell self-renewal. *Nature* 453, 519–523. doi: 10.1038/nature06968

Zhao, X., Gazy, I., Hayward, B., Pintado, E., Hwang, Y. H., Tassone, F., et al. (2019). Repeat instability in the fragile X-related disorders: lessons from a mouse model. *Brain Sci.* 9:E52.

Zhao, X., Lu, H., Dagur, P. K., and Usdin, K. (2020). Isolation and analysis of the CGG-repeat size in male and female gametes from a fragile X mouse model. *Methods Mol. Biol.* 2056, 173–186. doi: 10.1007/978-1-4939-9784-8_11

Zhao, X. N., Lokanga, R., Allette, K., Gazy, I., Wu, D., and Usdin, K. (2016). A MutSbeta-dependent contribution of mutsalpha to repeat expansions in fragile X premutation mice? *PLoS Genet.* 12:e1006190. doi: 10.1371/journal.pgen.1006190

Zhao, X. N., and Usdin, K. (2018). Timing of expansion of fragile X premutation alleles during intergenerational transmission in a mouse model of the fragile X-related disorders. *Front. Genet.* 9:314. doi: 10.3389/fgene.2018.00314

Zhou, Y., Kumari, D., Sciascia, N., and Usdin, K. (2016). CGG-repeat dynamics and *FMR1* gene silencing in fragile X syndrome stem cells and stem cell-derived neurons. *Mol. Autism* 7:42.

Conflict of Interest: The authors declare that the research was conducted in the absence of any commercial or financial relationships that could be construed as a potential conflict of interest.

frontiers in Molecular Biosciences

BRIEF RESEARCH REPORT
published: 14 July 2020
doi: 10.3389/fmolb.2020.00135

Effect of AGG Interruptions on *FMR1* Maternal Transmissions

Olatz Villate[1,2,3]*, *Nekane Ibarluzea*[1,3], *Hiart Maortua*[2,3], *Ana Belén de la Hoz*[1,3], *Laia Rodriguez-Revenga*[3,4,5], *Silvia Izquierdo-Álvarez*[6] *and María Isabel Tejada*[1,2,3]*

[1] Biocruces Bizkaia Health Research Institute, Barakaldo, Spain, [2] Genetics Service, Cruces University Hospital, Osakidetza Basque Health Service, Barakaldo, Spain, [3] Centre for Biomedical Research on Rare Diseases (CIBERER), ISCIII, Madrid, Spain, [4] Biochemistry and Molecular Genetics Department, Hospital Clinic, Barcelona, Spain, [5] Institut d'Investigació Biomèdica August Pi i Sunyer IDIBAPS, Barcelona, Spain, [6] Genetics Department of Clinical Biochemistry, Hospital Universitario Miguel Servet, Zaragoza, Spain

There are four classes of CGG repeat alleles in the *FMR1* gene: normal alleles have up to 44 repeats; patients with Fragile X Syndrome have more than 200 repeats; those between 55 and 200 CGGs are considered *FMR1* premutation alleles, because they are associated with maternal expansions of the number of CGGs in the next generation and finally, alleles between 45 and 54 CGGs are called intermediate or gray zone alleles. In these last categories, the stability depends on the presence of AGG interruptions, which usually occurs between 9 and 10 CGGs. In this context, we have studied retrospectively 66 women with CGG repeats between 45 and 65, and their offspring. In total 87 transmissions were analyzed with triplet repeat primed PCR using AmplideX® FMR1 PCR (Asuragen, Austin, TX, USA) and we found that alleles with CGG repeats between 45 and 58 do not expand in the next generation except two cases with 56 repeats and 0 AGG interruptions. Furthermore, we have found four females with alleles with more than 59 CGG repeats and 2 AGG interruptions that do not expand either. Alleles from 56 CGG repeats without AGGs expand in all cases. In light of these results and those of the literature, we consider that the risk of unstable transmissions should be based on the presence or absence of AGG interruptions and not on the classical cutoffs which define each category of *FMR1* alleles. The application of these results in the genetic and reproductive counseling is essential and AGG interruptions should always be studied.

Keywords: *FMR1* gene, fragile X syndrome, CGG repeats, AGG interruptions, premutation, genetic counseling

OPEN ACCESS

Edited by:
Giorgio Malpeli,
University of Verona, Italy

Reviewed by:
Marsha Mailick,
University of Wisconsin-Madison, United States
Shai E. Elizur,
Sheba Medical Center, Israel

***Correspondence:**
Olatz Villate
olatz.villatebejarano@osakidetza.eus
María Isabel Tejada
mariaisabel.tejadaminguez@osakidetza.eus

Specialty section:
This article was submitted to Cellular Biochemistry, a section of the journal Frontiers in Molecular Biosciences

Received: *28 April 2020*
Accepted: *05 June 2020*
Published: *14 July 2020*

Citation:
Villate O, Ibarluzea N, Maortua H, de la Hoz AB, Rodriguez-Revenga L, Izquierdo-Álvarez S and Tejada MI (2020) Effect of AGG Interruptions on FMR1 Maternal Transmissions. Front. Mol. Biosci. 7:135. doi: 10.3389/fmolb.2020.00135

INTRODUCTION

The *FMR1* gene is the gene responsible for Fragile X Syndrome (FXS) affecting ∼1/3,717 to 1/8,918 Caucasian males (Crawford et al., 2001). FXS occurs when FMR1 is silenced by methylation or inactivation due to an abnormal expansion of a CGG trinucleotide (>200 repeats and called Full mutation, FM), located in the untranslated sequence at 5′, before the *FMR1* gene's first exon (Oberle et al., 1991; Verkerk et al., 1991; Yu et al., 1991).

It has been established that the normal CGG repeat number is below 45 and alleles in this repeat range are transmitted stably from generation to generation. Those alleles carrying between 45 and 200 CGG repeats are premutation (55–200 repeats, PM) or intermediate alleles (45–54 CGGs, IAs). The American College of Medical Genetics (ACMG) guidelines for defining these ranges are currently followed (Maddalena et al., 2001).

The term PM has been used since the discovery of the *FMR1* gene (Oberle et al., 1991) to reflect the fact that PM carriers do not generally have intellectual disability (ID) but their alleles are usually unstable, resulting in an expansion of the CGG repeats when transmitted by a female. It has been demonstrated that the risk of expansion is related to the number of CGG repeats, with smaller alleles being less likely to expand to a full mutation than larger ones (Rousseau et al., 1994; Nolin et al., 2003; Berkenstadt et al., 2007; Strom et al., 2007; Tejada et al., 2014) that is, the instability of PM alleles increases with the size of alleles. The smallest PM that has been reported to expand to a FM allele in one generation is 56 CGGs (Fernandez-Carvajal et al., 2009), later registered in our published cohort (Tejada et al., 2014).

The number of women carrying PM alleles is really high: it seems that as many as 1/130–260 females are carriers of a PM (Hagerman, 2008). In addition, these women could be at risk of developing several disorders associated with being a PM carrier: fragile X-associated premature ovarian insufficiency (FXPOI) (Sullivan et al., 2011), fragile X-associated tremor/ataxia syndrome (FXTAS) (Jacquemont et al., 2003), and the recently described fragile X-associated neuropsychiatric disorders (FXAND) (Hagerman et al., 2018). It has been estimated that about 13–26% of PM carriers women develop FXPOI (Wittenberger et al., 2007) and that up to 13% of women with PM could have FXTAS (Adams et al., 2007). In Spanish women with PM, we found similar frequencies to that previously reported for FXPOI (22.61%) (Merino et al., 2016), and also for FXTAS with frequencies from 3.27% (Merino et al., 2016) up to 16% (Rodriguez-Revenga et al., 2009).

There is also another range, that of the IAs or gray zone alleles (45–54 CGG), so called because these alleles may or may not be unstable (Nolin et al., 2003). In fact, we previously found that four mothers with 50–54 repeats expanded to a PM allele in the next generation (Tejada et al., 2014) and that 2% expanded to a FM in two generations (Madrigal et al., 2011). These alleles are very common in the population (0.8–3.6% with some geographical variability) (Madrigal et al., 2011) but their clinical relevance is not comparable to that of PM and it has been highly controversial. In previous studies in Spain, no evidence of an association between IA and behavioral or cognitive phenotypes was found (Madrigal et al., 2011) and, in relation to FXPOI and FXTAS, we found no association for alleles below 50 CGGs but the clinical implication of IA $\geq$50 CGGs was not clear and remains to be further elucidated (Alvarez-Mora et al., 2018).

Coming back to the expansion of a *FMR1* allele, today it is known that the risk of expansion depends not only on the number of CGGs but also on the presence of AGG interruptions (Eichler et al., 1994, 1996). In the general population, almost 95% of alleles have one or two AGG interruptions, and usually occur after 9–10 CGG repeats (Eichler et al., 1994, 1996). In the case of PM alleles, a combined international study has recently shown that there is a significant number of women with 55-90 CGG repeats that have one or more AGG interruptions, even up to five in some cases (Domniz et al., 2018). The biological function of these interruptions appears to be to stabilize the gene during transmission and to decrease the risk of DNA polymerase slippage during DNA replication (Yrigollen et al., 2012, 2014; Nolin et al., 2013, 2015, 2019). Presumably, the alleles without AGGs confer a high risk of unstable transmission (Dombrowski et al., 2002; Domniz et al., 2018) and on the contrary, the presence of AGG interruptions within the CGG repeat tract significantly increases genetics stability and reduces the risk of expansion to a greater number of CGGs (Yrigollen et al., 2012). Therefore, knowledge of the distribution of these interruptions in IAs and PM alleles is of great importance for genetic counseling.

Since our previous works were done only with data recorded with the size of CGGs, we undertook the retrospective study of the published cases, adding new cases of recent years in order to determine the exact sequence of the CGG repeat tract with AGGs in our population. The overall aim of this study is to shed light on this topic to improve genetic and reproductive counseling in women with IA and PM alleles and to suggest that the risk of expansion should be based on the study of AGG interruptions which have not been taken into account in the established ranges followed nowadays.

MATERIALS AND METHODS

Study Design and Subjects

The design of the study was retrospective. Women with alleles between 45 and 65 CGG repeats were selected for the study. This range was selected based on the study of Nolin et al. (2013) where they found similar frequencies of unstable transmissions in the ranges of 60–64 CGG repeats and 65–69 CGG repeats and to understand the effect of AGGs in women with low PM (<65 CGG repeats) in order to provide a more accurate genetic counseling taking into account also recent studies on transmissions. In Cruces University Hospital these cases were taken anonymously from a database which includes the results of the *FMR1* alleles obtained between 1991 and 2018 in patients referred for Fragile X testing and their relatives in northern Spain. Collaborative hospitals from Barcelona and Zaragoza contributed with new cases for the study. In total, we studied 66 women (index cases) with CGG repeats between 45 and 65, and their children. Eighty-seven transmissions (47 males and 40 females) were analyzed. Informed consent approved by the clinical ethical committee was obtained in all cases prior to genetic testing.

Molecular Analyses

Genomic DNA was extracted from peripheral blood. DNA samples were amplified with the AmplideX®FMR1 PCR commercial kit (Asuragen, Austin, TX, USA) to obtain the exact number of repeats of both CGGs and AGGs. Sequences were analyzed with the Gene Mapper™ Software and the formula was annotated for each sample.

RESULTS

Index Cases

Table 1 shows the results of *FMR1* triplet repeat studies in the index cases (each woman with analyzed offspring) of the project indicating the CGG repeats and the AGG interruptions. The most common alleles found were those carrying 56 or 57 repeats with two AGG interruptions representing the 15% of our cases. We did

TABLE 1 | Results of triplet studies indicating CGG repeats and AGG interruptions in index cases.

Maternal CGGs	Maternal AGGs	Number of index cases	Total number of index cases
45	1	1	3
	2	2	
46	1	2	4
	2	2	
47	1	1	4
	2	3	
48	0	1	5
	1	1	
	2	3	
49	1	1	3
	2	2	
50	1	2	4
	2	2	
51	2	2	2
52	2	3	3
53	2	4	4
54	1	1	2
	2	1	
55	1	2	4
	2	2	
56	0	2	7
	2	5	
57	1	1	6
	2	5	
58	1	1	2
	2	1	
59	0	2	4
	2	2	
61	0	1	1
62	0	1	3
	2	2	
63	0	1	2
	1	1	
64	0	1	2
	2	1	
65	2	1	1
			Total = 66

For each woman only the intermediate allele or the allele with premutation is represented.

not find any cases of 60 repeats in our study as an index case. For each case, the formula of the CGG repeats and AGG interruptions was recorded.

Analysis of CGGs and AGGs Transmissions

For each index case, at least one generation was studied in order to analyze the transmission of the allele from 45 to 65 CGG repeats. In some cases, three generations of the same family could be studied. Also in several cases for each index case more than one child was studied, so the number of transmissions was greater than the number of index cases studied.

Table 2 shows the results of the transmission of alleles based on AGGs interruptions. Alleles with CGG repeats between 45 and

TABLE 2 | Transmissions of the alleles between 45 and 65 CGG repeats.

Maternal CGGs	Maternal AGGs	Number of index cases	CGGs (AGGs) in offspring	Total number of offspring
45	1	1	45 (1)	1
	2	2	45 (2)	2
46	1	2	46 (1)	2
	2	2	46 (2)	2
47	1	1	47 (1)	1
	2	3	47 (2)	3
48	0	1	48 (0)	1
	1	1	48 (1)	1
	2	3	48 (2)	3
49	1	1	49 (1)	1
	2	2	49 (2)	2
50	1	2	48 (1)	2
	2	2	50 (2)	2
51	2	2	51 (2)	2
52	2	3	52 (2)	3
53	2	4	53 (2)	9
54	1	1	54 (1)	1
	2	1	54 (2)	1
55	1	2	55 (1)	2
	2	2	55 (2)	2
56	0	1	62 (0)	1
		1	65 (0)	1
			77 (0)	1
	2	5	56 (2)	6
57	1	1	57 (1)	2
	2	5	57 (2)	7
58	1	1	57 (1)	1
	2	1	58 (2)	1
59	0	1	68 (0)	1
			74–82 (0)	1
		1	82 (0)	1
	2	2	59 (2)	3
61	0	1	71 (0)	1
			61–81 (0)	1
62	0	1	>200	1
	2	1	62 (1)	2
	2	1	64 (2)	1
63	0	1	66 (0)	1
	1	1	125–150 (0)	1
64	0	1	80 (0)	1
	2	1	64 (2)	2
65	2	1	70(0)	1
			88(0)	1

In the case of offspring with different formulas, they have been arranged on several lines. Alleles separated by a hyphen indicate the appearance of a mosaic in CGG triplets.

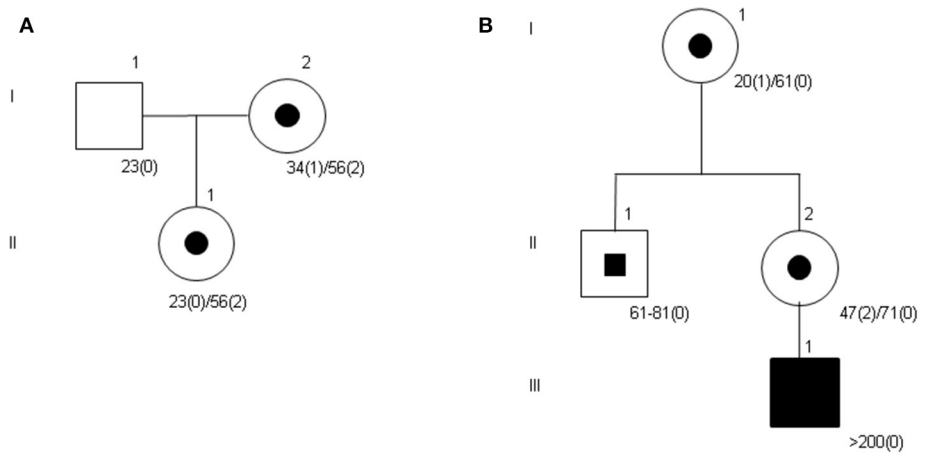

FIGURE 1 | Examples of pedigrees of studied families showing the expansion of the CGG repeats. **(A)** The allele with 56 CGG repeats and two AGG interruptions is inherited by the daughter without expansion. **(B)** In the third generation, the patient presents with Fragile X Syndrome with an allele of more than 200 repeats. Subject II-1 presents a mosaicism in the number of CGG repeats.

TABLE 3 | Results of triplet studies in different generations of families where the index case presented 0 AGG interruptions in her allele.

1st generation CGGs (AGGs)	2nd generation CGGs (AGGs)	3rd generation CGGs (AGGs)
56 (0)	62 (0)	>200 (0)
59 (0)	82 (0)	>200 (0)
59 (0)	74–82 (0)	>200 (0)
		>200 (0)
	68 (0)	N
61 (0)	71 (0)	>200 (0)
	61–81 (0)	N
64 (0)	80 (0)	>200 (0)

N, indicates no offspring.

58 do not expand in the next generation except two alleles with 56 repeats and no AGG interruptions which expand in one case to 62 repeats and in another case to 65 and 77 repeats in two different transmissions. Therefore, AGG interruptions confer stability to the alleles as is shown in **Figure 1A**. Furthermore, we have found four females with alleles with more than 59 CGG repeats and two AGG interruptions that do not expand either. Alleles from 56 CGG repeats without AGGs expand in all cases. Results of *FMR1* triplet repeat expansions over different generations within families where the index case presented no AGG interruptions in her PM allele are represented in **Table 3**. In all cases, the allele has expanded, leading in the third generation to a large expansion of CGG repeats and the appearance of FXS. In the second generation of these families where the index case does not present AGGs, in several cases CGG mosaicisms appear due to the instability of the allele. An example of the families where the allele has expanded due to the lack of AGG interruptions is represented in **Figure 1B**.

DISCUSSION

Although the importance of AGG interruptions in maintaining *FMR1* repeat stability has been well-documented (Yrigollen et al., 2012; Nolin et al., 2013, 2015; Domniz et al., 2018), nowadays clinicians use in genetic and reproductive counseling the laboratory reports where the American College of Medical Genetics definition for the ranges of IA (45–54) and PM (55–200) (Maddalena et al., 2001) are followed. These guidelines do not include the composition of the sequence (i.e., presence or not of AGG interruptions). This raises a great anxiety in many women due to the high frequency of IAs and PM (Madrigal et al., 2011) in our population.

The number of AGGs has a substantial impact on the risk and the magnitude of repeat change from the mother to her offspring. In our study we have found that alleles within the range of 45–59 CGG repeats and two AGG interruptions do not expand in the next generation. Moreover, there are two cases of 64 CGG repeats and two AGG interruptions which do not expand to the next generation either. Nolin et al. (2013) analyzed the effect of maternal repeat size and number of AGGs on unstable transmissions and full mutation expansions and found that in the range of 45–49 CGG repeats and two AGGs there is a 5% of risk of unstable transmissions as well as in the range of 55–59 CGG repeats and two AGGs. These results show that the risk of expansion is the same in these particular ranges belonging to IA and low PM classifications. Domniz et al. (2018) analyzed PM carriers with 55–90 CGG repeats and found that the risk of unstable transmissions for alleles between 55 and 59 CGGs with two AGGs was a little bit higher (14.5% in the combined study) decreasing to 0% when they have more than two AGGs. They also showed that the risk increases to 50% in the range of 60–64 CGGs with two or more AGGs. In our study including less cases, we have also found that alleles below 60 CGG repeats with two AGGs do not expand in the next generation but above 60 CGGs we observe a small increase in the risk of unstable

transmissions (two cases with 62 CGGs and two AGGs in **Table 2**; in one case there is a loss of one AGG and in the other case there is an expansion of two CGGs). Furthermore, in the previous Spanish study on IAs (Madrigal et al., 2011), the analysis of 100 transmissions of IAs showed that 95% of these alleles were stable, only 3% expanded within the same range and 2% expanded to a FM in two generations; these two cases had lost the AGG interruptions. In the present study and in the range of IAs, we have only found one case without AGGs (48 CGGs) that did not expand in the next generation (**Table 2**), but all the alleles from 56 CGG repeats without AGG interruptions, expanded in the next generation giving a FXS in the third generation. All FM expansions were transmitted from alleles lacking AGGs (**Table 3** and **Figure 1B**). These results show once again that AGG interruptions give stability to the allele as seen in other recent studies (Nolin et al., 2013, 2015, 2019; Yrigollen et al., 2014).

The discovery of AGG interruptions in IA or low PM has a great application in the genetic and reproductive counseling of carriers. Although we have a limited number of cases, with this study and the results of other recent studies, we suggest that the risk of expansion should be personalized and based on the study of AGG interruptions which have not been taken into account in the established ranges followed nowadays. In a previous study of CGG transmissions where AGG interruptions were not analyzed (Tejada et al., 2014) it was concluded that women with 55–59 CGG presented a risk of expansion to FM of 6.4%. And in this study we observe, for example, five index cases with 57 CGG repeats and two AGGs which do not expand in the seven transmissions analyzed. Finally, PM alleles may lose AGGs and CGGs through contractions and become normal, intermediate, or smaller premutation alleles (Nolin et al., 2019) so follow-up of women with a very low number of CGG repeats and no AGG interruptions should be recommended, despite the low risk of expansion in the next generation, like the case we have with 48 CGGs.

In conclusion, we strongly recommend that clinical laboratories study the total number of CGG repeats with the number of AGG interruptions as it was already said in previous studies (Yrigollen et al., 2012; Domniz et al., 2018) but unfortunately it is not a routine in many laboratories. In genetic counseling, it will be very important to convey this more accurate risk information to women carriers of alleles with 45–65 CGG repeats regarding their risk of expansion or not of their CGG repeats in the *FMR1* gene. This will serve to reassure women with very low risk of expansion even if they are classified as PM carrier according to the classic definition (i.e., <59 CGGs with two AGGs), and to follow-up those that have higher risk including those with IAs and no AGGs.

DATA AVAILABILITY STATEMENT

All datasets presented in this study are included in the article.

ETHICS STATEMENT

Informed consent approved by the clinical ethical committee was obtained in all cases prior to genetic testing and it includes the permission of using the data for statistical analyses.

AUTHOR CONTRIBUTIONS

OV and MT designed the study. OV wrote the manuscript. OV, NI, HM, AH, LR-R, and SI-Á collected data and performed the analyses. MT supervised the entire work. All authors revised the manuscript critically, approved the final manuscript as submitted and agreed to be accountable for all aspects of the work All authors contributed to the article and approved the submitted version.

FUNDING

This work was partially funded by the Jesús de Gangoiti Barrera Foundation and the Basque Fragile X Syndrome Association.

ACKNOWLEDGMENTS

We thank the families for their collaboration in this study. We would also like to thank Carmen Díez López for her technical work on patients' DNA extractions and amplifications by triplet PCRs.

REFERENCES

Adams, J. S., Adams, P. E., Nguyen, D., Brunberg, J. A., Tassone, F., Zhang, W., et al. (2007). Volumetric brain changes in females with fragile X-associated tremor/ataxia syndrome (FXTAS). *Neurology* 69, 851–859. doi: 10.1212/01.wnl.0000269781.10417.7b

Alvarez-Mora, M. I., Madrigal, I., Martinez, F., Tejada, M. I., Izquierdo-Alvarez, S., Sanchez-Villar de Saz, P., et al. (2018). Clinical implication of FMR1 intermediate alleles in a Spanish population. *Clin. Genet.* 94, 153–158. doi: 10.1111/cge.13257

Berkenstadt, M., Ries-Levavi, L., Cuckle, H., Peleg, L., and Barkai, G. (2007). Preconceptional and prenatal screening for fragile X syndrome: experience with 40,000 tests. *Prenat. Diagn.* 27, 991–994. doi: 10.1002/pd.1815

Crawford, D. C., Acuña, J. M., and Sherman, S. L. (2001). FMR1 and the fragile X syndrome: human genome epidemiology review. *Genet. Med* 3, 359–371. doi: 10.1097/00125817-200109000-00006

Dombrowski, C., Levesque, S., Morel, M. L., Rouillard, P., Morgan, K., and Rousseau, F. (2002). Premutation and intermediate-size FMR1 alleles in 10572 males from the general population: loss of an AGG interruption is a late event in the generation of fragile X syndrome alleles. *Hum. Mol. Genet.* 11, 371–378. doi: 10.1093/hmg/11.4.371

Domniz, N., Ries-Levavi, L., Cohen, Y., Marom-Haham, L., Berkenstadt, M., Pras, E., et al. (2018). Absence of AGG interruptions is a risk factor for full mutation expansion among israeli FMR1 premutation carriers. *Front. Genet.* 9:606. doi: 10.3389/fgene.2018.00606

Eichler, E. E., Holden, J., Popovich, B. W., Reiss, A. L., Snow, K., Thibodeau, S. N., et al. (1994). Length of uninterrupted CGG repeats determines instability in the FMR1 gene. *Nat. Genet.* 8, 88–94. doi: 10.1038/ng0994-88

Eichler, E. E., Macpherson, J. N., Murray, A., Jacobs, P. A., Chakravarti, A., and Nelson, D. L. (1996). Haplotype and intersperson analysis of the FMR1 CGG repeat indentifies two different mutational pathways for the origin of the fragile X syndrome. *Hum. Molec. Genet.* 5, 319–330. doi: 10.1093/hmg/5.3.319

Fernandez-Carvajal, I., Lopez Posadas, B., Pan, R., Raske, C., Hagerman, P. J., and Tassone, F. (2009). Expansion of an FMR1 grey-zone allele to a full mutation in two generations. *J. Mol. Diagn*. 11, 306–310. doi: 10.2353/jmoldx.2009.080174

Hagerman, P. J. (2008). The fragile X prevalence paradox. *J. Med. Genet.* 45, 498–499. doi: 10.1136/jmg.2008.059055

Hagerman, R. J., Protic, D., Rajaratnam, A., Salcedo-Arellano, M. J., Aydin, E. Y., and Schneider, A. (2018). Fragile X-associated neuropsychiatric disorders (FXAND). *Front. Psychiatry* 13:564. doi: 10.3389/fpsyt.2018.00564

Jacquemont, S., Hagerman, R. J., Leehey, M., Grigsby, J., Zhang, L., Brunberg, J. A., et al. (2003). Fragile X premutation tremor/ataxia syndrome: molecular, clinical, and neuroimaging correlates. *Am. J. Hum. Genet.* 72, 869–878. doi: 10.1086/374321

Maddalena, A., Richards, C. S., McGinniss, M. J., Brothman, A., Desnick, R. J., Grier, R. E., et al. (2001). Technical standards and guidelines for fragile X: the first of a series of disease-specific supplements to the standards and guidelines for clinical genetics laboratories of the american college of medical genetics. quality assurance subcommittee of the laboratory practice committee. *Genet. Med.* 3, 200–205. doi: 10.1097/00125817-200105000-00010

Madrigal, I., Xunclà, M., Tejada, M. I., Martínez, F., Fernández-Carvajal, I., Pérez-Jurado, L. A., et al. (2011). Intermediate FMR1 alleles and cognitive and/or behavioural phenotypes. *Eur. J. Hum. Genet*. 19, 921–923. doi: 10.1038/ejhg.2011.41

Merino, S., Ibarluzea, N., Maortua, H., Prieto, B., Rouco, I., López-Aríztegui, M. A., et al. (2016). Associated clinical disorders diagnosed by medical specialists in 188 FMR1 premutation carriers found in the last 25 years in the spanish basque country: a retrospective study. *Genes* 7:E90. doi: 10.3390/genes7100090

Nolin, S. L., Brown, W. T., Glicksman, A., Houck, G. E. Jr., Gargano, A. D., Sullivan, A., et al. (2003). Expansion of the fragile X CGG repeat in females with premutation or intermediate alleles. *Am. J. Hum. Genet*.72, 454–464. doi: 10.1086/367713

Nolin, S. L., Glicksman, A., Ersalesi, N., Dobkin, C., Brown, W. T., Cao, R., et al. (2015). Fragile X full mutation expansions are inhibited by one or more AGG interruptions in premutation carriers. *Genet. Med*. 17, 358–364. doi: 10.1038/gim.2014.106

Nolin, S. L., Glicksman, A., Tortora, N., Allen, E., Macpherson, J., Mila, M., et al. (2019). Expansions and contractions of the FMR1 CGG Repeat in 5,508 transmissions of normal, intermediate, and premutation alleles. *Am. J. Med. Genet. A* 179, 1148–1156. doi: 10.1002/ajmg.a.61165

Nolin, S. L., Sah, S., Glicksman, A., Sherman, S. L., Allen, E., Berry-Kravis, E., et al. (2013). Fragile X AGG analysis provides new risk predictions for 45-69 repeat alleles. *Am. J. Med. Genet. A* 161A, 771–778. doi: 10.1002/ajmg.a.35833

Oberle, I., Rousseau, F., Heitz, D., Kretz, C., Devys, D., Hanauer, A., et al. (1991). Instability of a 550-base pair DNA segment and abnormal methylation in fragile X syndrome. *Science* 252, 1097–1102. doi: 10.1126/science.252.5009.1097

Rodriguez-Revenga, L., Madrigal, I., Pagonabarraga, J., Xuncl,à, M., Badenas, C., Kulisevsky, J., et al. (2009). Penetrance of FMR1 premutation associated pathologies in fragile X syndrome families. *Eur. J. Hum. Genet*. 17, 1359–1362. doi: 10.1038/ejhg.2009.51

Rousseau, F., Heitz, D., Tarleton, J., MacPherson, J., Malmgren, H., Dahl, N., et al. (1994). A multicenter study on genotype-phenotype correlations in the fragile X syndrome, using direct diagnosis with probe StB12.3: the first 2,253 cases. *Am. J. Hum. Genet.* 55, 225–237.

Strom, C. M., Crossley, B., Redman, J. B., Buller, A., Quan, F., Peng, M., et al. (2007). Molecular testing for fragile X syndrome: lessons learned from 119,232 tests performed in a clinical laboratory. *Genet. Med*. 9, 46–51. doi: 10.1097/GIM.0b013e31802d833c

Sullivan, S. D., Welt, C., and Sherman, S. (2011). FMR1 and the continuum of primary ovarian insufficiency. *Semin. Reprod. Med.* 29, 299–307. doi: 10.1055/s-0031-1280915

Tejada, M. I., Glover, G., Martínez, F., Guitart, M., de Diego-Otero, Y., Fernández-Carvajal, I., et al. (2014). Molecular testing for fragile X: analysis of 5062 tests from 1105 fragile X families–performed in 12 clinical laboratories in Spain. *Biomed Res. Int*. 2014:195793. doi: 10.1155/2014/195793

Verkerk, A. J., Pieretti, M., Sutcliffe, J. S., Fu, Y. H., Kuhl, D. P., Pizzuti, A., et al. (1991). Identification of a gene (FMR-1) containing a CGG repeat coincident with a breakpoint cluster region exhibiting length variation in fragile X syndrome. *Cell* 65, 905–914. doi: 10.1016/0092-8674(91)90397-H

Wittenberger, M. D., Hagerman, R. J., Sherman, S. L., McConkie-Rosell, A., Welt, C. K., Rebar, R. W., et al. (2007). The FMR1 premutation and reproduction. *Fertil. Steril.* 87, 456–465. doi: 10.1016/j.fertnstert.2006.09.004

Yrigollen, C. M., Durbin-Johnson, B., Gane, L., Nelson, D. L., Hagerman, R., Hagerman, P. J., et al. (2012). AGG interruptions within the maternal FMR1 gene reduce the risk of offspring with fragile X syndrome. *Genet. Med.* 14, 729–736. doi: 10.1038/gim.2012.34

Yrigollen, C. M., Martorell, L., Durbin-Johnson, B., Naudo, M., Genoves, J., Murgia, A., et al. (2014). AGG interruptions and maternal age affect FMR1 CGG repeat allele stability during transmission. *J. Neurodev. Disord.* 6:24. doi: 10.1186/1866-1955-6-24

Yu, S., Pritchard, M., Kremer, E., Lynch, M., Nancarrow, J., Baker, E., et al. (1991). Fragile X genotype characterized by an unstable region of DNA. *Science* 252, 1179–1181. doi: 10.1126/science.252.5009.1179

Conflict of Interest: The authors declare that the research was conducted in the absence of any commercial or financial relationships that could be construed as a potential conflict of interest.

frontiers in Molecular Biosciences

MINI REVIEW
published: 18 September 2020
doi: 10.3389/fmolb.2020.571092

Metabolic Alterations in *FMR1* Premutation Carriers

Yiqu Cao[1,2†], *Yun Peng*[1,2†], *Ha Eun Kong*[1], *Emily G. Allen*[1*] *and Peng Jin*[1*]

[1] *Department of Human Genetics, School of Medicine, Emory University, Atlanta, GA, United States,* [2] *Department of Neurology, Xiangya Hospital, Central South University, Changsha, China*

FMR1 gene premutation carriers are at risk of developing Fragile X-associated tremor/ataxia syndrome (FXTAS) and Fragile X-associated primary ovarian insufficiency (FXPOI) in adulthood. Currently the development of biomarkers and effective treatments in *FMR1* premutations is still in its infancy. Recent metabolic studies have shown novel findings in asymptomatic *FMR1* premutation carriers and FXTAS, which provide promising insight through identification of potential biomarkers and therapeutic pathways. Here we review the latest advancements of the metabolic alterations found in asymptomatic *FMR1* premutation carriers and FXTAS, along with our perspective for future studies in this emerging field.

Keywords: FXTAS, *FMR1*, metabolomics, biomarker, therapeutic development

OPEN ACCESS

Edited by:
Rob Willemsen,
Erasmus Medical Center, Netherlands

Reviewed by:
Barbara Bardoni,
UMR 7275 Institut de Pharmacologie Moléculaire et Cellulaire (IPMC), France
Eleonora Napoli,
University of California, Davis, United States
Flora Tassone,
University of California, Davis, United States

***Correspondence:**
Emily G. Allen
emgrave@emory.edu
Peng Jin
peng.jin@emory.edu

†These authors have contributed equally to this work

Specialty section:
This article was submitted to Cellular Biochemistry, a section of the journal Frontiers in Molecular Biosciences

Received: *09 June 2020*
Accepted: *26 August 2020*
Published: *18 September 2020*

Citation:
Cao Y, Peng Y, Kong HE, Allen EG and Jin P (2020) Metabolic Alterations in FMR1 Premutation Carriers. Front. Mol. Biosci. 7:571092. doi: 10.3389/fmolb.2020.571092

INTRODUCTION

A 55–200 CGG repeat expansion in the 5′ UTR of the fragile X mental retardation 1 (*FMR1*) gene is the hallmark of premutation carriers. The *FMR1* premutation carriers are at risk of developing Fragile X-associated tremor/ataxia syndrome (FXTAS) and Fragile X-associated primary ovarian insufficiency (FXPOI) in adulthood (Allingham-Hawkins et al., 1999; Hagerman et al., 2001), as well as other unspecific syndromes (Mila et al., 2018). FXTAS is a neurodegenerative disorder predominantly in men, characterized by kinetic tremor, gait ataxia, parkinsonism, executive dysfunction, and neuropathy (Jacquemont et al., 2003; Hall and Berry-Kravis, 2018); and FXPOI is a condition in women characterized by reduced function of the ovaries (Man et al., 2017). In FXTAS, the two principal molecular mechanisms are: (1) RNA-gain-of function toxicity (Jin et al., 2003, 2007; Tassone et al., 2004; Sofola et al., 2007; Sellier et al., 2010), which leads to sequestration of various rCGG repeat-binding proteins; and (2) repeat-associated non-ATG (RAN) translation (Todd et al., 2013; Oh et al., 2015; Krans et al., 2016; Sellier et al., 2017), which produces the polyglycine (polyG) peptides toxic to cells. As another phenotype of *FMR1* premutation, FXPOI is believed to share similar molecular mechanisms with FXTAS based on current evidence, but still needs further research (Elizur et al., 2014, 2019; Buijsen et al., 2016; Man et al., 2017). Currently, there is no effective treatment for FXTAS and FXPOI, and the development of biomarkers is still in its infancy (Hagerman and Hagerman, 2016; Man et al., 2017).

Recently, several studies have made encouraging discoveries in the metabolomics of asymptomatic *FMR1* premutation carriers and FXTAS, which provide promising insight for the identification of potential biomarkers and therapeutic pathways. Currently, no metabolomic study in FXPOI has been reported. Therefore, in this review, we focus on the current knowledge of metabolic alterations in asymptomatic *FMR1* premutation carriers and FXTAS. We begin by describing the basic concepts of metabolism, then discuss the specific metabolic alterations associated with *FMR1* premutation carriers, and lastly provide an overview of future directions in this field.

METABOLOMICS

Metabolomics explores the metabolic alterations associated with health and disease (Adamski, 2020). More specifically, metabolomics detects the metabolites and small molecular chemicals in various sample types, including biofluids, cells, and tissues (Johnson et al., 2016). The common human sample types used in the metabolomics include plasma, cerebrospinal fluid (CSF), peripheral blood mononuclear cells (PBMCs), fibroblasts and muscle tissues. A combination of analytical tools is implemented to detect various chemicals in the samples, such as liquid chromatography – mass spectrometry (LC-MS) and gas chromatography – mass spectrometry (GC–MS) (Wishart, 2019). The subsequent data analysis requires the available well-established databases (e.g., METLIN, HMDB, LipidMaps, and MassBank) (Fahy et al., 2009; Horai et al., 2010; Guijas et al., 2018; Wishart et al., 2018).

There are two main study types in metabolomics: untargeted (global) and targeted metabolomics (Johnson et al., 2016). Untargeted metabolomics detects the widest range of metabolites extracted from a sample, identifying novel and unanticipated alterations, whereas targeted metabolic analysis detects the levels of specific metabolites based on prior knowledge, allowing for higher sensitivity and selectivity (Johnson et al., 2016).

The main advantage of metabolomics is the ability to detect subtle perturbations in biological pathways. The metabolic signals could be amplified greatly because the most downstream changes of the genome, epigenome, transcriptome, and proteome are being measured (Urbanczyk-Wochniak et al., 2003). Based on this advantage, metabolic profiling has identified perturbations and novel biomarkers in many neurodegenerative diseases, such as Parkinson's disease (PD) (Ahmed et al., 2009; Burte et al., 2017; Zhao et al., 2018), Alzheimer's disease (AD) (Chang et al., 2015; Van Assche et al., 2015; Wu et al., 2016) and Huntington disease (HD) (Verwaest et al., 2011).

METABOLIC ALTERATIONS ASSOCIATED WITH *FMR1* PREMUTATION

Carbohydrate Metabolism

Carbohydrate metabolism is fundamental for cellular energy balance and the biosynthesis of new cellular components (Dashty, 2013). In *FMR1* premutation carriers, researchers have identified alterations in carbohydrate metabolism pathways mainly in glycolysis, Krebs cycle, oxidative phosphorylation (OXPHOS), and the pentose phosphate shunt, as described below.

Glycolysis is the catabolic pathway that converts glucose into pyruvate, serving as the common initiation pathway of anaerobic and aerobic oxidation of glucose (**Figure 1**, red box). Studies have reported changes in the intermediates and products of glycolysis in *FMR1* premutation carriers. In the plasma of premutation carriers, the levels of pyruvate entering the Krebs cycle were diminished due to the inhibition of the pyruvate dehydrogenase complex (PDHC), which may be caused by a higher [NADH]/[NAD+] ratio (Giulivi et al., 2016b). In addition to PDHC, high [NADH]/[NAD+] ratios could also inhibit other NAD-dependent dehydrogenases in the Krebs cycle, such as α-ketoglutarate dehydrogenase (AKGDH) and isocitrate dehydrogenase (ICDH). Furthermore, the lower entry of pyruvate into the Krebs cycle resulted in higher lactate formation in premutation carriers (Giulivi et al., 2016b).

In another study, peripheral blood mononuclear cells (PBMCs) were used to investigate mitochondrial energy-providing systems, and a dynamic alteration of glycolysis was observed when comparing controls, FXTAS-free carriers and FXTAS-affected carriers (Napoli et al., 2016). Specifically, FXTAS-free carriers exhibited a comparable or higher abundance of glycolytic proteins (e.g., hexokinase, phosphofructokinase, and pyruvate kinase) than controls, indicating an up-regulation of glycolysis (Napoli et al., 2016). However, in FXTAS-affected carriers, almost all glycolytic proteins were lower compared to control cells, with the exception of glucose-6-phosphate-dehydrogenase, which was higher in FXTAS-affected carriers compared to both controls and FXTAS-free carriers (Napoli et al., 2016). This marked alteration in glycolysis in FXTAS-affected carriers may implicate glycolysis in FXTAS pathogenesis (Napoli et al., 2016).

The Krebs cycle [also known as citric acid cycle (CAC) or tricarboxylic acid cycle (TCA cycle)] is a series of cyclic reactions that begins with the oxidation of acetyl-CoA into carbon dioxide and adenosine triphosphate (ATP), serving as the common metabolic pathway of carbohydrate, lipid and protein oxygenolysis (**Figure 1**, blue circle). Several intermediates of the Krebs cycle, located in the first half of the cycle, namely citrate, isocitrate and aconitate, were increased in the plasma of carriers compared to controls, indicating a decreased Krebs cycle activity in premutation (Giulivi et al., 2016a,b). Consistently, most enzymes of the Krebs cycle also showed a lower abundance in the PBMCs of the FXTAS-affected compared to controls (Napoli et al., 2016).

Oxidative Phosphorylation (OXPHOS) is the metabolic pathway in which cells utilize a series of protein complexes to produce ATP (Schmidt-Rohr, 2020). The activities of OXPHOS protein complexes and citrate synthase were lower in the PBMCs of carriers than controls, consistent with the relatively lower overall OXPHOS capacity in premutation carriers (Napoli et al., 2016). The combination of decreased OXPHOS and increased glycolysis in FXTAS-free premutation carriers suggests a Warburg effect in which glucose is mainly oxidized to lactate rather than undergoing OXPHOS to produce ATP (Warburg, 1956; Lin et al., 2012). These findings were accompanied by the observation of higher production of reactive oxygen species (ROS) and proton leak, as well as other mitochondrial outcomes (impaired Complex I activity, impaired redox-regulated mitochondrial disulfide relay system and increased mtDNA deletions) in the PBMCs or fibroblasts of premutation carriers, together suggesting increased oxidative-nitrative damage (Napoli et al., 2016; Song et al., 2016). Nitrative damage of scaffolding proteins could alter cytoskeletal organization, cause mitochondrial damage, and affect neuron maintenance and remodeling (Song et al., 2016).

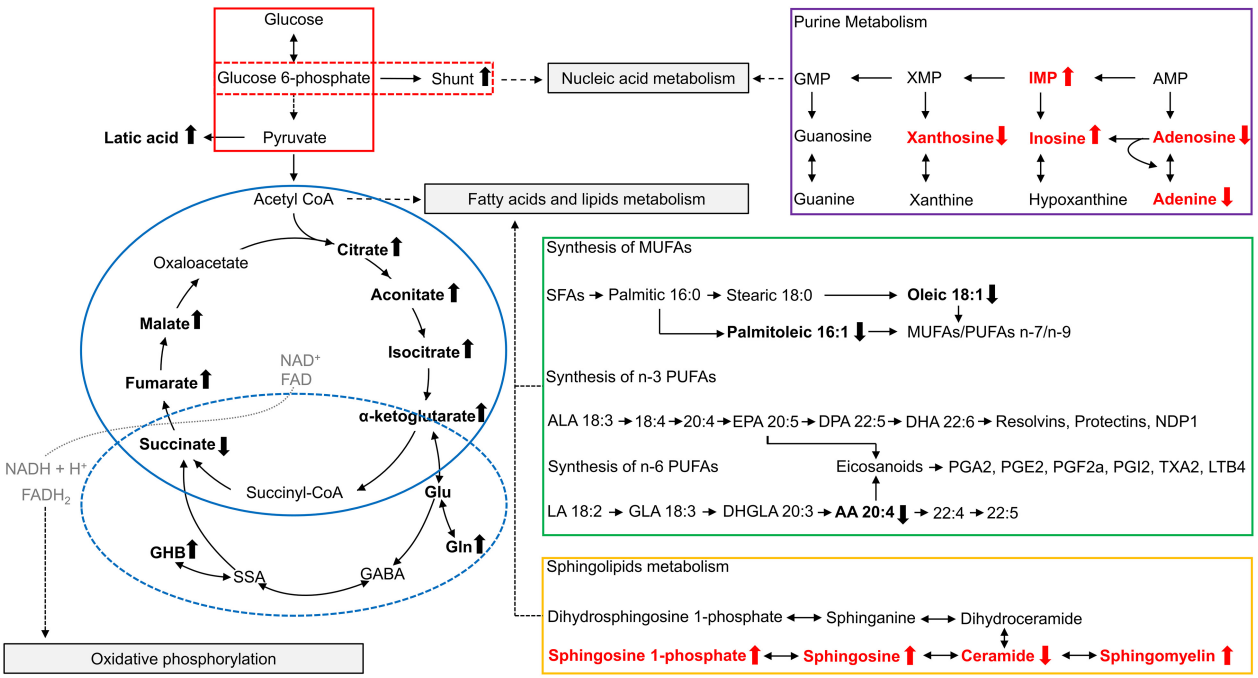

FIGURE 1 | Overview of metabolites related to *FMR1* premutation. Altered metabolites identified in studies of plasma from *FMR1* premutation carriers are shown in bold and in black. Altered metabolites identified in studies of FXTAS mice cerebellum are show in bold and in red. The up arrow indicates the increase, and the down arrow indicates the decrease. The "shunt" refers to the pentose phosphate shunt. The glycolysis pathway is outlined in red, with the pentose phosphate shunt outlined in a dashed red box. The TCA cycle is outlined in solid blue, and GABA metabolism is outlined in a dashed blue circle. Purine metabolism is outlined in purple, synthesis of polyunsaturated fatty acids is outlined in green, and sphingolipid metabolism is outlined in orange. AA, arachidonic acid; ALA, α-linolenic acid; AMP, Adenosine monophosphate; CoA, Coenzyme A; DHA, docosahexaenoic acid; DHGLA, dihomo-γ-linolenic acid; DPA, docosapentaenoic acid; EPA, eicosapentaenoic acid; FAD, Flavin adenine dinucleotide; GABA, γ-Aminobutyric acid; GHB, 4-hydroxybutyrate; GLA, Gamma linolenic acid; Gln, Glutamine; Glu, Glutamate; GMP, Guanosine monophosphate; IMP, Inosine monophosphate; LA, linoleic acid; LTB4, Leukotriene B4; MUFAs, monounsaturated fatty acids; NAD+, Nicotinamide adenine dinucleotide; PGA1, Prostaglandin A1; PGE2, Prostaglandin E2; PGF2a, Prostaglandin F2alpha; PGI2, prostaglandin I2; PUFAs, polyunsaturated fatty acids; SFAs, saturated fatty acids; SSA, succinic semialdehyde; TXA2, Thromboxane A2; XMP, Xanthosine monophosphate.

The pentose phosphate shunt is a metabolic pathway that utilizes glucose-6-phosphate to generate NADPH and ribose 5-phosphate (**Figure 1**, red dashed box). As mentioned above, most glycolytic proteins in PBMCs were diminished in FXTAS-affected carriers compared to controls, except glucose-6-phosphate dehydrogenase, which is the pentose phosphate shunt entry point (Napoli et al., 2016). The higher abundance of glucose-6-phosphate-dehydrogenase in FXTAS-affected carriers indicates a shift of glucose toward the pentose phosphate shunt, probably aiming to produce NADPH, reducing equivalents required for the antioxidant defenses (Napoli et al., 2016).

Amino Acids, Derivatives, and Biogenic Amines

The metabolism of amino acids, derivatives and biogenic amines has a profound effect on the nervous system by affecting the levels of structural proteins and neurotransmitters. In the plasma from premutation carriers, seventeen related metabolites (amino acids, derivatives or biogenic amines) were found to be altered, and among these, five amino acids or derivatives (proline, glycine, hydroxyproline, citrulline, and glutamylvaline) correlated with CGG repeat size, indicating a genotype-phenotype correlation (Giulivi et al., 2016b). Additionally, the increased plasma levels of glutamate and 4-hydroxybutyrate (GHB) may signal an imbalance in neurotransmission, which has been reported as a hallmark of anxiety disorders (Giulivi et al., 2016b). This observation is consistent with a higher incidence of anxiety/mood disorders in FXTAS-affected carriers (Bourgeois et al., 2007; Kogan et al., 2008).

Moreover, Giulivi et al. (2016a) hypothesized that given the increased levels of the Krebs cycle intermediates (citrate, isocitrate and aconitate), the activity of AKGDH is decreased in premutation carriers, resulting in an increased flux from alpha-ketoglutarate to glutamate, which subsequently culminates in the elevation of glutamine, GABA, and GHB levels (**Figure 1**, blue dashed circle). Consistently, researchers found that the metabotropic glutamate (Glu) receptor 5 and GABA pathways are altered in the brains of FXTAS patients (Pretto et al., 2014). Additionally, lower plasma concentrations of phenylethylamine (PEA) were also found in premutation carriers, which may reflect incipient nigrostriatal degeneration (Giulivi et al., 2016a).

In the cerebellum of FXTAS mice expressing r(CGG)$_{90}$ in Purkinje cells, our group also observed alterations of amino acids (41 out of 115) (Kong et al., 2019). For example, 5-oxoproline was decreased in aged FXTAS compared to aged

WT mice, suggesting that this metabolite is altered due to CGG-associated toxicity. 5-oxoproline was also decreased in the aged FXTAS compared to young FXTAS mice, implicating perturbation of this metabolite in the progression of FXTAS. Interestingly, subsequent genetic screening using a *Drosophila* model of FXTAS revealed that knockdown of *CG4306*, the fly ortholog of *Gamma-glutamylcyclotransferase (Ggct),* which encodes the enzyme responsible for catalyzing the formation of 5-oxoproline (Oakley et al., 2008), resulted in suppression of $(CGG)_{90}$ toxicity in *Drosophila*. This finding suggests *Ggct* as a genetic modifier of CGG-associated neurotoxicity (Kong et al., 2019), providing a novel therapeutic target for FXTAS.

Fatty Acids and Structural Lipids

Giulivi et al. (2016b) found overall fatty acids levels decreased in the plasma of premutation carriers. More specifically, they found lower plasma levels of free fatty acids, oleic and arachidonic acids, which are associated with depression and parkinsonism (Giulivi et al., 2016b). Additionally, they found a decreased ratio of polyunsaturated fatty acids (PUFA) of the n-3 series over that of the n-6 series, which might be related to impaired learning and memory in premutation carriers (**Figure 1**, green box) (Giulivi et al., 2016b). The decreased ratio of the n-3 series over the n-6 series could result in more pro-inflammatory prostaglandins produced via the Δ5–6 desaturase pathway, and an increased pro-inflammatory status (Giulivi et al., 2016b). Moreover, researchers observed a decrease in palmitoleic acid in plasma from premutation carriers, along with the lower estimated enzymatic activity of stearoyl-CoA desaturase 1 (SCD1), the rate-limiting enzyme in monounsaturated fatty acid biosynthesis (Ntambi and Miyazaki, 2004), which is necessary for axonogenesis, neuron differentiation and carbohydrate utilization in brain (Giulivi et al., 2016b).

Fatty acids and their derivatives also have an essential role in maintaining cellular integrity as structural lipids. Sphingolipids are structural lipids for eukaryotic cell membranes, consisting of the sphingoid backbone, which is N-acylated with various fatty acids to form ceramide species (Maceyka and Spiegel, 2014). Recently, sphingolipid metabolism was found to be altered in the cerebellum of FXTAS mice (**Figure 1**, orange box) (Kong et al., 2019). Specifically, levels of sphingosine, sphingosine 1-phosphate, and sphingomyelin were increased, while levels of ceramide were decreased in FXTAS mice compared to wildtype (Kong et al., 2019). Further pathway analysis and subsequent validation in a FXTAS *Drosophila* model confirmed two genes related to sphingosine metabolism, *Schlank* and *Sk2* (Kong et al., 2019). *Schlank* is the *Drosophila* ortholog of ceramide synthase, the enzyme synthesizing ceramide from sphingosine. *Sk2* is the *Drosophila* ortholog of sphingosine kinase responsible for phosphorylating sphingosine to yield S1P. Knockdown of *Schlank* and *Sk2* resulted in enhancement of premutation CGG repeat-mediated neurodegeneration in *Drosophila*, indicating that *Schlank* and *Sk2* interact with the CGG repeat of *FMR1* and act as genetic modifiers in the neurodegeneration of FXTAS (Kong et al., 2019). The above findings support sphingolipid metabolism as a potential path for therapeutic development, and further research in human premutation carriers are warranted.

Nucleotide Metabolism

In the same study (Kong et al., 2019), researchers found purine metabolism perturbed in the cerebellum of FXTAS mice, including increased inosine monophosphate (IMP) and inosine, and decreased xanthosine, adenosine, and adenine (**Figure 1**, purple box). Inosine 5′monophosphate dehydrogenase (Impdh) is the rate-limiting enzyme in guanine nucleotide biosynthesis, which catalyzes the conversion of IMP into xanthosine monophosphate (XMP). Knockdown of *Ras*, the fly ortholog of *Inosine Monophosphate Dehydrogenase 1 (Impdh1)*, which encodes Impdh, resulted in the enhancement of premutation CGG repeat-mediated neurodegeneration in the FXTAS *Drosophila* model (Kong et al., 2019). Consistently, disruptions in purine metabolism were also reported in the plasma from premutation carriers (Giulivi et al., 2016b). Imbalances in purine synthesis could affect multiple pathways including replication, transcription, and DNA repair, which may contribute to neurodegeneration in *FMR1* premutation carriers (Giulivi et al., 2016b; Kong et al., 2019).

THERAPEUTIC POTENTIAL TARGETING METABOLIC PATHWAYS

Several recent studies have highlighted the breadth of metabolic alterations in the pathogenesis of *FMR1* premutation. As a result, targeting these perturbed metabolic pathways is expected to be a promising new strategy in the treatment of *FMR1* premutation carriers.

Consistent with this expectation, researchers have identified several antioxidants, including scavengers of superoxide, hydrogen peroxide and hydroxyl radicals, which could recover citrate synthase activity and mitochondrial function in fibroblasts from *FMR1* premutation carriers (Song et al., 2016). In a 12-week intervention study, Napoli et al. found that allopregnanolone treatment improved cognition and memory of FXTAS patients (Napoli et al., 2019). Plasma metabolomic profiling of FXTAS patients showed an improved value of glutamate/glutamine, a trend toward higher contents of succinate, and a decreased GHB concentration after allopregnanolone treatment, suggesting improvements in the activity of the succinic semialdehyde dehydrogenase (SSADH) mediated pathway (Napoli et al., 2019). The researchers hypothesized that the neuroprotective effect of allopregnolone in FXTAS may be due to the reduction of excessive GHB. GHB is a neuropharmacologically active compound, and excessive GHB could be neurotoxic as an inhibitor of presynaptic dopamine release (Bernasconi et al., 1999; Maitre et al., 2000). Overall, this study was a step forward in exploring potential drugs by targeting the metabolic pathways altered in *FMR1* premutation carriers. However, given the small sample size of this study, replication studies in larger cohorts are needed to confirm these findings. In addition, future therapy studies are encouraged to test the other metabolic pathways identified in *FMR1* premutation.

CONCLUSION AND FUTURE DIRECTIONS

Diverse metabolic alterations have been found in *FMR1* premutation carriers, including perturbations in the metabolism of carbohydrates, amino acids and derivatives, biogenic amines, fatty acids, structural lipids, and nucleotide. Of note, many of those metabolic alterations can be attributed to mitochondrial dysfunction, such as decreased OXPHOS capacity, changed mitochondrial proteins and altered mitochondrial architecture, which are caused by RNA gain-of function toxicity and RAN translation (Hukema et al., 2014; Alvarez-Mora et al., 2017; Drozd et al., 2019; Gohel et al., 2019; Nobile et al., 2020). As the most downstream of *FMR1* premutation pathogenesis, the metabolic alterations discussed in this review could provide resources in the search for biomarkers and promising therapeutic targets for *FMR1* premutation carriers. Additionally, although current findings are based on the asymptomatic *FMR1* premutation and FXTAS, these findings may also benefit future studies in FXPOI as they share the same genetic mechanism – the *FMR1* premutation.

Moving forward, we suggest taking the following into consideration. First, using a disease model system has the advantage of being able to assess the metabolic alterations specifically in the affected tissues, such as the cerebellum in FXTAS. However, these results must be correlated with findings in human studies for validation. Second, for the human studies, using a blood sample would be convenient, but the metabolism as measured in blood may not accurately reflect the metabolome of the specific affected tissues. For example, the degree to which plasma metabolomes reflect central nervous system (CNS) neurobiology remains uncertain due to the limitation of the blood-brain barrier. Therefore, an important step to take in future studies would be to use the cerebrospinal fluid (CSF), or brain organoids derived from induced pluripotent cells (iPSC), which may more accurately reflect the metabolome in CNS. Additionally, it would be valuable to correlate the peripheral metabolic alteration with neuroimaging, such as Magnetic Resonance Spectroscopy (MRS). Third, the sample sizes in existing human studies are relatively small. It is generally challenging to enroll a large sample of patients in the study of rare diseases such as *FMR1* premutation. Thus, future efforts are encouraged to overcome this limitation by increasing the number of multi-center studies.

AUTHOR CONTRIBUTIONS

YC and YP wrote the manuscript. HK, EA, and PJ edited the manuscript. All authors contributed to the article and approved the submitted version.

FUNDING

This work was supported by the National Institutes of Health (NS111602 and NS051630 to PJ, NS091859 to EA and PJ, and AG065815 to EA).

REFERENCES

Adamski, J. (2020). "Chapter 1 – Introduction to metabolomics," in *Metabolomics for Biomedical Research*, ed. J. Adamski (Cambridge, MA: Academic Press), 1–15. doi: 10.1039/9781788019880-00001

Ahmed, S. S., Santosh, W., Kumar, S., and Christlet, H. T. (2009). Metabolic profiling of Parkinson's disease: evidence of biomarker from gene expression analysis and rapid neural network detection. *J. Biomed. Sci.* 16:63. doi: 10.1186/1423-0127-16-63

Allingham-Hawkins, D. J., Babul-Hirji, R., Chitayat, D., Holden, J. J., Yang, K. T., Lee, C., et al. (1999). Fragile X premutation is a significant risk factor for premature ovarian failure: the International Collaborative POF in Fragile X study–preliminary data. *Am. J. Med. Genet.* 83, 322–325. doi: 10.1002/(sici)1096-8628(19990402)83:4<322::aid-ajmg17>3.0.co;2-b

Alvarez-Mora, M. I., Rodriguez-Revenga, L., Madrigal, I., Guitart-Mampel, M., Garrabou, G., and Mila, M. (2017). Impaired mitochondrial function and dynamics in the pathogenesis of FXTAS. *Mol. Neurobiol.* 54, 6896–6902. doi: 10.1007/s12035-016-0194-7

Bernasconi, R., Mathivet, P., Bischoff, S., and Marescaux, C. (1999). Gamma-hydroxybutyric acid: an endogenous neuromodulator with abuse potential? *Trends Pharmacol. Sci.* 20, 135–141. doi: 10.1016/s0165-6147(99)01341-3

Bourgeois, J. A., Cogswell, J. B., Hessl, D., Zhang, L., Ono, M. Y., Tassone, F., et al. (2007). Cognitive, anxiety and mood disorders in the fragile X-associated tremor/ataxia syndrome. *Gen. Hosp. Psychiatry* 29, 349–356. doi: 10.1016/j.genhosppsych.2007.03.003

Buijsen, R. A., Visser, J. A., Kramer, P., Severijnen, E. A., Gearing, M., Charlet-Berguerand, N., et al. (2016). Presence of inclusions positive for polyglycine containing protein, FMRpolyG, indicates that repeat-associated non-AUG translation plays a role in fragile X-associated primary ovarian insufficiency. *Hum. Reprod.* 31, 158–168. doi: 10.1093/humrep/dev280

Burte, F., Houghton, D., Lowes, H., Pyle, A., Nesbitt, S., Yarnall, A., et al. (2017). metabolic profiling of Parkinson's disease and mild cognitive impairment. *Mov. Disord.* 32, 927–932.

Cai, R., Zhang, Y., Simmering, J. E., Schultz, J. L., Li, Y., Fernandez-Carasa, I., et al. (2019). Enhancing glycolysis attenuates Parkinson's disease progression in models and clinical databases. *J. Clin. Invest.* 129, 4539–4549. doi: 10.1172/jci129987

Chang, K. L., Pee, H. N., Tan, W. P., Dawe, G. S., Holmes, E., Nicholson, J. K., et al. (2015). Metabolic profiling of CHO-AbetaPP695 cells revealed mitochondrial dysfunction prior to amyloid-beta pathology and potential therapeutic effects of both PPARgamma and PPARalpha Agonisms for Alzheimer's disease. *J. Alzheimers Dis.* 44, 215–231. doi: 10.3233/jad-140429

Chaudhuri, A. D., Kabaria, S., Choi, D. C., Mouradian, M. M., and Junn, E. (2015). MicroRNA-7 promotes glycolysis to protect against 1-Methyl-4-phenylpyridinium-induced cell death. *J. Biol. Chem.* 290, 12425–12434. doi: 10.1074/jbc.m114.625962

Dashty, M. (2013). A quick look at biochemistry: carbohydrate metabolism. *Clin. Biochem.* 46, 1339–1352. doi: 10.1016/j.clinbiochem.2013.04.027

Drozd, M., Delhaye, S., Maurin, T., Castagnola, S., Grossi, M., Brau, F., et al. (2019). Reduction of Fmr1 mRNA levels rescues pathological features in cortical neurons in a model of FXTAS. *Mol. Ther. Nucleic Acids* 18, 546–553. doi: 10.1016/j.omtn.2019.09.018

Elizur, S. E., Friedman Gohas, M., Dratviman-Storobinsky, O., and Cohen, Y. (2019). Pathophysiology mechanisms in Fragile-X primary ovarian insufficiency. *Methods Mol. Biol.* 1942, 165–171. doi: 10.1007/978-1-4939-9080-1_14

Elizur, S. E., Lebovitz, O., Derech-Haim, S., Dratviman-Storobinsky, O., Feldman, B., Dor, J., et al. (2014). Elevated levels of FMR1 mRNA in granulosa cells are associated with low ovarian reserve in FMR1 premutation carriers. *PLoS One* 9:e105121. doi: 10.1371/journal.pone.0105121

Fahy, E., Subramaniam, S., Murphy, R. C., Nishijima, M., Raetz, C. R., Shimizu, T., et al. (2009). Update of the LIPID MAPS comprehensive classification system for lipids. *J. Lipid Res.* 50, S9–S14.

Giulivi, C., Napoli, E., Tassone, F., Halmai, J., and Hagerman, R. (2016a). Plasma biomarkers for monitoring brain pathophysiology in FMR1 premutation carriers. *Front. Mol. Neurosci.* 9:71. doi: 10.3389/fnmol.2016.00071

Giulivi, C., Napoli, E., Tassone, F., Halmai, J., and Hagerman, R. (2016b). Plasma metabolic profile delineates roles for neurodegeneration, pro-inflammatory damage and mitochondrial dysfunction in the FMR1 premutation. *Biochem. J.* 473, 3871–3888. doi: 10.1042/bcj20160585

Gohel, D., Sripada, L., Prajapati, P., Singh, K., Roy, M., Kotadia, D., et al. (2019). FMRpolyG alters mitochondrial transcripts level and respiratory chain complex assembly in Fragile X associated tremor/ataxia syndrome [FXTAS]. *Biochim. Biophys. Acta Mol. Basis Dis.* 1865, 1379–1388. doi: 10.1016/j.bbadis.2019.02.010

Gonzalez-Cabo, P., Ros, S., and Palau, F. (2010). Flavin adenine dinucleotide rescues the phenotype of frataxin deficiency. *PLoS One* 5:e8872. doi: 10.1371/journal.pone.0008872

Guijas, C., Montenegro-Burke, J. R., Domingo-Almenara, X., Palermo, A., Warth, B., Hermann, G., et al. (2018). METLIN: a technology platform for identifying knowns and unknowns. *Anal. Chem.* 90, 3156–3164. doi: 10.1021/acs.analchem.7b04424

Hagerman, R. J., and Hagerman, P. (2016). Fragile X-associated tremor/ataxia syndrome – features, mechanisms and management. *Nat. Rev. Neurol.* 12, 403–412. doi: 10.1038/nrneurol.2016.82

Hagerman, R. J., Leehey, M., Heinrichs, W., Tassone, F., Wilson, R., Hills, J., et al. (2001). Intention tremor, parkinsonism, and generalized brain atrophy in male carriers of fragile X. *Neurology* 57, 127–130. doi: 10.1212/wnl.57.1.127

Hall, D. A., and Berry-Kravis, E. (2018). Fragile X syndrome and fragile X-associated tremor ataxia syndrome. *Handb. Clin. Neurol.* 147, 377–391.

Horai, H., Arita, M., Kanaya, S., Nihei, Y., Ikeda, T., Suwa, K., et al. (2010). MassBank: a public repository for sharing mass spectral data for life sciences. *J. Mass Spectrom* 45, 703–714. doi: 10.1002/jms.1777

Hukema, R. K., Buijsen, R. A., Raske, C., Severijnen, L. A., Nieuwenhuizen-Bakker, I., Minneboo, M., et al. (2014). Induced expression of expanded CGG RNA causes mitochondrial dysfunction in vivo. *Cell Cycle* 13, 2600–2608. doi: 10.4161/15384101.2014.943112

Jacquemont, S., Hagerman, R. J., Leehey, M., Grigsby, J., Zhang, L., Brunberg, J. A., et al. (2003). Fragile X premutation tremor/ataxia syndrome: molecular, clinical, and neuroimaging correlates. *Am. J. Hum. Genet.* 72, 869–878.

Jin, P., Duan, R., Qurashi, A., Qin, Y., Tian, D., Rosser, T. C., et al. (2007). Pur alpha binds to rCGG repeats and modulates repeat-mediated neurodegeneration in a Drosophila model of fragile X tremor/ataxia syndrome. *Neuron* 55, 556–564. doi: 10.1016/j.neuron.2007.07.020

Jin, P., Zarnescu, D. C., Zhang, F., Pearson, C. E., Lucchesi, J. C., Moses, K., et al. (2003). RNA-mediated neurodegeneration caused by the fragile X premutation rCGG repeats in Drosophila. *Neuron* 39, 739–747. doi: 10.1016/s0896-6273(03)00533-6

Johnson, C. H., Ivanisevic, J., and Siuzdak, G. (2016). Metabolomics: beyond biomarkers and towards mechanisms. *Nat. Rev. Mol. Cell Biol.* 17, 451–459. doi: 10.1038/nrm.2016.25

Kogan, C. S., Turk, J., Hagerman, R. J., and Cornish, K. M. (2008). Impact of the Fragile X mental retardation 1 (FMR1) gene premutation on neuropsychiatric functioning in adult males without fragile X-associated Tremor/Ataxia syndrome: a controlled study. *Am. J. Med. Genet. B Neuropsychiatr. Genet.* 147B, 859–872. doi: 10.1002/ajmg.b.30685

Kong, H. E., Lim, J., Zhang, F., Huang, L., Gu, Y., Nelson, D. L., et al. (2019). Metabolic pathways modulate the neuronal toxicity associated with fragile X-associated tremor/ataxia syndrome. *Hum. Mol. Genet.* 28, 980–991. doi: 10.1093/hmg/ddy410

Krans, A., Kearse, M. G., and Todd, P. K. (2016). Repeat-associated non-AUG translation from antisense CCG repeats in fragile X tremor/ataxia syndrome. *Ann. Neurol.* 80, 871–881. doi: 10.1002/ana.24800

Lin, C. C., Cheng, T. L., Tsai, W. H., Tsai, H. J., Hu, K. H., Chang, H. C., et al. (2012). Loss of the respiratory enzyme citrate synthase directly links the Warburg effect to tumor malignancy. *Sci. Rep.* 2:785.

Maceyka, M., and Spiegel, S. (2014). Sphingolipid metabolites in inflammatory disease. *Nature* 510, 58–67. doi: 10.1038/nature13475

Maitre, M., Andriamampandry, C., Kemmel, V., Schmidt, C., Hode, Y., Hechler, V., et al. (2000). Gamma-hydroxybutyric acid as a signaling molecule in brain. *Alcohol* 20, 277–283. doi: 10.1016/s0741-8329(99)00092-0

Man, L., Lekovich, J., Rosenwaks, Z., and Gerhardt, J. (2017). Fragile X-associated diminished ovarian reserve and primary ovarian insufficiency from molecular mechanisms to clinical manifestations. *Front. Mol. Neurosci.* 10:290. doi: 10.3389/fnmol.2017.00290

Mila, M., Alvarez-Mora, M. I., Madrigal, I., and Rodriguez-Revenga, L. (2018). Fragile X syndrome: an overview and update of the FMR1 gene. *Clin. Genet.* 93, 197–205. doi: 10.1111/cge.13075

Napoli, E., Schneider, A., Wang, J. Y., Trivedi, A., Carrillo, N. R., Tassone, F., et al. (2019). Allopregnanolone treatment improves plasma metabolomic profile associated with GABA metabolism in Fragile X-associated tremor/ataxia syndrome: a pilot study. *Mol. Neurobiol.* 56, 3702–3713. doi: 10.1007/s12035-018-1330-3

Napoli, E., Song, G., Schneider, A., Hagerman, R., Eldeeb, M. A., Azarang, A., et al. (2016). Warburg effect linked to cognitive-executive deficits in FMR1 premutation. *FASEB J.* 30, 3334–3351. doi: 10.1096/fj.201600315r

Nobile, V., Palumbo, F., Lanni, S., Ghisio, V., Vitali, A., Castagnola, M., et al. (2020). Altered mitochondrial function in cells carrying a premutation or unmethylated full mutation of the FMR1 gene. *Hum. Genet.* 139, 227–245. doi: 10.1007/s00439-019-02104-7

Ntambi, J. M., and Miyazaki, M. (2004). Regulation of stearoyl-CoA desaturases and role in metabolism. *Prog. Lipid Res.* 43, 91–104. doi: 10.1016/s0163-7827(03)00039-0

Oakley, A. J., Yamada, T., Liu, D., Coggan, M., Clark, A. G., and Board, P. G. (2008). The identification and structural characterization of C7orf24 as gamma-glutamyl cyclotransferase. An essential enzyme in the gamma-glutamyl cycle. *J. Biol. Chem.* 283, 22031–22042. doi: 10.1074/jbc.m803623200

Oh, S. Y., He, F., Krans, A., Frazer, M., Taylor, J. P., Paulson, H. L., et al. (2015). RAN translation at CGG repeats induces ubiquitin proteasome system impairment in models of fragile X-associated tremor ataxia syndrome. *Hum. Mol. Genet.* 24, 4317–4326. doi: 10.1093/hmg/ddv165

Pretto, D. I., Kumar, M., Cao, Z., Cunningham, C. L., Durbin-Johnson, B., Qi, L., et al. (2014). Reduced excitatory amino acid transporter 1 and metabotropic glutamate receptor 5 expression in the cerebellum of fragile X mental retardation gene 1 premutation carriers with fragile X-associated tremor/ataxia syndrome. *Neurobiol. Aging* 35, 1189–1197. doi: 10.1016/j.neurobiolaging.2013.11.009

Schmidt-Rohr, K. (2020). Oxygen is the high-energy molecule powering complex multicellular life: fundamental corrections to traditional bioenergetics. *ACS Omega* 5, 2221–2233. doi: 10.1021/acsomega.9b03352

Sellier, C., Buijsen, R. A. M., He, F., Natla, S., Jung, L., Tropel, P., et al. (2017). Translation of expanded CGG repeats into FMRpolyG is pathogenic and may contribute to Fragile X Tremor ataxia syndrome. *Neuron* 93, 331–347. doi: 10.1016/j.neuron.2016.12.016

Sellier, C., Rau, F., Liu, Y., Tassone, F., Hukema, R. K., Gattoni, R., et al. (2010). Sam68 sequestration and partial loss of function are associated with splicing alterations in FXTAS patients. *Embo J* 29, 1248–1261. doi: 10.1038/emboj.2010.21

Sofola, O. A., Jin, P., Qin, Y., Duan, R., Liu, H., De Haro, M., et al. (2007). RNA-binding proteins hnRNP A2/B1 and CUGBP1 suppress fragile X CGG premutation repeat-induced neurodegeneration in a Drosophila model of FXTAS. *Neuron* 55, 565–571. doi: 10.1016/j.neuron.2007.07.021

Song, G., Napoli, E., Wong, S., Hagerman, R., Liu, S., Tassone, F., et al. (2016). Altered redox mitochondrial biology in the neurodegenerative disorder fragile X-tremor/ataxia syndrome: use of antioxidants in precision medicine. *Mol. Med.* 22, 548–559. doi: 10.2119/molmed.2016.00122

Tassone, F., Iwahashi, C., and Hagerman, P. J. (2004). FMR1 RNA within the intranuclear inclusions of fragile X-associated tremor/ataxia syndrome (FXTAS). *RNA Biol.* 1, 103–105. doi: 10.4161/rna.1.2.1035

Teo, E., Ravi, S., Barardo, D., Kim, H. S., Fong, S., Cazenave-Gassiot, A., et al. (2019). Metabolic stress is a primary pathogenic event in transgenic Caenorhabditis elegans expressing pan-neuronal human amyloid beta. *eLife* 8:e50069.

Todd, P. K., Oh, S. Y., Krans, A., He, F., Sellier, C., Frazer, M., et al. (2013). CGG repeat-associated translation mediates neurodegeneration in fragile X tremor ataxia syndrome. *Neuron* 78, 440–455. doi: 10.1016/j.neuron.2013.03.026

Urbanczyk-Wochniak, E., Luedemann, A., Kopka, J., Selbig, J., Roessner-Tunali, U., Willmitzer, L., et al. (2003). Parallel analysis of transcript and metabolic profiles: a new approach in systems biology. *EMBO Rep* 4, 989–993. doi: 10.1038/sj.embor.embor944

Van Assche, R., Temmerman, L., Dias, D. A., Boughton, B., Boonen, K., Braeckman, B. P., et al. (2015). Metabolic profiling of a transgenic *Caenorhabditis elegans* Alzheimer model. *Metabolomics* 11, 477–486. doi: 10.1007/s11306-014-0711-5

Verdin, E. (2015). NAD(+) in aging, metabolism, and neurodegeneration. *Science* 350, 1208–1213. doi: 10.1126/science.aac4854

Verwaest, K. A., Vu, T. N., Laukens, K., Clemens, L. E., Nguyen, H. P., Van Gasse, B., et al. (2011). (1)H NMR based metabolomics of CSF and blood serum: a metabolic profile for a transgenic rat model of Huntington disease. *Biochim. Biophys. Acta* 1812, 1371–1379. doi: 10.1016/j.bbadis.2011.08.001

Wang, X., Zhang, R., Lin, Y., and Shi, P. (2020). Inhibition of NF-kappaB might enhance the protective role of roflupram on SH-SY5Y cells under amyloid beta stimulation via PI3K/AKT/mTOR signaling pathway. *Int. J. Neurosci.* doi: 10.1080/00207454.2020.1759588 [Epub ahead of print].

Warburg, O. (1956). On respiratory impairment in cancer cells. *Science* 124, 269–270.

Wishart, D. S. (2019). Metabolomics for investigating physiological and pathophysiological processes. *Physiol. Rev.* 99, 1819–1875. doi: 10.1152/physrev.00035.2018

Wishart, D. S., Feunang, Y. D., Marcu, A., Guo, A. C., Liang, K., Vazquez-Fresno, R., et al. (2018). HMDB 4.0: the human metabolome database for 2018. *Nucleic Acids Res.* 46, D608–D617.

Wu, J., Fu, B., Lei, H., Tang, H., and Wang, Y. (2016). Gender differences of peripheral plasma and liver metabolic profiling in APP/PS1 transgenic AD mice. *Neuroscience* 332, 160–169. doi: 10.1016/j.neuroscience.2016.06.049

Yao, J., and Brinton, R. D. (2012). Estrogen regulation of mitochondrial bioenergetics: implications for prevention of Alzheimer's disease. *Adv. Pharmacol.* 64, 327–371. doi: 10.1016/b978-0-12-394816-8.00010-6

Zhao, H., Wang, C., Zhao, N., Li, W., Yang, Z., Liu, X., et al. (2018). Potential biomarkers of Parkinson's disease revealed by plasma metabolic profiling. *J. Chromatogr. B Anal. Technol. Biomed. Life Sci.* 1081-1082, 101–108. doi: 10.1016/j.jchromb.2018.01.025

Conflict of Interest: The authors declare that the research was conducted in the absence of any commercial or financial relationships that could be construed as a potential conflict of interest.

frontiers in Genetics

PERSPECTIVE
published: 08 October 2020
doi: 10.3389/fgene.2020.586910

Cardiovascular Problems in the Fragile X Premutation

*Nattaporn Tassanakijpanich[1,2], Jonathan Cohen[3], Rashelle Cohen[3], Uma N. Srivatsa[4] and Randi J. Hagerman[1,5]**

[1] UC Davis MIND Institute, UC Davis Health, Sacramento, CA, United States, [2] Department of Pediatrics, Faculty of Medicine, Prince of Songkla University, Songkhla, Thailand, [3] Fragile X Alliance Clinic, Genetic Clinics Australia, Melbourne, VIC, Australia, [4] Division of Cardiovascular Medicine, Department of Internal Medicine, UC Davis Medical Center, Sacramento, CA, United States, [5] Department of Pediatrics, University of California, Davis, Davis, School of Medicine, Sacramento, CA, United States

There is a dearth of information about cardiovascular problems in fragile X premutation carriers who have 55–200 CGG repeats in fragile X mental retardation 1 (*FMR1*) gene. The *FMR1* expansion in the premutation range leads to toxic RNA gain-of-function resulting in cellular dysregulation. The mechanism of RNA toxicity underlies all of the premutation disorders including fragile X-associated tremor/ataxia syndrome, fragile X-associated primary ovarian insufficiency, and fragile X-associated neuropsychiatric disorder. Cardiovascular problems particularly autonomic dysfunction, hypertension, and cardiac arrhythmias are not uncommon in premutation carriers. Some arterial problems and valvular heart diseases have also been reported. This article reviews cardiovascular problems in premutation carriers and discusses possible contributing mechanisms including RNA toxicity and mild fragile X mental retardation protein deficiency. Further research studies are needed in order to prove a direct association of the cardiovascular problems in fragile X premutation carriers because such knowledge will lead to better preventative treatment.

Keywords: fragile X, *FMR1*, premutation, cardiovascular, arrhythmia, autonomic dysfunction, hypertension

OPEN ACCESS

Edited by:
Renate K. Hukema, Rotterdam University of Applied Sciences, Netherlands

Reviewed by:
Rita Selvatici, University of Ferrara, Italy
Charlotte L. Alston, Wellcome Trust Centre for Mitochondrial Research (WT), United Kingdom

***Correspondence:**
Randi J. Hagerman
rjhagerman@ucdavis.edu

Specialty section:
This article was submitted to Genetics of Common and Rare Diseases, a section of the journal Frontiers in Genetics

Received: *24 July 2020*
Accepted: *21 September 2020*
Published: *08 October 2020*

Citation:
Tassanakijpanich N, Cohen J, Cohen R, Srivatsa UN and Hagerman RJ (2020) Cardiovascular Problems in the Fragile X Premutation. Front. Genet. 11:586910. doi: 10.3389/fgene.2020.586910

INTRODUCTION

The Fragile X Mental Retardation 1 (*FMR1*) gene is located at Xq27.3 and the 5′-untranslated region contains a trinucleotide repeat of cytosine-guanine-guanine (CGG), that has a normal range of 5 to 45 repeats with a mean of 30 in the general population. The full mutation of the *FMR1* gene contains >200 CGG repeats and this causes fragile X syndrome (FXS), the most common inherited cause of intellectual disability and the most common single gene cause of autism spectrum disorder. This condition leads to silencing of *FMR1* gene by methylation and subsequent loss of its product,

Abbreviations: ADHD, Attention-deficit/hyperactivity disorder; CGG, Cytosine-guanine-guanine; *FMR1*, Fragile X mental retardation 1; FMRP, Fragile X mental retardation protein; FXAND, Fragile X-associated neuropsychiatric disorders; FXPOI, Fragile X-associated primary ovarian insufficiency; FXS, Fragile X syndrome; FXTAS, Fragile X-associated tremor/ataxia syndrome; MMP, Matrix metalloproteinase; MRI, Magnetic resonance imaging; mRNA, Messenger RNA; SCAD, Spontaneous coronary artery dissection; SD, Standard deviation.

fragile X mental retardation protein (FMRP). FMRP is a messenger RNA (mRNA)-binding protein and regulates translation at the synapse of hundreds of mRNAs essential for synaptic plasticity. Therefore, its absence leads to significant cognitive and social impairment (Hagerman et al., 2017; Rajaratnam et al., 2017).

Moreover, cardiovascular problems including mitral valve prolapse, aortic root dilatation, and hypertension are commonly documented in individuals with FXS (Loehr et al., 1986; Waldstein and Hagerman, 1988; Sreeram et al., 1989; Utari et al., 2010; Ramírez-Cheyne et al., 2019). These problems were explained as a result of diminished or absent FMRP which leads to abnormal connective tissue structures including shortened and fragmented elastin fibers. However, cardiovascular conditions in premutation carriers, who have 55–200 CGG repeats on *FMR1* gene, are still rarely recognized except in occasional case studies (Riddle et al., 1998; Jacquemont et al., 2003; Coffey et al., 2008; Chonchaiya et al., 2010; Hunsaker et al., 2011; Hamlin et al., 2012). Since the premutation is common, 1 per 200 in women and 1 per 400 in men (Tassone et al., 2012b), the cardiovascular problems which can occur in carriers are relatively common. Our aim in this review is to advance understanding about possible risks and mechanisms of cardiovascular disorders in premutation carriers which will hopefully stimulate further research and treatment studies.

THE FRAGILE X PREMUTATION

Unlike individuals with FXS who usually have remarkable clinical features including intellectual disability, autism spectrum disorder, macroorchidism, hyperactivity, prominent ears, and hyperextensible finger joints, the premutation carriers have subtle presentations. Medical problems which are increased in carriers compared to controls without the premutation include autoimmune diseases (Winarni et al., 2012), premature menopause before age 40 and fertility problems (fragile X-associated primary ovarian insufficiency; FXPOI) (Wheeler et al., 2014; Campbell et al., 2016), and the neurodegenerative disorder involving an intention tremor, ataxia and cognitive decline later in life called the fragile X-associated tremor/ataxia syndrome (FXTAS) (Jacquemont et al., 2004; Hagerman and Hagerman, 2016). FXPOI is seen in approximately 20% of female carriers and FXTAS is seen in 40% of male carriers and approximately 13% of female carriers. In addition, psychiatric problems are common, particularly anxiety, depression, obsessive-compulsive disorder, mood disorder, and they fall under the umbrella term of fragile X-associated neuropsychiatric disorders (FXAND). One or more of these psychiatric problems can affect up to 50% of carriers (Wheeler et al., 2014; Hagerman et al., 2018).

Cardiovascular problems in premutation carriers have been documented but most cases were mentioned indirectly as a part of case studies or reviews about FXTAS. Here we present case histories of three carriers who had significant cardiovascular conditions along with a review of the literature of each condition in carriers.

CASE PRESENTATION

Case 1

A 61-year-old female with a *FMR1* premutation allele of 76 CGG repeats who is physically active. She has two children with FXS, so they were the initial probands. Her father also had FXTAS and he had ischemic heart disease. She has hyperextensible joints and recurrent knee dislocation with skiing. She had a 4 year history of paroxysmal atrial fibrillation largely controlled with sotalol hydrochloride 40 mg twice daily. Whilst not aware of palpitations, she did note exertional breathlessness and slight limitation of her physical activity. She also noted pre-syncopal symptoms related to conversion pauses which would occur on average 2–3 times per week. Holter electrocardiogram monitoring confirmed her to have paroxysmal episodes of atrial fibrillation up to 7 h at a time, with significant conversion pauses of up to 2.3 s in length. This also demonstrated periods of rapid ventricular response with up to 130 bpm. Her exercise thallium scan result was normal, and her echocardiogram and cardiac computer tomography revealed trivial pericardial effusion. Laboratory panel results were unremarkable. Medications included atorvastatin 40 mg daily, aspirin 100 mg daily, sotalol hydrochloride 40 mg twice daily, denosumab 60 mg twice yearly.

Physical examination showed normal vital signs although often with an irregular pulse consistent with atrial fibrillation. Aside from a narrow face and slightly protuberant ears, there were no other stigmata associated with her fragile X premutation of 76 CGG repeats. Cardiovascular examination was normal.

Primarily in view of her symptomatic conversion pauses and refractoriness and intolerance to higher doses of medications, pulmonary vein isolation and atrial ablation were successfully performed. She remained in sinus rhythm and was discharged home on sotalol 40 mg twice daily and dabigatran 110 mg twice daily for 2 months and is followed in cardiology clinic.

Review of Literature: Cardiac Arrhythmia in the Premutation

Cardiac arrhythmia is not uncommon in premutation carriers especially in those who have FXTAS. Characteristics include atrial fibrillation (Greco et al., 2006), sick sinus syndrome (Greco et al., 2006), and unspecified cardiac arrhythmia (Hunsaker et al., 2011; Tassone et al., 2012a) have been reported. Many carriers who are elderly have significant bradycardia or other arrhythmia which requires a pacemaker (Greco et al., 2006; Hunsaker et al., 2011; Tassone et al., 2012a). There is only a rare report of arrhythmias in carriers without FXTAS including one case of a 7-years 6-month-old boy with an unmethylated 58 CGG repeats on *FMR1* gene who had multiple premature ventricular contractions (Tassone et al., 2000b). However, no direct study about cardiac arrhythmia in carriers of the premutation has been published.

Case 2

Case 2 is a 60-year-old female with a *FMR1* premutation allele of 73 CGG repeats. Her father passed away at the age of 79 from FXTAS and congestive heart failure. Postural tremor in left

hand started at age 49 followed by handwriting and memory problem at age 52 and decrease vibration sense in both feet at age 58. White matter lesions on brain magnetic resonance imaging (MRI) findings were consistent with FXTAS.

Mitral valve prolapse and regurgitation was detected when she was 53 years old. She also had orthostatic hypotension and autonomic instability when she was 57 years old. Hypertension has been noted since age 58. Tricuspid valve regurgitation, smaller left ventricle, and left ventricular outflow tract obstruction were also documented. She takes 25 mg of metoprolol for her cardiac conditions.

Review of Literature: Autonomic Dysfunction in the Premutation

Autonomic dysfunction is a common problem in the premutation carriers especially with FXTAS and it usually precedes diagnosis of FXTAS (Jacquemont et al., 2003, 2004; Pugliese et al., 2004; Leehey, 2009; Hagerman and Hagerman, 2013). In non-FXTAS carriers, a study found that the premutation females had reduced vagal tone which reflects impaired parasympathetic response (Klusek et al., 2017). In terms of cardiovascular disorders, the clinical presentation of autonomic dysfunction includes episodic hypotension (Pugliese et al., 2004; Greco et al., 2006; Gokden et al., 2009; Hagerman and Hagerman, 2013) and hypertension (Jacquemont et al., 2003; Coffey et al., 2008; Chonchaiya et al., 2010; Hamlin et al., 2012). Hypertension is the only condition which has been studied directly compared to controls and it is increased in carriers particularly those with FXTAS (Coffey et al., 2008; Hamlin et al., 2012).

Hypertension is highly prevalent in the premutation carriers particularly in the carriers with FXTAS. Since the Jacquemont et al. (2003) paper found that 50% of the premutation males had hypertension, there have been several studies which focused on prevalence of hypertension in premutation carriers. In females, a study found that 16.4% of premutation females without FXTAS had been diagnosed with hypertension compared with 10.1% in the age-matched control females (Coffey et al., 2008). The association was significant in females with FXTAS, where 61.1% had a history of hypertension compared with 18% of age-match control females (Coffey et al., 2008). In addition, hypertension tended to be more prevalent in premutation females who were daughters of males with FXTAS than the other carriers although there was no statistical significance (18.09 vs. 8.33%, respectively; $p = 0.28$) (Chonchaiya et al., 2010).

In premutation males, the results were consistent with findings in premutation females. A study of Hamlin et al. (2012) found that premutation males age 40 and above had 1.61 higher risk of having hypertension than controls. Their mean systolic blood pressure was 136.73 (SD 14.5) and diastolic blood pressure was 81.45 (SD 7.99) even on hypertensive medication. The risk of having hypertension was significant in the premutation males with FXTAS. They had an odds ratio 3.22 to have hypertension compare with age-matched control males. This study found that 67% of the premutation males with FXTAS and 41.5% of the premutation males without FXTAS had hypertension compare with 27.4% in the control group. Data about age of onset is still inconclusive since it was gathered retrospectively; however, it seemed comparable between the carriers and age-matched controls (Chonchaiya et al., 2010; Hamlin et al., 2012).

Review of Literature: Valvular Heart Disease in the Premutation

Valvular heart disease including mitral regurgitation and aortic stenosis in premutation carriers have been reported in individuals with FXTAS and some of them needed valvular replacement (Greco et al., 2006; Hunsaker et al., 2011).

Case 3

A 41-year-old male with a *FMR1* premutation allele of 84 CGG repeats presented with a history of early connective tissue problems that included an umbilical hernia at 5 years old, recurrent bilateral muscle tears in the gastrocnemius muscles beginning at age 38, and spontaneous subluxation of the proximal interphalangeal joint of his right middle finger. Anxiety with panic attacks, migraine headaches, and obstructive sleep apnea has been described in his medical history. His daughter has the premutation and was the proband for the family.

At age 41, he was diagnosed with a dissection of the right upper cervical internal carotid artery extending into the proximal right petrous segment causing 60% luminal narrowing. He also had the right vertebral arterial dissection at C2 level, measuring 4 mm and a small left proximal cavernous internal carotid aneurysm. He did not undergo surgical intervention and was treated with aspirin 81 mg per day. Follow-up brain MRI was done 3 months after he was diagnosed which demonstrated significant resolution of the dissection and aneurysm.

Review of Literature: Arterial Dissection and Aneurysm in the Premutation

This is the first report of internal carotid artery dissection, vertebral artery dissection, and internal carotid aneurysm in the premutation. Similarly, thoracic aortic dissection and abdominal aortic aneurysm have been reported as a cause of death in a 69-year-old male with FXTAS (Gokden et al., 2009). Recently, three premutation females with spontaneous coronary artery dissection (SCAD) who presented with chest pain have been documented (Park et al., 2017; McKenzie et al., 2020). These conditions have shared pathophysiology which is weakening arterial wall integrity from abnormal connective tissue morphology and inflammation (Hashimoto et al., 2006; Dogan et al., 2008; Sadasivan et al., 2013; Hayes et al., 2018; Yetkin and Ozturk, 2018).

DISCUSSION

We report cases of atrial fibrillation, autonomic dysfunction, and vascular dissection in premutation carriers. To the best of our knowledge, this is the first perspective of cardiovascular problems in association with the fragile X premutation. We would like to postulate possible mechanisms for such an association: (1) RNA

toxicity and (2) FMRP deficiency. They both play a role in each condition, but they are not mutually exclusive (**Figure 1**).

The First Mechanism: RNA Toxicity

The concept of RNA toxicity has been reviewed extensively in FXTAS (Greco et al., 2006; Hagerman and Hagerman, 2013, 2016). In the premutation range, transcription of *FMR1* mRNA is enhanced compared to normal and the *FMR1* mRNA levels increase as the CGG repeat increases (Tassone et al., 2000a, 2007; Kenneson et al., 2001). Two mechanisms resulting from excessive mRNA are explained (Hagerman and Hagerman, 2015). The first mechanism is a post-transcriptional mechanism. The elevation of the mRNA sequestrates and binds to RNA binding proteins (i.e., DROSHA, DGCR8, Sam68, and HNRNPA2B1) and the sequestration of DROSHA/DGCR8 down regulates microRNA which are important for maintaining normal cellular functions (Garcia-Arocena and Hagerman, 2010; Sellier et al., 2010, 2013, 2014; Hagerman and Hagerman, 2013). The mRNA may also mistranslate because of RAN translation to FMRpolyG protein meaning FMRP with a polyglycine tail which is toxic to cells (Sellier et al., 2014, 2017). The second is a co-transcriptional mechanism. Increasing *FMR1* gene transcription links to elevation of R-loop formation and subsequently ineffective clearance of DNA damage repair responses (Loomis et al., 2014). These mechanisms cause mitochondrial dysfunction (Napoli et al., 2011; Song et al., 2016), disrupted intracellular calcium regulation (Robin et al., 2017), and eventually potentiate oxidative stress and inflammatory responses in the cells (Sellier et al., 2014; Hagerman and Hagerman, 2016). Elevated mRNA levels correlated with shorten neuronal survival and abnormal neuronal development in animal models with the *FMR1* premutation (Chen et al., 2010; Kaplan et al., 2012). Evidence of RNA toxicity and the sequestration of proteins is displayed as intranuclear inclusions in those with FXTAS which contain mRNA (Tassone et al., 2004) and the sequestered proteins (Iwahashi et al., 2006; Buijsen et al., 2014, 2016; Ma et al., 2019).

Other than in neuronal cells, the inclusions of FXTAS were also found in various organs including subepicardial autonomic ganglia, peripheral nervous system neurons, cardiomyocytes, and mitral valves (Greco et al., 2006; Gokden et al., 2009; Hunsaker et al., 2011; Buijsen et al., 2014) in addition to elevated mRNA levels (Greco et al., 2006; Hunsaker et al., 2011), therefore autonomic dysfunction which includes hypertension

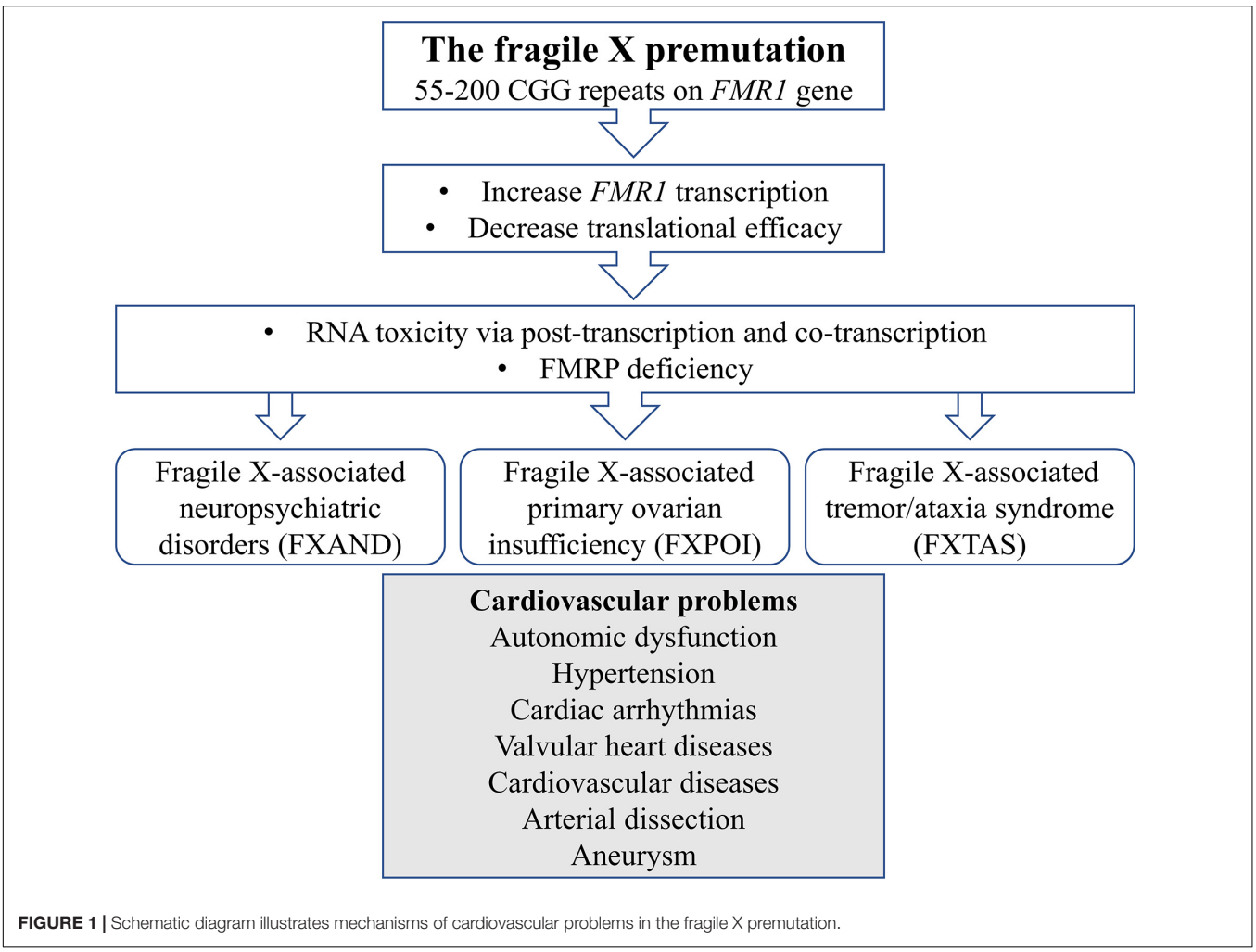

FIGURE 1 | Schematic diagram illustrates mechanisms of cardiovascular problems in the fragile X premutation.

and cardiac arrhythmia are hypothesized to be a consequence of RNA toxicity. Increasing CGG repeats are also positively correlated with the numbers of inclusions (Greco et al., 2006). Moreover, anatomical and functional changes as well as findings of inclusion bodies in brain areas which regulate autonomic functions also support the hypothesis of RNA toxicity as a mechanism of autonomic dysfunction (Greco et al., 2006; Brown and Stanfield, 2015).

The mechanism of RNA toxicity may partly contribute to the explanation of cardiovascular conditions which link to connective tissue problems; these are arterial dissection (Hayes et al., 2018), aneurysm (Hashimoto et al., 2006; Sadasivan et al., 2013; Yetkin and Ozturk, 2018), and valvular heart disease (El Sabbagh et al., 2018). Increase inflammation and oxidative stress in carriers stimulated by RNA toxicity, have been thought to be an underlying pathophysiology in intracranial aneurysm (Hashimoto et al., 2006; Sadasivan et al., 2013; Yetkin and Ozturk, 2018) and arterial dissection (Hayes et al., 2018).

The Second Mechanism: FMRP Deficiency

The mechanism might link to cardiovascular problems relate to connective tissue disorder in the carriers. The higher CGG repeats in carriers, especially more than 120 repeats, inversely correlate with FMRP levels (Pretto et al., 2014; Kim et al., 2019) which relates to some characteristics of connective tissue problems such as prominent ears (Riddle et al., 1998), elongated face, and hyperextensible finger joint (Loesch et al., 2003). The impact of FMRP deficiency on connective tissue has been well studied and reviewed in those with FXS (Ramírez-Cheyne et al., 2019). A pathological finding from a male with FXS showed abnormal structure and pattern of elastin, collagen, and acid mucopolysaccharide substrate in tissue samples from aorta, mitral and tricuspid valves, and forearm skin (Waldstein and Hagerman, 1988). From molecular studies, dysregulation of extracellular matrix-related proteins which are regulated by FMRP has been confirmed in FXS. These include matrix metalloproteinases (MMPs), elastin, and actin which are components of connective tissue structure (Ramírez-Cheyne et al., 2019).

The impact of FMRP deficiency on connective tissue in premutation carriers has not been studied. In respect to cardiovascular findings, diminished FMRP might affect endothelial integrity via alteration of MMP-9 expression which is hypothesized as a pathophysiology of dilating arteries (Hashimoto et al., 2006; Dogan et al., 2008; Sadasivan et al., 2013; Yetkin and Ozturk, 2018) and arterial dissection including SCAD (McKenzie et al., 2020). Moreover, the mechanism might lead to less elastic and stiffer vessels especially in those with a high CGG repeat range where FMRP is more deficient (Pretto et al., 2014).

Nonetheless, FMRP levels begin to be lower than average in individuals with a CGG above 120 (Pretto et al., 2014). RNA toxicity may also contribute to the connective tissue problems to some degree as a study found an association between some physical features of connective tissue disorder in the carriers who had normal FMRP level but high mRNA level (Basuta et al., 2011). Furthermore, intranuclear inclusions have been identified in mitral valve tissue from a carrier with mitral regurgitation who had high level of mRNA (Hunsaker et al., 2011). However, it is important to realize that mRNA and FMRP levels were measured in blood samples, so they might not represent actual levels in tissues (Tassone et al., 2000b) and need to be confirmed by direct studies.

Future Directions

To better understand the risk of having cardiovascular problems in premutation carriers, more direct studies are needed in aspects of prevalence, age of onset, and mechanisms involved. For clinical implications, previous data currently proves that the premutation carriers have high risk of having hypertension (Coffey et al., 2008; Hamlin et al., 2012). Untreated hypertension not only contributes to atherosclerosis, but also causes white matter hyperintensity lesions in the brain which relate to impaired executive function, activities of daily living, gait speed, and mood (Hajjar et al., 2011). Therefore, it is very important to monitor blood pressure and treat as indicated.

In the aspect of cardiovascular diseases, chronic hypoestrogenism in the premutation females with FXPOI probably heightens risk of cardiovascular diseases via various mechanisms particularly atherosclerosis (Morselli et al., 2017). Early detection for FXPOI is crucial and the role of hormonal replacement therapy to reduce risk of having cardiovascular disease needs to be considered (Cobin et al., 2017). Nevertheless, research about the risk of having cardiovascular diseases in the premutation carriers has not been published. Even though ischemic heart disease and congestive heart failure have been reported in individuals with FXTAS (Jacquemont et al., 2003; Greco et al., 2006; Gokden et al., 2009), most of them are males and the mechanism is still unclear. Since FXTAS is associated with increasing mitochondria dysfunction (Napoli et al., 2011; Song et al., 2016), it is likely that end stage FXTAS is associated with such severe mitochondrial dysfunction that the congestive heart failure is also related to the lack of energy from mitochondrial problems (Brown et al., 2017; Zhou and Tian, 2018). Further study to confirm the association is necessary and a treatment for the mitochondrial dysfunction may eventually help myocardial function in aging carriers.

Finally, since neuropsychiatric disorders in carriers called FXAND are very common (Hagerman et al., 2018) and a long history of emotional intensity can lead to enhanced catecholamine release which could aggravate cardiovascular problems including cardiomyopathy (Wittstein et al., 2005), hypertension (Hamlin et al., 2012), and SCAD (McKenzie et al., 2020), therefore, treatment of FXAND should be kept in mind.

CONCLUSION

The fragile X premutation carriers are likely to have health conditions throughout their life. This review underscores cardiovascular problems commonly seen in premutation carriers

and alerts cardiologists and other clinicians to test for the premutation when necessary, watch for these problems and treat the conditions that arise related to the premutation.

DATA AVAILABILITY STATEMENT

The original contributions presented in the study are included in the article/supplementary material, further inquiries can be directed to the corresponding author/s.

ETHICS STATEMENT

The studies involving human participants were reviewed and approved by Institutional Review Board at the University of California, Davis. The patients/participants provided their written informed consent to participate in this study. Written informed consent was obtained from the individual(s) for the publication of any potentially identifiable images or data included in this article.

AUTHOR CONTRIBUTIONS

NT, JC, RC, US, and RH discussed the manuscript content. JC, RC, and RH wrote case histories. NT wrote the first draft. All the authors reviewed and edited the manuscript before submission. All authors contributed to the article and approved the submitted version.

FUNDING

This work was supported by the National Institute of Child Health and Human Development grant R01 HD036071, the Tides Foundation, and the MIND Institute Intellectual and Development Disability Research Centers U54 HD079125.

ACKNOWLEDGMENTS

We thank Dr. Jordan I. Ziegler who provided imaging information for a case in this manuscript.

REFERENCES

Basuta, K., Narcisa, V., Chavez, A., Kumar, M., Gane, L., Hagerman, R., et al. (2011). Clinical phenotypes of a juvenile sibling pair carrying the fragile X premutation. *Am. J. Med. Genet. A.* 155A, 519–525. doi: 10.1002/ajmg.a.33446

Brown, D. A., Perry, J. B., Allen, M. E., Sabbah, H. N., Stauffer, B. L., Shaikh, S. R., et al. (2017). Mitochondrial function as a therapeutic target in heart failure. *Nat. Rev. Cardiol.* 14, 238–250. doi: 10.1038/nrcardio.2016.203

Brown, S. S. G., and Stanfield, A. C. (2015). Fragile X premutation carriers: a systematic review of neuroimaging findings. *J. Neurol. Sci.* 352, 19–28. doi: 10.1016/j.jns.2015.03.031

Buijsen, R. A., Sellier, C., Severijnen, L.-A. W., Oulad-Abdelghani, M., Verhagen, R. F., Berman, R. F., et al. (2014). FMRpolyG-positive inclusions in CNS and non-CNS organs of a fragile X premutation carrier with fragile X-associated tremor/ataxia syndrome. *Acta Neuropathol Commun.* 2:162. doi: 10.1186/s40478-014-0162-2

Buijsen, R. A. M., Visser, J. A., Kramer, P., Severijnen, E. A. W. F. M., Gearing, M., Charlet-Berguerand, N., et al. (2016). Presence of inclusions positive for polyglycine containing protein, FMRpolyG, indicates that repeat-associated non-AUG translation plays a role in fragile X-associated primary ovarian insufficiency. *Hum. Reprod.* 31, 158–168. doi: 10.1093/humrep/dev280

Campbell, S., Eley, S. E. A., McKechanie, A. G., and Stanfield, A. C. (2016). Endocrine dysfunction in female FMR1 premutation carriers: characteristics and association with ill health. *Genes* 7:101. doi: 10.3390/genes7110101

Chen, Y., Tassone, F., Berman, R. F., Hagerman, P. J., Hagerman, R. J., Willemsen, R., et al. (2010). Murine hippocampal neurons expressing Fmr1 gene premutations show early developmental deficits and late degeneration. *Hum. Mol. Genet.* 19, 196–208. doi: 10.1093/hmg/ddp479

Chonchaiya, W., Nguyen, D. V., Au, J., Campos, L., Berry-Kravis, E. M., Lohse, K., et al. (2010). Clinical involvement in daughters of men with fragile X-associated tremor ataxia syndrome. *Clin. Genet.* 78, 38–46. doi: 10.1111/j.1399-0004.2010.01448.x

Cobin, R. H., Goodman, N. F., and Aace Reproductive Endocrinology Scientific Committee. (2017). American association of clinical endocrinologists and American college of endocrinology position statement on menopause-2017 update. *Endocr. Pract.* 23, 869–880. doi: 10.4158/EP171828.PS

Coffey, S. M., Cook, K., Tartaglia, N., Tassone, F., Nguyen, D. V., Pan, R., et al. (2008). Expanded clinical phenotype of women with the FMR1 premutation. *Am. J. Med. Genet. A.* 146A, 1009–1016. doi: 10.1002/ajmg.a.32060

Dogan, A., Tuzun, N., Turker, Y., Akcay, S., Kaya, S., and Ozaydin, M. (2008). Matrix metalloproteinases and inflammatory markers in coronary artery ectasia: their relationship to severity of coronary artery ectasia. *Coron. Artery. Dis.* 19, 559–563. doi: 10.1097/MCA.0b013e3283109079

El Sabbagh, A., Reddy, Y. N. V., and Nishimura, R. A. (2018). Mitral valve regurgitation in the contemporary era: insights into diagnosis, management, and future directions. *Cardiovasc. Imaging.* 11, 628–643. doi: 10.1016/j.jcmg.2018.01.009

Garcia-Arocena, D., and Hagerman, P. J. (2010). Advances in understanding the molecular basis of FXTAS. *Hum. Mol. Genet.* 19, R83–R89. doi: 10.1093/hmg/ddq166

Gokden, M., Al-Hinti, J. T., and Harik, S. I. (2009). Peripheral nervous system pathology in fragile X tremor/ataxia syndrome (FXTAS). *Neuropathology.* 29, 280–284. doi: 10.1111/j.1440-1789.2008.00948.x

Greco, C. M., Berman, R. F., Martin, R. M., Tassone, F., Schwartz, P. H., Chang, A., et al. (2006). Neuropathology of fragile X-associated tremor/ataxia syndrome (FXTAS). *Brain* 129, 243–255. doi: 10.1093/brain/awh683

Hagerman, P. J., and Hagerman, R. J. (2015). Fragile X-associated tremor/ataxia syndrome. *Ann. N. Y. Acad. Sci.* 1338, 58–70. doi: 10.1111/nyas.12693

Hagerman, R., and Hagerman, P. (2013). Advances in clinical and molecular understanding of the FMR1 premutation and fragile X-associated tremor/ataxia syndrome. *Lancet. Neurol.* 12, 786–798. doi: 10.1016/S1474-4422(13)70125-X

Hagerman, R. J., Berry-Kravis, E., Hazlett, H. C., Bailey, D. B. Jr., Moine, H., Kooy, R. F., et al. (2017). Fragile X syndrome. *Nat. Rev. Dis. Primers.* 3:17065. doi: 10.1038/nrdp.2017.65

Hagerman, R. J., and Hagerman, P. (2016). Fragile X-associated tremor/ataxia syndrome - features, mechanisms and management. *Nat. Rev. Neurol.* 12, 403–412. doi: 10.1038/nrneurol.2016.82

Hagerman, R. J., Protic, D., Rajaratnam, A., Salcedo-Arellano, M. J., Aydin, E. Y., and Schneider, A. (2018). Fragile X-associated neuropsychiatric disorders (FXAND). *Front. Psychiatry.* 9:564. doi: 10.3389/fpsyt.2018.00564

Hajjar, I., Quach, L., Yang, F., Chaves, P. H. M., Newman, A. B., Mukamal, K., et al. (2011). Hypertension, white matter hyperintensities and concurrent impairments in mobility, cognition and mood: the cardiovascular health study. *Circulation* 123, 858–865. doi: 10.1161/CIRCULATIONAHA.110.978114

Hamlin, A. A., Sukharev, D., Campos, L., Mu, Y., Tassone, F., Hessl, D., et al. (2012). Hypertension in FMR1 premutation males with and without fragile X-associated tremor/ataxia syndrome (FXTAS). *Am. J. Med. Genet. A.* 158A, 1304–1309. doi: 10.1002/ajmg.a.35323

Hashimoto, T., Meng, H., and Young, W. L. (2006). Intracranial aneurysms: links among inflammation, hemodynamics and vascular remodeling. *Neurol. Res.* 28, 372–380. doi: 10.1179/016164106X14973

Hayes, S. N., Kim, E. S. H., Saw, J., Adlam, D., Arslanian-Engoren, C., Economy, K. E., et al. (2018). Spontaneous coronary artery dissection: current state of the science: a scientific statement from the American heart association. *Circulation* 137, e523–e557. doi: 10.1161/CIR.0000000000000564

Hunsaker, M. R., Greco, C. M., Spath, M. A., Smits, A. P. T., Navarro, C. S., Tassone, F., et al. (2011). Widespread non-central nervous system organ pathology in fragile X premutation carriers with fragile X-associated tremor/ataxia syndrome and CGG knock-in mice. *Acta. Neuropathol.* 122, 467–479. doi: 10.1007/s00401-011-0860-9

Iwahashi, C. K., Yasui, D. H., An, H.-J., Greco, C. M., Tassone, F., Nannen, K., et al. (2006). Protein composition of the intranuclear inclusions of FXTAS. *Brain* 129, 256–271. doi: 10.1093/brain/awh650

Jacquemont, S., Hagerman, R. J., Leehey, M., Grigsby, J., Zhang, L., Brunberg, J. A., et al. (2003). Fragile X premutation tremor/ataxia syndrome: molecular, clinical, and neuroimaging correlates. *Am. J. Hum. Genet.* 72, 869–878. doi: 10.1086/374321

Jacquemont, S., Hagerman, R. J., Leehey, M. A., Hall, D. A., Levine, R. A., Brunberg, J. A., et al. (2004). Penetrance of the fragile X-associated tremor/ataxia syndrome in a premutation carrier population. *JAMA* 291, 460–469. doi: 10.1001/jama.291.4.460

Kaplan, E. S., Cao, Z., Hulsizer, S., Tassone, F., Berman, R. F., Hagerman, P. J., et al. (2012). Early mitochondrial abnormalities in hippocampal neurons cultured from Fmr1 premutation mouse model. *J. Neurochem.* 123, 613–621. doi: 10.1111/j.1471-4159.2012.07936.x

Kenneson, A., Zhang, F., Hagedorn, C. H., and Warren, S. T. (2001). Reduced FMRP and increased FMR1 transcription is proportionally associated with CGG repeat number in intermediate-length and premutation carriers. *Hum. Mol. Genet.* 10, 1449–1454. doi: 10.1093/hmg/10.14.1449

Kim, K., Hessl, D., Randol, J. L., Espinal, G. M., Schneider, A., Protic, D., et al. (2019). Association between IQ and FMR1 protein (FMRP) across the spectrum of CGG repeat expansions. *PLoS. One* 14:e0226811. doi: 10.1371/journal.pone.0226811

Klusek, J., LaFauci, G., Adayev, T., Brown, W. T., Tassone, F., and Roberts, J. E. (2017). Reduced vagal tone in women with the FMR1 premutation is associated with FMR1 mRNA but not depression or anxiety. *J. Neurodev. Disord.* 9:16. doi: 10.1186/s11689-017-9197-6

Leehey, M. A. (2009). Fragile X-associated tremor/ataxia syndrome: clinical phenotype, diagnosis, and treatment. *J. Investig. Med.* 57, 830–836. doi: 10.2310/JIM.0b013e3181af59c4

Loehr, J. P., Synhorst, D. P., Wolfe, R. R., and Hagerman, R. J. (1986). Aortic root dilatation and mitral valve prolapse in the fragile X syndrome. *Am. J. Med. Genet.* 23, 189–194. doi: 10.1002/ajmg.1320230113

Loesch, D. Z., Huggins, R. M., Bui, Q. M., Taylor, A. K., and Hagerman, R. J. (2003). Relationship of deficits of FMR1 gene specific protein with physical phenotype of fragile X males and females in pedigrees: a new perspective. *Am. J. Med. Genet. A.* 118A, 127–134. doi: 10.1002/ajmg.a.10099

Loomis, E. W., Sanz, L. A., Chédin, F., and Hagerman, P. J. (2014). Transcription-associated R-Loop formation across the human FMR1 CGG-repeat region. *PLoS. Genet.* 10:e1004294. doi: 10.1371/journal.pgen.1004294

Ma, L., Herren, A. W., Espinal, G., Randol, J., McLaughlin, B., Martinez-Cerdeno, V., et al. (2019). Composition of the intranuclear inclusions of fragile X-associated tremor/ataxia syndrome. *Acta Neuropathol. Commun.* 7:143. doi: 10.1186/s40478-019-0796-1

McKenzie, F. J., Tassankijpanich, N., Epps, K. C., March, S. K., and Hagerman, R. J. (2020). Spontaneous coronary artery dissection in females with the fragile X FMR1 premutation. *JACC Case. Rep.* 2, 40–44. doi: 10.1016/j.jaccas.2019.11.058

Morselli, E., Santos, R. S., Criollo, A., Nelson, M. D., Palmer, B. F., and Clegg, D. J. (2017). The effects of oestrogens and their receptors on cardiometabolic health. *Nat. Rev. Endocrinol.* 13, 352–364. doi: 10.1038/nrendo.2017.12

Napoli, E., Ross-Inta, C., Wong, S., Omanska-Klusek, A., Barrow, C., Iwahashi, C., et al. (2011). Altered zinc transport disrupts mitochondrial protein processing/import in fragile X-associated tremor/ataxia syndrome. *Hum. Mol. Genet.* 20, 3079–3092. doi: 10.1093/hmg/ddr211

Park, H.-Y., Cho, J.-M., Kim, D.-H., Park, C.-B., and Kim, C.-J. (2017). Spontaneous coronary artery dissection in a female patient with fragile X syndrome. *Kosin. Med. J.* 32, 240–243. doi: 10.7180/kmj.2017.32.2.240

Pretto, D. I., Mendoza-Morales, G., Lo, J., Cao, R., Hadd, A., Latham, G. J., et al. (2014). CGG allele size somatic mosaicism and methylation in FMR1 premutation alleles. *J. Med. Genet.* 51, 309–318. doi: 10.1136/jmedgenet-2013-102021

Pugliese, P., Annesi, G., Cutuli, N., Arabia, G., Nicoletti, G., Annesi, F., et al. (2004). The fragile X premutation presenting as postprandial hypotension. *Neurology* 63, 2188–2189. doi: 10.1212/01.wnl.0000145709.61117.08

Rajaratnam, A., Shergill, J., Salcedo-Arellano, M., Saldarriaga, W., Duan, X., and Hagerman, R. (2017). Fragile X syndrome and fragile X-associated disorders. *F1000Res* 6:2112. doi: 10.12688/f1000research.11885.1

Ramírez-Cheyne, J. A., Duque, G. A., Ayala-Zapata, S., Saldarriaga-Gil, W., Hagerman, P., Hagerman, R., et al. (2019). Fragile X syndrome and connective tissue dysregulation. *Clin. Genet.* 95, 262–267. doi: 10.1111/cge.13469

Riddle, J. E., Cheema, A., Sobesky, W. E., Gardner, S. C., Taylor, A. K., Pennington, B. F., et al. (1998). Phenotypic involvement in females with the FMR1 gene mutation. *Am. J. Ment. Retard.* 102, 590–601. doi: 10.1352/0895-80171998102(0590:piifwt(2.0.co;2

Robin, G., López, J. R., Espinal, G. M., Hulsizer, S., Hagerman, P. J., and Pessah, I. N. (2017). Calcium dysregulation and Cdk5-ATM pathway involved in a mouse model of fragile X-associated tremor/ataxia syndrome. *Hum. Mol. Genet.* 26, 2649–2666. doi: 10.1093/hmg/ddx148

Sadasivan, C., Fiorella, D. J., Woo, H. H., and Lieber, B. B. (2013). Physical factors effecting cerebral aneurysm pathophysiology. *Ann. Biomed. Eng.* 41, 1347–1365. doi: 10.1007/s10439-013-0800-z

Sellier, C., Buijsen, R. A. M., He, F., Natla, S., Jung, L., Tropel, P., et al. (2017). Translation of expanded CGG repeats into FMRpolyG is pathogenic and may contribute to fragile X tremor ataxia syndrome. *Neuron* 93, 331–347. doi: 10.1016/j.neuron.2016.12.016

Sellier, C., Freyermuth, F., Tabet, R., Tran, T., He, F., Ruffenach, F., et al. (2013). Sequestration of DROSHA and DGCR8 by expanded CGG RNA repeats alters microRNA processing in fragile X-associated tremor/ataxia Syndrome. *Cell. Rep.* 3, 869–880. doi: 10.1016/j.celrep.2013.02.004

Sellier, C., Rau, F., Liu, Y., Tassone, F., Hukema, R. K., Gattoni, R., et al. (2010). Sam68 sequestration and partial loss of function are associated with splicing alterations in FXTAS patients. *EMBO. J.* 29, 1248–1261. doi: 10.1038/emboj.2010.21

Sellier, C., Usdin, K., Pastori, C., Peschansky, V. J., Tassone, F., and Charlet-Berguerand, N. (2014). The multiple molecular facets of fragile X-associated tremor/ataxia syndrome. *J. Neurodev. Disord.* 6:23. doi: 10.1186/1866-1955-6-23

Song, G., Napoli, E., Wong, S., Hagerman, R., Liu, S., Tassone, F., et al. (2016). Altered redox mitochondrial biology in the neurodegenerative disorder fragile X-tremor/ataxia syndrome: use of antioxidants in precision medicine. *Mol. Med.* 22, 548–559. doi: 10.2119/molmed.2016.00122

Sreeram, N., Wren, C., Bhate, M., Robertson, P., and Hunter, S. (1989). Cardiac abnormalities in the fragile X syndrome. *Br. Heart. J.* 61, 289–291. doi: 10.1136/hrt.61.3.289

Tassone, F., Beilina, A., Carosi, C., Albertosi, S., Bagni, C., Li, L., et al. (2007). Elevated FMR1 mRNA in premutation carriers is due to increased transcription. *RNA* 2007, 555–562. doi: 10.1261/rna.280807

Tassone, F., Greco, C. M., Hunsaker, M. R., Seritan, A. L., Berman, R. F., Gane, L. W., et al. (2012a). Neuropathological, clinical and molecular pathology in female fragile X premutation carriers with and without FXTAS. *Genes. Brain. Behav.* 11, 577–585. doi: 10.1111/j.1601-183X.2012.00779.x

Tassone, F., Hagerman, R. J., Taylor, A. K., Gane, L. W., Godfrey, T. E., and Hagerman, P. J. (2000a). Elevated levels of FMR1 mRNA in carrier males: a new mechanism of involvement in the fragile-X syndrome. *Am. J. Hum. Genet.* 66, 6–15. doi: 10.1086/302720

Tassone, F., Hagerman, R. J., Taylor, A. K., Mills, J. B., Harris, S. W., Gane, L. W., et al. (2000b). Clinical involvement and protein expression in individuals with the FMR1 premutation. *Am. J. Med. Genet.* 91, 144–152. doi: 10.1002/(sici)1096-8628(20000313)91:2(144:aid-ajmg14(3.0.co;2-v

Tassone, F., Iong, K. P., Tong, T.-H., Lo, J., Gane, L. W., Berry-Kravis, E., et al. (2012b). FMR1 CGG allele size and prevalence ascertained through newborn screening in the United States. *Genome. Med.* 4, 100. doi: 10.1186/gm401

Tassone, F., Iwahashi, C., and Hagerman, P. J. (2004). FMR1 RNA within the intranuclear inclusions of fragile X-associated tremor/ataxia syndrome (FXTAS). *RNA Biol.* 1, 103–105. doi: 10.4161/rna.1.2.1035

Utari, A., Adams, E., Berry-Kravis, E., Chavez, A., Scaggs, F., Ngotran, L., et al. (2010). Aging in fragile X syndrome. *J. Neurodev. Disord.* 2, 70–76. doi: 10.1007/s11689-010-9047-2

Waldstein, G., and Hagerman, R. (1988). Aortic hypoplasia and cardiac valvular abnormalities in a boy with fragile X syndrome. *Am. J. Med. Genet.* 30, 83–98. doi: 10.1002/ajmg.1320300107

Wheeler, A. C., Bailey, D. B., Berry-Kravis, E., Greenberg, J., Losh, M., Mailick, M., et al. (2014). Associated features in females with an FMR1 premutation. *J. Neurodev. Disord.* 6:30. doi: 10.1186/1866-1955-6-30

Winarni, T. I., Chonchaiya, W., Sumekar, T. A., Ashwood, P., Morales, G. M., Tassone, F., et al. (2012). Immune-mediated disorders among women carriers of fragile X premutation alleles. *Am. J. Med. Genet. A.* 158A, 2473–2481. doi: 10.1002/ajmg.a.35569

Wittstein, I. S., Thiemann, D. R., Lima, J. A. C., Baughman, K. L., Schulman, S. P., Gerstenblith, G., et al. (2005). Neurohumoral features of myocardial stunning due to sudden emotional stress. *N. Engl. J. Med.* 352, 539–548. doi: 10.1056/NEJMoa043046

Yetkin, E., and Ozturk, S. (2018). Dilating vascular diseases: pathophysiology and clinical aspects. *Int. J. Vasc. Med.* 2018:9024278. doi: 10.1155/2018/9024278

Zhou, B., and Tian, R. (2018). Mitochondrial dysfunction in pathophysiology of heart failure. *J. Clin. Invest.* 128, 3716–3726. doi: 10.1172/JCI120849

Conflict of Interest: RH has consulted with Zynerba and Fulcrum regarding treatment of Fragile X syndrome and she has received funding from the Azrieli Foundation, Ovid, and Zynerba to carry out treatment studies in Fragile X syndrome.

The remaining authors declare that the research was conducted in the absence of any commercial or financial relationships that could be construed as a potential conflict of interest.

frontiers in Molecular Biosciences

ORIGINAL RESEARCH
published: 22 October 2020
doi: 10.3389/fmolb.2020.578640

Characterization of the Metabolic, Clinical and Neuropsychological Phenotype of Female Carriers of the Premutation in the X-Linked *FMR1* Gene

*Eleonora Napoli[1], Yingratana Amabel McLennan[2], Andrea Schneider[2,3], Flora Tassone[2,4], Randi J. Hagerman[2,3] and Cecilia Giulivi[1,2]**

[1] Department of Molecular Biosciences, School of Veterinary Medicine, University of California, Davis, Davis, CA, United States, [2] MIND Institute, University of California Davis Medical Center, Sacramento, CA, United States, [3] Department of Pediatrics, University of California Davis Medical Center, Sacramento, CA, United States, [4] Department of Biochemistry and Molecular Medicine, School of Medicine, University of California, Davis, Davis, CA, United States

OPEN ACCESS

Edited by:
Simona Paladino,
University of Naples Federico II, Italy

Reviewed by:
Shai E. Elizur,
IVF Unit, Sheba Medical Center, Israel
Emily G. Allen,
Emory University, United States

***Correspondence:**
Cecilia Giulivi
cgiulivi@ucdavis.edu

Specialty section:
This article was submitted to Cellular Biochemistry, a section of the journal Frontiers in Molecular Biosciences

Received: 30 June 2020
Accepted: 24 September 2020
Published: 22 October 2020

Citation:
Napoli E, McLennan YA, Schneider A, Tassone F, Hagerman RJ and Giulivi C (2020) Characterization of the Metabolic, Clinical and Neuropsychological Phenotype of Female Carriers of the Premutation in the X-Linked FMR1 Gene. Front. Mol. Biosci. 7:578640. doi: 10.3389/fmolb.2020.578640

The X-linked *FMR1* premutation (PM) is characterized by a 55–200 CGG triplet expansion in the 5′-untranslated region (UTR). Carriers of the PM were originally thought to be asymptomatic; however, they may present general neuropsychiatric manifestations including learning disabilities, depression and anxiety, among others. With age, both sexes may also develop the neurodegenerative disease fragile X-associated tremor/ataxia syndrome (FXTAS). Among carriers, females are at higher risk for developing immune disorders, hypertension, seizures, endocrine disorders and chronic pain, among others. Some female carriers younger than 40 years old may develop fragile X-associated primary ovarian insufficiency (FXPOI). To date, no studies have addressed the metabolic footprint – that includes mitochondrial metabolism – of female carriers and its link to clinical/cognitive manifestations. To this end, we performed a comprehensive biochemical assessment of 42 female carriers (24–70 years old) compared to sex-matched non-carriers. By applying a multivariable correlation matrix, a generalized bioenergetics impairment was correlated with diagnoses of the PM, FXTAS and its severity, FXPOI and anxiety. Intellectual deficits were strongly correlated with both mitochondrial dysfunction and with CGG repeat length. A combined multi-omics approach identified a down-regulation of RNA and mRNA metabolism, translation, carbon and protein metabolism, unfolded protein response, and up-regulation of glycolysis and antioxidant response. The suboptimal activation of the unfolded protein response (UPR) and endoplasmic-reticulum-associated protein degradation (ERAD) response challenges and further compromises the PM genetic background to withstand other, more severe forms of stress. Mechanistically, some of the deficits were linked to

an altered protein expression due to decreased protein translation, but others seemed secondary to oxidative stress originated from the accumulation of either toxic mRNA or RAN-derived protein products or as a result of a direct toxicity of accumulated metabolites from deficiencies in critical enzymes.

Keywords: mitochondrial dysfunction, omics, cellular response to stress, oxidative phosphorylation, glycolysis, fragile X-associated primary ovarian insufficiency, fragile X-associated tremor and ataxia syndrome

INTRODUCTION

Carriers of the premutation (PM) are characterized by a moderate (55 to 200) expansion of the cytosine-guanine-guanine (CGG) nucleotide repeats in the first exon and promoter of the X-linked *FMR1* gene (Verkerk et al., 1991; Bagni et al., 2012). Originally, PM carriers were assumed to be free of any apparent phenotypic traits. However, over the last decade, a growing number of neuropsychiatric manifestations (including depression, anxiety, and insomnia), visuospatial deficits, and immune dysregulation have been reported to occur at a greater frequency among adult PM carriers than in the general population (Hagerman and Hagerman, 2013). Generally, PM carriers show lower performance in neuropsychological testing including full-scale intellectual quotient (FSIQ) and working memory (WM) subtests on the Wechsler Adult Intelligence Scale (Lozano et al., 2016). In the case of children with the PM, they are often diagnosed with ADHD, autism, anxiety, and other psychopathologies (Napoli et al., 2018). The PM has also been associated with conditions beyond those involving the CNS, such as hypertension, hypothyroidism, high blood glucose, as well as a higher incidence of thyroid, prostate and other cancers (Lozano et al., 2016). With age, both female and male carriers of the PM are at a higher risk for developing the late-onset (usually appearing after age 50) neurodegenerative disorder fragile X-associated tremor/ataxia syndrome [FXTAS; OMIM:300623; (Hagerman et al., 2001, 2004; Hagerman and Hagerman, 2013)]. FXTAS-affected carriers may exhibit intention tremor and gait ataxia, accompanied by cerebral atrophy, white matter disease, parkinsonism, neuropathy, autonomic dysfunction, and cognitive deficits (Berry-Kravis et al., 2007a; Bourgeois et al., 2007; Lozano et al., 2016; Claeys et al., 2020).

As it is the case for many X-linked disorders, women have a lower absolute risk of developing FXTAS symptoms compared to men (Hagerman and Hagerman, 2016). However, women carrying *FMR1* PM allele have a higher risk of developing premature or primary ovarian insufficiency (POI) [16% (Schwartz et al., 1994; Allingham-Hawkins et al., 1999; Rifé et al., 2004; Terracciano et al., 2004; Schuettler et al., 2011; Elizur et al., 2014; Pouresmaeili and Fazeli, 2014)] as compared to full mutation females (>200 CGG repeats), who carry the same risk for POI as the general population (1%). About 20 to 30% of female carriers experiencing irregular periods or amenorrhea due to ovarian insufficiency prior to age 40 are diagnosed with fragile X-associated primary ovarian insufficiency [FXPOI; (Allingham-Hawkins et al., 1999; Allen et al., 2007)]. Even PM carriers without signs of ovarian dysfunction have an earlier (on average by 5 years) age at menopause compared with non-carriers (Patsalis et al., 1999; Sullivan et al., 2005; Besterman et al., 2014). Women with alleles between 35–44 CGG repeats seem to present diminished ovarian function but regular menses and occult primary ovarian insufficiency (Streuli et al., 2009; Karimov et al., 2011; Pastore et al., 2012); however, other studies found no association between *FMR1* intermediate alleles and POI (Bennett et al., 2010; Murray et al., 2014; Voorhuis et al., 2014). Other medical and psychological issues reported in females are hypothyroidism, hypertension, endocrine dysfunctions, chronic pain, fibromyalgia, autoimmune diseases, neuropathies, migraines, dementia, and psychiatric conditions, such as anxiety and depression (Allen et al., 2007, 2020; Bailey et al., 2008; Hunter et al., 2010; Winarni et al., 2012; Wheeler et al., 2014a,b; Lozano et al., 2016; Movaghar et al., 2019). Collectively included under the term FXAND [fragile X–associated neuropsychiatric disorders; (Hagerman et al., 2018)], such emotional and neuropsychiatric disorders, have been shown to be more common in female carriers compared to non-carriers. In a recent work by Dr. S. Sherman's group, which investigated the association between the PM diagnosis and CGG repeat expansion in female carriers, the most common symptoms reported were anxiety and depression, migraine, headaches, and sleep problems (Allen et al., 2020).

Our team was the first to report mitochondrial dysfunction as a common feature in biological samples from PM carriers (Napoli et al., 2013, 2016a,b, 2018; Song et al., 2016) as well as in murine models of the PM (Napoli et al., 2016a). This decreased mitochondrial bioenergetics is present in PM carriers with and without FXTAS and even in some pediatric carriers (Napoli et al., 2018). However, to our knowledge, no study has to date characterized the metabolic footprint of the PM and related clinical and cognitive features in female carriers of the PM.

To bridge this gap in knowledge, we performed a comprehensive biochemical assessment (including metabolomics and proteomics profiling, and bioenergetics) in peripheral blood mononuclear cells (PBMC) and plasma samples obtained from 24- to 70-year-old female carriers. To elucidate peripheral bioenergetics markers that may function as surrogates for CNS function, we utilized a multivariable correlation matrix to identify correlations between mitochondrial outcomes and cognitive parameters (FSIQ), executive function (BDS-2), anxiety, tremor, and FXTAS (and its severity) and FXPOI diagnoses. As such, this study is ideally positioned to perform comprehensive deep metabolic and mitochondrial phenotyping by gathering complementary outcomes on genomics, proteomics, metabolomics, mitochondrial physiology

and clinical information to systematically develop a metabolic profile from established female carriers by taking advantage of a substantial repository of patient samples. This multi-faceted approach, as opposed to a simple model based on the statistical differences of few (and sometimes unconnected) metabolites or proteins between diagnostic groups. The profile generated will, for the first time, allow researchers to fully assess the larger biological impact of the premutation on metabolic status of female carriers, thereby providing unprecedented insight into the biological consequences of metabolic deficits and mitochondrial dysfunction, aiding the discovery of disease mechanisms. Importantly, due to the depth of the phenotyping across multiple readouts, the integrated metabolic profiles generated will have the detail required to cluster patients according to their clinical pathology when more patients' data will be available. This necessary step, in turn, will lead to truly novel and testable hypotheses regarding individualized pathogenesis and treatment.

MATERIALS AND METHODS

Subjects

Blood samples were obtained from 42 female carriers of the *FMR1* PM ranging from 24- to 70-year old, recruited through the Fragile X Treatment and Research Center at the MIND Institute at University of California, Davis. Blood samples were also obtained from 10 female non-carriers aged 25 to 60 years. The study was approved by the IRB ethics committee at University of California Davis Medical Center. Blood samples were obtained by venipuncture with informed consent. FXTAS was diagnosed utilizing criteria reported before (Jacquemont et al., 2003; Hagerman and Hagerman, 2016). For returning participants, outcomes evaluated at one single visit collected at the indicated age were included in the analysis.

Genotyping

CGG repeat expansion in all individuals included in this study were evaluated by both PCR and Southern Blot analysis, as previously described (Tassone et al., 2008; Filipovic-Sadic et al., 2010). The X-activation ratio (XAR), representing the percentage of cells with the normal allele on the active X chromosome, was calculated by the ratio of the densitometric intensity of the normal *FMR1* unmethylated band over the sum of the intensities of the normal unmethylated and methylated bands (Tassone et al., 1999; Berry-Kravis et al., 2003). In a population of normal (Z) distribution, 1.65 × SD leads to a tail that gives the probability of 5% of the data to be excluded from normal. If this value is subtracted from the mean XAR, then anything below this value has <5% probability of being significant. Thus, XAR values <36% of non-carrier ones were considered unfavorable (<0.2).

Lymphocyte Preparation

Blood (5–7 ml) was collected in BD vacutainer CPT tubes (BD Biosciences, Franklin Lakes, NJ, United States) and lymphocytes were isolated as previously described (Napoli et al., 2016a). Upon collection, lymphocyte suspension was divided into 2 aliquots in Eppendorf tubes and pelleted by centrifugation 1 min 2,000 rpm in a microfuge at 4°C. The supernatant was removed, and the pellet was used immediately for mitochondrial outcomes. An aliquot of PBMC was suspended in 0.5 ml cold 10 mM HEPES, pH 7.4, frozen at −80°C overnight and subsequently transferred for extended storage, into liquid nitrogen.

Mitochondrial Outcomes

All chemicals and biochemicals were of analytical grade or higher. Enzymatic activities of Complexes I–V in digitonin-permeabilized lymphocytes determined by polarography essentially as described before (Giulivi et al., 2010; Napoli et al., 2016a). Briefly, an aliquot ($0.5–1.0 \times 10^6$) of lymphocytes was added to the oxygen chamber in 0.3 ml of a buffer containing 0.22 M sucrose, 50 mM KCl, 1 mM EDTA, 10 mM KH_2PO_4, and 10 mM HEPES, pH 7.4. Oxygen consumption rates were evaluated in the presence of (i) 1 mM ADP plus 1 mM malate-10 mM glutamate followed by the addition of 5 μM rotenone; (ii) 10 mM succinate followed by the addition of 1 mM malonate; (iii) 1 mM α-glycerophosphate followed by the addition of 3.6 μM antimycin A; and (iv) 10 mM ascorbate and 0.2 mM *N,N,N′,N′*-tetramethyl-*p*-phenylenediamine followed by the addition of 1 mM KCN. Activities of individual electron transport chain (ETC) segments were evaluated as the difference of oxygen uptake recorded before and after the addition of specific inhibitors. Citrate synthase activity was evaluated spectrophotometrically with a Tecan Infinite M200 microplate reader equipped with the Magellan software (Austria) at 412 nm as described elsewhere (Napoli et al., 2016a). The respiratory control ratio (RCR) was calculated as the ratio between oxygen uptake rates of intact cells supplemented with 10 mM glucose (present in RPMI-1640) in State 3 μ (with 2 μM carbonylcyanide-*p*-trifluoromethoxyphenylhydrazone, or FCCP) and State 4 (with 0.2 μM oligomycin) (Giulivi et al., 2013). Mitochondrial ROS production was calculated from the oligomycin-resistant oxygen consumption rates and normalized by basal respiration in the presence of 10 mM glucose.

Plasma Metabolomics

Plasma samples were obtained from age-matched 8 non-carriers and 7 PM carriers as previously described (Napoli et al., 2016a), and metabolites were extracted and analyzed by mass spectrometry (Napoli et al., 2015). Briefly, 30-μl aliquots were extracted by 1 ml of degassed acetonitrile:isopropanol:water (3:3:2, V/V/V) at −20°C, centrifuged and decanted with subsequent evaporation of the solvent to complete dryness. A clean-up step with acetonitrile/water (1:1) removed membrane lipids and triglycerides. Details on the identification of metabolites and data analysis are reported in Napoli et al. (2015).

Proteomics

Peripheral blood mononuclear cells samples were hand-homogenized on ice in 20 mM HEPES pH 6.8, containing protease and phosphatase inhibitor cocktail (Sigma-Aldrich, St. Louis, MO, United States). Protein concentration was determined by BCA protein assay kit (Thermo Scientific, Sunnyvale, CA, United States) and samples from 7 controls and 7 PM carriers

were submitted to the UC Davis Mass Spectrometry Facility and analyzed as described in detail elsewhere (Napoli et al., 2016a).

Statistics

As the population assessed in this study did not follow a normal distribution, Spearman's correlation coefficients and correspondent p values for each pair of variables tested were computed with a correlation matrix for multiple variables. Due to the limited information available for some subjects on some of the variables included in our analysis (**Table 1**), and to exclude the possibility of considering significant interactions without true biological relevance, we applied a more stringent cut-off conditions by setting p values at $\leq$0.01. We did not employ a Bonferroni correction to adjust the p values for the number of variables tested as (i) it ignores dependencies among the data and is therefore too conservative if the number of tests is large, (ii) it assumes that all null hypotheses are true simultaneously, which was not our assumption, (iii) it increases the likelihood of type II errors, so that truly important differences are considered non-significant (Perneger, 1998). A two-way ANOVA was carried out to test for the contribution of age, diagnosis and age x diagnosis on the mitochondrial outcomes' variability. Graph Pad Prism v. 8.1.2 was used for all the statistical analyses. Metabolomics and proteomics data were analyzed as previously described (Giulivi et al., 2016; Napoli et al., 2016a,b).

RESULTS

Demographics and Clinical Characteristics of the Cohorts

Our cohorts consisted of women with the PM with and without FXTAS, and sex-matched non-carriers (named hereafter controls; **Table 1**). The control study group consisted of 25–60 year old women with CGG repeats at the 5′- untranslated region (UTR) of *FMR1* of 31 ± 1 (mean ± SEM; n = 10). The PM group included 24- to 70-year-old females (n = 42), from which about half (n = 20) were diagnosed with FXTAS. The FXTAS stages ranged from 1 to 4, with most subjects at stage 3. The CGG repeats of the mutant allele ranged from 57 to 137, with an average of 87 ± 4 for PM carriers without FXTAS and 90 ± 4 for FXTAS-affected carriers with no significant difference between these two groups (p = 0.156). Of the 42 carriers, 10 were diagnosed with FXPOI, and 3 had undergone hysterectomy between the age of 26 and 40 years. XAR ranged from 0.1 to 0.92 with an average of 0.57 ± 0.04 in PM without FXTAS and 0.57 ± 0.05 in FXTAS-affected with no significant difference between these two groups (p = 0.878), and not different from the expected random inactivation of the X-chromosome. Only 4 of 42 carriers had an unfavorable XAR.

Both cohorts were assessed for most of the neurological/neuropsychiatric outcomes. They included full-scale intellectual quotient (FSIQ; **Table 1**) assessed with the Wechsler Adult Intelligence Scale, WAIS-IV (Drozdick et al., 2012), and executive function [assessed by the Behavioral Dyscontrol Scale II or BDS-2; (Belanger et al., 2005)]. Subjects were also tested for generalized anxiety through the Structured Clinical Interview for Diagnosis of Mental Disorders (SCID)-1 [Diagnostic and Statistical Manual of Mental Disorders (DSM)-IV; **Table 1**].

Deficits in Peripheral Mitochondrial Energy Production Are Linked to Cognitive and Psychiatric Outcomes, and Diagnoses of FXPOI and FXTAS and Its Morbidity (FXTAS Stage)

A multivariable correlation matrix was built by utilizing as input data clinical, psychiatric and molecular outcomes from non-carriers and PM carriers (**Figure 1**). Continuous variables were used as such, whereas categorical ones (e.g., three diagnoses: non-carriers, PM, FXTAS; FXPOI diagnosis, and presence of anxiety) were assigned numerical values. Tremor, one of FXTAS hallmarks, was excluded from the correlation matrix as it was available for 23 of the 42 participants, of which only 2 showed tremors. Similarly, the XAR was not shown in **Figure 1**, as this outcome did not show any correlation with any of the other reported outcomes, due to the low frequency (9.5%) of unfavorable (<0.2) XAR in our cohort. The apparent discrepancy with the findings of other studies (Hagerman and Hagerman, 2004; Berry-Kravis et al., 2005, 2007b) could be bridged by considering that they utilized other neurological features (Berry-Kravis et al., 2007b); the use of an updated clinical diagnostic criteria for FXTAS (Hagerman and Hagerman, 2013).

Overall, demographic (age), clinical (diagnoses of PM and FXTAS, CGG repeats, diagnosis of FXPOI and FXTAS stage) and psychiatric (anxiety) variables correlated positively with each other. Notably, all of these outcomes were associated with increased oxidative stress as they were directly correlated with mitochondrial ROS production. As expected, these outcomes were inversely correlated with intellectual and functional capacities (FSIQ and BDS-2) and mitochondrial function (**Figure 1**).

In order to narrow down the significant associations among variables, the non-parametric Spearman's correlation coefficients, and correspondent p values were calculated.

Diagnoses of PM, FXTAS and FXPOI

Using the above mentioned significance threshold, FXTAS and PM diagnoses significantly and inversely correlated with (i) activity of citrate synthase, marker of mitochondrial mass, (CS; Spearman's $r = -0.361$, $p = 0.004$); (ii) mitochondrial ATP production supported by NADH- ($r = -0.397$, $p = 0.001$) and $FADH_2$-linked substrates ($r = -0.413$, $p = 0.001$); (iii) α-glycerophosphate-fueled ATP production (αGP; $r = -0.330$, $p = 0.01$); (iv) cytochrome c oxidase activity ($r = -0.402$, $p = 0.001$); (v) glucose-sustained mitochondrial ATP production ($r = -0.439$, $p < 0.0001$); and (vi) coupling between electron transport and ATP production ($r = -0.391$, $p = 0.002$). In turn, diagnoses directly correlated with mitochondrial ROS production ($r = 0.490$, $p < 0.0001$). The same biochemical outcomes, except for mitochondrial mass (CS activity) and αGP-mediated respiration, correlated with FXTAS severity (i.e., stage; **Figure 1**)

TABLE 1 | Demographic and clinical data of the women included in this study.

Clinical group	*Age (y)*	*CGG*	*XAR*	*FXTAS Stage*	*FXPOI*	*FSIQ*	*BDS2*	*Anx*
*C1**	25	29,30	ND	0	No	115	18	No
*C2**	26	24,33	ND	0	No	ND	ND	ND
C3	27	40,42	ND	0	No	121	ND	ND
C4¶*	29	20,33	ND	0	No	106	26	No
*C5**	33	30,37	ND	0	No	121	26	No
*C6**	44	23,30	ND	0	No	104	ND	No
*C7**	45	22,33	ND	0	No	ND	ND	No
*C8**	47	23,30	ND	0	No	ND	24	No
C9	54	30	ND	0	No	ND	ND	No
C10¶*	60	23,30	ND	0	No	133	25	Yes
P1¶*	24	30,79	0.78	0	No	125	24	No
*P2**	24	31,93	0.38	0	No	96	19	No
*P3**	33	30,137	0.55	0	No	96	22	Yes
P4	33	29,81	0.57	0	No	ND	ND	ND
P5	37	30,79	0.72	0	No	ND	ND	ND
P6(T)*	38	33,60	0.43	0	No	112	24	No
P7	38	43,78	0.15	0	No	ND	ND	ND
P8(T)*	43	30,106	0.55	0	No	98	22	No
*P9**	49	31,86	0.64	0	Yes	118	25	Yes
*P10**	50	20,98	0.88	0	No	123	26	No
P11	50	30,94	0.56	0	ND	ND	ND	ND
P12	50	22,119	0.68	0	No	90	20	Yes
P13¶*	52	29,81	0.68	0	No	105	23	No
P14¶*	56	30,69	0.42	0	Yes	114	26	Yes
P15¶*	57	30,68	0.40	0	ND	ND	ND	ND
P16	58	29,69	0.57	0	No	ND	23	No
P17	58	27,77	0.48	0	No	98	23	Yes
P18	60	30,84	0.90	0	No	ND	ND	ND
P19	60	23,87	0.86	0	Yes	ND	ND	ND
P20	62	30,84	0.15	0	No	100	26	Yes
P21	64	31,71	0.49	0	No	ND	23	Yes
P22	71	29,105,160	0.81	0	Yes	110	23	Yes
F1	54	31,102	0.68	2.5	Yes	104	25	Yes
F2	54	32,93	0.62	3	ND	ND	ND	ND
F3	56	30,93	0.15	3	HYS	ND	10	Yes
F4	57	30,99	0.76	2	No	96	21	Yes
F5	59	33,107	0.10	ND	No	ND	ND	ND
F6	60	37,70	0.62	3	No	ND	ND	ND
F7	60	31,100	0.53	3	No	ND	ND	ND
F8	62	37,107	0.57	2	No	131	25	No
F9	63	30,102	0.36	3	HYS	104	22	Yes
F10	64	30,82	0.60	4	No	92	23	Yes
F11	67	23,103	0.31	3	No	104	21	Yes
F12	68	23,88	0.92	3	ND	ND	ND	ND
F13	68	25,57	0.66	3	Yes	106	26	No
F14	68	30,74	0.68	3	Yes	115	21	Yes
F15	70	28,104	0.77	4	Yes	97	17	No
F16	70	20,85	0.52	2	No	103	19	Yes
F17	70	29,61	0.85	2	ND	ND	ND	ND
F18	70	30,110	0.42	3	No	ND	ND	ND
F19	70	29,105	0.64	2	HYS	105	17	Yes
F20	70	30,76	0.54	3	Yes	99	ND	Yes

**Metabolomics carried out in plasma. ¶ Proteomics carried out in PBMC. Anx, anxiety; BDS2, behavioral dyscontrol scale II; FSIQ, Full Scale IQ, calculated by Wechsler Adult Intelligence Scale, Fourth Edition (WAIS-IV) P and F indicate, respectively, PM carriers either without or with FXTAS; FXTAS stage refers to clinical evaluation determined by previous diagnosis and based on the score published in Jacquemont et al. (2003) and Hagerman et al. (2008). HYS indicates patients that underwent hysterectomy (F3 at 27 year; F9 at 40 year; F19 at 36 year). T indicates the presence of tremors. ND, not determined or determined but not yet available in the database.*

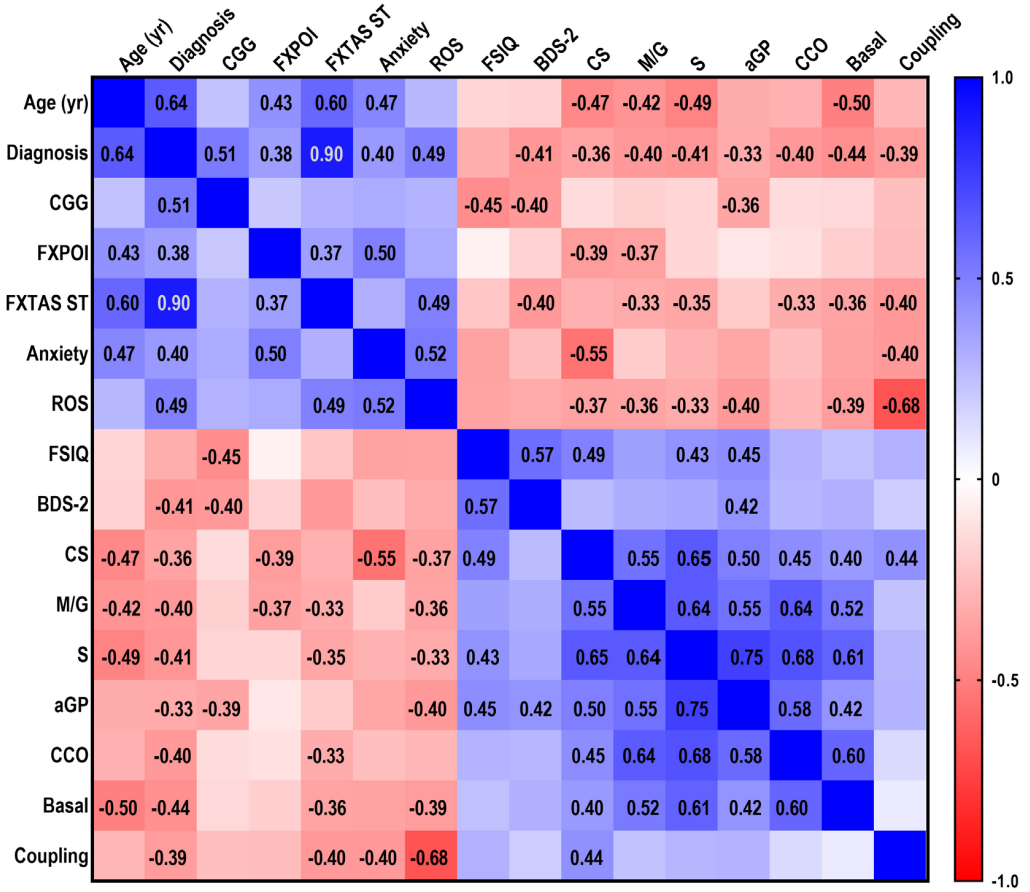

FIGURE 1 | Correlations between demographic, clinical and mitochondrial outcomes. A multivariable correlation matrix was built with demographic, clinical and functional data relative to PM without (n = 22) and with (n = 20) FXTAS symptoms and control (n = 10) women age 24–70 year, along with biochemical mitochondrial outcomes measured in lymphocytes obtained from the same individuals. Outcomes analyzed were: age, diagnosis, CGG (all with n = 52), FXPOI (n = 47), FXTAS stage (n = 51), anxiety (n = 36), Full Scale IQ (FSIQ; n = 31), Behavioral Dyscontrol Scale-2 (BDS-2; n = 32), ROS (n = 46), citrate synthase activity (CS; n = 52), NADH-fueled ATP-linked O_2 consumption (M/G; n = 52), succinate (S)-sustained $FADH_2$-fueled ATP-linked linked O_2 consumption (n = 52), α-glycerophosphate (αGP)-dependent ATP-linked O_2 consumption (n = 50), cytochrome c oxidase activity (CCO; 51), basal respiration (n = 51), coupling (n = 50). Categorical variables (i.e., diagnosis, FXPOI, anxiety) were assigned a numerical value. Diagnosis: control = 0, PM without FXTAS = 1, PM with FXTAS = 2; FXPOI and anxiety: absence = 0, presence = 1. Due to the non-Gaussian distribution of the data, the non-parametric Spearman test was run. R values are shown for those correlations which were statistically significant at $p \leq 0.01$. A scale showing the range of r values (from –1.0 for inversely correlated outcomes to 1.0 for positively correlated ones) is also shown.

indicating that the morbidity of this neurodegenerative disease is also reflected as a peripheral deficit in bioenergetics.

Lower CS activity and NADH-linked ATP production characterized FXPOI, diagnosis strongly linked to the occurrence of anxiety (r = 0.497, p = 0.001; **Figure 1**). While PM and FXTAS diagnoses, morbidity of FXTAS and FXPOI were all inversely correlated with CS activity, it could be assumed that the lower bioenergetics was a result of lower mitochondrial mass. However, even after normalization of the rates of ATP production by mitochondrial mass, several outcomes were still correlated (some directly and others inversely) highlighting the delicate balance among Complexes within the electron transport chain that needs to be preserved for its adequate production of ATP while minimizing ROS production. Among them (normalized by mitochondrial mass), NADH-linked ATP production with anxiety (r = 0.469; p = 0.002); succinate-linked ATP production with anxiety and PRI (r = 0.370; p = 0.01); CCO activity with FXPOI diagnosis (r = 0.310; p = 0.02), anxiety (r = 0.407; p = 0.008), PRI (r = −0.565; p = 0.01) and FSIQ (r = −0.369; p = 0.02); and basal respiration with PRI (r = −0.653; p = 0.003) and PSI (r = −0.517; p = 0.02).

Anxiety

Anxiety was inversely correlated with CS activity (r = −0.553, $p < 0.0001$) and coupling (r = −0.398, p = 0.01), and directly with mitochondrial ROS production (r = 0.521, p = 0.001).

Cognition and Executive Function

FSIQ strongly and positively correlated with executive function (BDS-2; r = 0.566, $p < 0.0001$; **Figure 1**). Similarly, and considering that the brain represents the main site of energy consumption with over 20% of body's total oxygen consumption

(Watts et al., 2018), a strong and direct correlation was identified between FSIQ and overall mitochondrial bioenergetics (**Figure 1**), with statistically significant associations with mitochondrial mass (CS, $r = 0.489$, $p = 0.002$), $FADH_2$-linked ATP production ($r = 0.427$, $p = 0.009$), and α-glycerophosphate-fueled ATP production (αGP; $r = 0.446$, $p = 0.008$). Overall, BDS-2 positively correlated with mitochondrial function, with the correlation with α-glycerophosphate-fueled ATP production resulting statistically significant ($r = 0.417$, $p = 0.008$). [NADH- and $FADH_2$-linked ATP production were significantly correlated with BDS-2 at $p < 0.05$ with $r = 0.318$ and 0.337, respectively].

FMR1 Gene Structure

No correlation was obtained between CGG expansions and FXPOI diagnosis likely due to the significant number of carriers with >100 CGG repeats (28.6%) as reported by others (Sullivan et al., 2005; Ennis et al., 2006; Allen et al., 2007). However, CGG repeats showed a statistically significant inverse correlation with α-glycerophosphate-fueled ATP production ($r = -0.391$, $p = 0.009$), probably indicating issues with the redox state and regulation of cellular energy metabolism, as well as with FSIQ ($r = -0.448$, $p = 0.008$) and BDS-2 performance ($r = -0.400$, $p = 0.01$).

Age

A strong and inverse correlation was observed between age and mitochondrial function in both carriers and non-carriers (**Figure 1**) consistent with the age-dependent decline of OXPHOS capacity (Burch et al., 1963; Cardellach et al., 1989; Linnane et al., 1989; Yen et al., 1989; Byrne et al., 1991; Cooper et al., 1992; Müller-Höcker, 1992; Torii et al., 1992; Münscher et al., 1993; Boffoli et al., 1994, 1996; Lezza et al., 1994; Wallace et al., 1995; Capkova et al., 2002) being more evident in tissues with high OXPHOS demand (Wallace, 1992; Ojaimi et al., 1999; Kwong and Sohal, 2000; Quiles et al., 2002). Relevant to our study, the overall age-dependent decline in the OXPHOS capacity is more evident in women (Cooper et al., 1992; Papa, 1996). To discriminate between the contribution of age- and the PM-dependent decline in mitochondrial function, we carried out a two-way ANOVA analysis for each mitochondrial outcome evaluated in PM and non-carriers at two age ranges, i.e., younger (23–43 year) and older (44–60) (**Table 2**). Then the same analysis was done with PM and FXTAS-affected females at two age ranges, i.e., younger (50–60 year) and older (60–70 year), to test for the contribution of age and FXTAS diagnosis (**Table 2**). When comparing controls and PM carriers, a simple main effect analysis showed that NADH- and $FADH_2$-linked ATP production along with the activity of CCO were solely attributed to the carrier status. Only CS activity showed a decline dependent with both age and PM status (**Table 2**). When the same analysis was performed to compare mitochondrial outcomes between PM and FXTAS-affected females, FXTAS diagnosis affected significantly both mtROS production and coupling, whereas all other outcomes were not influenced either by age or diagnosis. Of note, the observed correlation between age and FXPOI does not reflect the age at which these carriers first experienced ovarian insufficiency, but merely the age at which the PM carriers reported their medical history.

TABLE 2 | Effect of diagnosis, age and diagnosis x age interaction on mitochondrial outcomes evaluated in controls, PM and FXTAS female carriers.

	Diagnosis x age interaction	Diagnosis effect	Age effect
Controls vs. PM			
ROS (DFn = 1, DFd = 26)	*F* = 1.05e-003	*F* = 1.45	*F* = 0.01
	p = 0.9744	*p* = 0.2396	*p* = 0.9133
CS (DF*n* = 1, DFd = 24)	*F* = 0.57	*F* = 4.84	*F* = 6.83
	p = 0.4560	***p* = 0.0377**	***p* = 0.0153**
M/G (DFn = 1, DFd = 26)	*F* = 0.07	*F* = 4.75	*F* = 0.46
	p = 0.7989	***p* = 0.0385**	*p* = 0.5019
S (DFn = 1, DFd = 25)	*F* = 0.21	*F* = 4.80	*F* = 0.08
	p = 0.6542	***p* = 0.0381**	*p* = 0.7863
αGP (DFn = 1, DFd = 26)	*F* = 0.04	*F* = 8.08	*F* = 0.09
	p = 0.8433	***p* = 0.0086**	*p* = 0.7623
CCO (DFn = 1, DFd = 26)	*F* = 1.8e-003	*F* = 6.82	*F* = 0.02
	p = 0.9665	***p* = 0.0148**	*p* = 0.9026
Basal (DFn = 1, DFd = 27)	*F* = 0.01	*F* = 5.94	*F* = 4.16e-005
	p = 0.9362	***p* = 0.0217**	*p* = 0.9949
Coupling (DFn = 1, DFd = 26)	*F* = 0.08	*F* = 1.23	*F* = 1.23
	p = 0.7832	*p* = 0.2760	*p* = 0.4929
PM vs. FXTAS			
ROS (DFn = 1, DFd = 35)	*F* = 0.36	*F* = 9.36	*F* = 0.42
	p = 0.5537	***p* = 0.0042**	*p* = 0.5230
CS (DFn = 1, DFd = 41)	*F* = 2.20	*F* = 0.50	*F* = 1.67
	p = 0.1461	*p* = 0.4839	*p* = 0.2029
M/G (DFn = 1, DFd = 40)	*F* = 2.42	*F* = 0.28	*F* = 1.89
	p = 0.1279	*p* = 0.5971	*p* = 0.1766
S (DFn = 1, DFd = 39)	*F* = 1.24e-004	*F* = 3.48	*F* = 0.05
	p = 0.9912	*p* = 0.0697	*p* = 0.8193
αGP (DFn = 1, DFd = 39)	*F* = 0.09	*F* = 0.11	*F* = 0.11
	p = 0.7604	*p* = 0.7376	*p* = 0.7408
CCO (DFn = 1, DFd = 41)	*F* = 0.55	*F* = 2.54	*F* = 0.26
	p = 0.4632	*p* = 0.1189	*p* = 0.6161
Basal (DFn = 1, DFd = 40)	*F* = 0.40	*F* = 0.65	*F* = 0.55
	p = 0.5296	*p* = 0.4242	*p* < 0.4632
Coupling (DFn = 1, DFd = 40)	*F* = 1.71e-003	*F* = 5.00	*F* = 0.14
	p = 0.9672	***p* = 0.0312**	*p* = 0.7118

αGP, alpha-glycerophosphate; Basal, glucose-sustained mitochondrial ATP production; CCO, cytochrome c oxidase; CS, citrate synthase activity; M/G, malate/glutamate; ROS, reactive oxygen species; S, succinate. DF, degrees of freedom; DFn, number of groups -1; DFd, number of subjects – DFn. Numerosity of the groups is as follows. For the comparison between controls and PM: younger controls, n = 4; older controls n = 4; younger PM, n = 7, older PM, n = 13. For the comparison between younger and older carriers: younger PM, n = 17; older PM, n = 5; younger FXTAS, n = 5; older FXTAS, n = 15). Note: in some instances, outcomes for 1–6 samples were not tested for lack of biological material. Bolded are statistically significant p values (<0.05).

RNA and Protein Metabolism, Glycolysis and Cellular Response to Stress Is Differentially Regulated in Females With PM

Considering that impaired energy metabolism in the brain is integral to many CNS diseases, cells display complex

proteomic responses to energy deficits, including activation of UPR and limited protein synthesis, among others. To gain a deeper insight on the molecular mechanisms of the responses originating from the impaired energy deficit in a PM genetic background, we utilized a proteomics approach on PBMCs from a subset of carriers (see demographics details of this subset under **Table 1**). Proteins significantly altered between PM and non-carriers were uploaded with their corresponding fold change values (**Supplementary Dataset**) to STRING (Szklarczyk et al., 2019). Interactomes were algorithmically generated based on direct associations (physical or functional) between eligible proteins. STRING generated a score for each interactome which is a putative measure of probability, with the shading of each node being positively correlated with the magnitude of the fold change. The main functional interactome showed upregulation of the following pathways: HIF-1 signaling, glycolysis, sugars and carbon metabolism, pentose phosphate pathway, pathways involved in cancer-related faulty transcriptional regulation, and pathways affected in Alzheimer's disease (**Table 3**). Among the downregulated ones were ribosomal-, spliceosomal- (**Supplementary Figure 1**) and proteasomal-related pathways (**Table 3**; **Supplementary Figure 2**; **Supplementary Dataset**), pyruvate metabolism, amino acids degradation (in particular branched amino acids), RNA processing (**Table 3**; **Supplementary Figure 2**; **Supplementary Dataset**) and transport, fatty acid synthesis, and TCA (**Table 3**; **Figure 2A**; KEGG and REACTOME Pathway tabs of **Supplementary Dataset**). This interactome highlighted a shift in mitochondrial energy production (and consistent with the previous results on bioenergetics), enhanced endoplasmic reticulum (ER) stress and ribosomal dysfunction. A sub-interactome (named "Energy production interactome") was linked to energy-producing pathways including mitochondrial bioenergetics and glycolysis (**Figure 2B**; **Supplementary Figure 3**; **Supplementary Dataset**, tabs highlighted in gray). The decrease in proteins involved in butanoate metabolism, fatty acid elongation and beta-oxidation along with BCAA metabolism (ECH1, HSD17B10, and ECHS1) indicates a shift toward glycolysis (higher HK1, ALDOA, but lower LDHB) as alternative energy source without incurring into increased ketone bodies' metabolism.

Since the protein changes provided insight into the complex molecular alterations underpinning the cellular adaptation to the PM-mediated stress, we sought to evaluate circulating metabolites and biomarkers of mitochondrial dysfunction by performing untargeted plasma metabolomics. To this end, untargeted metabolomics was performed by using gas chromatography mass spectrometry in plasma from 7 carriers and 8 age-matched controls (see demographics details under **Table 1**). Similar to the metabolic disarray observed in some mitochondrial disorders, Krebs' cycle intermediates, dicarboxylic acids, and "other metabolites" associated with glycolysis and leucine metabolism were mostly up-regulated (**Supplementary Figure 4**), with levels of aconitate, succinate, lactic acid, and lactate-to-pyruvate, being significantly higher in PM than controls (**Supplementary Figure 4**). These results confirm and expand findings of increased Krebs' cycle intermediates, likely the result of an impaired TCA activity, already observed by our group in PM carriers of both sexes (Giulivi et al., 2016), with aconitate, and isocitrate being those that differentiated the most between diagnostic groups, along with oleamide (Giulivi et al., 2016). In this regard, levels of oleamide, along with tryptophan, were found significantly lower in female PM whereas those of cholesterol were significantly higher in PM (**Supplementary Figure 4**). The odds ratio (OR) for these metabolites to be altered in the PM (**Figure 2C** with $p < 0.1$) was significant for cholesterol, oleamide, tryptophan, aconitate, succinate, lactate, and lactate-to-pyruvate ratio, glycerate, alpha-glycerophosphate, 4-hydroxybutyrate and some of the dicarboxylic acids tested.

TABLE 3 | Differential expression of pathways in PBMC from PM females.

Upregulated	Raw p
HIF-1 signaling pathway	0.0011698
Glycolysis or Gluconeogenesis	0.013441
Fructose and mannose metabolism	0.02419
Neomycin, kanamycin and gentamicin biosynthesis	0.036192
Central carbon metabolism in cancer	0.091013
Bacterial invasion of epithelial cells	0.10011
Alzheimer disease	0.13034
Transcriptional misregulation in cancer	0.15592
Pentose phosphate pathway	0.19871
Downregulated	**Raw p**
Ribosome	1.24E-17
Spliceosome	0.016999
Propanoate metabolism	0.025582
Pyruvate metabolism	0.033013
Proteasome	0.042895
Valine, leucine and isoleucine degradation	0.0482
Thermogenesis	0.089012
Non-homologous end-joining	0.091438
Complement and coagulation cascades	0.1142
RNA transport	0.12057
Fatty acid elongation	0.18073
Butanoate metabolism	0.18677
Citrate cycle (TCA cycle)	0.19871

*For the detailed list of proteins identified by proteomics analysis see **Supplementary Dataset**. Proteomics analysis was evaluated in 2 controls and 3 PM without FXTAS (**Table 1**).*

DISCUSSION

Mounting evidence has shown that female carriers of the PM are at higher risk for developing several health-related issues compared to non-carrier females (Bailey et al., 2008; Hunter et al., 2010; Winarni et al., 2012; Wheeler et al., 2014b; Movaghar et al., 2019). Awareness of these risks and correlation of the clinical signs with the biochemical footprint of carriers could help to identify critical biomarkers in early diagnosis and likely prognosis. If ascertained, these associations could lead to an integrated approach between clinical specialties and basic science, which could be extremely beneficial in the management of

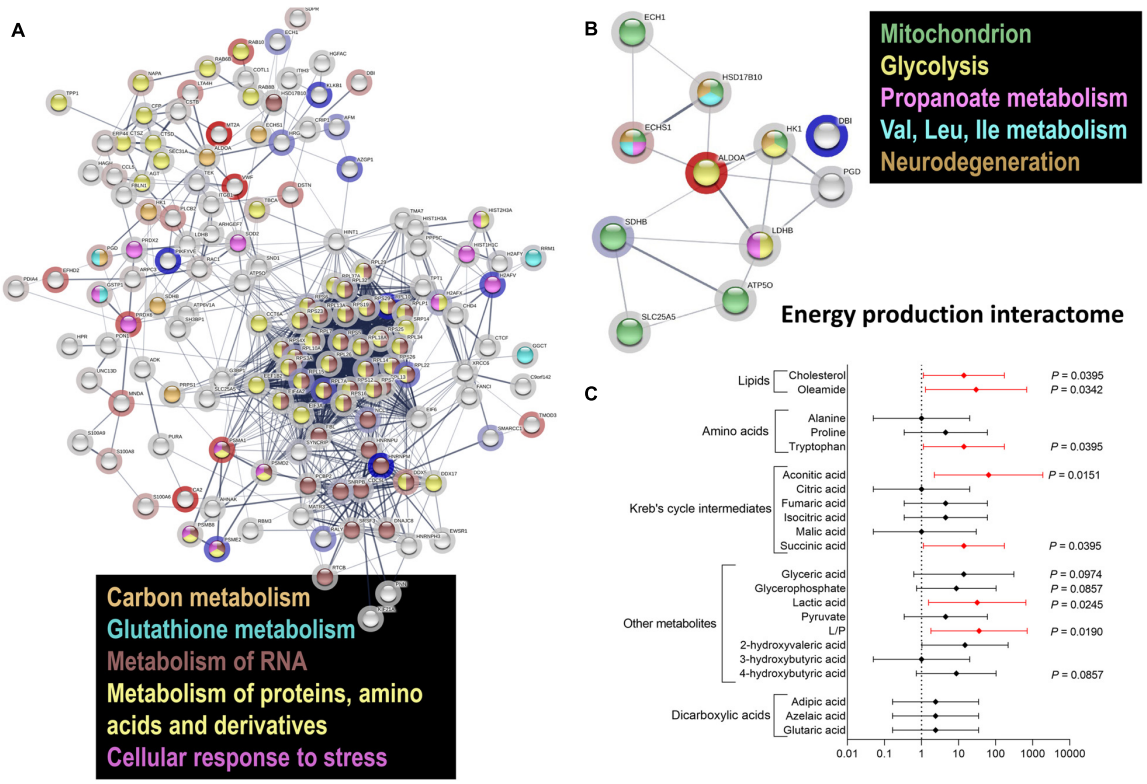

FIGURE 2 | Differential protein and metabolite enrichment in PM females. **(A)** Proteomics analysis was carried out in PBMC from PM females 29–63 year old and age-matched controls. Proteins detected in both PM and non-carriers were uploaded with their corresponding fold change values (see **Supplementary Dataset**) to STRING. Interactomes were algorithmically generated based on direct associations (physical or functional) between eligible proteins. The interactomes are color coded with blue nodes representing proteins that were down-regulated, red upregulated in PM, and clear when there were detected but whose levels were not statistically different between diagnostic groups. The shading of each node is correlated with the magnitude of the fold change. Differentially regulated metabolic pathways included carbon metabolism, metabolism of RNA, proteins, amino acids, and cellular response to oxidative stress. **(B)** A subset of differentially regulated proteins (**Supplementary Dataset**, tabs highlighted in gray) had key roles in mitochondrial function, glycolysis, fatty acid and amino acid metabolism, as well as in RNA processing (pathways reported in **Supplementary Figures 1–3**) and pathways affected in neurodegeneration. **(C)** Metabolomics analysis was performed in plasma from 8 controls and 7 age-matched PM carriers, 24–52 year, and age-matched controls. Differentially enriched metabolites are shown, with their respective *p* values, in **Supplementary Figure 4**. A forest plot was built with the odds ratios (*X* axis) and the 95% CI (error bars) calculated with control values for each selected metabolite based on its role in glycolysis and mitochondrial metabolism. In red are metabolites with statistically significant OR, indicating a higher probability to be affected in the PM, and as such considered as putative biomarkers for female carriers.

symptoms and challenges that female PM carriers experience in their day-to-day life.

The brain's high mitochondrial energy consumption makes neurons highly vulnerable to impaired glucose metabolism (Hyder et al., 2013). Then, it is not surprising that a decline in mitochondrial activity has been associated with memory loss and, particularly, with age-dependent cognitive impairment (Freeman and Young, 2000; Liu et al., 2002). Moreover, most mtDNA diseases are associated with brain disorders because adequate neuronal development (Atamna et al., 2002; Zini et al., 2002) and structure (Johnson and Byerly, 1993; Bristow et al., 2002; Liu et al., 2002) and axonal and synaptic activity (Freeman and Young, 2000; Zenisek and Matthews, 2000) all involve mitochondrial genes (Wallace, 1999; Schon, 2000). Mitochondrial dysfunction has been reported not only in neurodegeneration (Friedland et al., 1983; Minoshima et al., 1997; Chiaravalloti et al., 2015) but also in pre-symptomatic, genetically-susceptible individuals (Small et al., 1995; Reiman et al., 1996; Mosconi et al., 2006; Ossenkoppele et al., 2013). In line with these studies and our previous reports on the PM (Napoli et al., 2016a, 2018), our study strongly indicates that global impairment of bioenergetics, and likely the subsequent energy depletion, is one of the earliest functional changes prior to the onset of overt clinical symptoms. This is supported by the relatively milder mitochondrial dysfunction in PM carriers without FXTAS and FXPOI which is enhanced with the diagnosis and progression of FXTAS. While the decline in cognitive/intellectual (FSIQ) and executive (BDS-2) function was correlated with longer CGGs, intellectual decline (FSIQ) was significantly correlated with an overall mitochondrial deficit. This is highly suggestive that mitochondrial deficits may influence neuronal dysregulation and, over the years, degenerative mechanisms such as described for AD (Rice et al., 2014).

The metabolomics findings are particularly relevant in the context of several psychiatric and neurological symptoms experienced by some female carriers as oleamide has a critical

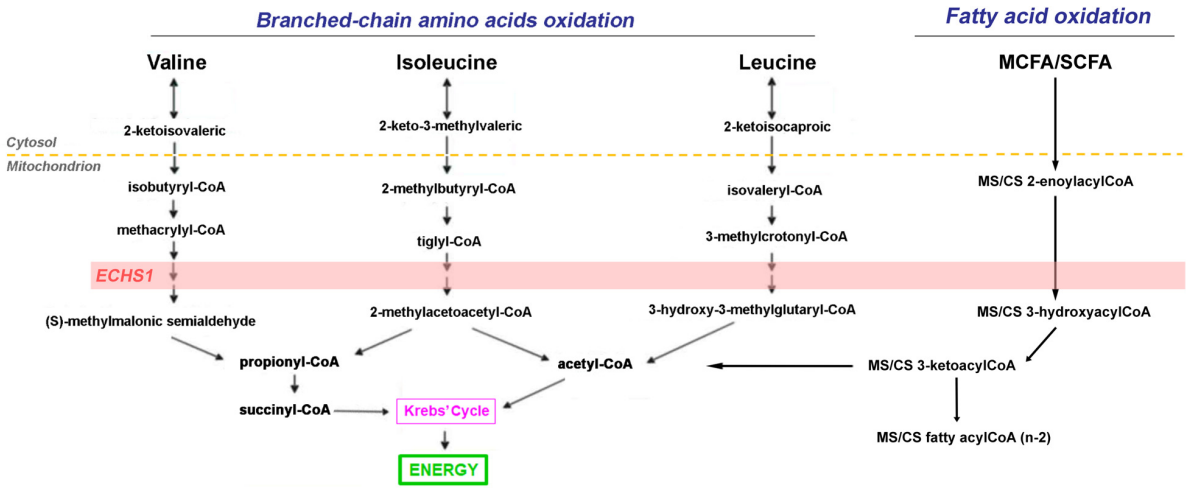

FIGURE 3 | Role of ECSH1 in branched-chain amino acids and short- and medium-chain fatty acid catabolism. The short-chain enoyl-CoA hydratase ECHS1 has a critical role in branched chain amino acid (BCAA) catabolism as well as fatty acid catabolism generating succinyl-CoA and acetyl-CoA which are fed into the Krebs' cycle for the generation of reducing equivalents.

role in mood and sleep disorders as well as depression due to its interaction with serotonergic and GABAergic neurotransmission (Mendelson and Basile, 2001). Similarly, tryptophan is not only an essential amino acid for protein synthesis but also a precursor of several biological mediators involved in stress response, antioxidant system, behavioral response, and immune system (Firk and Markus, 2009; Hoglund et al., 2017). Decreased tryptophan levels have been linked to lower serotonin levels, likely setting the basis for the establishment of neuropsychological symptoms including depression, anxiety, irritability, attention deficits, and insomnia (Jenkins et al., 2016). The higher cholesterol levels are of interest in the context of neurodegeneration, as mitochondrial cholesterol loading has recently emerged as a key player in the pathology of neurological disorders such as AD and Niemann-Pick Type C (NPC) disease (Elustondo et al., 2017; Torres et al., 2019).

In line with these findings, the lower fatty acid beta-oxidation resulting mainly from lower ABAD and ECHS1, deserves a separate discussion. Lower levels of ABAD may disrupt the ABAD-beta-amyloid interaction in mitochondria and suppresses apoptosis by increasing the levels of beta-amyloid as reported for AD patients and transgenic mouse models (Lustbader et al., 2004). Deficiency in ECHS1 results in metabolic acidosis with a combined respiratory chain deficiency (Sakai et al., 2015). Consistent with these findings, higher levels of lactic acid and a trend towards higher 2-hydroxyvaleric acid, proline and organic acids, such as adipic, azelaic and glutaric, were observed in plasma from female carriers (**Figures 2C**, **3**) similar to the cases reported by others (Fitzsimons et al., 2018). Then, the significant lower expression of ABAD and ECHS1 in female carriers makes them as interesting candidates to investigate further in terms of its regulation in the context of beta-amyloid and proteostasis. Furthermore, since the OXPHOS decline in ECHS1 deficiency has been attributed to the accumulation of inhibitory fatty acid intermediates and to the disruption of ETC Complex biogenesis and/or stability (Burgin and McKenzie, 2020), it would not be unlikely that these mechanisms are contributing to the OXPHOS deficiencies observed in the PM.

Proteomics analysis not only confirmed and extended the functional and metabolomics results, but also shed light into the proteostasis status of the PM. The biological consequence of higher mitochondrial ROS was identified with the higher levels of aconitate likely the result of inactivation of aconitase, an enzyme highly sensitive to oxidative stress damage. The increase in oxidative stress may contribute to proteotoxicity and to the generation of misfolded proteins that accumulate upon ER stress, as a result, increase in the detoxification demands. However, an uncoordinated proteomic response in the ER was identified in the PM. Only one chaperone, HSPA5, was higher in PM vs. non-carriers, and a mixed response was observed for subunits of the proteasome. These results suggest that proteasomal degradation, a fundamental mechanism for degrading the misfolded proteins that accumulate in response to the metabolic challenge, is somehow not coordinated to adequately cope with the proteotoxicity. Indeed, it has been a long-standing hypothesis that protein aggregates in diseased brain impair the protein degradation function of the 26S proteasome (Taylor et al., 2002; Ciechanover and Brundin, 2003; Valera et al., 2005), then it would be reasonable to hypothesize that as the UPR is not fully coordinated in female carriers, any proteasomal response expected to ensue in response to a metabolic, environmental or pharmacological challenge might be adversely affected.

Our findings are particularly relevant for female carriers, as mitochondria have a critical role in oocyte developmental competence and function (Dumollard et al., 2007; Wang et al., 2009), and in the development and function of the reproductive system fertility (Reynier et al., 2001; El Shourbagy et al., 2006; Santos et al., 2006; Cagnone et al., 2016; Demain et al., 2017) with an irrefutable implication in primary ovarian insufficiency (POI)

(Conca Dioguardi et al., 2016; Tiosano et al., 2019). The energy deficit along with the lower levels of ECHS1 in carriers, one of the genes identified as critical for oocyte developmental competence (Biase, 2017), set the basis for future research to identify more clearly the role of this protein in POI and FXPOI.

In conclusion, through a combined multi-omics approach in PBMC and plasma of PM females in association with thorough clinical and bioenergetics assessments, we found impaired metabolic pathways which can result from the direct action of toxic intermediates derived from the PM genetic background (either accumulation of mRNA or proteotoxicity of RAN-derived protein products). In this regard, we are adding the novel observation that the accumulation of aberrant metabolites resulting from deficiencies in critical metabolic steps may add to the altered interaction between fatty acid oxidation and the electron transport chain contributing to the overall OXPHOS decline as it has been described for ECHS1 deficiency (Burgin and McKenzie, 2020; **Figure 3**). In turn, either mechanism elicits a suboptimal activation of UPR and ERAD responses, setting a challenging scenario to withstand other, more severe forms of stress. Along these lines, the development of neurodegeneration or other clinical symptoms in older carriers could be linked to a lifetime accumulation of cellular damage, aggravated by the aging process.

Limitations

There are potential limitations to our study, starting with its partly retrospective design. Of all the participants included, neurocognitive testing and omics analyses were performed in a subset of individuals. The selection of the cohort was from a controlled sample of individuals enrolled in the study upon referral to the medical center clinic. For this reason, this cohort might not be representative of the full PM population range but rather the most affected ones. Similarly, a fraction of the controls included in our analysis were family members of probands with typical *FMR1* repeat sizes and, while they may represent the non-carrier group, they may be affected by extra emotional burden by having a relative or partner with PM diagnosis. The challenging recruitment of healthy donors is reflected in their relatively lower number particularly in the 60–70 year age bracket. Information on anxiety was self-reported. The OXPHOS variability could be ascribed to the lack of a clinical diagnosis of a mitochondrial disease (i.e., borderline OXPHOS capacity without overt mitochondrial disease symptoms) which is manifested in front of a challenge (high-intensity exercise, a co-morbidity, or aging), the influence of different dietary habits and lifestyle, and the contribution of mtDNA polymorphisms to cognitive deficits (Skuder et al., 1995).

FINANCIAL DISCLOSURE

RH has received funding from the Azrieli Foundation, Zynerba, Ovid and Neuren for treatment trials in fragile X syndrome, and consulted with Zynerba and Fulcrum regarding treatment for fragile X syndrome. FT has received funding from the Azrieli Foundation and Zynerba for studies on fragile X syndrome and has consulted with Zynerba. The other authors have no financial disclosures relevant to this article.

DATA AVAILABILITY STATEMENT

The raw data supporting the conclusions of this article will be made available by the authors, without undue reservation.

ETHICS STATEMENT

The studies involving human participants were reviewed and approved by IRB Ethics Committee at UC Davis Medical Center. The patients/participants provided their written informed consent to participate in this study.

AUTHOR CONTRIBUTIONS

EN processed all samples, carried out all polarographic and spectrophotometric measurements, performed correspondent statistical analyses, wrote the manuscript, and revised and approved the final version as submitted. YM collected and provided demographic, clinical, and molecular data, revised the manuscript, and approved the final version as submitted. AS carried out the neuropsychological testing and also revised the manuscript and approved the final as submitted. FT provided CGG repeats and XAR, revised the manuscript, and approved the final version as submitted. RH carried out clinical assessment of the women enrolled in this study and wrote clinical findings, revised the manuscript, and approved the final manuscript as submitted. CG conceptualized and designed the study, analyzed the omics data, wrote the manuscript, and approved the final manuscript as submitted.

FUNDING

This study was funded by the National Institutes of Health (HD036071). Support was also obtained from the MIND Institute Intellectual and Developmental Disabilities Research Center (U54 HD079125) and the Health and Human Administration of Developmental Disabilities grants 90DD0596 and UL1 TR001860.

ACKNOWLEDGMENTS

We wish to thank all women who provided these samples making this study possible.

SUPPLEMENTARY MATERIAL

The Supplementary Material for this article can be found online at: https://www.frontiersin.org/articles/10.3389/fmolb.2020.578640/full#supplementary-material

REFERENCES

Allen, E. G., Charen, K., Hipp, H. S., Shubeck, L., Amin, A., He, W., et al. (2020). Clustering of comorbid conditions among women who carry an FMR1 premutation. *Genet. Med.* 22, 758–766. doi: 10.1038/s41436-019-0733-5

Allen, E. G., Sullivan, A. K., Marcus, M., Small, C., Dominguez, C., Epstein, M. P., et al. (2007). Examination of reproductive aging milestones among women who carry the FMR1 premutation. *Hum. Reprod.* 22, 2142–2152. doi: 10.1093/humrep/dem148

Allingham-Hawkins, D. J., Babul-Hirji, R., Chitayat, D., Holden, J. J. A., Yang, K. T., Lee, C., et al. (1999). Fragile X premutation is a significant risk factor for premature ovarian failure: the international collaborative POF in fragile X study - Preliminary data. *Am. J. Med. Genet.* 83, 322–325. doi: 10.1002/(SICI)1096-8628(19990402)83:4<322::AID-AJMG17>3.0.CO;2-B

Atamna, H., Killilea, D. W., Killilea, A. N., and Ames, B. N. (2002). Heme deficiency may be a factor in the mitochondrial and neuronal decay of aging. *Proc. Natl. Acad. Sci. U.S.A.* 99, 14807–14812. doi: 10.1073/pnas.192585799

Bagni, C., Tassone, F., Neri, G., and Hagerman, R. (2012). Fragile X syndrome: causes, diagnosis, mechanisms, and therapeutics. *J. Clin. Invest.* 122, 4314–4322. doi: 10.1172/JCI63141

Bailey, D. B. Jr., Raspa, M., Olmsted, M., and Holiday, D. B. (2008). Co-occurring conditions associated with FMR1 gene variations: findings from a national parent survey. *Am. J. Med. Genet. A* 146A, 2060–2069. doi: 10.1002/ajmg.a.32439

Belanger, H. G., Wilder-Willis, K., Malloy, P., Salloway, S., Hamman, R. F., and Grigsby, J. (2005). Assessing motor and cognitive regulation in AD, MCI, and controls using the behavioral dyscontrol scale. *Arch. Clin. Neuropsychol.* 20, 183–189. doi: 10.1016/j.acn.2004.05.003

Bennett, C. E., Conway, G. S., Macpherson, J. N., Jacobs, P. A., and Murray, A. (2010). Intermediate sized CGG repeats are not a common cause of idiopathic premature ovarian failure. *Hum. Reprod.* 25, 1335–1338. doi: 10.1093/humrep/deq058

Berry-Kravis, E., Abrams, L., Coffey, S. M., Hall, D. A., Greco, C., Gane, L. W., et al. (2007a). Fragile X-associated tremor/ataxia syndrome: clinical features, genetics, and testing guidelines. *Mov. Disord.* 22, 2018–2030. doi: 10.1002/mds.21493

Berry-Kravis, E., Goetz, C. G., Leehey, M. A., Hagerman, R. J., Zhang, L., Li, L., et al. (2007b). Neuropathic features in fragile X premutation carriers. *Am. J. Med. Genet. A* 143A, 19–26. doi: 10.1002/ajmg.a.31559

Berry-Kravis, E., Lewin, F., Wuu, J., Leehey, M., Hagerman, R., Hagerman, P., et al. (2003). Tremor and ataxia in fragile X premutation carriers: blinded videotape study. *Ann. Neurol.* 53, 616–623. doi: 10.1002/ana.10522

Berry-Kravis, E., Potanos, K., Weinberg, D., Zhou, L., and Goetz, C. G. (2005). Fragile X-associated tremor/ataxia syndrome in sisters related to X-inactivation. *Ann. Neurol.* 57, 144–147. doi: 10.1002/ana.20360

Besterman, A. D., Wilke, S. A., Mulligan, T. E., Allison, S. C., Hagerman, R., Seritan, A. L., et al. (2014). Towards an understanding of neuropsychiatric manifestations in fragile X premutation carriers. *Fut. Neurol.* 9, 227–239. doi: 10.2217/fnl.14.11

Biase, F. H. (2017). Oocyte developmental competence: insights from cross-species differential gene expression and human oocyte-specific functional gene networks. *OMICS* 21, 156–168. doi: 10.1089/omi.2016.0177

Boffoli, D., Scacco, S. C., Vergari, R., Persio, M. T., Solarino, G., Laforgia, R., et al. (1996). Ageing is associated in females with a decline in the content and activity on the b-c1 complex in skeletal muscle mitochondria. *Biochim. Biophys. Acta* 1315, 66–72. doi: 10.1016/0925-4439(95)00107-7

Boffoli, D., Scacco, S. C., Vergari, R., Solarino, G., Santacroce, G., and Papa, S. (1994). Decline with age of the respiratory chain activity in human skeletal muscle. *Biochim. Biophys. Acta* 1226, 73–82. doi: 10.1016/0925-4439(94)90061-2

Bourgeois, J. A., Cogswell, J. B., Hessl, D., Zhang, L., Ono, M. Y., Tassone, F., et al. (2007). Cognitive, anxiety and mood disorders in the fragile X-associated tremor/ataxia syndrome. *Gen. Hosp. Psychiatry* 29, 349–356. doi: 10.1016/j.genhosppsych.2007.03.003

Bristow, E. A., Griffiths, P. G., Andrews, R. M., Johnson, M. A., and Turnbull, D. M. (2002). The distribution of mitochondrial activity in relation to optic nerve structure. *Arch. Ophthalmol.* 120, 791–796. doi: 10.1001/archopht.120.6.791

Burch, H. B., Lowry, O. H., Kuhlman, A. M., Skerjance, J., Diamant, E. J., Lowry, S. R., et al. (1963). Changes in patterns of enzymes of carbohydrate metabolism in the developing rat liver. *J. Biol. Chem.* 238, 2267–2273.

Burgin, H. J., and McKenzie, M. (2020). Understanding the role of OXPHOS dysfunction in the pathogenesis of ECHS1 deficiency. *FEBS Lett.* 594, 590–610. doi: 10.1002/1873-3468.13735

Byrne, E., Dennett, X., and Trounce, I. (1991). Oxidative energy failure in post-mitotic cells: a major factor in senescence. *Rev. Neurol.* 147, 6–7.

Cagnone, G. L., Tsai, T. S., Makanji, Y., Matthews, P., Gould, J., Bonkowski, M. S., et al. (2016). Restoration of normal embryogenesis by mitochondrial supplementation in pig oocytes exhibiting mitochondrial DNA deficiency. *Sci. Rep.* 6:23229. doi: 10.1038/srep23229

Capkova, M., Houstek, J., Hansikova, H., Hainer, V., Kunesova, M., and Zeman, J. (2002). Activities of cytochrome c oxidase and citrate synthase in lymphocytes of obese and normal-weight subjects. *Int. J. Obes. Relat. Metab. Disord.* 26, 1110–1117. doi: 10.1038/sj.ijo.0802055

Cardellach, F., Galofre, J., Cusso, R., and Urbano-Marquez, A. (1989). Decline in skeletal muscle mitochondrial respiration chain function with ageing. *Lancet* 334, 44–45. doi: 10.1016/S0140-6736(89)90282-1

Chiaravalloti, A., Martorana, A., Koch, G., Toniolo, S., Di Biagio, D., Di Pietro, B., et al. (2015). Functional correlates of t-Tau, p-Tau and Abeta(1)(-)(4)(2) amyloid cerebrospinal fluid levels in Alzheimer's disease: a (1)(8)F-FDG PET/CT study. *Nucl. Med. Commun.* 36, 461–468. doi: 10.1097/MNM.0000000000000272

Ciechanover, A., and Brundin, P. (2003). The ubiquitin proteasome system in neurodegenerative diseases: sometimes the chicken, sometimes the egg. *Neuron* 40, 427–446. doi: 10.1016/s0896-6273(03)00606-8

Claeys, T., Boogers, A., and Vanneste, D. (2020). MRI findings in fragile X-associated tremor/ataxia syndrome. *Acta Neurol. Belg.* 120, 181–183. doi: 10.1007/s13760-019-01237-w

Conca Dioguardi, C., Uslu, B., Haynes, M., Kurus, M., Gul, M., Miao, D. Q., et al. (2016). Granulosa cell and oocyte mitochondrial abnormalities in a mouse model of fragile X primary ovarian insufficiency. *Mol. Hum. Reprod.* 22, 384–396. doi: 10.1093/molehr/gaw023

Cooper, J. M., Mann, V. M., and Schapira, A. H. (1992). Analyses of mitochondrial respiratory chain function and mitochondrial DNA deletion in human skeletal muscle: effect of ageing. *J. Neurol. Sci.* 113, 91–98. doi: 10.1016/0022-510x(92)90270-u

Demain, L. A., Conway, G. S., and Newman, W. G. (2017). Genetics of mitochondrial dysfunction and infertility. *Clin. Genet.* 91, 199–207. doi: 10.1111/cge.12896

Drozdick, L. W., Wahlstrom, D., Zhu, J., and Weiss, L. G. (2012). "The Wechsler adult intelligence scale—fourth edition and the wechsler memory scale—fourth edition," in *Contemporary Intellectual Assessment: Theories, Tests, and Issues*, 3rd Edn, eds D. P. Flanagan and P. L. Harrison (New York, NY: The Guilford Press), 197–223.

Dumollard, R., Duchen, M., and Carroll, J. (2007). The role of mitochondrial function in the oocyte and embryo. *Curr. Top. Dev. Biol.* 77, 21–49. doi: 10.1016/S0070-2153(06)77002-8

El Shourbagy, S. H., Spikings, E. C., Freitas, M., and St John, J. C. (2006). Mitochondria directly influence fertilisation outcome in the pig. *Reproduction* 131, 233–245. doi: 10.1530/rep.1.00551

Elizur, S. E., Lebovitz, O., Derech-Haim, S., Dratviman-Storobinsky, O., Feldman, B., Dor, J., et al. (2014). Elevated levels of FMR1 mRNA in granulosa cells are associated with low ovarian reserve in FMR1 premutation carriers. *PLoS One* 9:e0105121. doi: 10.1371/journal.pone.0105121

Elustondo, P., Martin, L. A., and Karten, B. (2017). Mitochondrial cholesterol import. *Biochim. Biophys. Acta Mol. Cell. Biol. Lipids* 1862, 90–101. doi: 10.1016/j.bbalip.2016.08.012

Ennis, S., Ward, D., and Murray, A. (2006). Nonlinear association between CGG repeat number and age of menopause in FMR1 premutation carriers. *Europ. J. Hum. Genet.* 14, 253–255. doi: 10.1038/sj.ejhg.5201510

Filipovic-Sadic, S., Sah, S., Chen, L., Krosting, J., Sekinger, E., Zhang, W., et al. (2010). A novel FMR1 PCR method for the routine detection of low abundance expanded alleles and full mutations in fragile X syndrome. *Clin. Chem.* 56, 399–408. doi: 10.1373/clinchem.2009.136101

Firk, C., and Markus, C. R. (2009). Mood and cortisol responses following tryptophan-rich hydrolyzed protein and acute stress in healthy subjects with

high and low cognitive reactivity to depression. *Clin. Nutr.* 28, 266–271. doi: 10.1016/j.clnu.2009.03.002

Fitzsimons, P. E., Alston, C. L., Bonnen, P. E., Hughes, J., Crushell, E., Geraghty, M. T., et al. (2018). Clinical, biochemical, and genetic features of four patients with short-chain enoyl-CoA hydratase (ECHS1) deficiency. *Am. J. Med. Genet. A* 176, 1115–1127. doi: 10.1002/ajmg.a.38658

Freeman, F. M., and Young, I. G. (2000). The mitochondrial benzodiazepine receptor and avoidance learning in the day-old chick. *Pharmacol. Biochem. Behav.* 67, 355–362. doi: 10.1016/S0091-3057(00)00373-7

Friedland, R. P., Budinger, T. F., Ganz, E., Yano, Y., Mathis, C. A., Koss, B., et al. (1983). Regional cerebral metabolic alterations in dementia of the Alzheimer type: positron emission tomography with [18F]fluorodeoxyglucose. *J. Comput. Assist. Tomogr.* 7, 590–598. doi: 10.1097/00004728-198308000-00003

Giulivi, C., Napoli, E., Schwartzer, J., Careaga, M., and Ashwood, P. (2013). Gestational exposure to a viral mimetic poly(i:C) results in long-lasting changes in mitochondrial function by leucocytes in the adult offspring. *Mediators Inflamm.* 2013:609602. doi: 10.1155/2013/609602

Giulivi, C., Napoli, E., Tassone, F., Halmai, J., and Hagerman, R. (2016). Plasma biomarkers for monitoring brain pathophysiology in FMR1 premutation carriers. *Front. Mol. Neurosci.* 9:71. doi: 10.3389/fnmol.2016.00071

Giulivi, C., Zhang, Y. F., Omanska-Klusek, A., Ross-Inta, C., Wong, S., Hertz-Picciotto, I., et al. (2010). Mitochondrial dysfunction in autism. *JAMA* 304, 2389–2396. doi: 10.1001/jama.2010.1706

Hagerman, P. J., and Hagerman, R. J. (2004). The fragile-X premutation: a maturing perspective. *Am. J. Hum. Genet.* 74, 805–816. doi: 10.1086/386296

Hagerman, R., and Hagerman, P. (2013). Advances in clinical and molecular understanding of the FMR1 premutation and fragile X-associated tremor/ataxia syndrome. *Lancet Neurol.* 12, 786–798. doi: 10.1016/S1474-4422(13)70125-X

Hagerman, R. J., and Hagerman, P. (2016). Fragile X-associated tremor/ataxia syndrome - features, mechanisms and management. *Nat. Rev. Neurol.* 12, 403–412. doi: 10.1038/nrneurol.2016.82

Hagerman, R. J., Hall, D. A., Coffey, S., Leehey, M., Bourgeois, J., Gould, J., et al. (2008). Treatment of fragile X-associated tremor ataxia syndrome (FXTAS) and related neurological problems. *Clin. Interv. Aging* 3, 251–262. doi: 10.2147/cia.s1794

Hagerman, R. J., Leavitt, B. R., Farzin, F., Jacquemont, S., Greco, C. M., Brunberg, J. A., et al. (2004). Fragile-X-associated tremor/ataxia syndrome (FXTAS) in females with the FMR1 premutation. *Am. J. Hum. Genet.* 74, 1051–1056. doi: 10.1086/420700

Hagerman, R. J., Leehey, M., Heinrichs, W., Tassone, F., Wilson, R., Hills, J., et al. (2001). Intention tremor, parkinsonism, and generalized brain atrophy in male carriers of fragile X. *Neurology* 57, 127–130. doi: 10.1212/wnl.57.1.127

Hagerman, R. J., Protic, D., Rajaratnam, A., Salcedo-Arellano, M. J., Aydin, E. Y., and Schneider, A. (2018). Fragile X-associated neuropsychiatric disorders (FXAND). *Front. Psychiatry* 9:564. doi: 10.3389/fpsyt.2018.00564

Hoglund, E., Overli, O., Andersson, M. A., Silva, P., Laursen, D. C., Moltesen, M. M., et al. (2017). Dietary l-tryptophan leaves a lasting impression on the brain and the stress response. *Br. J. Nutr.* 117, 1351–1357. doi: 10.1017/S0007114517001428

Hunter, J. E., Rohr, J. K., and Sherman, S. L. (2010). Co-occurring diagnoses among FMR1 premutation allele carriers. *Clin. Genet.* 77, 374–381. doi: 10.1111/j.1399-0004.2009.01317.x

Hyder, F., Rothman, D. L., and Bennett, M. R. (2013). Cortical energy demands of signaling and nonsignaling components in brain are conserved across mammalian species and activity levels. *Proc. Natl. Acad. Sci. U.S.A.* 110, 3549–3554. doi: 10.1073/pnas.1214912110

Jacquemont, S., Hagerman, R. J., Leehey, M., Grigsby, J., Zhang, L., Brunberg, J. A., et al. (2003). Fragile X premutation tremor/ataxia syndrome: molecular, clinical, and neuroimaging correlates. *Am. J. Hum. Genet.* 72, 869–878. doi: 10.1086/374321

Jenkins, T. A., Nguyen, J. C., Polglaze, K. E., and Bertrand, P. P. (2016). Influence of tryptophan and serotonin on mood and cognition with a possible role of the gut-brain axis. *Nutrients* 8:56. doi: 10.3390/nu8010056

Johnson, B. D., and Byerly, L. (1993). A cytoskeletal mechanism for Ca2+ channel metabolic dependence and inactivation by intracellular Ca2+. *Neuron* 10, 797–804. doi: 10.1016/0896-6273(93)90196-X

Karimov, C. B., Moragianni, V. A., Cronister, A., Srouji, S., Petrozza, J., Racowsky, C., et al. (2011). Increased frequency of occult fragile X-associated primary ovarian insufficiency in infertile women with evidence of impaired ovarian function. *Hum. Reprod.* 26, 2077–2083. doi: 10.1093/humrep/der168

Kwong, L. K., and Sohal, R. S. (2000). Age-related changes in activities of mitochondrial electron transport complexes in various tissues of the mouse. *Arch. Biochem. Biophys.* 373, 16–22. doi: 10.1006/abbi.1999.1495

Lezza, A. M. S., Boffoli, D., Scacco, S., Cantatore, P., and Gadaleta, M. N. (1994). Correlation between mitochondrial DNA 4977-bp deletion and respiratory chain enzyme activities in aging human skeletal muscles. *Biochem. Biophys. Res. Commun.* 205, 772–779. doi: 10.1006/bbrc.1994.2732

Linnane, A., Ozawa, T., Marzuki, S., and Tanaka, M. (1989). Mitochondrial DNA mutations as an important contributor to ageing and degenerative diseases Lancet. *Lancet* 333, 642–645. doi: 10.1016/S0140-6736(89)92145-4

Liu, J., Head, E., Gharib, A. M., Yuan, W., Ingersoll, R. T., Hagen, T. M., et al. (2002). Memory loss in old rats is associated with brain mitochondrial decay and RNA/DNA oxidation: Partial reversal by feeding acetyl-L-carnitine and/or R-α-lipoic acid. *Proc. Natl. Acad. Sci. U.S.A.* 99, 2356–2361. doi: 10.1073/pnas.261709299

Lozano, R., Saito, N., Reed, D., Eldeeb, M., Schneider, A., Hessl, D., et al. (2016). Aging in Fragile X Premutation carriers. *Cerebellum* 15, 587–594. doi: 10.1007/s12311-016-0805-x

Lustbader, J. W., Cirilli, M., Lin, C., Xu, H. W., Takuma, K., Wang, N., et al. (2004). ABAD directly links Abeta to mitochondrial toxicity in Alzheimer's disease. *Science* 304, 448–452. doi: 10.1126/science.1091230

Mendelson, W. B., and Basile, A. S. (2001). The hypnotic actions of the fatty acid amide, oleamide. *Neuropsychopharmacol.* 25, S36–S39. doi: 10.1016/S0893-133X(01)00341-4

Minoshima, S., Giordani, B., Berent, S., Frey, K. A., Foster, N. L., and Kuhl, D. E. (1997). Metabolic reduction in the posterior cingulate cortex in very early Alzheimer's disease. *Ann. Neurol.* 42, 85–94. doi: 10.1002/ana.410420114

Mosconi, L., Sorbi, S., De Leon, M. J., Li, Y., Nacmias, B., Myoung, P. S., et al. (2006). Hypometabolism exceeds atrophy in presymptomatic early-onset familial Alzheimer's disease. *J. Nucl. Med.* 47, 1778–1786.

Movaghar, A., Page, D., Brilliant, M., Baker, M. W., Greenberg, J., Hong, J., et al. (2019). Data-driven phenotype discovery of FMR1 premutation carriers in a population-based sample. *Sci. Adv.* 5:eaaw7195. doi: 10.1126/sciadv.aaw7195

Müller-Höcker, J. (1992). Mitochondria and ageing. *Brain Pathol.* 2, 149–158. doi: 10.1111/j.1750-3639.1992.tb00683.x

Münscher, C., Müller-Höcker, J., and Kadenbach, B. (1993). Human aging is associated with various point mutations in trna genes of mitochondrial DNA. *Biol. Chem. Hoppe Seyler* 374, 1099–1104. doi: 10.1515/bchm3.1993.374.7-12.1099

Murray, A., Schoemaker, M. J., Bennett, C. E., Ennis, S., Macpherson, J. N., Jones, M., et al. (2014). Population-based estimates of the prevalence of FMR1 expansion mutations in women with early menopause and primary ovarian insufficiency. *Genet. Med.* 16, 19–24. doi: 10.1038/gim.2013.64

Napoli, E., Schneider, A., Hagerman, R., Song, G., Wong, S., Tassone, F., et al. (2018). Impact of FMR1 premutation on neurobehavior and bioenergetics in young monozygotic twins. *Front. Genet.* 9:338. doi: 10.3389/fgene.2018.00338

Napoli, E., Song, G., Schneider, A., Hagerman, R., Eldeeb, M. A., Azarang, A., et al. (2016a). Warburg effect linked to cognitive-executive deficits in FMR1 premutation. *FASEB J.* 30, 3334–3351. doi: 10.1096/fj.201600315R

Napoli, E., Song, G., Wong, S., Hagerman, R., and Giulivi, C. (2016b). Altered bioenergetics in primary dermal fibroblasts from adult carriers of the FMR1 premutation before the onset of the neurodegenerative disease Fragile X-Associated Tremor/Ataxia Syndrome. *Cerebellum* 15, 552–564. doi: 10.1007/s12311-016-0779-8

Napoli, E., Tassone, F., Wong, S., Angkustsiri, K., Simon, T. J., Song, G., et al. (2015). Mitochondrial citrate transporter-dependent metabolic signature in the 22q11.2 deletion syndrome. *J. Biol. Chem.* 290, 23240–23253. doi: 10.1074/jbc.M115.672360

Napoli, E., Wong, S., Hung, C., Ross-Inta, C., Bomdica, P., and Giulivi, C. (2013). Defective mitochondrial disulfide relay system, altered mitochondrial morphology and function in Huntington's disease. *Hum. Mol. Genet.* 22, 989–1004. doi: 10.1093/hmg/dds503

Ojaimi, J., Masters, C. L., Opeskin, K., Mckelvie, P., and Byrne, E. (1999). Mitochondrial respiratory chain activity in the human brain as a function of age. *Mech. Ageing Dev.* 111, 39–47. doi: 10.1016/s0047-6374(99)00071-8

Ossenkoppele, R., Van Der Flier, W. M., Zwan, M. D., Adriaanse, S. F., Boellaard, R., Windhorst, A. D., et al. (2013). Differential effect of APOE genotype on amyloid load and glucose metabolism in AD dementia. *Neurology* 80, 359–365. doi: 10.1212/WNL.0b013e31827f0889

Papa, S. (1996). Mitochondrial oxidative phosphorylation changes in the life span. Molecular aspects and physiopathological implications. *Biochim. Biophys. Acta* 1276, 87–105. doi: 10.1016/0005-2728(96)00077-1

Pastore, L. M., Young, S. L., Baker, V. L., Karns, L. B., Williams, C. D., and Silverman, L. M. (2012). Elevated prevalence of 35-44 FMR1 trinucleotide repeats in women with diminished ovarian reserve. *Reprod. Sci.* 19, 1226–1231. doi: 10.1177/1933719112446074

Patsalis, P. C., Sismani, C., Hettinger, J. A., Holden, J. J. A., Lawson, J. S., Chalifoux, M., et al. (1999). Frequencies of' 'grey-zone' and premutation-size FMR1 CGG-repeat alleles in patients with developmental disability in Cyprus and Canada [1]. *Am. J. Med. Genet.* 84, 195–197. doi: 10.1002/(SICI)1096-8628(19990528)84:3<195::AID-AJMG4<3.0.CO;2-1

Perneger, T. V. (1998). What's wrong with bonferroni adjustments. *BMJ* 316, 1236–1238. doi: 10.1136/bmj.316.7139.1236

Pouresmaeili, F., and Fazeli, Z. (2014). Premature ovarian failure: a critical condition in the reproductive potential with various genetic causes. *Intl. J. Fert. Steril.* 8, 1–12.

Quiles, J. L., Martinez, E., Ibanez, S., Ochoa, J. J., Martin, Y., Lopez-Frias, M., et al. (2002). Ageing-related tissue-specific alterations in mitochondrial composition and function are modulated by dietary fat type in the rat. *J. Bioenerg. Biomembr.* 34, 517–524. doi: 10.1023/a:1022530512096

Reiman, E. M., Caselli, R. J., Yun, L. S., Chen, K., Bandy, D., Minoshima, S., et al. (1996). Preclinical evidence of Alzheimer's disease in persons homozygous for the epsilon 4 allele for apolipoprotein E. *N. Engl. J. Med.* 334, 752–758. doi: 10.1056/NEJM199603213341202

Reynier, P., May-Panloup, P., Chretien, M. F., Morgan, C. J., Jean, M., Savagner, F., et al. (2001). Mitochondrial DNA content affects the fertilizability of human oocytes. *Mol. Hum. Reprod.* 7, 425–429. doi: 10.1093/molehr/7.5.425

Rice, A. C., Keeney, P. M., Algarzae, N. K., Ladd, A. C., Thomas, R. R., Bennett, J. P. Jr., et al. (2014). Mitochondrial DNA copy numbers in pyramidal neurons are decreased and mitochondrial biogenesis transcriptome signaling is disrupted in Alzheimer's disease hippocampi. *J. Alzheimers Dis.* 40, 319–330. doi: 10.3233/JAD-131715

Rifé, M., Nadal, A., Milà, M., and Willemsen, R. (2004). Immunohistochemical FMRP studies in a full mutated female fetus. *Am. J. Med. Genet.* 124, 129–132. doi: 10.1002/ajmg.a.20342

Sakai, C., Yamaguchi, S., Sasaki, M., Miyamoto, Y., Matsushima, Y., and Goto, Y. (2015). ECHS1 mutations cause combined respiratory chain deficiency resulting in Leigh syndrome. *Hum. Mutat.* 36, 232–239. doi: 10.1002/humu.22730

Santos, T. A., El Shourbagy, S., and St John, J. C. (2006). Mitochondrial content reflects oocyte variability and fertilization outcome. *Fertil. Steril.* 85, 584–591. doi: 10.1016/j.fertnstert.2005.09.017

Schon, E. A. (2000). Mitochondrial genetics and disease. *Trends Biochem. Sci.* 25, 555–560. doi: 10.1016/S0968-0004(00)01688-1

Schuettler, J., Peng, Z., Zimmer, J., Sinn, P., Von Hagens, C., Strowitzki, T., et al. (2011). Variable expression of the Fragile X Mental Retardation 1 (FMR1) gene in patients with premature ovarian failure syndrome is not dependent on number of $(CGG)_n$ triplets in exon 1. *Hum. Reprod.* 26, 1241–1251. doi: 10.1093/humrep/der018

Schwartz, C. E., Dean, J., Howard-Peebles, P. N., Bugge, M., Mikkelsen, M., Tommerup, N., et al. (1994). Obstetrical and gynecological complications in fragile X carriers: a multicenter study. *Am. J. Med. Genet.* 51, 400–402. doi: 10.1002/ajmg.1320510419

Skuder, P., Plomin, R., Mcclearn, G. E., Smith, D. L., Vignetti, S., Chorney, M. J., et al. (1995). A polymorphism in mitochondrial DNA associated with IQ? *Intelligence* 21, 1–11. doi: 10.1016/0160-2896(95)90035-7

Small, G. W., Mazziotta, J. C., Collins, M. T., Baxter, L. R., Phelps, M. E., Mandelkern, M. A., et al. (1995). Apolipoprotein E type 4 allele and cerebral glucose metabolism in relatives at risk for familial Alzheimer disease. *JAMA* 273, 942–947.

Song, G., Napoli, E., Wong, S., Hagerman, R., Liu, S., Tassone, F., et al. (2016). Altered redox mitochondrial biology in the neurodegenerative disorder fragile X-tremor/ataxia syndrome: use of antioxidants in precision medicine. *Mol. Med.* 22, 548–559. doi: 10.2119/molmed.2016.00122

Streuli, I., Fraisse, T., Ibecheole, V., Moix, I., Morris, M. A., and De Ziegler, D. (2009). Intermediate and premutation FMR1 alleles in women with occult primary ovarian insufficiency. *Fertil. Steril.* 92, 464–470. doi: 10.1016/j.fertnstert.2008.07.007

Sullivan, A. K., Marcus, M., Epstein, M. P., Allen, E. G., Anido, A. E., Paquin, J. J., et al. (2005). Association of FMR1 repeat size with ovarian dysfunction. *Hum. Reprod.* 20, 402–412. doi: 10.1093/humrep/deh635

Szklarczyk, D., Gable, A. L., Lyon, D., Junge, A., Wyder, S., Huerta-Cepas, J., et al. (2019). STRING v11: protein-protein association networks with increased coverage, supporting functional discovery in genome-wide experimental datasets. *Nucleic Acids Res.* 47, D607–D613. doi: 10.1093/nar/gky1131

Tassone, F., Hagerman, R. J., Ikle, D. N., Dyer, P. N., Lampe, M., Willemsen, R., et al. (1999). FMRP expression as a potential prognostic indicator in fragile X syndrome. *Am. J. Med. Genet.* 84, 250–261. doi: 10.1002/(SICI)1096-8628(19990528)84:3<250::AID-AJMG17<3.0

Tassone, F., Pan, R., Amiri, K., Taylor, A. K., and Hagerman, P. J. (2008). A rapid polymerase chain reaction-based screening method for identification of all expanded alleles of the fragile X (FMR1) gene in newborn and high-risk populations. *J. Mol. Diagn.* 10, 43–49. doi: 10.2353/jmoldx.2008.070073

Taylor, J. P., Hardy, J., and Fischbeck, K. H. (2002). Toxic proteins in neurodegenerative disease. *Science* 296, 1991–1995. doi: 10.1126/science.1067122

Terracciano, A., Pomponi, M. G., Marino, G. M. E., Chiurazzi, P., Rinaldi, M. M., Dobosz, M., et al. (2004). Expansion to full mutation of a FMR1 intermediate allele over two generations. *Europ. J. Hum. Genet.* 12, 333–336. doi: 10.1038/sj.ejhg.5201154

Tiosano, D., Mears, J. A., and Buchner, D. A. (2019). Mitochondrial dysfunction in primary ovarian insufficiency. *Endocrinology* 160, 2353–2366. doi: 10.1210/en.2019-00441

Torii, K., Sugiyama, S., Takagi, K., Satake, T., and Ozawa, T. (1992). Age-related decrease in respiratory muscle mitochondrial function in rats. *Am. J. Resp. Cell. Mol. Biol.* 6, 88–92. doi: 10.1165/ajrcmb/6.1.88

Torres, S., Garcia-Ruiz, C. M., and Fernandez-Checa, J. C. (2019). Mitochondrial cholesterol in Alzheimer's disease and niemann-pick type C Disease. *Front. Neurol.* 10:1168. doi: 10.3389/fneur.2019.01168

Valera, A. G., Diaz-Hernandez, M., Hernandez, F., Ortega, Z., and Lucas, J. J. (2005). The ubiquitin-proteasome system in Huntington's disease. *Neuroscientist* 11, 583–594. doi: 10.1177/1073858405280639

Verkerk, A. J. M. H., Pieretti, M., Sutcliffe, J. S., Fu, Y. H., Kuhl, D. P. A., Pizzuti, A., et al. (1991). Identification of a gene (FMR-1) containing a CGG repeat coincident with a breakpoint cluster region exhibiting length variation in fragile X syndrome. *Cell* 65, 905–914. doi: 10.1016/0092-8674(91)90397-H

Voorhuis, M., Onland-Moret, N. C., Janse, F., Ploos Van Amstel, H. K., Goverde, A. J., Lambalk, C. B., et al. (2014). The significance of fragile X mental retardation gene 1 CGG repeat sizes in the normal and intermediate range in women with primary ovarian insufficiency. *Hum. Reprod.* 29, 1585–1593. doi: 10.1093/humrep/deu095

Wallace, D. C. (1992). Diseases of the mitochondrial DNA. *Annu. Rev. Biochem.* 61, 1175–1212. doi: 10.1146/annurev.bi.61.070192.005523

Wallace, D. C. (1999). Mitochondrial diseases in man and mouse. *Science* 283, 1482–1488. doi: 10.1126/science.283.5407.1482

Wallace, D. C., Bohr, V. A., Cortopassi, G., Kadenbach, B., Linn, S., Linnane, A. W., et al. (1995). "Group report: the role of bioenergetics and mitochondrial DNA mutations in aging and age-related diseases," in *Molecular Aspects of Aging*, eds K. Esser and G. M. Martin (England: Wiley), 199–226.

Wang, L. Y., Wang, D. H., Zou, X. Y., and Xu, C. M. (2009). Mitochondrial functions on oocytes and preimplantation embryos. *J. Zhejiang Univ. Sci. B* 10, 483–492. doi: 10.1631/jzus.B0820379

Watts, M. E., Pocock, R., and Claudianos, C. (2018). Brain energy and oxygen metabolism: emerging role in normal function and disease. *Front. Mol. Neurosci.* 11:216. doi: 10.3389/fnmol.2018.00216

Wheeler, A. C., Bailey, D. B. Jr., Berry-Kravis, E., Greenberg, J., Losh, M., Mailick, M., et al. (2014a). Associated features in females with an FMR1 premutation. *J. Neurodev. Disord.* 6:30. doi: 10.1186/1866-1955-6-30

Wheeler, A. C., Raspa, M., Green, A., Bishop, E., Bann, C., Edwards, A., et al. (2014b). Health and reproductive experiences of women with an FMR1

premutation with and without fragile X premature ovarian insufficiency. *Front. Genet.* 5:300. doi: 10.3389/fgene.2014.00300

Winarni, T. I., Chonchaiya, W., Sumekar, T. A., Ashwood, P., Morales, G. M., Tassone, F., et al. (2012). Immune-mediated disorders among women carriers of fragile X premutation alleles. *Am. J. Med. Genet. A* 158A, 2473–2481. doi: 10.1002/ajmg.a.35569

Yen, T. C., Chen, Y. S., King, K. L., Yeh, S. H., and Wei, Y. H. (1989). Liver mitochondrial respiratory functions decline with age. *Biochem. Biophys. Res. Comm.* 165, 994–1003. doi: 10.1016/0006-291X(89)92701-0

Zenisek, D., and Matthews, G. (2000). The role of mitochondria in presynaptic calcium handling at a ribbon synapse. *Neuron* 25, 229–237. doi: 10.1016/S0896-6273(00)80885-5

Zini, R., Morin, C., Bertelli, A., Bertelli, A. A. E., and Tillement, J. P. (2002). Resveratrol-induced limitation of dysfunction of mitochondria isolated from rat brain in an anoxia-reoxygenation model. *Life Sci.* 71, 3091–3108. doi: 10.1016/S0024-3205(02)02161-6

Conflict of Interest: The authors declare that the research was conducted in the absence of any commercial or financial relationships that could be construed as a potential conflict of interest.

frontiers in Genetics

BRIEF RESEARCH REPORT
published: 13 November 2020
doi: 10.3389/fgene.2020.557147

Development and Validation of a Mathematical Model to Predict the Complexity of *FMR1* Allele Combinations

*Bárbara Rodrigues[1,2], Emídio Vale-Fernandes[2,3], Nuno Maia[1,2], Flávia Santos[1,2], Isabel Marques[1,2], Rosário Santos[1,2], António J. A. Nogueira[4] and Paula Jorge[1,2]**

[1] Molecular Genetics Unit, Centro de Genética Médica Dr. Jacinto Magalhães (CGMJM), Centro Hospitalar Universitário do Porto (CHUP), Porto, Portugal, [2] Unit for Multidisciplinary Research in Biomedicine (UMIB), Institute of Biomedical Sciences Abel Salazar (ICBAS), University of Porto, Porto, Portugal, [3] Centre for Medically Assisted Procreation/Public Gamete Bank, Centro Materno-Infantil do Norte Dr. Albino Aroso (CMIN), Centro Hospitalar Universitário do Porto (CHUP), Porto, Portugal, [4] Center for Environmental and Marine Studies (CESAM), Department of Biology, University of Aveiro, Aveiro, Portugal

OPEN ACCESS

Edited by:
Laia Rodriguez-Revenga, Hospital Clínic de Barcelona, Spain

Reviewed by:
María Isabel Alvarez-Mora, University Hospital October 12, Spain
Carolyn M. Yrigollen, University of California, Davis, United States

***Correspondence:**
Paula Jorge
paulajorge.cgm@chporto.min-saude.pt

Specialty section:
This article was submitted to Genetics of Common and Rare Diseases, a section of the journal Frontiers in Genetics

Received: *29 April 2020*
Accepted: *13 October 2020*
Published: *13 November 2020*

Citation:
Rodrigues B, Vale-Fernandes E, Maia N, Santos F, Marques I, Santos R, Nogueira AJA and Jorge P (2020) Development and Validation of a Mathematical Model to Predict the Complexity of FMR1 Allele Combinations. Front. Genet. 11:557147. doi: 10.3389/fgene.2020.557147

The polymorphic trinucleotide repetitive region in the *FMR1* gene 5′UTR contains AGG interspersions, particularly in normal-sized alleles (CGG < 45). In this range repetitive stretches are typically interrupted once or twice, although alleles without or with three or more AGG interspersions can also be observed. AGG interspersions together with the total length of the repetitive region confer stability and hinder expansion to pathogenic ranges: either premutation (55 < CGG < 200) or full mutation (CGG > 200). The AGG interspersions have long been identified as one of the most important features of *FMR1* repeat stability, being particularly important to determine expansion risk estimates in female premutation carriers. We sought to compute the combined AGG interspersion numbers and patterns, aiming to define *FMR1* repetitive tract complexity combinations. A mathematical model, the first to compute this cumulative effect, was developed and validated using data from 131 young and healthy females. Plotting of their allelic complexity enabled the identification of two statistically distinct groups – *equivalent* and *dissimilar* allelic combinations. The outcome, a numerical parameter designated *allelic score*, depicts the repeat substructure of each allele, measuring the allelic complexity of the *FMR1* gene including the AGGs burden, thus allowing new behavioral scrutiny of normal-sized alleles in females.

Keywords: *FMR1* gene, CGG repeats, AGG interspersion pattern, modeling allelic complexity, *allelic score*

INTRODUCTION

The fragile X-related disorders result from the expansion of a CGG-repeat tract in the 5′ untranslated region of the *FMR1* gene (Xq27.3), coding for the fragile X mental retardation protein (FMRP), an RNA-binding protein that regulates expression of several genes (Man et al., 2017). Depending on the number of CGG repeats, *FMR1* alleles can be categorized into four classes: normal (CGG < 45), intermediate or "gray zone" (45 < CGG < 54), premutation

(55 < CGG < 200), and full mutation (CGG > 200) (Biancalana et al., 2015). Premutations causing *FMR1* mRNA overexpression and reduced FMRP synthesis, underly both fragile X-associated tremor/ataxia syndrome (FXTAS, OMIM #300623) and fragile X-associated primary ovarian insufficiency (FXPOI, OMIM #311360). The full mutation alleles undergo hypermethylation, leading to gene silencing and absence of FMRP, causing fragile X syndrome (FXS, OMIM #300624), the most common heritable cause of intellectual disability (Man et al., 2017). Due to the repeat tract instability, above a threshold expansions and contractions can be observed both in the germline and in the somatic cells. Some rare contraction events can originate mosaicism with mutated and normal alleles in clinically typical fragile-X phenotypes (Maia et al., 2016). In the normal population, the vast majority of the alleles contain one or more AGG interspersions within the repetitive tract, usually at every 9 or 10 CGG repeat intervals, being highly stable. In higher repeat ranges, the number of AGGs tends to be progressively smaller as the size of the repetitive tract increases (Yrigollen et al., 2012; Mila et al., 2018; Manor et al., 2019). The AGG interspersions together with the repetitive region's total length confer stability and hinder expansion to pathogenic size-ranges (Latham et al., 2014; Domniz et al., 2018; McGinty and Mirkin, 2018). In premutation female carriers, the risk of having a child with FXS depends on both the repeat length and AGG interspersions (Ardui et al., 2018). The incidence of normal pure alleles (without interspersions) is low and their origin as well as the phenotypic impact in females, are still debatable. It has been proposed that "low zone" alleles, variably determined to be CGG $\leq$ 26 or CGG $\leq$ 23, are associated with different phenotypic outcomes (Mailick et al., 2014; Gleicher et al., 2015; Rehnitz et al., 2018). Some studies show that they are associated with decreased ovarian reserve and fertility issues, due to a mechanism not yet elucidated, possibly different from that involved in premutated alleles (Gleicher et al., 2015; Wang et al., 2017), although such negative effects were not corroborated by others (Spitzer et al., 2012; Ruth et al., 2016). These contradictory assumptions require further studies to elucidate the clinical impact of "low zone" alleles.

Few studies focus on AGG interspersion patterns to assess allele stability, within the normal range. Given the importance of understanding the cumulative effect of the CGG repeat tract length and its AGG interspersions, we developed a mathematical model that considers these patterns and produces a functional model predicting the complexity of allele combinations (*allelic score*).

MATERIALS AND METHODS

Study Population

Young and potentially fertile females were recruited among candidates for oocyte donation at the Portuguese Public Gamete Bank, Centro Materno-Infantil do Norte Dr. Albino Aroso (CMIN), Centro Hospitalar Universitário do Porto (CHUP). The donor population, originating from the entire national territory, includes actively recruited students from major Portuguese universities, with a wide range of nationalities. Around 10% of the donor candidates were of foreign nationality, 95% were Caucasian and about 30% of those who donated at our center lived outside Porto (Galvão et al., 2017). Two independent cohorts were used for development (cohort 1) and for validation (cohort 2) studies. Cohort 1, n = 50, mean age 25.4 $\pm$ 3.93 years (range 18–33), recruited between 2016 and 2017. Cohort 2, n = 81, mean age 26.5 $\pm$ 3.86 years (range 19–33), collected between 2018 and 2019. All participants provided written informed consent, and this project was approved by the Hospital's Ethics Committee (2018.231/201-DEFI/200-CES).

FMR1 Repeat Region Substructure Profile

Sizing of *FMR1* alleles had been previously obtained as part of the routine oocyte donor's protocol, on blood samples. Categorizing the respective genotype followed the ACMG/EMQN guidelines: normal (CGG < 45), intermediate or "gray zone" (45 < CGG < 54), premutation (55 < CGG < 200), and full mutation (CGG > 200) (Monaghan et al., 2013; Biancalana et al., 2015). AGG interspersion pattern was determined by Triplet Repeat Primed-PCR using FRAXA PCR kit LabGscan™ (Diagnostica Longwood, Zaragoza, Spain), according to the manufacturer's instructions. This method allowed the confirmation of the total repeat length and the characterization of the CGG/AGG substructure. Thirteen samples with different patterns were additionally verified by Sanger sequencing to confirm the previously determined CGG/AGG pattern.

Statistical Analysis

Hierarchical Cluster Analysis using euclidean distance as a metric to evaluate similarity was used in statistical software SPSS® version 26 (IBM developer, 2019: SPSS Statistics version 26 – Armonk, New York, United States). Linear regression of the linearized form of an exponential model [i.e., regression of ln(score 2) against score 1] was used to obtain a functional model to relate the complexity of both alleles in each sample. The analysis of covariance (ANCOVA), as outlined by Zar (2010), was used to compare the regression models, and derive common regression lines, with *allelic scores* as variables [i.e., score 1 and ln(score 2)]. All statistical tests were carried out for a significance level of 0.05.

Determination of X-Chromosome Inactivation Pattern and *FMR1* Methylation Status

X-chromosome inactivation (XCI) pattern was determined by the human androgen-receptor assay (HUMARA), resorting to the CAG trinucleotide repeat located in the first exon and two methylation-sensitive endonuclease sites located upstream of the *AR* gene (Allen et al., 1992). The percentage of allele activity was determined using the peak heights, and normalized to the corresponding undigested allele peak

height. The *FMR1* methylation status was determined using AmplideX® mPCR *FMR1* kit (Asuragen, Inc., Austin, TX, United States), according to the manufacturer's instructions. The mPCR assay determines both the number of CGG repeats and the percentage promoter methylation of each *FMR1* allele.

RESULTS

A similar *FMR1* CGG size distribution was obtained in both cohorts with normal alleles, ranging from 15 to 40 CGG in cohort 1 and from 15 to 44 CGG in cohort 2 (n = 127, 97%) and intermediate genotypes, one allele with 48 CGG in cohort 1 and three alleles with 45 CGG in cohort 2 (n = 4, 3%) (**Tables 1**, **2**). Homozygosity was observed in eleven samples (22%, cohort 1), of which nine shared the same CGG/AGG substructure, and in seventeen samples (21%, cohort 2), of which thirteen shared the same AGG pattern. In line with previous publications, the vast majority of the alleles (93%) showed one or two AGGs, 5% were pure (4, cohort 1 and 9, cohort 2) and the remaining 2% showed three AGG interspersions. The most common structure, $(CGG)_{10}AGG(CGG)_9AGG(CGG)_9$, was identified in 29 (29%, cohort 1) and 40 alleles (25%, cohort 2). Similar to other worldwide populations, a highly polymorphic CGG/AGG substructure was observed: forty-one and fifty-five unique patterns were identified in cohorts 1 and 2, respectively (**Tables 1**, **2**; Yrigollen et al., 2014).

Development of the Mathematical Model

A mathematical model was developed to integrate the AGG interspersion number and pattern and the total repeat length, reflecting the CGG/AGG substructure. The result score, named *allelic score*, was calculated separately for each allele as follows:

$$Allelic\ score = \left(\sum_{i=1}^{n} R_i \times\ 4^{i-1}\right) + \left(R_{n+1} \times\ 4^{n}\right)$$

where,

R_i: number of CGG repeats before the first AGG interspersion of order i;

i: CGG repeat order number;

n: total number of AGG interspersions;

R_{n+1}: number of CGG repeats after the last AGG interspersion.

Base-4 numeral system was used to ensure that the *allelic score* is unique to each of the AGG interspersion patterns and sufficiently spaced.

For the purpose of addressing allelic complexity, two different aspects of the allelic structure are considered: number of AGG interspersions and number of CGG repeats between interspersions. Higher relevance is given to the number of interspersions as, for alleles with identical number of CGG repeats, higher number of AGG interspersions is usually linked with allelic stability (Maia et al., 2016; Manor et al., 2019). As example, an allele with two AGGs shows an *allelic score* of 193 whereas an allele with a similar length but only one AGG has an *allelic score* of 59.

$$Allelic\ score\left[(CGG)_9\,AGG\,(CGG)_{10}\,AGG\,(CGG)_9\right] =$$
$$[(9 \times 4^{1-1}) + (10 \times 4^{2-1})] + (9 \times 4^2) = 193$$
$$Allelic\ score\left[(CGG)_{10}\,AGG\,(CGG)_{19}\right] =$$
$$(19 \times 4^{1-1}) + (10 \times 4^1) = 59$$

This mathematical model is protected with a national patent (reference – 115244) and international patent application submitted on december 6, 2019 (reference – PCT/IB2019/060520).

Application and Validation of the Mathematical Model

Allelic scores ranged from 15 to 825 (cohort 1) and 15 to 828 (cohort 2), with most samples scoring below 220 (95.4%) and six with a score in the order of 800, due to the presence of three AGG interspersions (**Tables 1**, **2**). Scores under 220 either represent zero, one or two AGG interspersions; above two AGG interspersions, the *allelic score* grows exponentially. An exploratory cluster analysis identified four major clusters, with observations within each quadrant separated in both axes by an *allelic score* of 150 (**Supplementary Figures 1**, **2**). Similar behaviors were observed among the two quadrants where *allelic scores* were both lower than 150 or both higher than 150, and the other two where alleles show low and high *allelic score*, allowing the definition of two groups. The *equivalent* group contains samples where both alleles show a similar complexity, and the *dissimilar* group with samples where alleles show a different complexity. These groups include samples with three AGGs as the behavior of their alleles fits that of other samples in the same quadrant (**Supplementary Figures 1**, **2**). In both groups, an exponential model was used to describe the correlation between the *allelic score* of each allele. Significant correlations were found: cohort 1 – *equivalent* group: r = 0.8092; df = 24; $p < 0.0001$ and *dissimilar* group: $r = -0.7067$; df = 22; $p < 0.0001$ (**Supplementary Figure 3**). To validate the mathematical models and their reproducibility, a covariance (ANCOVA) analysis was used to compare the models calculated for cohort 1 and the same models computed using cohort 2 data (*equivalent* group: r = 0.8603; df = 43; $p < 0.0001$ and *dissimilar* group: $r = -0.8716$; df = 33; $p < 0.0001$) (**Supplementary Figure 4**). There was no statistically significant difference between cohort 1 (development cohort) and cohort 2 (validation cohort) with respect to the *equivalent* and *dissimilar* group's models, as demonstrated by the coincident regression lines (**Supplementary Figure 5**). A more robust model including all observations (both cohorts) was derived: *equivalent* group – $F_{(2,68)} = 1.8048$; $p = 0.1723$: ln(score 2) = 3.6452 + 0.0088 × score 1 and *dissimilar* group – $F_{(2,55)} = 0.9574$; $p = 0.3902$: ln(score 2) = 5.6944 – 0.0065 × score 1.

Seven samples from each group (cohort 2) were tested for XCI pattern (**Supplementary Table 1**). Interestingly, in a sample

TABLE 1 | Cohort 1 data used to calculate the *allelic scores*, and identify the two groups, *equivalent* (white background) and *dissimilar* (gray background).

Allele 1			Allele 2		
CGG/AGG Pattern	**Repeat length**	***Allelic score***	**CGG/AGG Pattern**	**Repeat length**	***Allelic score***
$(CGG)_{8}AGG(CGG)_{9}$	$18^{\$}$	**41**	$(CGG)_{23}AGG(CGG)_{9}$	33	**101**
$(CGG)_{10}AGG(CGG)_{9}$	$20^{\$}$	**49**	$(CGG)_{10}AGG(CGG)_{9}$	$20^{\$}$	**49**
$(CGG)_{9}AGG(CGG)_{8}AGG(CGG)_{9}$	$20^{\$}$	**185**	$(CGG)_{10}AGG(CGG)_{8}AGG(CGG)_{9}$	29	**201**
$(CGG)_{10}AGG(CGG)_{9}$	$20^{\$}$	**49**	$(CGG)_{20}AGG(CGG)_{9}$	30	**89**
$(CGG)_{10}AGG(CGG)_{9}$	$20^{\$}$	**49**	$(CGG)_{13}AGG(CGG)_{9}$	$23^{\$}$	**61**
$(CGG)_{9}AGG(CGG)_{11}$	$21^{\$}$	**47**	$(CGG)_{12}AGG(CGG)_{16}$	29	**64**
$(CGG)_{10}AGG(CGG)_{11}$	$22^{\$}$	**51**	$(CGG)_{13}AGG(CGG)_{16}$	30	**68**
$(CGG)_{9}AGG(CGG)_{13}$	$23^{\$}$	**49**	$(CGG)_{12}AGG(CGG)_{25}$	38	**73**
$(CGG)_{9}AGG(CGG)_{15}$	$25^{\$}$	**51**	$(CGG)_{10}AGG(CGG)_{19}$	30	**59**
$(CGG)_{9}AGG(CGG)_{9}AGG(CGG)_{9}$	29	**189**	$(CGG)_{10}AGG(CGG)_{9}AGG(CGG)_{9}$	30	**205**
$(CGG)_{9}AGG(CGG)_{9}AGG(CGG)_{9}$	29	**189**	$(CGG)_{10}AGG(CGG)_{9}AGG(CGG)_{10}$	31	**206**
$(CGG)_{9}AGG(CGG)_{9}AGG(CGG)_{9}$	29	**189**	$(CGG)_{10}AGG(CGG)_{9}AGG(CGG)_{9}$	30	**205**
$(CGG)_{9}AGG(CGG)_{9}AGG(CGG)_{9}$	29	**189**	$(CGG)_{9}AGG(CGG)_{9}AGG(CGG)_{9}$	29	**189**
$(CGG)_{9}AGG(CGG)_{9}AGG(CGG)_{9}$	29	**189**	$(CGG)_{10}AGG(CGG)_{9}AGG(CGG)_{9}$	30	**205**
$(CGG)_{9}AGG(CGG)_{9}AGG(CGG)_{9}$	29	**189**	$(CGG)_{10}AGG(CGG)_{9}AGG(CGG)_{9}$	30	**205**
$(CGG)_{9}AGG(CGG)_{10}AGG(CGG)_{9}$	30	**193**	$(CGG)_{10}AGG(CGG)_{9}AGG(CGG)_{14}$	35	**210**
$(CGG)_{9}AGG(CGG)_{10}AGG(CGG)_{9}$	30	**193**	$(CGG)_{10}AGG(CGG)_{11}AGG(CGG)_{9}$	32	**213**
$(CGG)_{10}AGG(CGG)_{9}AGG(CGG)_{9}$	30	**205**	$(CGG)_{10}AGG(CGG)_{9}AGG(CGG)_{9}$	30	**205**
$(CGG)_{10}AGG(CGG)_{9}AGG(CGG)_{9}$	30	**205**	$(CGG)_{10}AGG(CGG)_{9}AGG(CGG)_{9}$	30	**205**
$(CGG)_{9}AGG(CGG)_{9}AGG(CGG)_{10}$	30	**190**	$(CGG)_{10}AGG(CGG)_{9}AGG(CGG)_{8}AGG(CGG)_{9}$	39	**825**
$(CGG)_{10}AGG(CGG)_{9}AGG(CGG)_{9}$	30	**205**	$(CGG)_{10}AGG(CGG)_{9}AGG(CGG)_{9}$	30	**205**
$(CGG)_{10}AGG(CGG)_{9}AGG(CGG)_{9}$	30	**205**	$(CGG)_{10}AGG(CGG)_{9}AGG(CGG)_{9}$	30	**205**
$(CGG)_{10}AGG(CGG)_{9}AGG(CGG)_{9}$	30	**205**	$(CGG)_{10}AGG(CGG)_{9}AGG(CGG)_{9}$	30	**205**
$(CGG)_{10}AGG(CGG)_{9}AGG(CGG)_{9}$	30	**205**	$(CGG)_{10}AGG(CGG)_{9}AGG(CGG)_{9}$	30	**205**
$(CGG)_{9}AGG(CGG)_{10}AGG(CGG)_{9}$	30	**193**	$(CGG)_{10}AGG(CGG)_{11}AGG(CGG)_{9}$	32	**213**
$(CGG)_{10}AGG(CGG)_{9}AGG(CGG)_{9}$	30	**205**	$(CGG)_{10}AGG(CGG)_{9}AGG(CGG)_{9}$	30	**205**
$(CGG)_{9}AGG(CGG)_{9}AGG(CGG)_{12}$	32	**192**	$(CGG)_{10}AGG(CGG)_{9}AGG(CGG)_{18}$	39	**214**
$(CGG)_{8}AGG(CGG)_{9}AGG(CGG)_{21}$	40	**185**	$(CGG)_{9}AGG(CGG)_{8}AGG(CGG)_{29}$	$48^{\#}$	**205**
$(CGG)_{15}$	$15^{\$}$	**15**	$(CGG)_{10}AGG(CGG)_{9}AGG(CGG)_{9}$	30	**205**
$(CGG)_{7}AGG(CGG)_{9}$	$17^{\$}$	**37**	$(CGG)_{10}AGG(CGG)_{9}AGG(CGG)_{9}$	30	**205**
$(CGG)_{10}AGG(CGG)_{9}$	$20^{\$}$	**49**	$(CGG)_{10}AGG(CGG)_{9}AGG(CGG)_{9}$	30	**205**
$(CGG)_{10}AGG(CGG)_{9}$	$20^{\$}$	**49**	$(CGG)_{10}AGG(CGG)_{9}AGG(CGG)_{10}$	31	**206**
(CGG)10AGG(CGG)9	$20^{\$}$	**49**	$(CGG)_{10}AGG(CGG)_{9}AGG(CGG)_{9}$	30	**205**
$(CGG)_{10}AGG(CGG)_{9}$	$20^{\$}$	**49**	$(CGG)_{10}AGG(CGG)_{10}AGG(CGG)_{10}$	32	**210**
$(CGG)_{9}AGG(CGG)_{10}$	$20^{\$}$	**46**	$(CGG)_{10}AGG(CGG)_{8}AGG(CGG)_{9}AGG(CGG)_{9}$	39	**813**
$(CGG)_{9}AGG(CGG)_{10}$	$20^{\$}$	**46**	$(CGG)_{10}AGG(CGG)_{8}AGG(CGG)_{9}$	29	**201**
$(CGG)_{9}AGG(CGG)_{10}$	$20^{\$}$	**46**	$(CGG)_{10}AGG(CGG)_{9}AGG(CGG)_{9}$	30	**205**
$(CGG)_{10}AGG(CGG)_{9}$	$20^{\$}$	**49**	$(CGG)_{10}AGG(CGG)_{9}AGG(CGG)_{8}AGG(CGG)_{9}$	39	**825**
$(CGG)_{9}AGG(CGG)_{10}$	$20^{\$}$	**46**	$(CGG)_{10}AGG(CGG)_{8}AGG(CGG)_{7}AGG(CGG)_{9}$	37	**805**
$(CGG)_{9}AGG(CGG)_{10}$	$20^{\$}$	**46**	$(CGG)_{9}AGG(CGG)_{12}AGG(CGG)_{9}$	32	**201**
$(CGG)_{25}$	$25^{\$}$	**25**	$(CGG)_{10}AGG(CGG)_{9}AGG(CGG)_{10}$	31	**206**
$(CGG)_{15}AGG(CGG)_{9}$	$25^{\$}$	**69**	$(CGG)_{10}AGG(CGG)_{9}AGG(CGG)_{10}$	31	**206**
$(CGG)_{9}AGG(CGG)_{9}AGG(CGG)_{9}$	29	**189**	$(CGG)_{9}AGG(CGG)_{29}$	39	**65**
$(CGG)_{9}AGG(CGG)_{9}AGG(CGG)_{9}$	29	**189**	$(CGG)_{11}AGG(CGG)_{20}$	32	**64**
$(CGG)_{10}AGG(CGG)_{9}AGG(CGG)_{9}$	30	**205**	$(CGG)_{10}AGG(CGG)_{22}$	33	**62**
$(CGG)_{10}AGG(CGG)_{9}AGG(CGG)_{9}$	30	**205**	$(CGG)_{10}AGG(CGG)_{20}$	31	**60**
$(CGG)_{10}AGG(CGG)_{9}AGG(CGG)_{9}$	30	**205**	$(CGG)_{10}AGG(CGG)_{22}$	33	**62**
$(CGG)_{30}$	30	**30**	$(CGG)_{10}AGG(CGG)_{9}AGG(CGG)_{9}$	30	**205**
$(CGG)_{10}AGG(CGG)_{9}AGG(CGG)_{9}$	30	**205**	$(CGG)_{10}AGG(CGG)_{20}$	31	**60**
$(CGG)_{30}$	30	**30**	$(CGG)_{10}AGG(CGG)_{9}AGG(CGG)_{9}$	30	**205**

Homoallelism for CGG-repeat length (black background) and homozygosity for both CGG-repeat length and AGG pattern (allelic score in green background).
[#] *intermediate size.*
[$] *normal "low zone" alleles (see section "Discussion").*

TABLE 2 | Cohort 2 data used to calculate the *allelic scores*, and identify the two groups, *equivalent* (white background) and *dissimilar* (gray background).

Allele 1			Allele 2		
CGG/AGG Pattern	**Repeat length**	***Allelic score***	**CGG/AGG Pattern**	**Repeat length**	***Allelic score***
$(CGG)_{15}$	15[$]	**15**	$(CGG)_{10}AGG(CGG)_{9}$	20[$]	**49**
$(CGG)_{18}$	18[$]	**18**	$(CGG)_{10}AGG(CGG)_{9}$	20[$]	**49**
$(CGG)_{10}AGG(CGG)_{9}$	20[$]	**49**	$(CGG)_{25}AGG(CGG)_{9}$	35	**109**
$(CGG)_{10}AGG(CGG)_{9}$	20[$]	**49**	$(CGG)_{10}AGG(CGG)_{9}$	20[$]	**49**
$(CGG)_{10}AGG(CGG)_{9}$	20[$]	**49**	$(CGG)_{20}$	20[$]	**20**
$(CGG)_{10}AGG(CGG)_{9}$	20[$]	**49**	$(CGG)_{10}AGG(CGG)_{19}$	30	**59**
$(CGG)_{11}AGG(CGG)_{9}$	21[$]	**53**	$(CGG)_{12}AGG(CGG)_{10}$	23[$]	**58**
$(CGG)_{9}AGG(CGG)_{13}$	23[$]	**49**	$(CGG)_{9}AGG(CGG)_{19}$	29	**55**
$(CGG)_{9}AGG(CGG)_{13}$	23[$]	**49**	$(CGG)_{12}AGG(CGG)_{32}$	45[#]	**80**
$(CGG)_{13}AGG(CGG)_{9}$	23[$]	**61**	$(CGG)_{24}$	24[$]	**24**
$(CGG)_{10}AGG(CGG)_{13}$	24[$]	**53**	$(CGG)_{13}AGG(CGG)_{16}$	30	**68**
$(CGG)_{16}AGG(CGG)_{9}$	26[$]	**73**	$(CGG)_{29}$	29	**29**
$(CGG)_{9}AGG(CGG)_{18}$	28	**54**	$(CGG)_{9}AGG(CGG)_{28}$	38	**64**
$(CGG)_{9}AGG(CGG)_{9}AGG(CGG)_{9}$	29	**189**	$(CGG)_{9}AGG(CGG)_{9}AGG(CGG)_{9}$	29	**189**
$(CGG)_{9}AGG(CGG)_{9}AGG(CGG)_{9}$	29	**189**	$(CGG)_{10}AGG(CGG)_{9}AGG(CGG)_{9}$	30	**205**
$(CGG)_{10}AGG(CGG)_{8}AGG(CGG)_{9}$	29	**201**	$(CGG)_{10}AGG(CGG)_{9}AGG(CGG)_{8}$	29	**204**
$(CGG)_{9}AGG(CGG)_{9}AGG(CGG)_{9}$	29	**189**	$(CGG)_{9}AGG(CGG)_{9}AGG(CGG)_{9}$	29	**189**
$(CGG)_{9}AGG(CGG)_{9}AGG(CGG)_{9}$	29	**189**	$(CGG)_{10}AGG(CGG)_{9}AGG(CGG)_{9}$	30	**205**
$(CGG)_{9}AGG(CGG)_{9}AGG(CGG)_{9}$	29	**189**	$(CGG)_{9}AGG(CGG)_{12}AGG(CGG)_{9}$	32	**201**
$(CGG)_{9}AGG(CGG)_{9}AGG(CGG)_{9}$	29	**189**	$(CGG)_{10}AGG(CGG)_{9}AGG(CGG)_{9}$	30	**205**
$(CGG)_{9}AGG(CGG)_{9}AGG(CGG)_{10}$	30	**190**	$(CGG)_{10}AGG(CGG)_{9}AGG(CGG)_{16}$	37	**212**
$(CGG)_{9}AGG(CGG)_{10}AGG(CGG)_{9}$	30	**193**	$(CGG)_{10}AGG(CGG)_{11}AGG(CGG)_{9}$	32	**213**
$(CGG)_{9}AGG(CGG)_{10}AGG(CGG)_{9}$	30	**193**	$(CGG)_{10}AGG(CGG)_{11}AGG(CGG)_{9}$	32	**213**
$(CGG)_{9}AGG(CGG)_{9}AGG(CGG)_{10}$	30	**190**	$(CGG)_{10}AGG(CGG)_{9}AGG(CGG)_{9}AGG(CGG)_{8}$	39	**828**
$(CGG)_{10}AGG(CGG)_{9}AGG(CGG)_{9}$	30	**205**	$(CGG)_{10}AGG(CGG)_{10}AGG(CGG)_{10}$	32	**210**
$(CGG)_{10}AGG(CGG)_{9}AGG(CGG)_{9}$	30	**205**	$(CGG)_{10}AGG(CGG)_{9}AGG(CGG)_{9}$	30	**205**
$(CGG)_{9}AGG(CGG)_{10}AGG(CGG)_{9}$	30	**193**	$(CGG)_{10}AGG(CGG)_{14}AGG(CGG)_{9}$	35	**225**
$(CGG)_{10}AGG(CGG)_{9}AGG(CGG)_{9}$	30	**205**	$(CGG)_{10}AGG(CGG)_{9}AGG(CGG)_{9}$	30	**205**
$(CGG)_{10}AGG(CGG)_{9}AGG(CGG)_{9}$	30	**205**	$(CGG)_{10}AGG(CGG)_{9}AGG(CGG)_{9}$	30	**205**
$(CGG)_{9}AGG(CGG)_{9}AGG(CGG)_{10}$	30	**190**	$(CGG)_{10}AGG(CGG)_{9}AGG(CGG)_{20}$	41	**216**
$(CGG)_{10}AGG(CGG)_{9}AGG(CGG)_{9}$	30	**205**	$(CGG)_{10}AGG(CGG)_{9}AGG(CGG)_{9}$	30	**205**
$(CGG)_{9}AGG(CGG)_{10}AGG(CGG)_{9}$	30	**193**	$(CGG)_{10}AGG(CGG)_{11}AGG(CGG)_{9}$	32	**213**
$(CGG)_{10}AGG(CGG)_{9}AGG(CGG)_{9}$	30	**205**	$(CGG)_{10}AGG(CGG)_{9}AGG(CGG)_{9}$	30	**205**
$(CGG)_{9}AGG(CGG)_{9}AGG(CGG)_{10}$	30	**190**	$(CGG)_{10}AGG(CGG)_{9}AGG(CGG)_{19}$	40	**215**
$(CGG)_{10}AGG(CGG)_{9}AGG(CGG)_{9}$	30	**205**	$(CGG)_{10}AGG(CGG)_{9}AGG(CGG)_{9}$	30	**205**
$(CGG)_{10}AGG(CGG)_{9}AGG(CGG)_{9}$	30	**205**	$(CGG)_{10}AGG(CGG)_{9}AGG(CGG)_{9}$	30	**205**
$(CGG)_{10}AGG(CGG)_{9}AGG(CGG)_{9}$	30	**205**	$(CGG)_{10}AGG(CGG)_{9}AGG(CGG)_{9}$	30	**205**
$(CGG)_{10}AGG(CGG)_{9}AGG(CGG)_{9}$	30	**205**	$(CGG)_{10}AGG(CGG)_{9}AGG(CGG)_{9}$	30	**205**
$(CGG)_{9}AGG(CGG)_{9}AGG(CGG)_{10}$	30	**190**	$(CGG)_{9}AGG(CGG)_{11}AGG(CGG)_{9}$	31	**197**
$(CGG)_{9}AGG(CGG)_{10}AGG(CGG)_{9}$	30	**193**	$(CGG)_{10}AGG(CGG)_{11}AGG(CGG)_{9}$	32	**213**
$(CGG)_{10}AGG(CGG)_{9}AGG(CGG)_{9}$	30	**205**	$(CGG)_{10}AGG(CGG)_{10}AGG(CGG)_{9}$	31	**209**
$(CGG)_{9}AGG(CGG)_{10}AGG(CGG)_{9}$	30	**193**	$(CGG)_{10}AGG(CGG)_{11}AGG(CGG)_{9}$	32	**213**
$(CGG)_{10}AGG(CGG)_{9}AGG(CGG)_{9}$	30	**205**	$(CGG)_{10}AGG(CGG)_{12}AGG(CGG)_{9}$	33	**217**
$(CGG)_{10}AGG(CGG)_{9}AGG(CGG)_{10}$	31	**206**	$(CGG)_{10}AGG(CGG)_{9}AGG(CGG)_{10}$	31	**206**
$(CGG)_{9}AGG(CGG)_{9}AGG(CGG)_{11}$	31	**191**	$(CGG)_{10}AGG(CGG)_{9}AGG(CGG)_{17}$	38	**213**
$(CGG)_{9}AGG(CGG)_{9}AGG(CGG)_{19}$	39	**199**	$(CGG)_{9}AGG(CGG)_{9}AGG(CGG)_{9}AGG(CGG)_{15}$	45[#]	**771**
$(CGG)_{10}AGG(CGG)_{5}$	16[$]	**45**	$(CGG)_{10}AGG(CGG_{9}AGG(CGG)_{10}$	31	**206**
$(CGG)_{10}AGG(CGG_{9}$	20[$]	**49**	$(CGG)_{10}AGG(CGG)_{9}AGG(CGG)_{9}$	30	**205**
$(CGG)_{9}AGG(CGG)_{10}$	20[$]	**46**	$(CGG)_{10}AGG(CGG)_{9}AGG(CGG)_{8}$	29	**204**
$(CGG)_{10}AGG(CGG)_{9}$	20[$]	**49**	$(CGG)_{10}AGG(CGG)_{9}AGG(CGG)_{9}$	30	**205**

(Continued)

TABLE 2 | Continued

Allele 1			Allele 2		
CGG/AGG Pattern	**Repeat length**	***Allelic score***	**CGG/AGG Pattern**	**Repeat length**	***Allelic score***
$(CGG)_{10}AGG(CGG)_9$	20[§]	**49**	$(CGG)_{10}AGG(CGG)_{10}AGG(CGG)_{10}$	32	**210**
$(CGG)_{10}AGG(CGG)_9$	20[§]	**49**	$(CGG)_{10}AGG(CGG)_9AGG(CGG)_9$	30	**205**
$(CGG)_9AGG(CGG)_{10}$	20[§]	**46**	$(CGG)_{10}AGG(CGG)_{11}AGG(CGG)_9$	32	**213**
$(CGG)_9AGG(CGG)_{10}$	20[§]	**46**	$(CGG)_{10}AGG(CGG)_8AGG(CGG)_9$	29	**201**
$(CGG)_{20}$	20[§]	**20**	$(CGG)_9AGG(CGG)_9AGG(CGG)_9$	29	**189**
$(CGG)_{10}AGG(CGG)_9$	20[§]	**49**	$(CGG)_{10}AGG(CGG)_9AGG(CGG)_9$	30	**205**
$(CGG)_9AGG(CGG)_{10}$	20[§]	**46**	$(CGG)_{10}AGG(CGG)_9AGG(CGG)_9$	30	**205**
$(CGG)_{10}AGG(CGG)_9$	20[§]	**49**	$(CGG)_{10}AGG(CGG)_9AGG(CGG)_9$	30	**205**
$(CGG)_9AGG(CGG)_{10}$	20[§]	**46**	$(CGG)_{10}AGG(CGG)_8AGG(CGG)_9$	29	**201**
$(CGG)_{10}AGG(CGG)_9$	20[§]	**49**	$(CGG)_{10}AGG(CGG)_9AGG(CGG)_9$	30	**205**
$(CGG)_{10}AGG(CGG)_{11}$	22[§]	**51**	$(CGG)_{12}AGG(CGG)_7AGG(CGG)_9$	30	**229**
$(CGG)_{13}AGG(CGG)_9$	23[§]	**61**	$(CGG)_{10}AGG(CGG)_9AGG(CGG)_9$	30	**205**
$(CGG)_{12}AGG(CGG)_{10}$	23[§]	**58**	$(CGG)_9AGG(CGG)_{10}AGG(CGG)_9$	30	**193**
$(CGG)_{13}AGG(CGG)_9$	23[§]	**61**	$(CGG)_{10}AGG(CGG)_9AGG(CGG)_9$	30	**205**
$(CGG)_{13}AGG(CGG)_9$	23[§]	**61**	$(CGG)_{10}AGG(CGG)_9AGG(CGG)_9$	30	**205**
$(CGG)_{13}AGG(CGG)_9$	23[§]	**61**	$(CGG)_{10}AGG(CGG)_9AGG(CGG)_9$	30	**205**
$(CGG)_{27}$	27	**27**	$(CGG)_{10}AGG(CGG)_9AGG(CGG)_9$	30	**205**
$(CGG)_9AGG(CGG)_9AGG(CGG)_9$	29	**189**	$(CGG)_{29}AGG(CGG)_9$	39	**125**
$(CGG)_9AGG(CGG)_9AGG(CGG)_9$	29	**189**	$(CGG)_{38}$	38	**38**
$(CGG)_9AGG(CGG)_{19}$	29	**55**	$(CGG)_{10}AGG(CGG)_9AGG(CGG)_9$	30	**205**
$(CGG)_9AGG(CGG)_9AGG(CGG)_9$	29	**189**	$(CGG)_{10}AGG(CGG)_{20}$	31	**60**
$(CGG)_9AGG(CGG)_{19}$	29	**55**	$(CGG)_{10}AGG(CGG)_9AGG(CGG)_{10}$	31	**206**
$(CGG)_{10}AGG(CGG)_9AGG(CGG)_9$	30	**205**	$(CGG)_{22}AGG(CGG)_9$	32	**97**
$(CGG)_{10}AGG(CGG)_{19}$	30	**59**	$(CGG)_{10}AGG(CGG)_9AGG(CGG)_{10}$	31	**206**
$(CGG)_9AGG(CGG)_{10}AGG(CGG)_9$	30	**193**	$(CGG)_{10}AGG(CGG)_{19}$	30	**59**
$(CGG)_{30}$	30	**30**	$(CGG)_{10}AGG(CGG)_9AGG(CGG)_{10}$	31	**206**
$(CGG)_{10}AGG(CGG)_9AGG(CGG)_9$	30	**205**	$(CGG)_{33}AGG(CGG)_9$	43	**141**
$(CGG)_{10}AGG(CGG)_9AGG(CGG)_9$	30	**205**	$(CGG)_{10}AGG(CGG)_{19}$	30	**59**
$(CGG)_{10}AGG(CGG)_{20}$	31	**60**	$(CGG)_{10}AGG(CGG)_9AGG(CGG)_{23}$	44	**219**
$(CGG)_9AGG(CGG)_{21}$	31	**57**	$(CGG)_{10}AGG(CGG)_8AGG(CGG)_{25}$	45[#]	**217**
$(CGG)_{10}AGG(CGG)_{20}$	31	**60**	$(CGG)_{10}AGG(CGG)9AGG(CGG)_{10}$	31	**206**

Homoallelism for CGG-repeat length (black background) and homozygosity for both CGG-repeat length and AGG pattern (allelic score in green background).
[#]intermediate size. [§]normal "low zone" alleles (see section "Discussion").

belonging to the *dissimilar* group, *FMR1* mPCR showed extreme skewing (85%) toward the smallest "low zone" allele.

DISCUSSION

Our study focused on developing a tool to score and evaluate the complexity of the *FMR1* gene repetitive tract structure. To this end, a mathematical model was designed that computes the *FMR1* gene CGG repeat length, as well as the AGG interspersion number and pattern. The output, a number designated *allelic score*, deciphers a functional model to predict the complexity of allele combinations. Two cohorts of young, healthy, and potentially fertile females were used independently for development and validation studies. The fact that two statistically significant groups, *equivalent* and *dissimilar*, were identified in both cohorts, justified the pooling of data. Furthermore, the identification of two groups shows the model's ability to compare the complexity of the two alleles. Interestingly, the *dissimilar* group is enriched with "low zone" heterozygous samples (herein defined as CGG $\leq$ 26). It has been proposed that these "low zone" alleles may exert negative effects, although controversial (Spitzer et al., 2012; Mailick et al., 2014; Gleicher et al., 2015; Ruth et al., 2016). Another study claims that normal *FMR1* repeat length outside 26 > CGG > 34 concur with a higher XCI skew, a putative mechanism underlying the ovarian reserve impairment (as assessed by AMH), particularly in infertile older females (Barad et al., 2017). Moreover, the AGG "protective" effect toward a decreased risk of ovarian malfunction was observed in females carrying premutated alleles with two or more interspersions (Lekovich et al., 2018). According to our model, these alleles would show a high *allelic score*, which seems to suggest a correlation between the allelic complexity and a protective effect. Replication of these results is still required

using larger control and patient cohorts. Nonetheless, with this mathematical model developed to calculate the *FMR1 allelic score*, further research can now be undertaken with a different perspective in terms of *FMR1* characterization.

DATA AVAILABILITY STATEMENT

The original contributions presented in the study are included in the article/supplementary material, further inquiries can be directed to the corresponding author.

ETHICS STATEMENT

The studies involving human participants were reviewed and approved by the Ethics Committe of Centro Hospitalar Universitário do Porto. Written informed consent from the participants was obtained in accordance with the national legislation (lei 12/2005) and the institutional requirements. The participants provided their written informed consent to participate in this study.

AUTHOR CONTRIBUTIONS

PJ conceived and designed the study together with BR. AN developed the mathematical model and performed the statistical analysis with BR who also carried out laboratory work, analyzed the data, and drafted the manuscript. FS performed methylation/inactivation studies. EV-F, NM, IM, and RS provided critical feedback, helped conduct the research, and contributed toward the manuscript. All authors discussed the final results and critically reviewed the manuscript.

FUNDING

This work was supported by national funds: FCT/MCTES (Fundação para a Ciência e a Tecnologia) – Project Reference SFRH/BD/136398/2018 to BR, UMIB (Unidade Multidisciplinar de Investigação Biomédica) – Reference UIDP/00215/2020 and UIDB/00215/2020, DEFI (Departamento de Ensino, Formação e Investigação) – Reference 2015-DEFI/145/12, and CESAM (Centro de Estudos do Ambiente e do Mar) – Reference UIDP/50017/2020 and UIDB/50017/2020.

ACKNOWLEDGMENTS

We gratefully acknowledge the Center for Medically Assisted Procreation/Public Gamete Bank, Centro Materno-Infantil do Norte Dr. Albino Aroso (CMIN), Centro Hospitalar Universitário do Porto (CHUP). Without the invaluable help of all collaborators (potential donors, clinicians, nurses, and embryologists), our work would not have been possible. Special thanks to Isabel Sousa Pereira for recruiting cohort 1 participants. We are also grateful for important feedback from international reviewers.

REFERENCES

Allen, R. C., Zoghbi, H. Y., Annemarie, B., Moseley, H. M. R., and Belmont, J. W. (1992). Methylation of *Hpall* and *Hhal* sites near the polymorphic CAG repeat in the human androgen-receptor gene correlates with X chromosome inactivation. *Am. J. Hum. Genet.* 51, 1229–1212. doi: 10.1158/1538-7445.am2014-ct404

Ardui, S., Race, V., de Ravel, T., Van Esch, H., Devriendt, K., and Matthijs, G. (2018). Detecting AGG interruptions in females with a *FMR1* premutation by long-read single-molecule sequencing: a 1 year clinical experience. *Front. Genet.* 9:150. doi: 10.3389/fgene.2018.00150

Barad, D. H., Darmon, S., Weghofer, A., Latham, G. J., Wang, Q., Kushnir, V. A., et al. (2017). Association of skewed X-chromosome inactivation with *FMR1* CGG repeat length and anti-mullerian hormone levels: a cohort study. *Reprod. Biol. Endocrinol.* 15:34. doi: 10.1186/s12958-017-0250-9

Biancalana, V., Glaeser, D., McQuaid, S., and Steinbach, P. (2015). EMQN best practice guidelines for the molecular genetic testing and reporting of fragile X syndrome and other fragile X-associated disorders. *Eur. J. Hum. Genet.* 23, 417–425. doi: 10.1038/ejhg.2014.185

Domniz, N., Ries-Levavi, L., Cohen, Y., Marom-Haham, L., Berkenstadt, M., Pras, E., et al. (2018). Absence of AGG interruptions is a risk factor for full mutation expansion among israeli fmr1 premutation carriers. *Front. Genet.* 9:606. doi: 10.3389/fgene.2018.00606

Galvão, A., Vale-Fernandes, E., Pereira, I. S., Fraga, S., Lourenço, C., Morgado, A., et al. (2017). "Applicants for oocyte donors from the Portuguese public gamete bank: who are they?," in *CMIN SUMMIT 17 - Inovações e Controvérsias na Saúde da Mulher e da Criança* (Porto).

Gleicher, N., Yu, Y., Himaya, E., Barad, D. H., Weghofer, A., Wu, Y., et al. (2015). Early decline in functional ovarian reserve in young women with low (CGGn <26) *FMR1* gene alleles. *Transl. Res.* 166, 502–507. doi: 10.1016/j.trsl.2015.06.014

Latham, G. J., Coppinger, J., Hadd, A. G., and Nolin, S. L. (2014). The role of AGG interruptions in fragile X repeat expansions: a twenty-year perspective. *Front. Genet.* 5:244. doi: 10.3389/fgene.2014.00244

Lekovich, J., Man, L., Xu, K., Canon, C., Lilienthal, D., Stewart, J. D., et al. (2018). CGG repeat length and AGG interruptions as indicators of fragile X–associated diminished ovarian reserve. *Genet. Med.* 20, 957–964. doi: 10.1038/gim.2017.220

Maia, N., Loureiro, J. R., Oliveira, B., Marques, I., Santos, R., Jorge, P., et al. (2016). Contraction of fully expanded *FMR1* alleles to the normal range: predisposing haplotype or rare events? *J. Hum. Genet.* 62, 1–7. doi: 10.1038/jhg.2016.122

Mailick, M. R., Hong, J., Rathouz, P., Baker, M. W., Greenberg, J. S., Smith, L., et al. (2014). Low-normal *FMR1* CGG repeat length: phenotypic associations. *Front. Genet.* 5:309. doi: 10.3389/fgene.2014.00309

Man, L., Lekovich, J., Rosenwaks, Z., and Gerhardt, J. (2017). Fragile X-associated diminished ovarian reserve and primary ovarian insufficiency from molecular mechanisms to clinical manifestations. *Front. Mol. Neurosci.* 10:290. doi: 10.3389/fnmol.2017.00290

Manor, E., Gonen, R., Sarussi, B., Keidar-Friedman, D., Kumar, J., Tang, H. T., et al. (2019). The role of AGG interruptions in the *FMR1* gene stability: a survey in ethnic groups with low and high rate of consanguinity. *Mol. Genet. Genomic Med.* 7, 1–14. doi: 10.1002/mgg3.946

McGinty, R. J., and Mirkin, S. M. (2018). Cis- and trans-modifiers of repeat expansions: blending model systems with human genetics. *Trends Genet.* 34, 448–465. doi: 10.1016/j.tig.2018.02.005

Mila, M., Alvarez-Mora, M. I., Madrigal, I., and Rodriguez-Revenga, L. (2018). Fragile X syndrome: an overview and update of the *FMR1* gene. *Clin. Genet.* 93, 197–205. doi: 10.1111/cge.13075

Monaghan, K. G., Lyon, E., and Spector, E. B. (2013). ACMG standards and guidelines for fragile X testing: a revision to the disease-specific supplements to the standards and guidelines for clinical genetics laboratories of the American

College of medical genetics and genomics. *Genet. Med.* 15, 575–586. doi: 10.1038/gim.2013.61

Rehnitz, J., Alcoba, D. D., Brum, I. S., Dietrich, J. E., Youness, B., Hinderhofer, K., et al. (2018). *FMR1* expression in human granulosa cells increases with exon 1 CGG repeat length depending on ovarian reserve. *Reprod. Biol. Endocrinol.* 16:65 doi: 10.1186/s12958-018-0383-5

Ruth, K. S., Bennett, C. E., Schoemaker, M. J., Weedon, M. N., Swerdlow, A. J., and Murray, A. (2016). Length of *FMR1* repeat alleles within the normal range does not substantially affect the risk of early menopause. *Hum. Reprod.* 31, 2396–2403. doi: 10.1093/humrep/dew204

Spitzer, L. T., Johnstone, E. B., Huddleston, H. G., Cedars, L. M., Davis, G., and Fujimoto, V. (2012). *FMR1* repeats and ovarian reserve: CGG repeat number does not influence antral follicle count. *J. Fertil. Vitr.* 02, 10–13. doi: 10.4172/2165-7491.1000105

Wang, Q., Kushnir, V. A., Darmon, S., Barad, D. H., Wu, Y., Zhang, L., et al. (2017). Reduced RNA expression of the *FMR1* gene in women with low (CGGn<26) repeats. *Fertil. Steril.* 108:e143. doi: 10.1016/j.fertnstert.2017.07.432

Yrigollen, C. M., Durbin-Johnson, B., Gane, L., Nelson, D. L., Hagerman, R., Hagerman, P. J., et al. (2012). AGG interruptions within the maternal *FMR1* gene reduce the risk of offspring with fragile X syndrome. *Genet. Med.* 14, 729–736. doi: 10.1038/gim.2012.34

Yrigollen, C. M., Sweha, S., Durbin-Johnson, B., Zhou, L., Berry-Kravis, E., Fernandez-Carvajal, I., et al. (2014). Distribution of AGG interruption patterns within nine world populations. *Intractable Rare Dis. Res.* 3, 153–161. doi: 10.5582/irdr.2014.01028

Zar, J. H. (2010). *Bioestatistical Analysis*, 5th Edn. Upper Saddle River, NJ: Prentice Hall, doi: 10.1007/978-1-4939-2917-7

Conflict of Interest: The authors declare that the research was conducted in the absence of any commercial or financial relationships that could be construed as a potential conflict of interest.

frontiers in Molecular Biosciences

ORIGINAL RESEARCH
published: 14 December 2020
doi: 10.3389/fmolb.2020.599101

Lack of a Clear Behavioral Phenotype in an Inducible FXTAS Mouse Model Despite the Presence of Neuronal FMRpolyG-Positive Aggregates

Saif N. Haify[1], Ruchira S. D. Mankoe[1,2], Valerie Boumeester[1], Esmay C. van der Toorn[1], Rob F. M. Verhagen[1], Rob Willemsen[1], Renate K. Hukema[1,3] and Laurens W. J. Bosman[2]**

[1] Department of Clinical Genetics, Erasmus MC, Rotterdam, Netherlands, [2] Department of Neuroscience, Erasmus MC, Rotterdam, Netherlands, [3] Department of Health Care Studies, Rotterdam University of Applied Sciences, Rotterdam, Netherlands

OPEN ACCESS

Edited by:
Eleonora Napoli,
University of California, Davis,
United States

Reviewed by:
Barbara Bardoni,
UMR 7275 Institut de Pharmacologie Moléculaire et Cellulaire (IPMC), France
Frank Kooy,
University of Antwerp, Belgium

***Correspondence:**
Saif N. Haify
s.haify@erasmusmc.nl
Laurens W. J. Bosman
l.bosman@erasmusmc.nl

Specialty section:
This article was submitted to Cellular Biochemistry, a section of the journal Frontiers in Molecular Biosciences

Received: 26 August 2020
Accepted: 23 November 2020
Published: 14 December 2020

Citation:
Haify SN, Mankoe RSD, Boumeester V, van der Toorn EC, Verhagen RFM, Willemsen R, Hukema RK and Bosman LWJ (2020) Lack of a Clear Behavioral Phenotype in an Inducible FXTAS Mouse Model Despite the Presence of Neuronal FMRpolyG-Positive Aggregates. Front. Mol. Biosci. 7:599101. doi: 10.3389/fmolb.2020.599101

Fragile X-associated tremor/ataxia syndrome (FXTAS) is a rare neurodegenerative disorder caused by a 55–200 CGG repeat expansion in the 5′ untranslated region of the Fragile X Mental Retardation 1 (*FMR1*) gene. FXTAS is characterized by progressive cerebellar ataxia, Parkinsonism, intention tremors and cognitive decline. The main neuropathological hallmark of FXTAS is the presence of ubiquitin-positive intranuclear inclusions in neurons and astrocytes throughout the brain. The molecular pathology of FXTAS involves the presence of 2 to 8-fold elevated levels of *FMR1* mRNA, and of a repeat-associated non-AUG (RAN) translated polyglycine peptide (FMRpolyG). Increased levels of *FMR1* mRNA containing an expanded CGG repeat can result in cellular toxicity by an RNA gain-of-function mechanism. The increased levels of CGG repeat-expanded *FMR1* transcripts may create RNA foci that sequester important cellular proteins, including RNA-binding proteins and FMRpolyG, in intranuclear inclusions. To date, it is unclear whether the FMRpolyG-positive intranuclear inclusions are a cause or a consequence of FXTAS disease pathology. In this report we studied the relation between the presence of neuronal intranuclear inclusions and behavioral deficits using an inducible mouse model for FXTAS. Neuronal intranuclear inclusions were observed 4 weeks after dox-induction. After 12 weeks, high numbers of FMRpolyG-positive intranuclear inclusions could be detected in the hippocampus and striatum, but no clear signs of behavioral deficits related to these specific brain regions were found. In conclusion, the observations in our inducible mouse model for FXTAS suggest a lack of correlation between the presence of intranuclear FMRpolyG-positive aggregates in brain regions and specific behavioral phenotypes.

Keywords: FXTAS, nuclear inclusions, mouse behavior, *FMR1*, repeat expansion

INTRODUCTION

Fragile X-associated tremor/ataxia syndrome (FXTAS) is a late-onset neurodegenerative disease that is characterized mainly by essential tremor, cerebellar ataxia, Parkinsonism, peripheral neuropathy and cognitive decline (Hagerman et al., 2001; Tassone et al., 2007; Hagerman and Hagerman, 2013, 2016). FXTAS leads to cerebral and cerebellar atrophy, with increased T2 signal intensity in MRI images of the middle cerebellar peduncles as diagnostic hallmark (Brown and Stanfield, 2015). Carriers of a premutation in the *FMR1* gene, consisting of a 55–200 CGG repeat expansion, are at risk of developing FXTAS. Such intermediate repeat expansions lead to elevated levels of *FMR1* mRNA (Tassone et al., 2000; Kenneson et al., 2001; Salcedo-Arellano et al., 2020). In contrast, longer repeat expansions, more than 200 units, induce silencing of *FMR1* mRNA, which results in a lack of FMRP protein, causing the neurodevelopmental Fragile X syndrome (Bassell and Warren, 2008; Salcedo-Arellano et al., 2020).

Several mechanisms by which the premutation and the consequential increase in *FMR1* mRNA levels may lead to the development of FXTAS have been proposed. Of these, arguably the most studied process is the formation of intranuclear inclusions that has been very well-documented in patients as well as in animal models and their occurrence has been linked to alterations at the cellular level in neurons and astrocytes (Louis et al., 2006; Jin et al., 2007; Berman et al., 2014; Ma et al., 2019; Haify et al., 2020). The intranuclear inclusions are mainly composed of proteins and to date more than 200 different proteins have been identified in nuclear inclusions (Iwahashi et al., 2006; Ma et al., 2019). *FMR1* mRNA containing a CGG repeat expansion, although present itself only in relatively low concentrations in the nuclear inclusions, could act as a scaffold binding place for the other components (Cid-Samper et al., 2018; Langdon et al., 2018; Ma et al., 2019). The putative pathogenicity of these inclusions could be based on depleting essential molecules, including RNA-binding proteins (Jin et al., 2007; Sofola et al., 2007; Qurashi et al., 2011; Sellier et al., 2013). Another, not necessarily mutually exclusive, potential pathogenic mechanism is repeat-associated non-AUG (RAN) translation through which a toxic polyglycine (FMRpolyG) protein is produced from the elongated *FMR1* CGG repeat mRNA (Todd et al., 2013; Sellier et al., 2017; Krans et al., 2019). To date, the relative contributions of the RNA-based inclusions and the expression of toxic FMRpolyG to human pathology are still matter of debate. It has even been suggested that in early disease state, the inclusions may serve a protective function by sequestering FMRpolyG (Greco et al., 2006; Hagerman and Hagerman, 2016).

Our current clinical, molecular and histopathological understanding of FXTAS in patients is mostly derived from studies in mouse models. Several mouse models have been generated to study the (neuro)pathology and behavioral effects of FXTAS. Initially two knock-in (KI) mouse models were generated: the Dutch (CGG_{dut}) and the NIH (CGG_{nih}) KI mouse model. Both KI mouse models display FXTAS pathology at the genetic, molecular, histological and behavioral level with slight differences. Both show ubiquitin-positive intranuclear inclusions throughout the entire brain, but these inclusions are more common in the CGG_{dut} KI mice. Behavioral examination of both CGG KI mice revealed memory impairment (Hunsaker et al., 2009), increased levels of anxiety in the CGG_{dut} KI mice while CGG_{nih} KI mice show decreased levels of anxiety. Also, assessment of motor function in the CGG_{dut} KI mouse model showed impairment with increasing age of the mice (Van Dam et al., 2005). This observed cognitive decline and motor function impairment in these mice may reflect the progressive cognitive decline and functionality impairment observed in FXTAS patients. Although both KI mouse models nicely recapitulate FXTAS disease pathology, the time to generate a phenotype is a major disadvantage. It takes roughly up to 52–72 weeks before any phenotype is observed in these mice. Therefore, several transgenic mouse models were developed to study specific research questions of FXTAS disease pathology such as RAN-translation, mRNA containing expanded CGG repeat and potential therapeutic interventions. We refer the reader to more advanced and detailed reviews covering all available mouse models for the premutation and FXTAS (Berman et al., 2014; Haify et al., 2020). All these mouse models show presence of ubiquitin-positive and FMRpolyG-positive inclusions in the central nervous system (CNS) in neurons and astrocytes as well as in non-CNS organs, thus display the most prominent neuropathological hallmark in FXTAS disease pathology, with the notable exception of the intention tremor.

We studied the occurrence of intranuclear inclusions in a novel inducible mouse model for FXTAS, and related these to quantitative alterations in mouse behavior. To avoid interactions during development, we induced—in adult mice—the expression of a randomly integrated 103× CGG repeat expansion in the mouse under control of the neuron-specific Ca^{2+}/calmodulin-dependent protein kinase II alpha (*CamKII*-α) promoter. The *CamKII*-α driver induces expression throughout the entire forebrain, but also in several other regions in the cerebrum such as the hippocampus and the basal ganglia, which are regions known to be involved in FXTAS disease pathology (Greco et al., 2002; Wang et al., 2013). In this report we mainly focused on the dentate gyrus (DG) and CA3 region of the hippocampus, and the striatum, being part of the basal ganglia. These regions are believed to contribute to several behavioral impairments in FXTAS such as in motor learning and coordination, and memory (Scaglione et al., 2008; Hagerman and Hagerman, 2013; Haify et al., 2020). Also, cognitive decline based on performance in spatial learning, memory tasks, executive motor function impairments and anxiety associated disorders are observed in premutation carriers and FXTAS patients (Hasegawa et al., 2009). For a period of 3 months after induction, we quantified the formation of inclusions in the brain and characterized the behavioral performance. As expected, and in line with the expression pattern of the *CamKII*-α promoter (Burgin et al., 1990), we found intranuclear inclusions in the hippocampus and the striatum, already appearing 4 weeks after dox-induction. To our surprise, however, virtually no impact on behavioral performance

was detectable even after 3 months of dox-induction. We therefore propose based on this study that intranuclear inclusions do not have an immediate detrimental effect on neuronal function and this may point to a protective function of inclusion formation in the early-onset of disease-progression in FXTAS.

MATERIALS AND METHODS

Mice

For this study, male and female *CamKII*-α-rtTA/TRE-103CGG-GFP-mice with a C57BL6/J background were used (**Figure 1A**). This *CamKII*-α inducible mouse model was generated similarly to the ubiquitous inducible mouse model by random integration of the transgenes in the genome (Hukema et al., 2014). The TRE-103CGG-GFP mice were crossed with the *CamKII*-α-rtTA driver line to generate double transgenic mice using the Tet-On system. Dox-treatment was initiated at the age of 9 weeks in these mice. Dox drinking water contained 2 mg/ml doxycycline hyclate (Sigma) in 5% sucrose (Sigma) and was refreshed every 2–3 days.

Genotyping

For genotyping, toe clips from P5–7 mice and, after sacrificing, lung tissue, were incubated overnight in 300 µl tail digestion buffer [TDB; 50 mM KCl, 10 mM Tris-HCl pH 9, 0.1% Triton X-100 and 0.15 µg proteinase K (Roche)] at 55°C. The following day, samples were heat inactivated for 5′ at 95°C and centrifuged to remove debris. Next, 1 µl of supernatant was used as template DNA in PCR. Templates were checked for presence of rtTA and/or TRE. The following PCR mix was used: 10× FastStart DNA Polymerase buffer with $MgCl_2$ (Roche), 25 mM dNTPs, primers (10 mM), FastStart DNA polymerase (5 U/µl; Roche) and sterilized water. The PCR program consisted of 4′ denaturation at 94°C, followed by 30 cycles of amplification through 30″ at 94°C, 30′ at 60°C, and 90″ at 72°C, and ended with 5′ at 72°C. PCR products were visualized by adding 10 µl 3× loading mix [30% Orange G (Sigma), 0.2% GelRed (Biotium) in H_2O] to 5 µl of PCR product and separating using gel electrophoresis on a 1.5% agarose gel. Gels were scanned using Gel Doc XR+ (Bio-Rad) Molecular Imager with Image Lab software. The TRE transgene was amplified using forward primer 5′-GCTTAGATCTCTCGAGTTTAC-3′ and reverse primer 5′-ATGGAGGTCAAAACAGCGTG-3′. The rtTA transgene was amplified using forward primer 5′-CAGCAGGCAGCATATCAAGGT-3′ and reverse primer 5′-GCCGTGGGCCACTTTACAC-3′.

Repeat Length PCR

Repeat length was determined according to an in-house PCR protocol. Brain tissue from mice having 11CGGs (positive control), wildtype mice (negative control) and TRE-103CGG-GFP 4 weeks old mice were incubated overnight in 300 µl tail mix buffer [50 mM Tris pH = 7.5, 10 mM EDTA, 150 mM NaCl, 1% SDS and 20 µl proteinase K (10 mg/ml; Roche Cat. #3115852)] at 55°C. The next day, 100 µl 6 M NaCl was added to the samples and samples were shaken very well to induce

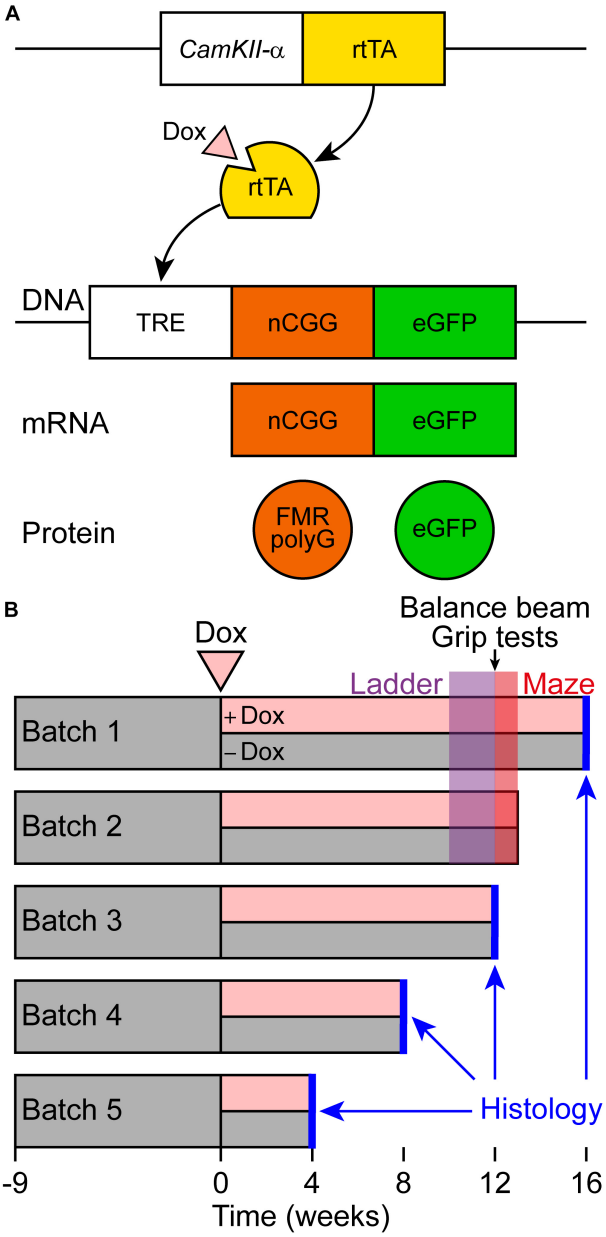

FIGURE 1 | Schematic representation of the Tet-On system and behavioral testing of a new brain-specific mouse model for FXTAS. **(A)** Brain-specific expression of the expanded CGG repeat RNA coupled to GFP was studied in the *CamKII*-α-rtTA/TRE-103CGG-GFP inducible mouse model with a C57BL6/J background. The Tet-On system was used to generate double transgenic mice expressing the expanded CGG repeat at the RNA level. Expression of the reverse tetracycline transactivator (rtTA) is controlled by the *CamKII*-α promoter on a separate transgene. Upon dox administration, rtTA will be activated and can bind the tet response element (TRE) on another transgene, which induces expression of the expanded CGG repeat at the RNA level and GFP at the protein level. As the transgene contains the 5′-UTR of the FMR1 gene with an expanded CGG repeat, the FMRpolyG polypeptide is produced from the expanded CGG repeat by RAN translation. **(B)** Schematic overview of the experimental schedule for histological analysis and behavioral testing. At around 9 weeks of age, dox-treatment started. Around 10 weeks later, ErasmusLadder tests were performed, followed by balance beam and grip tests. Finally, the mice were subjected to the Morris water maze test.

precipitation of cell debris. Samples were centrifuged (10,000 *g* at RT for 10 min) to remove cell debris. The supernatant was transferred to a new tube and 1 ml 100% EtOH was added (shake very well). Tubes were centrifuged at 10,000 *g* for 10 min to form DNA pellet. Next, the supernatant was discarded and DNA pellet was washed with 500 µl 70% EtOH. Samples were centrifuged at 10,000 *g* for 5–10 min. The supernatant with EtOH was discarded and the DNA pellet was left to dry to the air for a couple of minutes. The DNA pellet was resuspended in 100 µl sterilized water. Next, 1 µl of supernatant was used as template DNA in the PCR reaction mix (total volume 21 µl). Following PCR mix was used: 10 µl Betaine (5 M), 4 µl 5× expand HF buffer without Mg^{2+}, 1.5 µl $MgCl_2$ (25 mM) 1 µl forward primer (10 µM), 1 µl reverse primer (10 µM), 0.2 µl dNTP mix (100 mM) (25 mM each), 0.2 µl FastStart Taq DNA polymerase (5 U/µl; Roche) and 2.1 µl sterilized water. The PCR program consisted of 10' denaturation at 98°C, followed by 35 cycles of amplification through 35 s at 98°C, 35 s at 58°C and 3 min at 72°C, and ended with a cooling step at 15°C. For quantification of the DNA size, 1 µl 1 Kb Plus DNA ladder (Thermo Fisher Scientific; Cat. # 10787018) was used with and without 0.2% GelRed (Biotium) in dH_2O. Staining with GelRed after electrophoresis run is necessary because GelRed interferes with the DNA and therefore influences CGG repeat measurement. To front track DNA separation during gel electrophoresis, 10 µl 30% Orange G (Sigma) loading dye was added to 5 µl of PCR product on the 1.5% agarose gel. After gel electrophoresis run, the agarose gel was stained for 30 min in 500 ml 1X TBE-buffer (1L 5X TBE-buffer: 54 g Tris (CAS #77-86-1), 27.5 g boric acid (CAS #10043-35-3) and 20 ml 0.5 M EDTA pH = 8.0 (CAS #60-00-4) + 50 µl 0.2% GelRed (Biotium). Gels were scanned using Gel Doc XR+ (Bio-Rad) Molecular Imager with Image Lab software. The CGG repeat was amplified using the following forward primer 5'-ATCCACGCTGTTTTGACCTC-3' and reverse primer 5'-CCAGTGCCTCACGACCAAC-3'.

RNA Isolation and cDNA Synthesis

RNA isolation was performed on dox and sucrose treated 16 weeks old *CamKII*-α-rtTA/TRE-103CGG-GFP mice. Per treatment group $n = 3$ brains were used for RNA isolation. Prior to lysing, samples were thawed on ice and supplied with RIPA-buffer containing 0.05% protease inhibitors (Roche), 0.3% 1 M DTT (Invitrogen) and 40U RNase Out (Roche). Samples were mechanically lysed, followed by 30 min of incubation on ice. After 30 min of incubation, mechanical lysing was repeated to ensure total homogenization. Homogenate was added to RNA Bee (Tel-Test) in a 1:10 (v/v) ratio and mixed thoroughly. Chloroform (Millipore) was added to mixture in a 1:5 ratio (v/v), mixed thoroughly and incubated on ice for 15 min. After incubation the mixture was centrifuged for 15 min at 4°C and supernatant was collected and supplied with 0.6× (v/v) 100% 2-propanol (Honeywell). After 15 min centrifugation at 4°C, supernatant was discarded. Remaining pellet was washed with 80% EtOH (Honeywell) in duplicate with brief centrifugation at 4°C between washes. Following removal of residual supernatant, 50 µl dH_2O was added and concentration was determined using the NanoDrop 2000 (Thermo Fisher Scientific).

Quantitative Real-Time PCR

Reverse transcriptase (RT) was performed using 1 µg of RNA with the iScript cDNA synthesis kit (Biorad) according to manufacturer's instructions. RNA was treated with DNase before cDNA synthesis. Q-PCR using iTaq Supermix (BioRad) was performed on 0.1 µl RT product. Cycling conditions were an initial denaturation of 3 min at 95°C, followed by 35 cycles of each 5 s at 95°C and 30 s at 60°C. As a reference gene GAPDH was used. For statistical analysis the two-sample unpaired *t*-test assuming equal variance was used.

Immunohistochemical Staining

Tissues were fixed overnight in 4% paraformaldehyde (PFA) at 4°C and embedded in paraffin according to in-house protocols. Sections of 6 µm were cut and placed on silane coated slides (Klinipath). The sections were deparaffinized in decreasing concentrations of alcohol—starting with xylene and ending in demineralized H_2O—before performing antigen retrieval by microwave treatment in 0.01 M sodium citrate (pH = 6). Endogenous peroxidase activity was blocked with 0.6% H_2O_2 in PBS. When staining for FMRpolyG an additional incubation with proteinase K (5 µg/ml) was performed for 20–30 min at 37°C to ensure optimal antibody binding. Staining was performed overnight at 4°C with primary antibodies diluted in PBS/0.5% milk/0.15% glycine (PBS+). Staining with secondary antibodies was performed at RT for 60 min. Antigen-antibody complexed were visualized using DAB-substrate (DAKO), after which slides were counterstained with hematoxylin for 5 min and subsequently mounted with Entellan (Merck Milipore International). Antibodies used are listed in **Table 1** hereafter.

Behavioral Testing

Muscle function was tested using a hanging wire test. A metal wire with a diameter of 2 mm was suspended around 20 cm above a cage. The mouse was brought to the wire so that he could grasp the wire with his front paws after which the latency to fall was recorded. The maximal trial duration was 60 s. In addition, we used the Bioseb grip strength test (Bioseb, Vitrolles, France). For this test, the mouse was placed on a metal grid and after he clamped to the grid with all four limbs, he was gently pulled down by the base of his tail. The maximal force was measured and the average of three consecutive trials was calculated.

The fine motor coordination of the mice was tested on the balance beam. During 2 consecutive days, the mice were habituated to the setup that consisted of a horizontal wooden beam with a diameter of 12 mm and a length of 100 cm located

TABLE 1 | Antibodies.

Target	Dilution	Host	Source	Catalog No.
FMRpolyG (8FM)	1:10	Mouse	Gift from N. Charlet-Berguerand, IGBMC	X
GFP	1:2000	Mouse	Roche	11814460 001

Mouse specific anti-GFP and anti-FMRpolyG (8FM) antibodies were used to visualize GFP expression and the FMRpolyG protein aggregates in mouse brain, respectively.

approximately 50 cm above a table. Each mouse was placed on one side of the beam and walked over the beam to a home cage at the other side of the beam. After two trials, the beam was replaced by one with a diameter of 8 mm and also on this beam two trials were performed. On the third day, the performance of the mice was quantified by counting the number foot slips and falls. Each mouse crossed each beam twice and the average time required to reach the other side of the beam was measured, taking only trials without falls into account.

Locomotor patterns were recorded on a horizontal ladder flanked by two plexiglass walls spaced 2 cm apart (ErasmusLadder, Noldus, Wageningen, Netherlands) as described previously (Vinueza Veloz et al., 2015). The ladder consisted of two rows of 37 rungs placed in an alternated high/low pattern. The rungs were spaced 15 mm apart and the height difference between high and low rungs was 9 mm. Each rung was connected to a pressure sensor recording rung touch. During a trial, the mouse had to walk from a shelter box on one side of the ladder to another on the other end. Trial start was indicated by lighting an LED in the shelter box followed 3 s later by a strong tail wind. Early escapes, thus before the LED was switched on, were discouraged as they triggered a strong head wind. In between trials, there was a resting period. Mice were first habituated to the setup by letting them freely explore the ladder for 15 min during which no light or air cues were given. On the next day, training started with 44 trials on each day. The initial training consisted of six daily sessions, after which the mice were measured once a week. Sensor touches were filtered to delete single backsteps or fake hind limb steps using the factory settings. For the further analysis, we used the touches of the front limbs with the first and the last step of each trial being deleted.

Using the water maze test, we quantified the spatial memory of the mice. Each mouse was placed on the border of a circular pool with a diameter of 120 cm filled with a mixture of water and non-toxic white paint kept constant at 26°C. In the pool, a platform with a diameter of 11 cm diameter was hidden 1 cm below the water surface. The time to find the platform was recorded on two trials each day on 5 consecutive days. When the mouse did not find the platform within 60 s, the trial was stopped. On days 6 and 7, a probe trial was given. During the probe trials, the platform was absent and the mice were allowed to swim for 60 s while their trajectory was tracked (EthoVision XT11, Noldus, Wageningen, Netherlands). The data of the probe trials were analyzed by subdividing the pool in four quadrants, with the original position of the platform in the middle of quadrant 3. We marked the original platform position as well as the same shape at the corresponding position in the other three quadrants and counted how often the mouse passed the borders of each of these positions per trial. We considered a crossing if it involved more than 50% of the body of the mouse. On top of that, we also quantified the time spent in each quadrant.

The battery of behavioral tests is schematically represented in time in **Figure 1B**.

Statistics

Behavioral performance on each paradigm was compared between mice treated with and without doxycycline. The statistical tests used are mentioned in the Results section, whereby we used non-parametric tests for data that were not normally distributed. Throughout the manuscript, we considered a p-value of 0.05 or less as indication for statistical significance.

RESULTS

Expanded CGG Expression Results in Inclusion Formation in the Hippocampus and Basal Ganglia

First of all, we studied the expression pattern of the FMRpolyG-GFP fusion protein in *CamKII*-α-rtTA/TRE-103CGG-GFP mice after induction of transgene expression by the addition of doxycycline (dox) to the drinking water. First, repeat length in the transgene was verified using an in-house PCR protocol. Repeat length PCR shows the repeat size of 103× CGGs at approximately 480 bp compared to the control 11 CGGs length at 290 bp (**Supplementary Figure S1A**). To verify whether dox treatment did not affect murine *Fmr1* mRNA expression, we performed quantitative real-time PCR on brain tissue of treated and control mice. The data show that dox treatment had no effect on *Fmr1* mRNA expression in the brain as tested in the hippocampus (**Supplementary Figure S1B**). Since the transgene expression was under the *CamKII*-α promoter, we expected the FMRpolyG protein to be present in neurons of, among other regions, the hippocampus, the neocortex, the basal ganglia, and in the posterior part of the cerebellum, more specifically lobule X (Hasegawa et al., 2009; Wang et al., 2013). In our hands, already after 4 weeks of dox treatment, GFP expression, indicative of FMRpolyG expression, was found in all aforementioned brain regions. After 12 weeks of dox treatment, the expanded CGG repeat was strongly expressed in the striatum of the basal ganglia, the hippocampus, the neocortex, and lobule X of the cerebellum (**Figures 2A,B,D,E**). Low to modest expression of GFP was present at 12 weeks in the hypothalamus, the colliculus inferior and superior (**Figures 2C,D**), and other sub-regions of the midbrain.

Next, we investigated whether FMRpolyG expression was associated with the formation of nuclear inclusions in the *CamKII*-α-rtTA/TRE-103CGG-GFP mice. To this end, we compared brain sections stained for FMRpolyG from mice that did receive dox with those from mice that did not. As expected, we could not detect any inclusions in the control mice. However, the mice treated with dox developed spherical FMRpolyG-positive inclusions in most of the brain regions in which GFP expression was observed. The highest density of inclusions was found in the striatum, the CA3 region of the hippocampus and the hypothalamus (**Figures 3B–D**). Lower densities were present in the DG region of the hippocampus, as well as in the inferior and the superior colliculus (**Figures 3A,E**). We did not observe a perfect correlation between GFP expression and the occurrence of inclusions: in lobule X of the cerebellum, no inclusions were found despite the presence of GFP (**Figures 2E,F**). In general, during 12 weeks of dox treatment, the number of inclusions increased over time with regional differences. Quantification

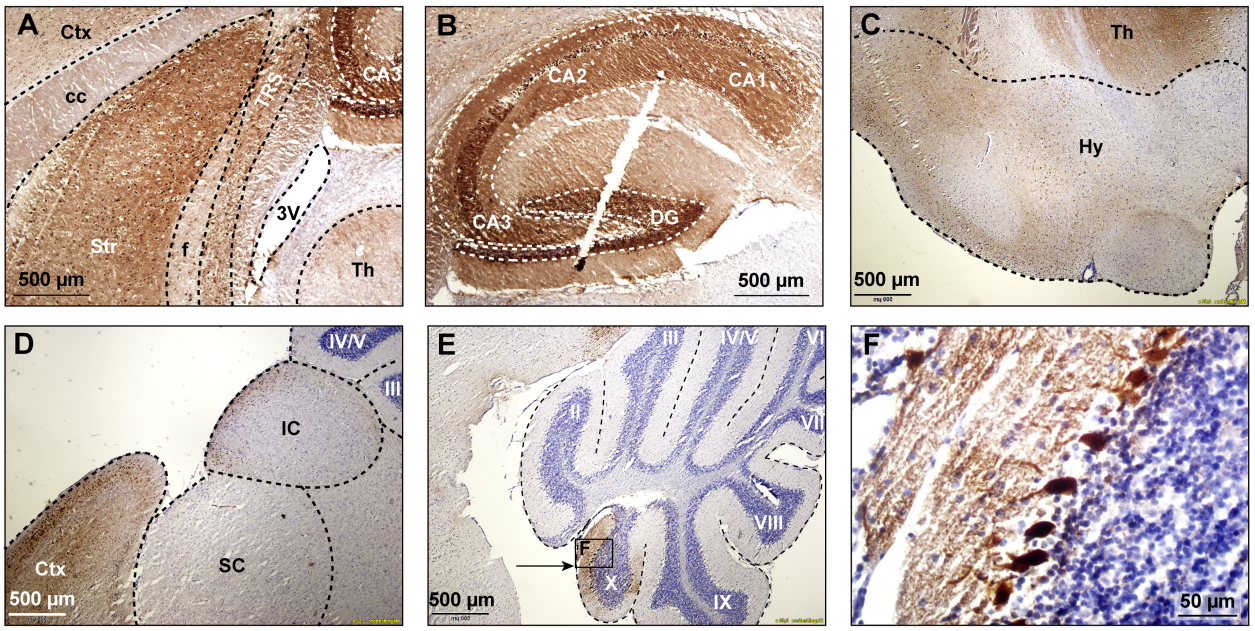

FIGURE 2 | GFP expression in multiple brain regions. GFP expression (brown staining) was visualized using immunohistochemical staining with a mouse specific anti-GFP antibody in sagittal brain sections at 12 weeks after onset of dox-treatment. Strong expression of GFP was present in the striatum **(A)**, the hippocampus **(B)**, the hypothalamus **(C)**, and the cerebral cortex **(D)**. Lower levels of expression were present in the superior and inferior colliculus **(D)**. In the cerebellum, GFP expression was only observed in vermal lobule X (**E**, indicated area amplified in **F**). 3V, third ventricle; cc, corpus callosum, Ctx, cerebral cortex; DG, dentate gyrus; f, fornix; Hy, hypothalamus; IC, inferior colliculus; SC, superior colliculus; Str, striatum; Th, thalamus; TRS, triangular nucleus of the septum.

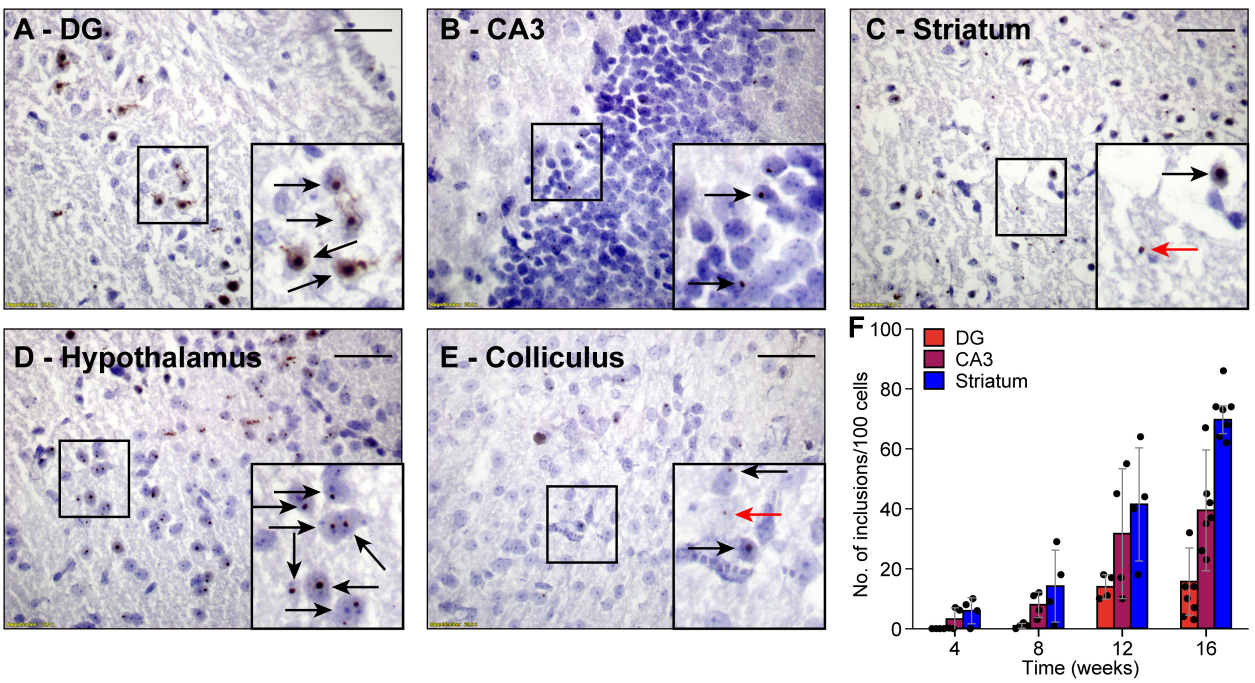

FIGURE 3 | FMRpolyG-positive inclusions are predominantly located in the nucleus. FMRpolyG-positive inclusions, visible as black dots, were stained using the mouse anti-FMRpolyG (8FM) antibody. Most often, the FMRpolyG-positive inclusions were observed in the nuclei (black arrows) but occasionally also outside the nuclei (red arrows). FMRpolyG-positive inclusions were found in the dentate gyrus (DG, **A**) and the CA3 region of the hippocampus **(B)**, the striatum **(C)**, the hypothalamus **(D)**, and in the colliculi **(E)**. Rectangles indicate areas enlarged in insets. Scale bars = 50 µm. **(F)** The prevalence of FMRpolyG-positive inclusions increased over time after onset of dox treatment. Bars indicated average values and error bars the sd.

of FMRpolyG-positive inclusions (**Figure 3F**) was only done in the hippocampus and the striatum of the basal ganglia, since these regions are known to be involved in FXTAS disease pathology (Greco et al., 2002). Irrespective of the brain region involved, most inclusions were located intranuclearly. Sometimes two or more smaller inclusions were located in the same nucleus. In summary, dox induced the production of CGG RNA in *CamKII*-α-rtTA/TRE-103CGG-GFP mice in several brain regions, which resulted in the formation of FMRpolyG-positive nuclear inclusions, predominantly in the striatum and the hippocampal CA3 region.

Absence of Behavioral Phenotype in Mice Expressing FMRpolyG-Positive Inclusions

To test whether the expression of the CGG repeat and the resulting nuclear inclusions had any impact on mouse behavior, we subjected the mice to a battery of behavioral tests. To control for possible confounding problems with the general condition of the mice, we first tested the muscle strength using the hanging wire and the Bioseb grip strength tests 12 weeks after the start of the dox treatment. The latency to fall was 22.0 ± 11.0 vs. 26.5 ± 10.2 s (control vs. dox mice, averages ± s.d., $p = 0.385$, $t = 0.944$, $df = 17$, *t*-test **Figure 4A**) during the hanging wire test and the force was 1.79 ± 0.37 vs. 1.53 ± 0.39 N (control vs. dox mice, averages ± s.d., $p = 0.336$, $t = 0.991$, $df = 17$, *t*-test **Figure 4B**) during the Bioseb grip strength test. We therefore conclude that there were no indications for changes in muscle strength due to the dox treatment.

Next, we tested the overall motor control and balance on the balance beam after 12 weeks of dox treatment. The numbers of hind foot slips per trial were comparable between control and dox mice [thick beam: 2.0 (inter-quartile range (IQR): 1.5) vs. 1.5 (IQR: 0.9), $p = 0.876$, $U = 47.5$; thin beam: 1.0 (IQR: 1.4) vs. 2.5 (IQR: 2.5), $p = 0.220$, $U = 33.5$, medians, Mann-Whitney tests, **Figure 4C**]. Also the time required to cross the beam were not really different between control and dox mice [thick beam: 8.3 (IQR: 2.5) vs. 7.0 (IQR: 1.9) s, $p = 0.593$, $U = 42.5$; thin beam: 9.8 (IQR: 8.6) vs. 12.5 (IQR: 9.1), $p = 0.820$, $U = 46.5$, medians, Mann-Whitney tests, **Figure 4C**]. We take this as a sign that the treatment did not impair the overall motor control and ability to keep balance.

We continued by describing the behavior on the ErasmusLadder, which is a horizontal ladder consisting of two rows of rungs in an alternating high/low pattern spanning the space between two shelter boxes. After habituation and initial training, we measured the performance at 10, 11, and 12 weeks after the start of dox treatment. The start of each trial was indicated by switching on an LED in the start box and this was followed by a strong tail wind 3 s later. In roughly 75% of the trials, the mice waited until the tail wind started before leaving the start box. Leaving upon perception of the visual cue or even before that was observed less often. Changes in this pattern could be a sign of cognitive impairment (Vinueza Veloz et al., 2012), but these were not observed between control and dox mice ($p = 0.516$, 3 × 2 Fisher's exact test, **Figure 4D**).

Next, we characterized the stepping pattern on the ErasmusLadder. Wild type C57BL/6J mice have a tendency to avoid the lower rungs and typically make steps from one high rung to the next or the second next high rung (Vinueza Veloz et al., 2015). We considered these small and regular steps, respectively. Long steps, skipping at least two higher rungs, and lower rung steps occurred much less often, as did other irregular steps such as backwards walking. Thus, also regarding the stepping pattern, no impact of the dox treatment was observed (**Table 2** and **Figures 4E–G**).

Finally, to test for putative defects in spatial memory formation, we subjected the mice to the Morris water maze test around 12 weeks after the start of the dox treatment. During 5 consecutive days, the mice were trained to find a hidden platform just below the surface of an opaque, circular pool. Over the sessions, both control and dox-treated mice managed to be faster in finding the hidden platform, with no statistically significant differences between the two groups [$p = 0.134$, $F_{(1, 17)} = 2.479$, repeated measures ANOVA, **Figure 4H**]. On the next 2 days, the experiment was repeated—but without a hidden platform. On these probe trials we made video recordings of the mice (**Figure 4I**). First, we counted how often the mice crossed the location where the hidden platform had been during the training sessions and compared these with crosses of the analogous locations in the other three quadrants. During the first probe trial, both control and dox treated mice had a preference for the real location (in quadrant 3) over the other areas (control: 2.2 ± 1.5 crosses per trial of the real location vs. 1.0 ± 0.9 crosses of the other locations, $p = 0.021$, $U = 60.5$, Mann-Whitney test, dox mice 2.0 ± 2.2 vs. 0.6 ± 0.7 crosses, averaged ± ss, $p = 0.107$, $U = 101.5$, Mann-Whitney test, control vs. dox mice: $p = 0.813$, $\chi^2 = 0.95$, χ^2 test). During the second probe trial, the preference of the control mice for the real location was gone (1.8 ± 1.2 vs. 1.6 ± 1.3 crosses, $p = 0.624$, $U = 108.0$, Mann-Whitney test), but remained present in the dox treated mice (3.3 ± 2.3 vs. 1.1 ± 1.1 crosses per trial, $p = 0.005$, $U = 63.0$, Mann-Whitney test). This difference between control and dox mice was on the border of statistical significance ($p = 0.061$, $\chi^2 = 7.36$, χ^2-test, **Figure 4J**). This might indicate that the dox-treated mice had more trouble understanding that the hidden platform was no longer in place. This, however, was not reflected in the relative dwell times per quadrant [$p = 1.00$, $F_{(1, 17)} = 0.000$, repeated measures ANOVA, **Figure 4K**], which leads us to conclude that also the Morris water maze did not reveal convincing differences in behavior due to activation of the premutation.

DISCUSSION

Wide-spread occurrence of nuclear inclusions is a major hallmark of FXTAS. To date, it is a matter of debate whether these inclusions contribute to cellular pathology in FXTAS, or—in contrast—slow down the disease process by sequestering toxic RNA and proteins. Such a protective function has been suggested for FXTAS (Greco et al., 2006; Hagerman and Hagerman, 2016), but also for other protein-aggregation disorders, such as Huntington's disease and SCA1 (Klement et al., 1998;

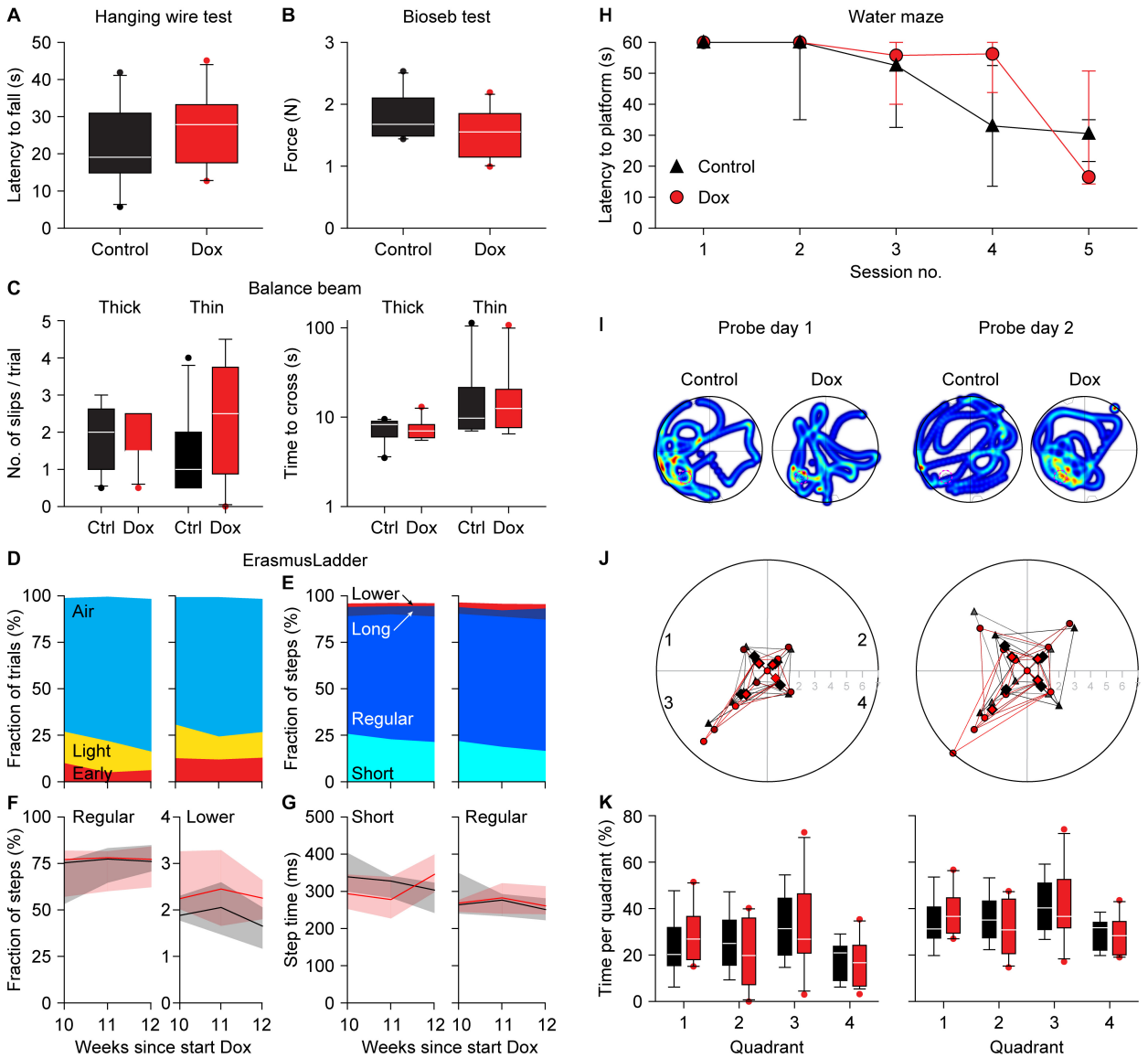

FIGURE 4 | Absence of a clear behavioral phenotype in dox-treated mice. Neither the hanging wire test **(A)** nor the Bioseb grip strength test **(B)** demonstrated an impact of dox-treatment on muscle strength. **(C)** Also, the balance beam test failed to find consistent differences in either the number of slips (left) or the time to cross (right). The tests were performed on a thick (12 mm diameter) and a thin (8 mm diameter) wooden beam. **(D)** On the ErasmusLadder, trial starts were indicated by lighting an LED in the start box, followed 3 s later by a strong tail wind. The fraction of trials with starts before the visual cue ("Early"), during the visual cue ("Light") or after the start of the tail wind ("Air") were comparable between control and dox-treated mice. Data recorded at 10, 11, and 12 weeks after the start of dox-treatment. **(E)** The ErasmusLadder consists of alternating high and low rungs. The fractions of short steps (from one high rung to the next), regular steps (from one high rung to the second high rung), long steps (from on high rung to another, skipping at least two) and lower rung touches were also similar for both groups, as further illustrated for the fraction of regular steps and lower rung touches **(F)** as well as for step times **(G)**. The data in **(F,G)** show the medians with the shades indicating the inter-quartile range. See **Table 2** for a more extensive statistical analysis of the ErasmusLadder test. **(H)** In the water maze, the mice had to find a platform hidden just below the water surface. As the water was made opaque, the mice could not see the platform. During 5 consecutive training days, the latency to find the platform decreased both in control and dox-treated mice. **(I)** On the next 2 days, the hidden platform was removed (probe trials) and the trajectories of the mice were recorded. The heat maps indicate the time spent per area of two exemplary mice. The original location of the hidden platform is indicated by a pink dashed circle in quadrant 3. **(J)** On the first probe day, the mice crossed the location where the hidden platform had been more often than the analogous regions of the other quadrants. On the second day, the control mice no longer searched more often in the area where the hidden platform had been ($p = 0.624$, Mann-Whitney test), while the dox-treated mice kept searching specifically around the location where the hidden platform had been ($p = 0.005$, Mann-Whitney test). **(K)** This retention, however, was not noticeable when comparing the times spent per quadrant. Unless indicated otherwise, behavioral tests were performed during the 12th week of dox-treatment. Group sizes were 10 mice.

TABLE 2 | Step size statistics for the ErasmusLadder.

	Treatment	Median	IQR	*p*	F	df	Test
Step lengths (%)							
Short steps (step size = 2)	-Dox	6.4	15.8	0.687	0.168	1	Repeated measures ANOVA
	+Dox	7.1	22.8				
Regular steps (step size = 4)	-Dox	76.1	14.2	0.699	0.154	1	Repeated measures ANOVA
	+Dox	77.2	22.0				
Long steps (step size ≥ 6)	-Dox	3.4	7.9	0.688	0.166	1	Repeated measures ANOVA
	+Dox	5.1	4.1				
Lower rung steps	-Dox	1.7	0.9	0.153	2.226	1	Repeated measures ANOVA
	+Dox	2.3	0.8				
Backsteps	-Dox	1.3	1.0	0.629	0.241	1	Repeated measures ANOVA
	+Dox	2.1	1.8				
Step times (ms)							
Short steps (step size = 2)	-Dox	303	82	0.751	0.104	1	Repeated measures ANOVA
	+Dox	346	101				
Regular steps (step size = 4)	-Dox	251	59	0.588	0.304	1	Repeated measures ANOVA
	+Dox	261	75				

The percentages of steps to higher rungs, being either short, regular or long, as well as those to lower steps (irrespective of stride length), and backward steps were compared at 10, 11, and 12 weeks after onset of dox treatment. Note that the percentages do not add to 100% as some irregular types of steps were not considered here (in particular, steps starting from lower rungs). Of the two most frequent step categories, also the step times are indicated and compared. The values were first calculated per mouse, and then compared between the two groups (n = 10 mice/group). The median and interquartile range (IQR) values in this table refer to the recording session at 12 weeks after onset of dox treatment. All values refer to front paw movements. p-values reflect the between-subject comparisons of repeated measures ANOVAs. Since not a single p-value was close to the threshold for significance, no correction for multiple comparisons was applied.

Saudou et al., 1998; Cummings et al., 1999; Arrasate et al., 2004). To study the relation between the development of intranuclear inclusions and behavioral deficits, we used a novel, inducible and neuron-specific mouse model for FXTAS under the control of the *CamKII*-α promoter. Expression of an expanded 103CGG repeat RNA transgene is induced by dox and is under the control of the Tet-On system. This inducible mouse model shows no evidence of expression in the absence of dox (i.e., no leakage of expression), and was induced after completion of normal development to avoid interaction with developmental processes. Within a month after transgene induction, FMRpolyG-positive nuclear inclusions were found in the striatum and the CA3 region of the hippocampus. Two months after the occurrence of the first nuclear inclusions, the inclusions were abundant in most brain areas in which the *CamKII*-α promoter is active such as the hippocampus, neocortex and the striatum. Yet, we could not identify a robust behavioral phenotype that could be caused by the inclusion pathology in these mice. Several mouse models have significantly contributed to our understanding of the molecular mechanisms underlying FXTAS and have characterized disease progression. Previously, we found in a different inducible mouse model for FXTAS, using the heterogeneous nuclear ribonucleoproteins (*hnRNP*) promoter, a rapid death after dox-induction. The neuronal level of transgene expression in these mice was low, and nuclear inclusions were sparse or even absent in the brain (Hukema et al., 2014). In contrast, in a third mouse line, under control of the brain-specific protease-resistant-protein (*PrP*) promoter, we observed both the formation of nuclear inclusions and behavioral deficits (Hukema et al., 2015). These mice developed only a deficit in the compensatory eye movement pathway after 20 weeks of treatment with dox. Although expression of the transgene containing the expanded CGG repeat mRNA was found in the hippocampus, lobule X of the cerebellum and the striatum, these expression levels were low with the exception of lobule X of the cerebellum where expression was the most profound. Together, these results lead us to question whether the development of nuclear inclusions is indeed the cause of developing FXTAS symptoms. Therefore, we developed a new inducible transgenic mouse model under the control of the *CamKII*-α promoter expecting stronger expression in the brain.

In our *CamKII*-α-rtTA/TRE-103CGG-GFP mouse model, the expression of GFP followed that of the previously described distribution of the *CamKII*-α promoter (Wang et al., 2013). Immunohistochemical staining shows the strongest GFP expression in the striatum, the CA3 region of the hippocampus and lobule X of the cerebellum. Moderate GFP expression was found in the neocortex, the dentate gyrus, the hypothalamus and several midbrain areas. In all of these regions, with the notable exception of the cerebellum, also nuclear inclusions were formed. If nuclear inclusions in these areas would result in functional deficits, a broad range of behavioral impairments is to be expected. As a consequence, typical cerebellar symptoms, although prominent in FXTAS patients (Hagerman et al., 2001; Tassone et al., 2007; Hagerman and Hagerman, 2013, 2016), were not expected in our mouse model since the *CamKII*-α is only expressed in a very limited part of the cerebellum. We therefore focused on spatial learning, that has previously been shown to be affected in a knock-in mouse model ("the Dutch mouse") (Van Dam et al., 2005; Hunsaker et al., 2009), and striatal motor coordination functions, as they also occur as parkinsonism in patients (Hagerman et al., 2001).

An intact hippocampus is essential for normal spatial learning in the water maze (D'Hooge and De Deyn, 2001; Okada and Okaichi, 2009; Laeremans et al., 2015). Our mice showed no, or only marginal, deficits at the water maze test, arguing against a severely impaired hippocampal function. The striatum is vital for motor control and striatal damage leads to impaired behavior on the balance beam (Shear et al., 1998; Feng et al., 2014), which was not observed in our mice. This lack of an effect on motor coordination was further substantiated by equal performance of treated and control mice on the ErasmusLadder and the grip tests. Although we cannot exclude that there were subtle behavioral deficits that we did not observe, it is safe to state that there were no major changes in behavioral performance in spite of the abundance of nuclear inclusion in the dox treated mice.

The expanded CGG RNA and proteins can aggregate with many other molecules into nuclear inclusions (Ma et al., 2019). The expanded CGG RNA on itself is not enough to induce toxicity and that the production of an out-of-frame FMRpolyG protein due to RAN translation is necessary for cellular toxicity (Galloway and Nelson, 2009; Hashem et al., 2009; Sellier et al., 2017; Derbis et al., 2018). Our present results indicate that the development of FMRpolyG-positive nuclear inclusions themselves are probably not very detrimental to the function of neurons. It remains to be seen whether aggregation is an active process, aimed at sequestering toxic molecules and thereby slowing down the disease progression, or more an epiphenomenon that is a physical consequence of the molecular structure of the expanded CGG RNA and/or RAN translation protein FMRpolyG.

DATA AVAILABILITY STATEMENT

The raw data supporting the conclusions of this article will be made available by the authors, without undue reservation, to any qualified researcher.

ETHICS STATEMENT

All experiments involving mice were performed according to Dutch law and following institutional guidelines (Erasmus MC, Rotterdam, Netherlands) in confirmation with EU directive 2010/63. Prior to the start of the experiments, project licenses were obtained from the national authority (Centrale Commissie Dierproeven, The Hague, Netherlands) after review by an independent ethical committee (DEC Consult, Soest, Netherlands) and filed under numbers AVD101002015290 and AVD1010020197846.

AUTHOR CONTRIBUTIONS

SH, RH, and LB conceived the project. SH, RM, ET, VB, and RV performed the experiments. SH, RM, RW, RH, and LB analyzed the data. SH, RW, and LB wrote the manuscript with input from all authors.

FUNDING

RW contributed to funding by the ZonMw Grant the ANR-14-RARE-0003 E-RARE "Drug_FXSPreMut."

ACKNOWLEDGMENTS

We thank Nicolas Charlet-Berguerand for the nCGG-GFP plasmids and the FMRpolyG 8FM mouse monoclonal antibody.

SUPPLEMENTARY MATERIAL

The Supplementary Material for this article can be found online at: https://www.frontiersin.org/articles/10.3389/fmolb.2020.599101/full#supplementary-material

Supplementary Figure 1 | CGG repeat length verification and *Fmr1* mRNA expression in dox-induced transgenic mice. **(A)** Gel electrophoresis analysis shows that the CGG repeat length in the *CamKII*-α-rtTA/TRE-103CGG-GFP transgenic mice is in the premutation range. Repeat length PCR shows the repeat size of 103× CGGs and 11× CGGs at approximately 480 and 290 bp, respectively. +L = Ladder with GelRed; -L = Ladder without GelRed; MUT = TRE-103CGG-GFP (mouse ID: 20464-1); 11CGG = normal repeat length (positive control); WT = wildtype (negative control); H_2O = water control. **(B)** Quantification of *Fmr1* mRNA expression in the hippocampus of dox-induced (n = 3) and control (sucrose; n = 2) mice 16 weeks after start of the dox treatment. Dox-induction does not affect *Fmr1* mRNA expression levels in these transgenic mice. Measurements were repeated twice with the same conditions using q-RT-PCR and normalized to the average level found in the control-dox mice.

REFERENCES

Arrasate, M., Mitra, S., Schweitzer, E. S., Segal, M. R., and Finkbeiner, S. (2004). Inclusion body formation reduces levels of mutant huntingtin and the risk of neuronal death. *Nature* 431, 805–810. doi: 10.1038/nature02998

Bassell, G. J., and Warren, S. T. (2008). Fragile X syndrome: loss of local mRNA regulation alters synaptic development and function. *Neuron* 60, 201–214. doi: 10.1016/j.neuron.2008.10.004

Berman, R. F., Buijsen, R. A., Usdin, K., Pintado, E., Kooy, F., Pretto, D., et al. (2014). Mouse models of the fragile X premutation and fragile X-associated tremor/ataxia syndrome. *J. Neurodev. Disord.* 6:25.

Brown, S. S. G., and Stanfield, A. C. (2015). Fragile X premutation carriers: a systematic review of neuroimaging findings. *J. Neurol. Sci.* 352, 19–28. doi: 10.1016/j.jns.2015.03.031

Burgin, K. E., Waxham, M. N., Rickling, S., Westgate, S. A., Mobley, W. C., and Kelly, P. T. (1990). *In situ* hybridization histochemistry of Ca2+/calmodulin-dependent protein kinase in developing rat brain. *J. Neurosci.* 10, 1788–1798. doi: 10.1523/jneurosci.10-06-01788.1990

Cid-Samper, F., Gelabert-Baldrich, M., Lang, B., Lorenzo-Gotor, N., Ponti, R. D., and Bolognesi, B. (2018). An integrative study of protein-RNA condensates identifies scaffolding RNAs and reveals players in fragile X-associated tremor/ataxia syndrome. *Cell Rep.* 25, 3422–3434.e7.

Cummings, C. J., Reinstein, E., Sun, Y., Antalffy, B., Jiang, Y., Ciechanover, A., et al. (1999). Mutation of the E6-AP ubiquitin ligase reduces nuclear inclusion frequency while accelerating polyglutamine-induced pathology in SCA1 mice. *Neuron* 24, 879–892. doi: 10.1016/s0896-6273(00)81035-1

Derbis, M., Konieczny, P., Walczak, A., Sekrecki, M., and Sobczak, K. (2018). Quantitative evaluation of toxic polyglycine biosynthesis and aggregation in cell models expressing expanded CGG Repeats. *Front. Genet.* 9:216. doi: 10.3389/fgene.2018.00216

D'Hooge, R., and De Deyn, P. P. (2001). Applications of the Morris water maze in the study of learning and memory. *Brain Res. Brain Res. Rev.* 36, 60–90. doi: 10.1016/s0165-0173(01)00067-4

Feng, Q., Ma, Y., Mu, S., Wu, J., Chen, S., Ouyang, L., et al. (2014). Specific reactions of different striatal neuron types in morphology induced by quinolinic acid in rats. *PLoS One* 9:e91512. doi: 10.1371/journal.pone.0091512

Galloway, J. N., and Nelson, D. L. (2009). Evidence for RNA-mediated toxicity in the fragile X-associated tremor/ataxia syndrome. *Future Neurol.* 4:785. doi: 10.2217/fnl.09.44

Greco, C. M., Berman, R. F., Martin, R. M., Tassone, F., Schwartz, P. H., Chang, A., et al. (2006). Neuropathology of fragile X-associated tremor/ataxia syndrome (FXTAS). *Brain* 129, 243–255.

Greco, C. M., Hagerman, R. J., Tassone, F., Chudley, A. E., Del Bigio, M. R., Jacquemont, S., et al. (2002). Neuronal intranuclear inclusions in a new cerebellar tremor/ataxia syndrome among fragile X carriers. *Brain* 125, 1760–1771. doi: 10.1093/brain/awf184

Hagerman, R., and Hagerman, P. (2013). Advances in clinical and molecular understanding of the *FMR1* premutation and fragile X-associated tremor/ataxia syndrome. *Lancet Neurol.* 12, 786–798. doi: 10.1016/s1474-4422(13)70125-x

Hagerman, R. J., and Hagerman, P. (2016). Fragile X-associated tremor/ataxia syndrome - features, mechanisms and management. *Nat. Rev. Neurol.* 12, 403–412. doi: 10.1038/nrneurol.2016.82

Hagerman, R. J., Leehey, M., Heinrichs, W., Tassone, F., Wilson, R., Hills, J., et al. (2001). Intention tremor, parkinsonism, and generalized brain atrophy in male carriers of fragile X. *Neurology* 57, 127–130. doi: 10.1212/wnl.57.1.127

Haify, S. N., Botta-Orfila, T., Hukema, R. K., and Tartaglia, G. G. (2020). *In silico*, *in vitro*, and *in vivo* approaches to identify molecular players in fragile x tremor and ataxia syndrome. *Front. Mol. Biosci.* 7:31. doi: 10.3389/fmolb.2020.00031

Hasegawa, S., Furuichi, T., Yoshida, T., Endoh, K., Kato, K., Sado, M., et al. (2009). Transgenic up-regulation of alpha-CaMKII in forebrain leads to increased anxiety-like behaviors and aggression. *Mol. Brain* 2:6. doi: 10.1186/1756-6606-2-6

Hashem, V., Galloway, J. N., Mori, M., Willemsen, R., Oostra, B. A., Paylor, R., et al. (2009). Ectopic expression of CGG containing mRNA is neurotoxic in mammals. *Hum. Mol. Genet.* 18, 2443–2451. doi: 10.1093/hmg/ddp182

Hukema, R. K., Buijsen, R. A., Raske, C., Severijnen, L. A., Nieuwenhuizen-Bakker, I., Minneboo, M., et al. (2014). Induced expression of expanded CGG RNA causes mitochondrial dysfunction *in vivo*. *Cell Cycle* 13, 2600–2608. doi: 10.4161/15384101.2014.943112

Hukema, R. K., Buijsen, R. A., Schonewille, M., Raske, C., Severijnen, L. A., Nieuwenhuizen-Bakker, I., et al. (2015). Reversibility of neuropathology and motor deficits in an inducible mouse model for FXTAS. *Hum. Mol. Genet.* 24, 4948–4957. doi: 10.1093/hmg/ddv216

Hunsaker, M. R., Wenzel, H. J., Willemsen, R., and Berman, R. F. (2009). Progressive spatial processing deficits in a mouse model of the fragile X premutation. *Behav. Neurosci.* 123, 1315–1324. doi: 10.1037/a0017616

Iwahashi, C. K., Yasui, D. H., An, H. J., Greco, C. M., Tassone, F., Nannen, K., et al. (2006). Protein composition of the intranuclear inclusions of FXTAS. *Brain* 129, 256–271. doi: 10.1093/brain/awh650

Jin, P., Duan, R., Qurashi, A., Qin, Y., Tian, D., Rosser, T. C., et al. (2007). Pur α binds to rCGG repeats and modulates repeat-mediated neurodegeneration in a *Drosophila* model of fragile X tremor/ataxia syndrome. *Neuron* 55, 556–564. doi: 10.1016/j.neuron.2007.07.020

Kenneson, A., Zhang, F., Hagedorn, C. H., and Warren, S. T. (2001). Reduced FMRP and increased *FMR1* transcription is proportionally associated with CGG repeat number in intermediate-length and premutation carriers. *Hum. Mol. Genet.* 10, 1449–1454. doi: 10.1093/hmg/10.14.1449

Klement, I. A., Skinner, P. J., Kaytor, M. D., Yi, H., Hersch, S. M., Clark, H. B., et al. (1998). Ataxin-1 nuclear localization and aggregation: role in polyglutamine-induced disease in SCA1 transgenic mice. *Cell* 95, 41–53.

Krans, A., Skariah, G., Zhang, Y., Bayly, B., and Todd, P. K. (2019). Neuropathology of RAN translation proteins in fragile X-associated tremor/ataxia syndrome. *Acta Neuropathol. Commun.* 7:152.

Laeremans, A., Sabanov, V., Ahmed, T., Nys, J., Van de Plas, B., Vinken, K., et al. (2015). Distinct and simultaneously active plasticity mechanisms in mouse hippocampus during different phases of Morris water maze training. *Brain Struct. Funct.* 220, 1273–1290. doi: 10.1007/s00429-014-0722-z

Langdon, E. M., Qiu, Y., Ghanbari Niaki, A., McLaughlin, G. A., Weidmann, C. A., Gerbich, T. M., et al. (2018). mRNA structure determines specificity of a polyQ-driven phase separation. *Science* 360, 922–927. doi: 10.1126/science.aar7432

Louis, E., Moskowitz, C., Friez, M., Amaya, M., and Vonsattel, J. P. G. (2006). Parkinsonism, dysautonomia, and intranuclear inclusions in a fragile X carrier: a clinical-pathological study. *Mov. Disord.* 21, 420–425. doi: 10.1002/mds.20753

Ma, L., Herren, A. W., Espinal, G., Randol, J., McLaughlin, B., Martinez-Cerdeño, V., et al. (2019). Composition of the intranuclear inclusions of fragile X-associated Tremor/Ataxia Syndrome. *Acta Neuropathol. Commun.* 7:143.

Okada, K., and Okaichi, H. (2009). Functional differentiation and cooperation among the hippocampal subregions in rats to effect spatial memory processes. *Behav. Brain Res.* 200, 181–191. doi: 10.1016/j.bbr.2009.01.011

Qurashi, A., Li, W., Zhou, J. Y., Peng, J., and Jin, P. (2011). Nuclear accumulation of stress response mRNAs contributes to the neurodegeneration caused by Fragile X premutation rCGG repeats. *PLoS Genet.* 7:e1002102. doi: 10.1371/journal.pgen.1002102

Salcedo-Arellano, M. J., Dufour, B., McLennan, Y., Martinez-Cerdeno, V., and Hagerman, R. (2020). Fragile X syndrome and associated disorders: clinical aspects and pathology. *Neurobiol. Dis.* 136:104740. doi: 10.1016/j.nbd.2020.104740

Saudou, F., Finkbeiner, S., Devys, D., and Greenberg, M. E. (1998). Huntingtin acts in the nucleus to induce apoptosis but death does not correlate with the formation of intranuclear inclusions. *Cell* 95, 55–66. doi: 10.1016/s0092-8674(00)81782-1

Scaglione, C., Ginestroni, A., Vella, A., Dotti, M. T., Nave, R. D., Rizzo, G., et al. (2008). MRI and SPECT of midbrain and striatal degeneration in fragile X-associated tremor/ataxia syndrome. *J. Neurol.* 255, 144–146. doi: 10.1007/s00415-007-0711-8

Sellier, C., Freyermuth, F., Tabet, R., Tran, T., He, F., Ruffenach, F., et al. (2013). Sequestration of DROSHA and DGCR8 by expanded CGG RNA repeats alters microRNA processing in fragile X-associated tremor/ataxia syndrome. *Cell Rep.* 3, 869–880. doi: 10.1016/j.celrep.2013.02.004

Sellier, C., Ronald, A. M. B., Fang, H., Sam, N., Laura, J., Philippe, T., et al. (2017). Translation of expanded CGG repeats into FMRpolyG Is pathogenic and may contribute to fragile X tremor ataxia syndrome. *Neuron* 93, 331–347. doi: 10.1016/j.neuron.2016.12.016

Shear, D. A., Dong, J., Gundy, C. D., Haik-Creguer, K. L., and Dunbar, G. L. (1998). Comparison of intrastriatal injections of quinolinic acid and 3-nitropropionic acid for use in animal models of Huntington's disease. *Prog. Neuropsychopharmacol. Biol. Psychiatry* 22, 1217–1240. doi: 10.1016/s0278-5846(98)00070-0

Sofola, O. A., Jin, P., Qin, Y., Duan, R., Liu, H., de Haro, M., et al. (2007). RNA-binding proteins hnRNP A2/B1 and CUGBP1 suppress fragile X CGG premutation repeat-induced neurodegeneration in a *Drosophila* model of FXTAS. *Neuron* 55, 565–571. doi: 10.1016/j.neuron.2007.07.021

Tassone, F., Adams, J., Berry-Kravis, E. M., Cohen, S. S., Brusco, A., Leehey, M. A., et al. (2007). CGG repeat length correlates with age of onset of motor signs of the fragile X-associated tremor/ataxia syndrome (FXTAS). *Am. J. Med. Genet. B Neuropsychiatr. Genet.* 144B, 566–569. doi: 10.1002/ajmg.b.30482

Tassone, F., Hagerman, R. J., Taylor, A. K., Gane, L. W., Godfrey, T. E., and Hagerman, P. J. (2000). Elevated levels of *FMR1* mRNA in carrier males: a new mechanism of involvement in the fragile-X syndrome. *Am. J. Hum. Genet.* 66, 6–15. doi: 10.1086/302720

Todd, P. K., Oh, S. Y., Krans, A., He, F., Sellier, C., Frazer, M., et al. (2013). CGG repeat-associated translation mediates neurodegeneration in fragile X tremor ataxia syndrome. *Neuron* 78, 440–455. doi: 10.1016/j.neuron.2013.03.026

Van Dam, D., Errijgers, V., Kooy, R. F., Willemsen, R., Mientjes, E., Oostra, B. A., et al. (2005). Cognitive decline, neuromotor and behavioural disturbances in a mouse model for fragile-X-associated tremor/ataxia syndrome (FXTAS). *Behav. Brain Res.* 162, 233–239. doi: 10.1016/j.bbr.2005.03.007

Vinueza Veloz, M. F., Buijsen, R. A. M., Willemsen, R., Cupido, A., Bosman, L. W. J., Koekkoek, S. K. E., et al. (2012). The effect of an mGluR5 inhibitor on procedural memory and avoidance discrimination impairments in *Fmr1* KO mice. *Genes Brain Behav.* 11, 325–331. doi: 10.1111/j.1601-183x.2011.00763.x

Vinueza Veloz, M. F., Zhou, K., Bosman, L. W. J., Potters, J. W., Negrello, M., Seepers, R. M., et al. (2015). Cerebellar control of gait and interlimb coordination. *Brain Struct. Funct.* 220, 3513–3536.

Wang, X., Zhang, C., Szabo, G., and Sun, Q. Q. (2013). Distribution of CaMKIIalpha expression in the brain in vivo, studied by CaMKIIalpha-GFP mice. *Brain Res.* 1518, 9–25. doi: 10.1016/j.brainres.2013.04.042

Conflict of Interest: The authors declare that the research was conducted in the absence of any commercial or financial relationships that could be construed as a potential conflict of interest.

frontiers in Molecular Biosciences

ORIGINAL RESEARCH
published: 12 January 2021
doi: 10.3389/fmolb.2020.577246

Differential Progression of Motor Dysfunction Between Male and Female Fragile X Premutation Carriers Reveals Novel Aspects of Sex-Specific Neural Involvement

Danuta Z. Loesch[1], Flora Tassone[2,3], Anna Atkinson[1], Paige Stimpson[4], Nicholas Trost[5], Dean L. Pountney[6] and Elsdon Storey[7]*

[1] Department of Psychology and Counselling, School of Psychology and Public Health, La Trobe University, Bundoora, VIC, Australia, [2] Department of Biochemistry and Molecular Medicine, School of Medicine, University of California, Davis, Davis, CA, United States, [3] MIND Institute, University of California Davis Medical Center, Davis, CA, United States, [4] Wellness and Recovery Centre, Monash Medical Centre, Clayton, VIC, Australia, [5] Medical Imaging Department, St Vincent's Hospital, University of Melbourne, Parkville, VIC, Australia, [6] Neurodegeneration Research Group, School of Medical Science, Griffith University, Gold Coast Campus, Southport, NC, Australia, [7] Department of Medicine (Neuroscience), Monash University, Alfred Hospital Campus, Melbourne, VIC, Australia

OPEN ACCESS

Edited by:
Renate K. Hukema, Rotterdam University of Applied Sciences, Netherlands

Reviewed by:
Marsha Mailick, University of Wisconsin-Madison, United States
Tri Indah Winarni, Diponegoro University, Indonesia

***Correspondence:**
Danuta Z. Loesch
d.loesch@latrobe.edu.au

Specialty section:
This article was submitted to Cellular Biochemistry, a section of the journal Frontiers in Molecular Biosciences

Received: *29 June 2020*
Accepted: *09 December 2020*
Published: *12 January 2021*

Citation:
Loesch DZ, Tassone F, Atkinson A, Stimpson P, Trost N, Pountney DL and Storey E (2021) Differential Progression of Motor Dysfunction Between Male and Female Fragile X Premutation Carriers Reveals Novel Aspects of Sex-Specific Neural Involvement. Front. Mol. Biosci. 7:577246. doi: 10.3389/fmolb.2020.577246

Expansions of the CGG repeat in the non-coding segment of the FMR1 X-linked gene are associated with a variety of phenotypic changes. Large expansions (>200 repeats), which cause a severe neurodevelopmental disorder, the fragile x syndrome (FXS), are transmitted from the mothers carrying smaller, unstable expansions ranging from 55 to 200 repeats, termed the fragile X premutation. Female carriers of this premutation may themselves experience a wide range of clinical problems throughout their lifespan, the most severe being the late onset neurodegenerative condition called "Fragile X-Associated Tremor Ataxia Syndrome" (FXTAS), occurring between 8 and 16% of these carriers. Male premutation carriers, although they do not transmit expanded alleles to their daughters, have a much higher risk (40–50%) of developing FXTAS. Although this disorder is more prevalent and severe in male than female carriers, specific sex differences in clinical manifestations and progress of the FXTAS spectrum have been poorly documented. Here we compare the pattern and rate of progression (per year) in three motor scales including tremor/ataxia (ICARS), tremor (Clinical Tremor Rating scale, CRST), and parkinsonism (UPDRS), and in several cognitive and psychiatric tests scores, between 13 female and 9 male carriers initially having at least one of the motor scores ≥10. Moreover, we document the differences in each of the clinical and cognitive measures between the cross-sectional samples of 21 female and 24 male premutation carriers of comparable ages with FXTAS spectrum disorder (FSD), that is, who manifest one or more features of FXTAS. The results of progression assessment showed that it was more than twice the rate in male than in female carriers for the ICARS-both gait ataxia and kinetic tremor domains and twice as high in males on the CRST scale. In contrast, sex difference was negligible for the rate of progress in UPDRS, and all the cognitive measures.

The overall psychiatric pathology score (SCL-90), as well as Anxiety and Obsessive/Compulsive domain scores, showed a significant increase only in the female sample. The pattern of sex differences for progression in motor scores was consistent with the results of comparison between larger, cross-sectional samples of male and female carriers affected with the FSD. These results were in concert with sex-specific distribution of MRI T2 white matter hyperintensities: all males, but no females, showed the middle cerebellar peduncle white matter hyperintensities (MCP sign), although the distribution and severity of these hyperintensities in the other brain regions were not dissimilar between the two sexes. In conclusion, the magnitude and specific pattern of sex differences in manifestations and progression of clinically recorded changes in motor performance and MRI lesion distribution support, on clinical grounds, the possibility of certain sex-limited factor(s) which, beyond the predictable effect of the second, normal FMR1 alleles in female premutation carriers, may have neuroprotective effects, specifically concerning the cerebellar circuitry.

Keywords: FMR1 premutation, CGG repeat, female carriers, motor scores, progression rates, gender differences

INTRODUCTION

The fragile X premutation, consisting of a small expansion of a CGG repeat ranging from 55 to 200 in the non-coding section of the Fragile X Mental Retardation 1 (*FMR1*) X-linked gene, is associated with the variety of abnormal conditions (Hagerman and Hagerman, 2004). These premutation (PM) alleles are relatively common, with the population prevalence ranging from 1 in 130 to 1 in 250 females, and from 1 in 250 to 1 in 810 males (Hagerman, 2008; Fernandez-Carvajal et al., 2009). The premutation-size unstable CGG repeat may expand into a larger (>200) repeat size from the female carriers to their offspring, causing the severe neurodevelopmental disorder-Fragile X syndrome (FXS) (Loesch and Hagerman, 2011). The most severe premutation-associated condition affecting both male and female carriers of the PM allele is the late-onset progressive neurodegenerative condition termed Fragile X-Associated Tremor/Ataxia Syndrome (FXTAS). This affects 40–50% of males over the age of 55, but only 8–16.5% female carriers in the same age group (Cronister et al., 1991; Rodriguez-Revenga et al., 2009; Loesch and Hagerman, 2011; Hagerman and Hagerman, 2013). The much lower risk of FXTAS in female than in male carriers can be, at least partly, attributed to the mitigating effect of the normal *FMR1* allele on the second X chromosome (Jacquemont et al., 2004).

Traditionally, the standard diagnostic (core) neurological features of FXTAS comprise intention tremor, gait ataxia, and MRI T2 hyperintensities in the middle cerebellar peduncles (MCP sign) (Brunberg et al., 2002; Hagerman and Hagerman, 2016). Additional, non-core features contributing to the diagnosis, include parkinsonism, cognitive decline seen in the later stages of this condition (executive function and episodic memory deficits), neuropathy (Soontarapornchai et al., 2008; Apartis et al., 2012), and other MRI findings, such as global brain atrophy and white matter disease (Jacquemont et al., 2004; Adams et al., 2007; Rodriguez-Revenga et al., 2009; Loesch et al., 2011; Apartis et al., 2012; Wheeler et al., 2014; Hermanson et al., 2015), especially in the splenium of the corpus callosum, and the basis pontis, but also around lateral ventricles and in the deep white matter of brain hemispheres. Typical FXTAS neuropathological changes consist of ubiquitin-positive intranuclear inclusions abundant in neurones and astrocytes (Greco et al., 2002), extending to autonomic nervous and neuroendocrine systems and myocardial cells (Louis et al., 2006; Greco et al., 2007; Hunsaker et al., 2011).

One component of the nuclear inclusions is the *FMR1* mRNA (Tassone et al., 2004), which has previously been found to be elevated in the blood of corresponding to increased CGG repeat number (Tassone et al., 2000). These findings have led to a hypothesized pathogenetic mechanism that involves a toxic gain-of-function of the expanded CGG-repeat mRNA, which arises through the adventitious binding/sequestration by the CGG repeat of one or more proteins, contributing to dysfunction and/or death of the cell (Jin et al., 2003; Polussa et al., 2014). An alternative model for FXTAS pathogenesis has been proposed, in which "toxic" peptides are generated by initiating translation at non-AUG codons located upstream of the CGG-repeat element. It has been shown that this process, known as Repeat-associated non-AUG (RAN) translation, which is proportional to the extent of expanded *FMR1* mRNA elevation, leads to "chimeric" peptide synthesis including a poly-glycine peptide that is toxic to cells. This peptide is detectable in both the intranuclear inclusions of subjects with FXTAS and in the inclusions of the Dutch premutation CGG-repeat mouse model (Todd et al., 2013; Boivin et al., 2018; Glineburg et al., 2018). These and other postulated additional mechanisms, associated with CGG expansions within the premutation range, and leading to the severe neuropathological changes underlying FXTAS, have been reviewed in 2015 (Hagerman and Hagerman, 2015).

The most common premutation-associated condition in females, occurring in ∼20% of carriers of this allele, is premature

ovarian failure (FXPOI). This term indicates early menopause (defined as occurring before 40 years of age; Hagerman and Hagerman, 2013). However, the effect of the PM alleles may extend beyond those two definitive disorders, FXTAS and FXPOI, especially in the female carriers, where other physical changes, such as autoimmune thyroid disease and other immune-related disorders, as well as psychiatric problems including social phobia, hostility, obsessive/compulsive behavior, and anxiety/depression can be seen; in addition, common disorders such as fibromyalgia, hypertension and migraines have been reported to be more common in female carriers that in the general population (Coffey et al., 2008; Soontarapornchai et al., 2008; Bourgeois et al., 2009, 2011; Roberts et al., 2009; Leehey et al., 2011; Loesch and Hagerman, 2011; Seltzer et al., 2012; Winarni et al., 2012; Au et al., 2013; Wheeler et al., 2014). However, most of the data obtained by comparing samples of carriers with non-carriers have yielded inconsistent results, in part attributable to selection bias (Hunter et al., 2008; Allen et al., 2020), and thus provide limited insight into the effects of PM alleles on female phenotypes.

There have been fewer studies exploring subtle impairments that might be directly related to pre-symptomatic brain changes in either male or female PM carriers, in the absence of overt neurological symptoms or signs. In males, the studies based on MRI analyses revealed subtle changes in the integrity of white matter without, or prior to, the occurrence of FXTAS (Wang et al., 2012, 2013; Battistella et al., 2013), and abnormal trajectories of cerebellar and brain stem volume loss from early adulthood (Wang et al., 2017). In female carriers, the findings of deficits on a range of tasks of executive functioning requiring rapid temporal responses (Shelton et al., 2016), or of subtle impairment of postural stability (O'Keeffe et al., 2019), compared with control non-carriers, suggested that there may be a slow but measurable decline in executive functioning and/or degradation of motor control in apparently asymptomatic individuals. The presence of intranuclear inclusions typical of FXTAS has been reported in both FXTAS and non-FXTAS female carriers (Tassone et al., 2012), and reinforces evidence for an accumulation of subclinical pathological processes over a broad age range associated with PM carriage. However, the progression and outcome of these sub-symptomatic changes in older age, including the core FXTAS manifestations of tremor, gait ataxia and the MCP sign, have not yet been addressed. Moreover, despite the large volume of studies to identify possible physical and mental health problems in female PM carriers, there is still insufficient understanding of the effect of skewed X-inactivation on the phenotypic changes and their trajectory in these carriers. This difficulty can be attributed to the well documented brain-blood difference in *FMR1* mRNA expression, and potentially of the CGG expansion (Tassone et al., 2004; Pretto et al., 2014a,b; Zhao et al., 2019). This reflects the absence of a relationship between epigenetic measure (activation ratio, AR) and clinical phenotypes, which has been commonly observed in PM females in a number of the relevant studies, reviewed in: Jiraanont et al. (2017). These authors acknowledge the complexity of the mechanisms linking the PM allele to female clinical phenotypes, and they suggest the existence of other still unidentified factors impacting on these phenotypes.

In this study we aimed to test the hypothesis that subtle phenotypic changes, once initiated, continue to progress, but generally at a much slower and less uniform rate in female than in male PM carriers. Our second aim was to delineate the pattern of sex differences in clinical motor, cognitive, and psychiatric involvement in those carriers classified as Fragile X Spectrum Disorder (FSD), that is, manifesting at least one major or two minor features consistent with FXTAS. The relationships of severity and progression of phenotypic scores with the CGG repeat size were also assessed for each sex separately. These results, combined with evidence from relevant MRI FLAIR images showing sex differences in a topography of white matter lesions, suggest the existence of specific factors that may alleviate the severity and progress of particular neurological manifestations in female PM carriers.

METHODS

Subjects

There were two aspects of this study that require two different (but overlapping) sources of participants, all of whom were adults (>50 years of age) carrying the PM allele. The first source of both male and female participants was a major research project continuing from 2012 at La Trobe University and supported by the National Institutes of Health, USA. This project's male and female participants (later termed "*current*" sample as they are still being studied in a longitudinal fashion) were originally recruited through fragile X families' admissions to the Victorian Genetic Counselling Clinic of the Murdoch Institute, or referred from several neurology clinics associated with the University of Melbourne and Monash University; the minority (some residing in the other states) were self-referred by postings in the community through The Australian Fragile X Association. The second source of female participants (later termed the *"retrospective"* sample) was our earlier 2008–2010 project supported by a research grant from the National Health and Medical Research of Australia (NHMRC) to ES and DZL. These females had originally been ascertained either through their FXS children diagnosed at the Genetic Counselling clinics in Victoria and South Australia, or were more distant relatives of these probands identified through cascade testing. Except for one Asian (Chinese) male and one (Thai) female, all participants were white Caucasians. The two-*current* and *retrospective* -samples were used in both progression rate and male-female comparisons aspects of this study, using the inclusion criteria specified below in section "Cross-Sectional Male-Female Comparisons", and in a flowchart (**Figure 1**), where sample sizes at every step of sample selection are also provided.

Progression Rate

The sample of 13 females aged 37–66 years has been selected by retrospective inspection of the results of motor scale scores from the sample of 57 adult females carrying the premutation allele, who underwent comprehensive neurological testing between 2008 and 2010, conducted by two specialist neurologists (ES and DZL-authors of this manuscript). In this same study (supported by the NHMRC project grant), these females also underwent

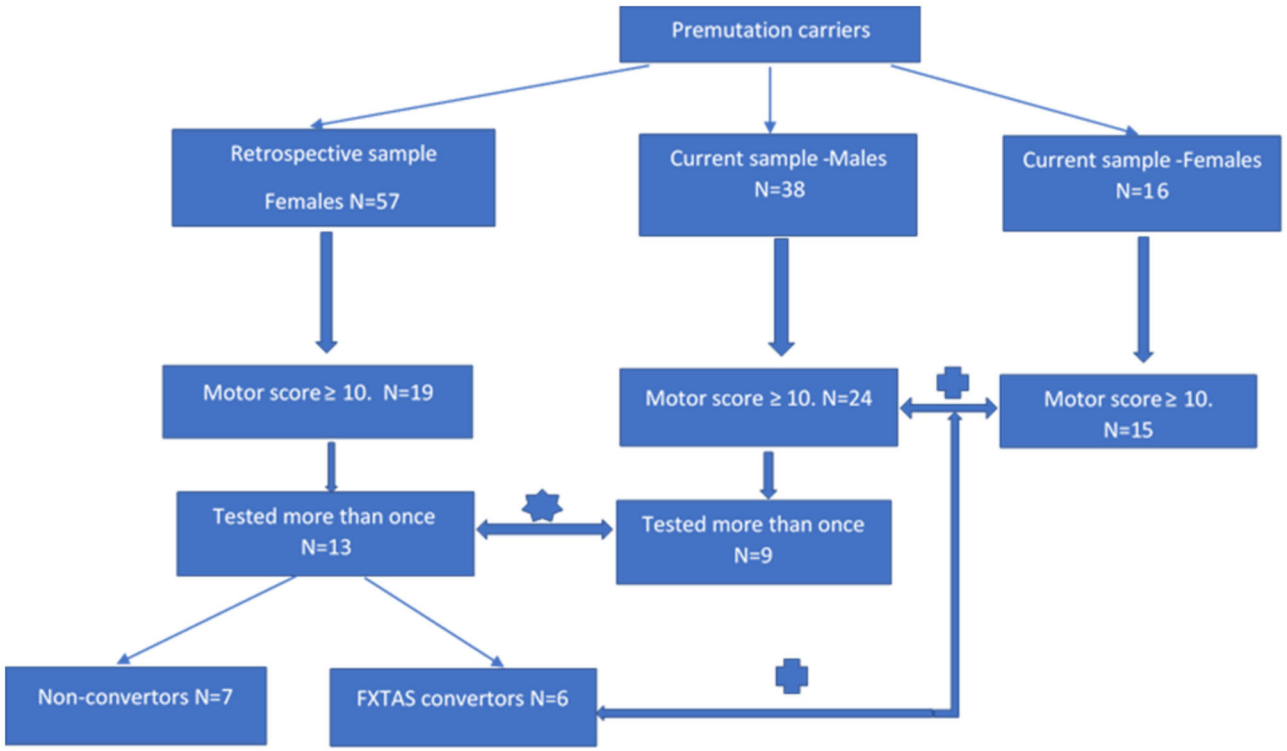

FIGURE 1 | Flowchart showing individual steps of recruitment of the participants of progression and cross-sectional aspects of analysis. rate of progression study; male-female comparison study.

a battery of neuropsychological and psychiatric pathology tests under the supervision of ES, using standard protocols. Partial retrospective analysis of SCL-90 data collected in this sample was described in our 2015 publication (Loesch et al., 2015). Our inspection of the raw data from this earlier ("*retrospective*") sample revealed that, amongst apparently asymptomatic carriers, 19 individuals scored ≥10 on the ICARS (2 SD above the mean) and/or ≥10 on the CRST (1 SD above average), and we decided to re-test these individuals after a 9–10 years interval. Thirteen of the 19 females from this subgroup (aged 36–66) were available for the follow-up testing within the present progression study (two declined, two have died of unknown cause, and two were not contactable). The follow-up 2019 assessment comprised, as far as possible, the same battery that had been used in the first run of testing in 2009. Based on the results of the follow-up assessment, six of these females met our criteria for the category of FSD (converters from the *"retrospective"* group in **Figure 1**), and they were also combined with 15 female carriers from the "*current*" group for the second part of this study aimed at comparing the phenotypic scores between male and female carriers classified as affected category.

The sample of nine male PM carriers aged 50–72 years, was used to compare with the data on the rate of progression obtained from the female sample. These individuals were selected from amongst 38 PM carriers who have been undergoing routine testing within our major NIH 2012–2021 longitudinal *("current")* study. In order to match the criteria of inclusion between the two sexes as close as possible, we only selected those (nine) males from this total sample who have been tested at least twice and, like female participants, had at least one (ICARS or CRST) motor score ≥10 on initial testing. The remaining differences between male and female samples, which could have potentially biased the results of comparison, were accounted for as described in "Statistical Analysis" and "Results" sections.

Cross-Sectional Male-Female Comparisons

The total sample of 24 male participants aged 48–80, and 21 female participants aged 37–78 were included in the second part of this analysis, which compared all phenotypic scores between the male and female carriers classified as having FSD, and displayed elevation of at least one motor score ≥10 (complying with the criterion applied to the 13 females from the *"retrospective"* sample). All male individuals were participants in the ongoing NIH-supported project ("*current*" sample). Six females were selected from the "*retrospective*" group (as described above), and 15 -from the "*current*" group. Within this group, the average follow-up period was 5.00 (2–7) years for males and 10.15

(9–11) years for females. The CGG repeat size averaged 85.1 in males and 80.2 in females; the difference in average repeat length of five repeats is expected to be negligible considering test error of ± 2 repeats and the PM range of 55–200.

Testing Protocols

Neurological and Cognitive Measures

Two neurologists specializing in movement disorders (ES and DZL), with relevant experience in these scales from previous studies, administered the three motor rating scales. These scales consisted of the Unified Parkinson's Disease Rating Scale Part III-Motor (UPDRS-III) (Fahn et al., 1987), the International Cooperative Ataxia Rating Scale (ICARS) (Trouillas et al., 1997), and the Clinical Rating Scale for Tremor (CRST) (Fahn et al., 1993), the first two of which have established inter-rater reliabilities (Richards et al., 1994; Storey et al., 2004; Stacy et al., 2007). The Vocabulary and Matrix Reasoning subtests of the Wechsler Adult Intelligence Scale (Third Edition; WAIS-III) were used to calculate a prorated Full-Scale IQ score (Wechsler, 1997), with Matrix Reasoning providing a measure of non-verbal reasoning. WAIS-III Digit Spans (forward and backward separately) were employed as measures of attention and working memory, respectively (Wechsler, 1997).

Psychiatric Pathology Test Scores

The SCL-90-R (Derogatis, 1994)—a 90 item self-administered questionnaire was chosen as an instrument that can efficiently provide information on a broad range of relevant symptom clusters and psychological concerns. It has good validity and reliability (test-retest: 0.80–0.90). Each of the 90- items is rated on a five-point Likert scale of distress, ranging from "not at all" (0) to "extremely." The subject is asked to respond to questions based on how much a given problem has "distressed or bothered" him or her during the past week, including the present day. It is typically completed in about 12–15 min. Here we report the data on a summary score providing a measure of overall psychological distress—the Global Severity Index (GSI), and on nine primary symptom dimensions: Somatization, Obsessive-compulsive, Interpersonal Sensitivity, Depression, Anxiety, Hostility, Phobic Anxiety, Paranoid Ideation, and Psychoticism.

Genetic Molecular Measures

CGG Sizing

Genomic DNA was isolated from peripheral blood lymphocytes using standard methods (Purygene Kit; Gentra, Inc., Minneapolis, MN). For Southern blot analysis, 10 mg of isolated DNA were digested with EcoRI and NruI. Hybridization was performed using the specific *FMR1* genomic dig-labeled StB12.3 probe as previously described (Tassone et al., 2008). Genomic DNA was also amplified by PCR (Filipovic-Sadic et al., 2010) DNA analysis was performed in the Laboratory of Dr. Tassone at the MIND Institute, UC Davis.

FMR1 mRNA Expression Level Measurements

This assay was also conducted at the MIND Institute. Total RNA was isolated from 3 mL of blood collected in Tempus tubes (Applied Biosystems, Foster City, California, USA). The measurement of *FMR1* mRNA expression levels was carried out by quantitative Real-Time qRT-PCR using custom-designed Taqman gene expression assays (Applied Biosystems) as previously described (Tassone et al., 2000).

Activation Ratio

Activation ratio (AR) indicates the proportion of cells that carry the normal allele on the active X chromosome, so that AR = 1.00 indicates a normal allele active in 100% of the cells. It was measured based on the intensity of the appropriate bands on Southern blots as described in Tassone et al. (1999).

Statistical Analysis

Data were analyzed using the Statistical Package for the Social Sciences version 26 (SPSS; IBM Corporation; Armonk, NY, USA). Summary statistics for sample characteristics, cognitive, psychiatric, and motor scores are presented as means and standard deviations (SD). Gender differences in parameters, and progression per year, were analyzed using independent sample *t*-tests. To account for inter-individual differences in baseline scores, progression change for each of the parameters was calculated as the percentage change between baseline (T1) and follow up (T2), with the following formula: Percentage Progression per year = [(T2 score – T1 score)/T1 score * 100]/ years between sessions. Paired sample *t*-tests were conducted to examine progression between Time 1 and Time 2 for each sex. There was no significant age difference between the sexes, and therefore age was not adjusted for in any analyses: for T1: $P = 0.054$, 95% CI −18.4, 0.19; for T2: $P = 0.375$, 95% CI −13.0, 5.13. (both *t*-test for unequal variances). Neither was there any significant age differences between the sexes for the cross-sectional component of the study (see **Table 2**), so correction for age was, again, unnecessary. The relationship between each of the phenotypic scores, and percentage progression per year (as outcome), and CGG repeat size and *FMR1* mRNA, was assessed using linear regression.

RESULTS

In this study, we considered the threshold for inclusion to be a score of ≥10 for the ICARS, which is 2 SD above average (4.07, SD 2.19) (Fitzpatrick et al., 2012). We are unaware of any relevant published normative values for the CRST, but used a sensitive cut off ≥10, being 1 SD above average in the control group of non-carrier males from our previous study (6.1, SD 4.85) (Loesch et al., 2005). Abnormality on UPDRS was signified by a score of ≥ 7, being two SD above average (1.9 ± 2.0) (Postuma et al., 2012). However, given that parkinsonism is not the major feature of FXTAS and is relatively common in the general population, the UPDRS score was used purely for analysis. Among 19 carriers who were selected based on these criteria, four presented with an elevation of ICARS score only, seven showed elevation of both ICARS and CRST scores, one presented with an elevation of UPDRS score in addition to elevation of their ICARS score, and seven with elevation of only CRST.

TABLE 1 | Summary statistics for all phenotypic scores at Time 1 and Time 2 in male (A) and female (B) samples included in the progression analysis, and the *p* values for significance of the T2-T1 differences for each sex separately.

							Paired differences			
Variable	***N***	**T1 Mean**	**SD**	***N***	**T2 Mean**	**SD**	**Mean diff. [95% CI]**	**SEM**	***P* value**	**Effect size (*g*)**
A										
Age	9	61.6	7.8	9	66.6	7.7	5 [3.7, 6.3]	0.56	N/A	N/A
UPDRS	9	9.8	10.0	9	17.3	13.7	7.6 [0.5, 15.6]	3.5	0.062	0.57
CRST	7	28.6	24.8	9	40.4	30.1	11.3 [5.3, 17.3]	2.4	**0.004**	0.37
ICARS total	9	17.9	11.8	9	28.7	13.5	10.8 [6.7, 14.9]	1.8	**0.000**	0.77
ICARS gait	9	4.6	3.0	9	8.3	4.1	3.8 [1.6, 5.9]	0.94	**0.004**	0.94
ICARS kinetic	9	11.3	7.3	9	17	7.2	5.7 [3.9, 7.4]	0.76	**0.000**	0.70
Vocab SS	9	9.2	3.3	9	10.2	3.2	1 [−0.3, 3.3]	0.58	0.122	0.28
MR SS	7	12.0	2.0	9	11.7	3.2	−1.4 [−3.9, 1]	0.99	0.202	0.52
DS Forwards	8	9.5	3.0	9	9.8	2.7	0 [−2.3, 2.3]	0.96	1.000	0.40
DS Backwards	8	6.8	2.1	9	5.9	1.4	−0.9 [−2.7, 1]	0.79	0.304	0.43
Pro-rated IQ	9	102.1	12.0	9	106.1	15.9	4 [−4.7, 12.7]	3.8	0.318	0.26
SCL-90 GSI	6	58.3	19.6	9	55.7	13.8	−2.7 [−19.6, 14.3]	6.6	0.703	0.13
B										
Age	13	52.5	13.0	13	62.6	12.7	10.1 [9.7, 10.6]	0.22	N/A	N/A
UPDRS	13	4.5	4.5	13	8.7	4.9	4.1 [1.1 ,7]	1.34	**0.011**	0.78
CRST	13	12.7	5.6	13	16.3	7.1	3.6 [−2, 9.3]	2.60	0.189	0.53
ICARS total	13	10.1	4.2	13	15.7	6.2	5.8 [3.4, 8.3]	1.13	**0.000**	0.99
ICARS gait	13	3.6	1.9	13	4.9	2.2	1.3 [0.48, 2.1]	0.38	**0.005**	0.59
ICARS kinetic	13	5.8	2.7	13	9.1	3.9	3.2 [1.45, 5]	0.82	**0.002**	0.91
Vocab SS	12	8.3	2.8	11	10	1.5	1.1 [0.07, 2.1]	0.46	**0.038***	0.54
MR SS	13	9.4	3.5	12	8.9	3.3	−1.1 [−3.4, 1.2]	1.1	0.327	0.32
DS Forwards	12	9.3	1.9	12	9.5	2.1	0.09 [−0.97, 1.2]	0.48	0.852	0.05
DS Backwards	12	5.8	1.9	12	5.3	1.0	−0.6 [−1.8, 0.54]	0.52	0.255	0.39
Pro-rated IQ	12	96.8	7.5	11	97.6	7.1	0.73 [−5.7, 7.1]	2.88	0.806	0.09
SCL-90 GSI	13	52.1	9.8	11	57	2.8	4.9 [1.7, 8.2]	1.46	**0.007**	0.48

All males came from the current sample, all females came from the retrospective sample.

Vocab SS, vocabulary scaled score from WAIS-3; MR SS, matrix reasoning from WAIS-3; DS forwards, digit span raw scores separately from WAIS-3. P values are for the two-sided t-test. Figures in bold were statistically significant at $p < 0.05$.

**T2-T1 difference is positive. p values are for the two-sided paired t-test; CI, confidence intervals.*

Progression Rate

Thirteen female carriers were available for the progression component of the study. Descriptive statistics of this group, including at baseline (T1) and at the follow-up assessment (T2) on the motor scales and cognitive and psychiatric pathology scores, are given in **Table 1B**. The significance of progression rate in these scores between times T1 and T2 (*p*-values from the *t*-test and confidence intervals, CI), are also given. In addition, the values of effect sizes are also reported. The corresponding parameters are also presented in **Table 1A**, for nine males selected from a larger- *current* -sample of PM carriers using the same motor scale criteria. Although the time length between the two assessments was typically shorter for males than for the female sample, it is evident that the T2-T1 differences are consistently greater in the males. This difference is much greater than should be expected in females assuming random X-inactivation. This especially applies to ICARS-gait and stance- domains, and CRST, where these differences are three times higher in males than in females, not reaching significance in the latter. This is in contrast with the ICARS (kinetic) domain, where the T2-T1 difference in males is less than twice that of the female value. The same applies to the UPDRS, where the progress is relatively small in either sex, without reaching statistical significance in the male sample. Although the progress assessed by T2-T1 differences in cognitive scores, including the Pro-Rated IQ and the Wechsler subtests, was negligible in either sex, it was evident (and highly significant) for the SCL90 GSI (summary) score.

The results of the follow-up assessments for the SCL90 GSI (summary) score, as well as SCL-90 profiles based on all 9 domains in female and male samples, respectively are illustrated

in **Figure 2**. The rate of increase per year is significant for the GSI score (**Figure 2** and **Table 1**), as well as for Anxiety and Obsessive-Compulsive domains, in females (**Figure 2A**) but not in males (**Figure 2B**). Sex differences for the rate of increase for these (**Figure 2C**), and for all other SCL 90 domains or GSI scores, were not statistically significant.

The magnitude and pattern of progression for all motor and cognitive measures are displayed in **Figures 3A,B,** respectively, including the *p*-values for male-female differences in progression rates. Since there was no significant male-female difference in age in either T1 (baseline) or T2, no age correction was applied. However, in order to allow comparison between males and females, the T2-T1 difference for each individual measure was divided by the number of years between the two assessments, to yield annual progression rates. Moreover, when assessing sex differences in the progression of motor and cognitive impairment, we also expressed measures of progression for each sex as a proportion of baseline (T1) value, to correct for possible baseline severity bias caused by differences between male and female samples. The *p* values from the *t*-tests representing significance of gender differences for the rate of progression, given in the Legend to **Figure 3,** are given both, with and without adjustment for baseline (T1) scores, respectively. The outcome was similar for these two models, with the exception of the CRST score, where male-female difference was significant only for the model without T1 adjustment, reflecting the possibility of T1-related bias. This, apart from a limited accuracy of the *t*-test in small samples, explains rare inconsistencies between the estimates of *p* values given in this figure and in **Table 2**, respectively.

The data presented in **Figure 3** show that sex differences for the rate of score increases are most prominent (and highly significant) for the ICARS scale. The rate for the total ICARS in males is more than twice that in females; for the ICARS Kinetic domain the rate in males is nearly three times of that in females; and for the ICARS Gait domain- nearly four time greater in males than in females. In contrast, the male-female difference in the rate of increase is much smaller (and insignificant) on the CRST, and negligible on the UPDRS. There is noticeable decline, in males only, on two Wechsler subtests- MR and DS Backward (compared with negligible change in the females), but this difference is not significant, reflecting the small samples available.

Cross-Sectional Male-Female Comparisons

Summary statistics, and the results of comparison of the motor and cognitive scale scores between cross-sectional samples of male and female carriers with FSD, including effect sizes, are shown in **Table 2**. There are no significant differences either in the age of the participants or in the size of the premutation allele, which falls within the range known to be associated with the highest risk for the occurrence of FSD in either sex. Comparison between the three motor scales revealed significant male-female differences for the ICARS (with a slightly greater size effect for Kinetic than Gait domains) and CRST scores, but not between UPDRS scores. There were no significant differences between male and female samples in cognitive test scores, with the trend toward slightly higher Prorated IQ score in the female than in the male sample (likely accounted for by somewhat higher Vocabulary test scores in the former); notably, the Prorated IQ remained within the population mean in both carrier samples. The differences either in the overall SCL-90 GSI (**Table 2**) or in any individual SCL-90 domains (data not shown) are insignificant.

Genotype-Phenotype Relationships

We assessed the regression of the motor and cognitive scores, listed in **Table 2,** on the number of CGG repeats, in male and female samples. The ICARS total score was the only motor scale showing a significant relationship with the CGG repeat size in both sexes: in the male sample, the correlation coefficient was 0.420, $p = 0.046$; in the female sample, it was 0.737, $p = 0.000$ (scatterplots shown in **Figure 4A**). These relationships remained significant for both gait ($p = 0.003$) and kinetic ($p = 0.002$) domains in females, but not in males. UPDRS scores were significantly correlated with CGG repeat size in both males (0.435, $p = 0.043$) and females (0.747, $p = 0.000$). Since there was no statistically significant difference in the UPDRS scores between males and females, we conducted this analysis in the combined sample, resulting in a highly significant regression of UPDRS score on CGG repeat size, with the correlation coefficient of 0.531, and $p = 0.000$ (**Figure 4B**). None of the other motor dysfunction or cognitive decline measures showed significant correlations with the CGG repeat size, with correlation coefficients not exceeding ∼0.250. The interpretation of the results of correlation analysis between the motor and cognitive scores and the *FMR1* mRNA levels is limited because of small sample sizes. Nevertheless, the only significant correlation encountered in the female sample was for the ICARS, with correlation coefficient of 0.649, $p = 0.016$, for the total score (**Figure 4C**), and 0.633, $p = 0.020$, for the Kinetic domain score. There was no relationship between any phenotypic scores and the (highly variable) activation ratio (AR), which averaged 0.57, SD = 0.33, and was assessed only in a sample of 13 females included in progression analysis.

Magnetic Resonance Imaging Data

The visual examination of T2-Flair MR images of the location of the *wmhs* available to us from 16 male and 12 female carriers included in this cross-sectional analysis revealed the MCP sign in all the males but none of the females, while the *wmhs* in the splenium occurred at the same rate in both males or females. Likewise, the *wmhs* changes within deep hemispheric and periventricular locations were not dissimilar between males and females, though less prominent in the latter. The discrepancy in these manifestations between males and females in the context of the clinical status is exemplified by two of the FXTAS patients included in **Table 2**, whose illustrative MRI FLAIR images are presented in **Figures 5A,B,** respectively.

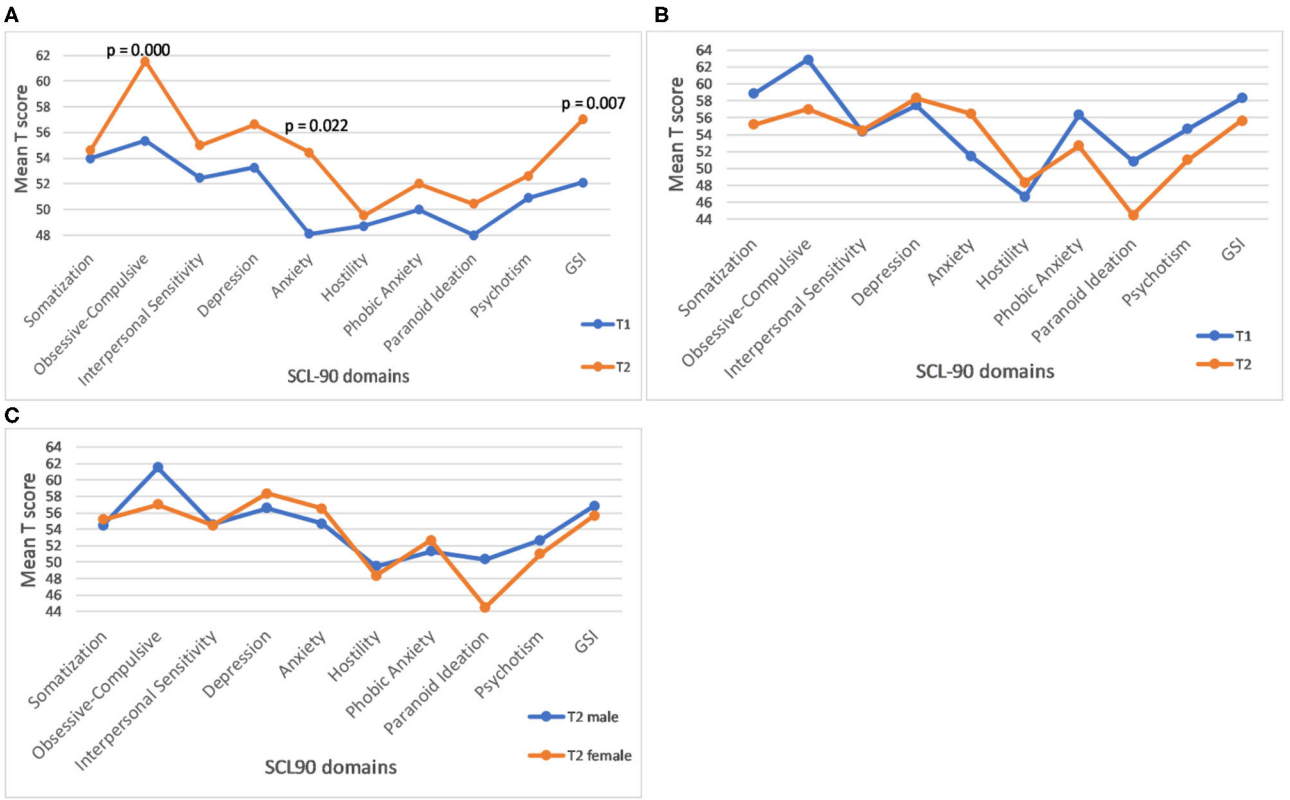

FIGURE 2 | Profile plot of mean baseline and follow-up of SCL-90 in female carriers. **(A)** The *p* values represent significance of the rate of progression. **(B)** Profile plot of mean baseline and follow-up of SCL-90 in male carriers. **(C)** Gender differences in the rate of progression of SCL-90 GSI score and individual domains in male and female carriers. **(C)** None of the male-female differences is statistically significant.

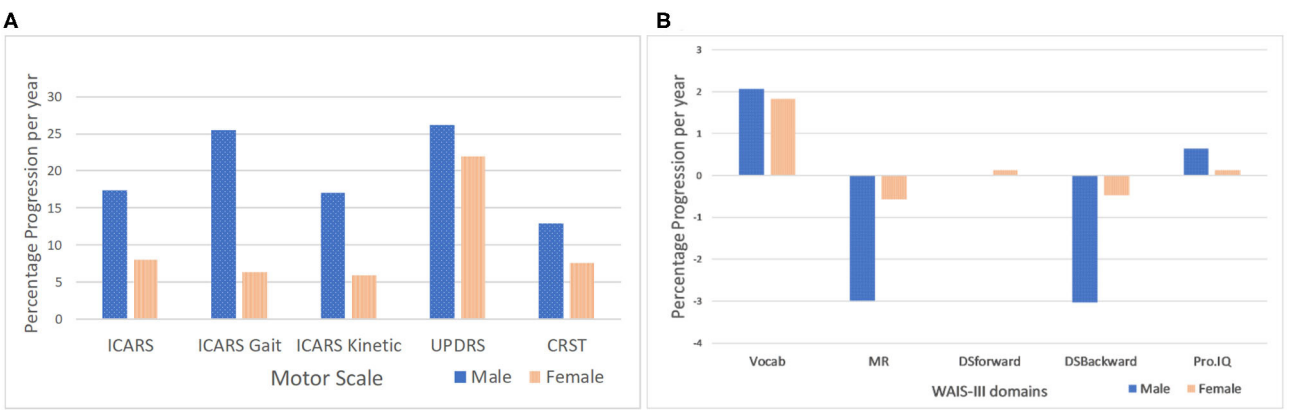

FIGURE 3 | Male-female differences in the rate of progression per year in motor scores adjusted for T1 scores. **(A)** *P* values are for statistically significant differences between males and females for rate of progression (**t*-test for unequal variances). *P* values for T2-T1 measures (male-female differences) adjusted for T1 scores: ICARS total ($p = 0.029$); ICARS Gait ($p = 0.013$); ICARS Kinetic ($p = 0.026$*); CSRT and UPDRS ($p > 0.05$)- *P* values for T2-T1 measures (male-female differences) not adjusted for T1 scores: ICARS total ($p = 0.003$*); ICARS Gait ($p = 0.02$*); ICARS Kinetic ($p = 0.008$*); and CSRT ($p = 0.000$*); UPDRS ($p > 0.05$). Male-female differences in the rate of progression per year in WAIS-III scores adjusted for T1 scores. **(B)** Males did not progress significantly in any Wechsler subscale scores or in Prorated IQ between T1 and T2. Females only showed (marginally) significant improvement in the Vocabulary subscale ($p = 0.038$).

DISCUSSION

This is the first study to explore male-female differences in manifestions and progression of both the major and minor (including sub-symptomatic) phenotypic changes relevant to FSD, using a quantitative approach. We assessed the rate of progression, over a period of 9–10 years, in all three motor scores (ICARS, UPDRS, and CRST), in several Wechsler cognitive test

TABLE 2 | Cross sectional study.

Variable	Males			Females			Gender differences			
	N	Mean	SD	N	Mean	SD	Mean diff. [95% CI]	SE	*P* value	Effect size (*d*)
Age	24	64.3	8.1	21	63.1	10.9	−1.19 [−6.9, 2.8]	2.84	0.667	0.12
CGG repeats	23	85.1	20.2	18	76.6[a]	18.6	−8.5 [−20.9, 3.9]	6.13	0.173	0.43[b]
RNA level	16	2.46	1.1	13	1.24	0.5	−1.22 [−1.9, −0.6]	0.3	**0.001**	1.33[b]
UPDRS	23	14.3	13.2	21	9.6	6.8	−4.77 [−11.1, 1.6]	3.12	**0.135***	0.46
CRST	24	30.4	25.3	21	17.5	7.5	−12.89 [−24.0, −1.8]	5.42	**0.025***	0.69
ICARS total	24	24.5	13.9	21	16.95	7.2	−7.6 [−14.1, −0.99]	3.25	**0.025***	0.68
ICARS gait	24	7.9	5.0	21	5.0	3.0	−2.87 [−5.3, −0.4]	1.21	**0.023***	0.70
ICARS kinetic	24	14.0	7.5	21	10.4	4.6	−3.62 [−7.3, 0.08]	1.82	0.055*	0.58
Vocab SS	23	10.1	2.9	19	11.1	2.3	0.97 [−0.7, 2.6]	0.83	0.245	0.36[b]
MR SS	23	10.6	4.0	20	10.3	3.5	−0.32 [−2.6, 2.0]	1.16	0.787	0.08
DS Forwards	23	9.7	2.4	20	9.6	2.0	−0.15 [−1.5, 1.2]	0.68	0.832	0.07
DS Backwards	23	5.8	1.6	20	5.6	0.9	−0.23 [−1.1, 0.6]	0.42	0.590	0.17
Pro-rated IQ	23	101.7	19.3	19	104.5	12.6	2.73 [−7.3, 12.8]	4.95	0.584*	0.16[b]
SCL90 GSI	15	56.2	13.0	18	56.8	7.9	0.56 [−7.1, 8.2]	3.65	0.881	0.05[b]

Summary statistics for genetic and phenotypic scores in FSD males and females, and between-group differences. All male data come from the current sample, female data comes from the current (15) and the retrospective (6) samples.

[a] *The values for two premutation/full mutation female mosaics excluded from this estimate.*

[b] *Hedges' g.*

**t-test for unequal variances. Figures in bold were statistically significant at $p < 0.05$.*

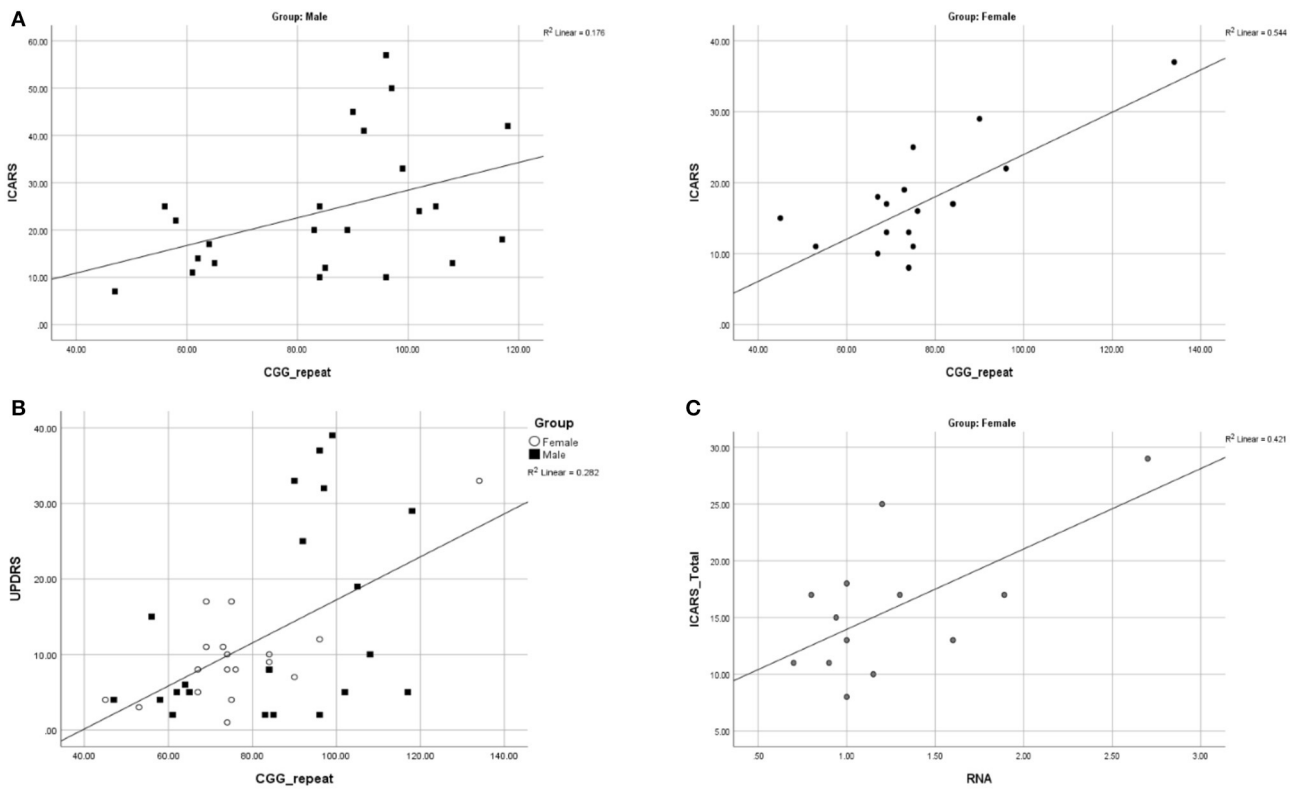

FIGURE 4 | (A) Scatterplots illustrating significant relationships between CGG repeat size and ICARS Total in males and females. **(B)** Scatterplot illustrating a significant relationship between CGG repeat size and UPDRS in males and females combined. **(C)** Scatterplots illustrating significant relationships between *FMR1* mRNA and ICARS total in females.

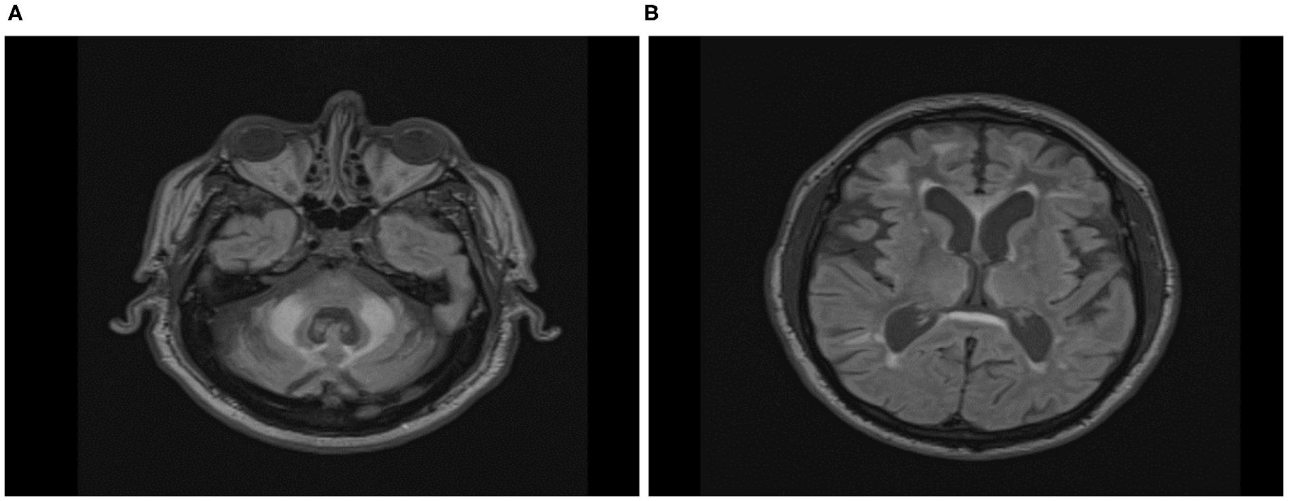

FIGURE 5 | Axial Fluid Attenuated Inversion Recovery (FLAIR) Magnetic Resonance Imaging in FXTAS male **(A)** and female **(B)** premutation carriers. **(A)** Seventy-five-year-old male participant, carrier of 58 CGG repeats, with overt features of FXTAS. ICARS = 22/100; UPDRS = 4/108; CRST:20/156; Prorated IQ = 103. *Wmhs* scattered in both hemispheres, mainly in the frontal region, thick periventricular and splenial bands, and bilateral MCP sign. **(B)** Sixty-seven-year-old female participant, carrier of 73 CGG repeats, with overt features of FXTAS and fibromyalgia. ICARS = 19/100; UPDRS = 11/108; CRST:14/156; Prorated IQ = 84. Few small *wmhs* scattered in both hemispheres, thick periventricular and splenial bands, but absence of *whms* in middle cerebellar peduncles.

subscores, and in aspects of psychiatric status, in female PM carriers who were sub-symptomatic at the first examination, but who nevertheless showed an elevation in either the ICARS or the CRST, at baseline. Of those sub-symptomatic females for whom longitudinal data was available (13), half (6) converted to a symptomatic form, with half of these (3) presenting a single feature occuring in FXTAS, and the other half-with diagnosable FXTAS. Analysis of the numerical data from the motor scales showed significant progression for both ICARS and UPDRS scores. Significant progression in all but one (UPDRS) motor scores was also encountered in male carriers selected using the same criteria as for the females. In order to account for the difference between male and female samples in the interval between the two assessments, we considered the rate of progress in relation to the length of this interval in each individual. There was no deterioration in any cognitive score in females, compared with obvious decline (though not significant in this small sample) in the MS, and DS Backward Wechsler subtests in males, both these tests being reliant on various aspects of executive function. However, females demonstrated significant deterioration in psychiatric pathology shown by an increase in the overall SCL90 scale score, and, more specifically, in the Obsessive-Compulsive and Anxiety domain scores, which reflect the prevalent changes reported in cross-sectional surveys (Bourgeois et al., 2009, 2011; Schneider et al., 2016). In contrast, male carriers did not show significant progression either in the SCL90 overall, or in any of its specific domains. Clearly, the significant progression in psychiatric symptoms- especially the anxiety observed in our female carriers-may have important clinical implications by drawing attention to the need for preventative measures, such as psychological intervention, as they age. The only other longitudinal study of anxiety in adult female carriers, although it applied different tools (DSM-IV-I) in a sample of younger females tested 3 years apart, showed concordant results for anxiety, and led the authors to emphasize the importance of attending to psychiatric health in fragile X families (Roberts et al., 2016).

Our data on progression of the premutation-associated changes from sub-symptomatic to clinical forms, especially in females, may have an important impact on future research, as well as on clinical approaches, because it introduces the concept of continuity. Combined with earlier evidence for the existence of subclinical neural or metabolic changes in both male and female carriers over a broad age range (Tassone et al., 2012; Wang et al., 2012, 2013, 2017; Battistella et al., 2013; Shelton et al., 2016; Loesch et al., 2017, 2018; Hocking et al., 2019; O'Keeffe et al., 2019), these data have shown that the focus of such research should be on trajectories rather than on the final outcome of the premutation-associated process. The most recent study, based on a wide range of metabolic and proteomic biomarkers, showed a decline of mitochondrial activities in pre-symptomatic female PM carriers, leading the authors to the conclusion that the development of neurodegeneration or other clinical symptoms in older carriers could be linked to a lifetime accumulation of cellular damage, aggravated by the aging process (Napoli et al., 2020).

The notion of "FXTAS spectrum" (Loesch and Hagerman, 2011; Hagerman and Hagerman, 2013; Roberts et al., 2016), here termed FSD, encompassing manifestations insufficient to formally diagnose FXTAS, and which could simply represent "FXTAS in the making," has been the first step in this direction. The utility of current strict diagnostic categories for FXTAS is even more questionable considering that one-third of the 19 apparently asymptomatic female carriers in our retrospective

sample had significant elevation in at least one motor score, with further marked elevation of these scores over time, evolving into FXTAS-like overt manifestations in over one-third of the "at risk" group over a period of 9–10 years. Notably, in another study, nearly half of premutation females were not aware of having tremor, as shown by CATSYS results (Juncos et al., 2011). Long-term follow-up studies of sub-symptomatic and monosymptomatic carriers would allow determination of the true proportion of subjects in whom elevated motor scores could be considered prodromal of syndromic FXTAS, or in whom the subclinical manifestations become symptomatic.

The major thrust of this study concerned differences between male and female carriers in the trajectory of measurable phenotypic changes. The two earlier studies applied motor scales in both male and female carriers, but these scores were compared, for each sex, between the carriers and control non-carriers. One of these studies, based on a small sample of affected carriers aged over 50, found significant differences in all three (ICARS, UPDRS, and CRST) scores between male, but not female, carriers compared with normal controls (Berry-Kravis et al., 2003). Similar results were obtained in another study using a much larger sample of premutation carriers recruited regardless of their neurological status and employing The FXTAS Rating Scale (a compilation of items from the three standard motor scales). While these scores were significantly worse in the entire group of male carriers compared with non-carrier controls, there was only a trend toward a difference in these scores between female carriers and controls (Leehey et al., 2008). These earlier results gave rise to the notion that there might be other sex-related protective effects on the female FSD phenotype besides the second X chromosome (Leehey et al., 2008). Although neither of these findings can be compared with our data, especially as direct comparisons between male and female carrier samples were not conducted, they provided early quantitative evidence for a large discrepancy in neural involvement between male and female carriers, either symptomatic or sub-symptomatic. In contrast, in the present study, we conducted direct statistical comparison of the rate of progression in the three motor scale scores, and cognitive and psychiatric scores. Although there was significant progression in the ICARS and UPDRS scale scores over the 9–10 years period in the sample of apparently asymptomatic females, the rate of progression on the ICARS, especially the ICARS Gait domain, was demonstrably less than in the male sample. This differs from the negligible sex difference in the rate of progression for parkinsonian rest tremor on the UPDRS, and for the CRST. The latter result is not unpredictable, considering that this scale measures both kinetic (as in the ICARS) and parkinsonian (as a component of UPDRS) types of tremor.

Our findings concerning sex differences in the rate of progression are supported by the parallel cross-sectional study results comparing male and female carriers affected by FSD, group-matched for age. While there are large, highly significant differences between males and females on the ICARS, especially the ICARS Gait domain scores, this difference is negligible for the UPDRS score. Notably, the UPDRS was the only measure showing significant correlation with CGG repeat size in both male and female samples. Although the interpretation of these UPDRS findings is currently unclear, they throw new light on the relevance of the trajectory of parkinsonian features, as part of the FXTAS spectrum, to the premutation allele. Our results showing (highly) significant relationships between ICARS scores and CGG repeat size in females are also novel and intriguing. One earlier study reported significant relationships between CGG repeat size and the FXTAS Rating Scale scores in a relatively large sample of males, comprising both affected and non-affected premutation carriers, with a similar trend in the corresponding female sample (Leehey et al., 2008). We reported borderline significance of correlation between ICARS total and CGG in the male sample, but no significance with the gait or kinetic domains, possibly on account of extensive variability of these scores and the small sample size; a similar argument may apply to the CRST score, especially as they included the C domain of CRST, which is based on (highly subjective) reporting.

The pathogenesis of FSD involves an unstable "gain of function" mutation. The lower penetrance with respect to neural involvement in female compared with male premutation carriers is sometimes attributed to the effect of the second normal (and active) *FMR1* allele. However, the rates of progression in motor scores for tremor/ataxia observed in this study, being up to three times higher in males than in females, are greater than anticipated from the effect of random inactivation, which, in our study, was 0.57. This does not indicate skewed inactivation, and indeed, the level of mRNA in our female sample is almost exactly half of that in the male sample, which is as expected from random inactivation. However, the male-female differences in phenotype we observed were greater than would be expected from this, raising the possibility that other phenotype-modifying factors are operative in female carriers, even allowing for a discrepancy between blood and brain AR status (Tassone et al., 2004; Pretto et al., 2014a,b; Zhao et al., 2019). Earlier evidence for this view was provided by the absence of correlation between cognitive and/or neuropsychiatric scores and relevant molecular measures (CGG repeat, *FMR1* mRNA, and AR) in premutation females (Gossett et al., 2016; Jiraanont et al., 2017; Allen et al., 2020). Consistent with these data, there was no relationship between AR status and any of the phenotypic scores in a sample of 13 females from the "retrospective" sample included in this study (data not shown).

The present results provide further, more specific information on sex differences in motor dysfunction. Although these data are based on small samples, moderate to high effect sizes (Cohen, 1988) that we calculated for the differences in all motor scores give us sufficient confidence in the statistical assessment, and thus allow us to advance possible causes underlying these sex-related effects. The largest differences in males vs. females in both the progression rate in the longitudinal sample, and in the magnitude of motor impairment in the cross-sectional FXTAS sample, seen in the ICARS scores, suggested differential sex involvement of cerebellar vermal and anterior hemispheric structures. This sex difference appeared to be particularly evident for balance and gait dysfunction, reflected by ICARS (especially ICARS gait) subscores. Cognitive decline, affecting aspects of

executive function, was evident only in male carriers. This is concordant with the motor findings, since these executive skills involve circuits that include the inferolateral cerebellar hemispheres (O'Halloran et al., 2012). Indeed, both the motor and the executive circuits' cortico-pontocerebellar afferents enter the cerebellum via the MCP. Given that the MCP sign, implying white matter degeneration, is very common in carrier males, but largely absent in carrier females, it is perhaps unsurprising that the sexes differ with respect to these two features of FSD. Unlike the tremor ataxia/scores, the parkinsonian score (UPDRS) showed similar values in both male and female FXTAS samples, as well as in the rate of progression. These results are consistent with the neuroradiological observation that, apart from the MCP sign, the pattern of white matter involvement is similar in the two sexes. For the illustration in **Figure 4**, we have shown, an example of a female who, despite an advanced form of FXTAS, did not show the MCP sign, whereas this sign was evident in a male with a milder form of FXTAS. Overall, we have encountered the MCP sign in all 24 FXTAS males, but in none of the females included in our cross-sectional analysis. Our clinical and neuroradiological data, showing disproportionately large gender differences in cerebellar manifestations, combined with small and/or insignificant gender differences in parkinsonian features, led to the conclusion that the cortico-cerebellar afferents (comprising the MCP) may be specifically protected in female carriers beyond the effect of the second normal (and active) allele. There is a possibility, though, that the activation ratio may be extremely biased in the cerebellar system, reflecting the wide variation of *FMR1* mRNA levels across different brain locations (Tassone et al., 2004). It is unlikely, however, since the elevation of this transcript in females is, in our study, half of that in males, and no evidence for any relationship of these levels with severity of cerebellar dysfunction. These results, though based on small samples, are interesting and indicative of the need for future studies based on larger samples and more direct approach to assess AR/mRNA relationships.

The most obvious limitation of this study is the smallness of our samples, implying that reliance on the *t*-test is potentially limited, mainly due to the elevated risk of Type II error. However, the moderate to large effect sizes regarding male-female differences in both progression rate and cross-sectional analysis of motor scores indicate that this risk is low for these comparisons. Although these effects are small to moderate for cognitive scores, the statistical results concerning motor scores provide critical evidence for this study's main hypothesis. Moreover, the effect of potentially large variances in some measures contributing to limited accuracy of the tests of significance has been reduced in this study by scoring, at each time point, being conducted by the same two neurologists. It may be noted that the confidence intervals (CI) determination were consistent with the results of the *t*-test for every measurement and in both progression and cross-sectional analysis. Another limitation relates to imperfect matching of male and female samples with respect to ascertainment, clinical categories, and interval between the repeat testing, though the latter was adjusted for in the analysis. However, it is practically impossible to achieve a perfect match between male and female carriers because, with rare exceptions, the trajectory and pattern of manifestations of the FSD, especially with respect to major features, is overtly different between the two genders. This difference may also have an impact on the mechanism of ascertainment, which may itself result in group differences. Moreover, our analysis makes the assumptions of linearity of both disease progression and assessment scales, whereas, in reality FXTAS may not necessarily progress evenly across time. We therefore corrected for these biases by adjusting the rate of progress data for the (T1) value representing baseline severity of involvement.

Using the term FSD to encompass a wide range of manifestations reminiscent of FXTAS, instead of classifying the affected individuals studied using the standard criteria for definitive, probable and possible categories (Hagerman and Hagerman, 2007), might be considered one of this study's limitations, especially since it restricts comparisons with other published results. However, our study has demonstrated that the transition from FSD to syndromic probable FXTAS is gradual; therefore, separating FXTAS from mild FSD may be artifactual. Furthermore, encompassing all the symptomatic carriers within the spectrum was determined by both small sample size and the lack of MRI results in some cases, and our reliance on the results of the motor rating scores. This approach is not only more relevant than the categorical one when employing these quantitative assessments, but it also reinforced the concept of a continuum of the effect of PM alleles with respect to neurological consequences.

However, despite these limitations, there is a consistent trend in the results from different aspects of the analysis., Our study reveal specific differences in the level and type of motor dysfunction between male and female carriers, and supports the hypothesis advanced in the study's aims: that subtle phenotypic changes, once initiated, continue to progress, but generally at a much slower and less uniform rate in female than in male PM carriers. These data, being suggestive of the existence of some sex-limited neuroprotective factors linked to the diminished cerebellar involvement in female carriers of the *FMR1* premutation allele, may indicate an avenue for future, more direct, neuropathological, and biochemical studies.

The search for possible protective factors in females should commence with investigation of cellular pathomechanisms already known to be involved in FXTAS. Mitochondrial dysfunction in FXTAS brains has been well documented (Giulivi et al., 2016; Alvarez-Mora et al., 2017), while the Rotterdam knock-in pre-CGG mouse model demonstrates raised cytoplasmic calcium levels (Robin et al., 2017). Neuronal calcium homeostasis is tightly controlled via regulation of mitochondrial and endoplasmic reticulum stores, and by several calcium-binding proteins including Calbindin D-28k, calretinin and parvalbumin (Bu et al., 2003). Calbindin levels are higher in the cerebellum and frontal cortex in female vs. male mice, and Calbindin D-28k null mice develop an ataxic phenotype (Barski et al., 2003). Calbindin levels are known to be controlled in part by estrogen receptor activation, although female estrogen receptor knock-out female XX mice still showed higher Calbindin levels than male XY receptor-knock-out mice (Abel

et al., 2011). Therefore, Calbindin's effect on calcium regulation and the latter's interaction with mitochondrial function would appear to be a logical avenue for further exploration.

DATA AVAILABILITY STATEMENT

The raw data supporting the conclusions of this article will be made available by the authors, without undue reservation.

ETHICS STATEMENT

The studies involving human participants were reviewed and approved by La Trobe University HREC Monash University HREC. The patients/participants provided their written informed consent to participate in this study.

AUTHOR CONTRIBUTIONS

DZL: conception, organization, and partial execution of research project, neurological assessments and motor scales scoring, review of statistical analysis, and co-writing (with ES) a manuscript. FT: conduct and interpretation of genetic molecular assays, review, and critique of manuscript. AA: contribution to cognitive testing and scoring, creating study database, execution of statistical analysis, contribution to review, and final editing of manuscript. NT: execution and description of the MR images in all study participants, review, and critique of manuscript. PS: conduct and interpretation of neuropsychological and psychiatric pathology assessments, organization, and partial execution of research project. DP: contribution to overall planning of this avenue of investigation and to interpretation of results in context with own data, and significant input to writing the Discussion. ES: conception and partial execution of research project, neurological assessments and motor scales scoring, neuropsychological assessments or supervision of assessments, and co-writing (with DZL) of manuscript. All authors: contributed to the article and approved the submitted version.

FUNDING

This study was supported by the National Institutes of Child Health and Human Development Grant, US, No HD 36071, to DZL and FT, and by National Health and Medical Research Australia project Grant No CF06/0269 to ES, DZL, and FT.

ACKNOWLEDGMENTS

We thank all participants and their families for their long-term commitment to this study.

REFERENCES

Abel, J. M., Witt, D. M., and Rissman, E. F. (2011). Sex differences in the cerebellum and frontal cortex: roles of estrogen receptor alpha and sex chromosome genes. *Neuroendocrinology* 93, 230–240. doi: 10.1159/000324402

Adams, J. S., Adams, P. E., Nguyen, D., Brunberg, J. A., Tassone, F., Zhang, W., et al. (2007). Volumetric brain changes in females with fragile X-associated tremor/ataxia syndrome (FXTAS). *Neurology* 69, 851–859. doi: 10.1212/01.wnl.0000269781.10417.7b

Allen, E. G., Charen, K., Hipp, H. S., Shubeck, L., Amin, A., He, W., et al. (2020). Clustering of comorbid conditions among women who carry an FMR1 premutation. *Genet. Med.* 22, 758–766. doi: 10.1038/s41436-019-0733-5

Alvarez-Mora, M. I., Rodriguez-Revenga, L., Madrigal, I., Guitart-Mampel, M., Garrabou, G., and Milà, M. (2017). Impaired mitochondrial function and dynamics in the pathogenesis of FXTAS. *Mol. Neurobiol.* 54, 6896–6902. doi: 10.1007/s12035-016-0194-7

Apartis, E., Blancher, A., Meissner, W. G., Guyant-Marechal, L., Maltete, D., De Broucker, T., et al. (2012). FXTAS: new insights and the need for revised diagnostic criteria. *Neurology* 79, 1898–1907. doi: 10.1212/WNL.0b013e318271f7ff

Au, J., Akins, R. S., Berkowitz-Sutherland, L., Tang, H. T., Chen, Y., Boyd, A., et al. (2013). Prevalence and risk of migraine headaches in adult fragile X premutation carriers. *Clin. Genet.* 84, 546–551. doi: 10.1111/cge.12109

Barski, J. J., Hartmann, J., Rose, C. R., Hoebeek, F., Mörl, K., Noll-Hussong, M., et al. (2003). Calbindin in cerebellar Purkinje cells is a critical determinant of the precision of motor coordination. *J. Neurosci.* 23, 3469–3477. doi: 10.1523/JNEUROSCI.23-08-03469.2003

Battistella, G., Niederhauser, J., Fornari, E., Hippolyte, L., Perrin, A. G., Lesca, G., et al. (2013). Brain structure in asymptomatic FMR1 premutation carriers at risk for fragile X-associated tremor/ataxia syndrome. *Neurobiol. Aging* 34, 1700–1707. doi: 10.1016/j.neurobiolaging.2012.12.001

Berry-Kravis, E., Lewin, F., Wuu, J., Leehey, M., Hagerman, R., Hagerman, P., et al. (2003). Tremor and ataxia in fragile X premutation carriers: blinded videotape study. *Ann. Neurol.* 53, 616–623. doi: 10.1002/ana.10522

Boivin, M., Willemsen, R., Hukema, R. K., and Sellier, C. (2018). Potential pathogenic mechanisms underlying Fragile X Tremor Ataxia Syndrome: RAN translation and/or RNA gain-of-function? *Eur. J. Med. Genet.* 61, 674–679. doi: 10.1016/j.ejmg.2017.11.001

Bourgeois, J., Coffey, S., Rivera, S. M., Hessl, D., Gane, L. W., Tassone, F., et al. (2009). Fragile X premutation disorders–expanding the psychiatric perspective. *J. Clin. Psychiatry* 70:852. doi: 10.4088/JCP.08r04476

Bourgeois, J. A., Seritan, A. L., Casillas, E. M., Hessl, D., Schneider, A., Yang, Y., et al. (2011). Lifetime prevalence of mood and anxiety disorders in fragile X premutation carriers. *J. Clin. Psychiatr.* 72:175. doi: 10.4088/JCP.09m05407blu

Brunberg, J. A., Jacquemont, S., Hagerman, R. J., Berry-Kravis, E. M., Grigsby, J., Leehey, M. A., et al. (2002). Fragile X premutation carriers: characteristic MR imaging findings of adult male patients with progressive cerebellar and cognitive dysfunction. *AJNR Am. J. Neuroradiol.* 23, 1757–1766.

Bu, J., Sathyendra, V., Nagykery, N., and Geula, C. (2003). Age-related changes in calbindin-D28k, calretinin, and parvalbumin-immunoreactive neurons in the human cerebral cortex. *Exp. Neurol.* 182, 220–231. doi: 10.1016/S0014-4886(03)00094-3

Coffey, S. M., Cook, K., Tartaglia, N., Tassone, F., Nguyen, D. V., Pan, R., et al. (2008). Expanded clinical phenotype of women with the FMR1 premutation. *Am. J. Med. Genet. A* 146A, 1009–1016. doi: 10.1002/ajmg.a.32060

Cohen, J. (1988). *Statistical Power Analysis for the Behavioral Sciences, 2nd Edn.* Hillsdale, NJ: Lawrence Erlbaum Associates Publishers.

Cronister, A., Schreiner, R., Wittenberger, M., Amiri, K., Harris, K., and Hagerman, R. J. (1991). Heterozygous fragile X female: historical, physical, cognitive, and cytogenetic features. *Am. J. Med. Genet.* 38, 269–274. doi: 10.1002/ajmg.1320380221

Derogatis, L. (1994). *SCL-90-R: Symptom Checklist-90-R. Administration, Scoring and Procedures Manual*. Minneapolis, MN: NCS Pearson.

Fahn, S., Elton, R., and and, U. P. D. R.S., Development Committee (1987). "The Unified Parkinson's Disease Rating Scale," in *Recent Developments in Parkinson's Disease, 2 Edn,* eds S. Fahn, C. D. Marsden, D. B. Calne, and M. Goldstein (Florham Park, NJ: Macmillan Healthcare Information), 153–163, 293–304.

Fahn, S., Tolosa, E., and Marin, C. (1993). "Clinical Rating Scale for Tremor," in *Parkinson's Disease and Movement Disorders, 2nd Edn,* eds J. Jankovic, and E. Tolosa (Baltimore: Williams and Wilkins), 271–280.

Fernandez-Carvajal, I., Walichiewicz, P., Xiaosen, X., Pan, R., Hagerman, P. J., and Tassone, F. (2009). Screening for expanded alleles of the FMR1 gene in blood spots from newborn males in a Spanish population. *J. Mol. Diagn.* 11, 324–329. doi: 10.2353/jmoldx.2009.080173

Filipovic-Sadic, S., Sah, S., Chen, L., Krosting, J., Sekinger, E., Zhang, W., et al. (2010). A novel FMR1 PCR method for the routine detection of low abundance expanded alleles and full mutations in fragile X syndrome. *Clin. Chem.* 56, 399–408. doi: 10.1373/clinchem.2009.136101

Fitzpatrick, L. E., Jackson, M., and Crowe, S. F. (2012). Characterization of cerebellar ataxia in chronic alcoholics using the International Cooperative Ataxia Rating Scale (ICARS). *Alcohol. Clin. Exp. Res.* 36, 1942–1951. doi: 10.1111/j.1530-0277.2012.01821.x

Giulivi, C., Napoli, E., Tassone, F., Halmai, J., and Hagerman, R. (2016). Plasma metabolic profile delineates roles for neurodegeneration, pro-inflammatory damage and mitochondrial dysfunction in the FMR1 premutation. *Biochem. J.* 473, 3871–3888. doi: 10.1042/BCJ20160585

Glineburg, M. R., Todd, P. K., Charlet-Berguerand, N., and Sellier, C. (2018). Repeat-associated non-AUG (RAN) translation and other molecular mechanisms in fragile X tremor ataxia syndrome. *Brain Res.* 151693, 43–54. doi: 10.1016/j.brainres.2018.02.006

Gossett, A., Sansone, S., Schneider, A., Johnston, C., Hagerman, R., Tassone, F., et al. (2016). Psychiatric disorders among women with the fragile X premutation without children affected by fragile X syndrome. *Am. J. Med. Genet. B* 171, 1139–1147. doi: 10.1002/ajmg.b.32496

Greco, C., Hagerman, R. J., Tassone, F., Chudley, A., Del Bigio, M., Jacquemont, S., et al. (2002). Neuronal intranuclear inclusions in a new cerebellar tremor/ataxia syndrome among fragile X carriers. *Brain* 125, 1760–1771.

Greco, C. M., Soontrapornchai, K., Wirojanan, J., Gould, J. E., Hagerman, P. J., and Hagerman, R. J. (2007). Testicular and pituitary inclusion formation in fragile X associated tremor/ataxia syndrome. *J. Urol.* 177, 1434–1437. doi: 10.1093/brain/awf184

Hagerman, P. J. (2008). The fragile X prevalence paradox. *J. Med. Genet.* 45, 498–499. doi: 10.1136/jmg.2008.059055

Hagerman, P. J., and Hagerman, R. J. (2004). The fragile-X premutation: a maturing perspective. *Am. J. Hum. Genet.* 74, 805–816. doi: 10.1086/386296

Hagerman, P. J., and Hagerman, R. J. (2007). Fragile X-associated tremor/ataxia syndrome—an older face of the fragile X gene. *Nat. Clin. Pract.* 3, 107–112. doi: 10.1038/ncpneuro0373

Hagerman, P. J., and Hagerman, R. J. (2015). Fragile X-associated tremor/ataxia syndrome. *Ann. N.Y. Acad. Sci.* 1338:58. doi: 10.1111/nyas.12693

Hagerman, R., and Hagerman, P. (2013). Advances in clinical and molecular understanding of the FMR1 premutation and fragile X-associated tremor/ataxia syndrome. *Lancet Neurol.* 12, 786–798. doi: 10.1016/S1474-4422(13)70125-X

Hagerman, R. J., and Hagerman, P. (2016). Fragile X-associated tremor/ataxia syndrome—features, mechanisms and management. *Nat. Rev. Neurol.* 12:403. doi: 10.1038/nrneurol.2016.82

Hermanson, M., Jhaveri, M., Stebbins, G., Dunn, E., Merkitch, D., Berry-Kravis, E., et al. (2015). The splenium of the corpus callosum sign in fragile X associated tremor ataxia syndrome (FXTAS) (P2.125). *Neurology* 84, P2.125.

Hocking, D. R., Loesch, D. Z., Trost, N., Bui, M. Q., Hammersley, E., Francis, D., et al. (2019). Total and regional white matter lesions are correlated with motor and cognitive impairments in carriers of the FMR1 premutation. *Front. Neurol.* 10:832. doi: 10.3389/fneur.2019.00832

Hunsaker, M. R., Greco, C. M., Spath, M. A., Smits, A. P., Navarro, C. S., Tassone, F., et al. (2011). Widespread non-central nervous system organ pathology in fragile X premutation carriers with fragile X-associated tremor/ataxia syndrome and CGG knock-in mice. *Acta Neuropathol.* 122, 467–479. doi: 10.1007/s00401-011-0860-9

Hunter, J. E., Allen, E. G., Abramowitz, A., Rusin, M., Leslie, M., Novak, G., et al. (2008). No evidence for a difference in neuropsychological profile among carriers and noncarriers of the FMR1 premutation in adults under the age of 50. *Am. J. Hum. Genet.* 83, 692–702. doi: 10.1016/j.ajhg.2008.10.021

Jacquemont, S., Hagerman, R. J., Leehey, M. A., Hall, D. A., Levine, R. A., Brunberg, J. A., et al. (2004). Penetrance of the fragile X–associated tremor/ataxia syndrome in a premutation carrier population. *JAMA* 291, 460–469. doi: 10.1001/jama.291.4.460

Jin, P., Zarnescu, D. C., Zhang, F., Pearson, C. E., Lucchesi, J. C., Moses, K., et al. (2003). RNA-mediated neurodegeneration caused by the fragile X premutation rCGG repeats in Drosophila. *Neuron* 39, 739–747. doi: 10.1016/S0896-6273(03)00533-6

Jiraanont, P., Sweha, S. R., AlOlaby, R. R., Silva, M., Tang, H.-T., Durbin-Johnson, B., et al. (2017). Clinical and molecular correlates in fragile X premutation females. *eNeurologicalSci* 7, 49–56. doi: 10.1016/j.ensci.2017.04.003

Juncos, J. L., Lazarus, J. T., Graves-Allen, E., Shubeck, L., Rusin, M., Novak, G., et al. (2011). New clinical findings in the fragile X-associated tremor ataxia syndrome (FXTAS). *Neurogenetics* 12, 123–135. doi: 10.1007/s10048-010-0270-5

Leehey, M. A., Berry-Kravis, E., Goetz, C. G., Zhang, L., Hall, D. A., Li, L., et al. (2008). FMR1 CGG repeat length predicts motor dysfunction in premutation carriers. *Neurology* 70, 1397–1402. doi: 10.1212/01.wnl.0000281692.98200.f5

Leehey, M. A., Legg, W., Tassone, F., and Hagerman, R. (2011). Fibromyalgia in fragile X mental retardation 1 gene premutation carriers. *Rheumatology* 50, 2233–2236. doi: 10.1093/rheumatology/ker273

Loesch, D., Churchyard, A., Brotchie, P., Marot, M., and Tassone, F. (2005). Evidence for, and a spectrum of, neurological involvement in carriers of the fragile X pre-mutation: FXTAS and beyond. *Clin. Genet.* 67, 412–417. doi: 10.1111/j.1399-0004.2005.00425.x

Loesch, D., and Hagerman, R. (2011). "Unstable mutations in the FMR1 gene and the phenotypes," in *Tandem Repeat Polymorphisms: Genetic Plasticity, Neural Diversity and Disease,* ed A. J. Hannan (New York, NY: Springer), 78–114. doi: 10.1007/978-1-4614-5434-2_6

Loesch, D. Z., Annesley, S. J., Trost, N., Bui, M. Q., Lay, S. T., Storey, E., et al. (2017). Novel blood biomarkers are associated with white matter lesions in Fragile X- Associated Tremor/Ataxia Syndrome. *Neurodegener. Dis.* 17, 22–30. doi: 10.1159/000446803

Loesch, D. Z., Bui, M. Q., Hammersley, E., Schneider, A., Storey, E., Stimpson, P., et al. (2015). Psychological status in female carriers of premutation FMR1 allele showing a complex relationship with the size of CGG expansion. *Clin. Genet.* 87, 173–178. doi: 10.1111/cge.12347

Loesch, D. Z., Kotschet, K., Trost, N., Greco, C. M., Kinsella, G., Slater, H. R., et al. (2011). White matter changes in basis pontis in small expansion FMR1 allele carriers with parkinsonism. *Am. J. Med. Genet. B* 156B, 502–506. doi: 10.1002/ajmg.b.31189

Loesch, D. Z., Trost, N., Bui, M. Q., Hammersley, E., Lay, S. T., Annesley, S. J., et al. (2018). The spectrum of neurological and white matter changes and premutation status categories of older male carriers of the FMR1 alleles are linked to genetic (CGG and FMR1 mRNA) and cellular stress (AMPK) markers. *Front. Genet.* 9, 531–531. doi: 10.3389/fgene.2018.00531

Louis, E., Moskowitz, C., Friez, M., Amaya, M., and Vonsattel, J. P. G. (2006). Parkinsonism, dysautonomia, and intranuclear inclusions in a fragile X carrier: a clinical–pathological study. *Mov. Disord.* 21, 420–425. doi: 10.1002/mds.20753

Napoli, E., McLennan, Y. A., Schneider, A., Tassone, F., Randi, J., Hagerman, R. J., and and Giulivi, C. (2020). Characterization of the metabolic, clinical and neuropsychological phenotype of female carriers of the premutation in the X-linked FMR1 gene. *Front. Mol. Biosci.*| doi: 10.3389/fmolb.2020.578640

O'Halloran, C. J., Kinsella, G. J., and Storey, E. (2012). The cerebellum and neuropsychological functioning: a critical review. *J. Clin. Exp. Neuropsychol.* 34, 35–56. doi: 10.1186/s12984-019-0560-6

O'Keeffe, C., Taboada, L. P., Feerick, N., Gallagher, L., Lynch, T., and Reilly, R. B. (2019). Complexity based measures of postural stability provide novel evidence of functional decline in fragile X premutation carriers. *J. Neuroeng. Rehabil.* 16, 87. doi: 10.1080/13803395.2011.614599

Polussa, J., Schneider, A., and Hagerman, R. (2014). Molecular advances leading to treatment implications for Fragile X premutation carriers. *Brain Disord. Ther.* 3:1000119.

Postuma, R., Lang, A., Gagnon, J., Pelletier, A., and Montplaisir, J. (2012). How does parkinsonism start? Prodromal parkinsonism motor changes in idiopathic REM sleep behaviour disorder. *Brain* 135, 1860–1870. doi: 10.1093/brain/aws093

Pretto, D., Yrigollen, C. M., Tang, H.-T., Williamson, J., Espinal, G., Iwahashi, C. K., et al. (2014a). Clinical and molecular implications of mosaicism in FMR1 full mutations. *Front Genet* 5, 318–318. doi: 10.3389/fgene.2014.00318

Pretto, D. I., Mendoza-Morales, G., Lo, J., Cao, R., Hadd, A., Latham, G. J., et al. (2014b). CGG allele size somatic mosaicism and methylation in FMR1 premutation alleles. *J. Med. Genet.* 51, 309–318. doi: 10.1136/jmedgenet-2013-102021

Richards, M., Marder, K., Cote, L., and Mayeux, R. (1994). Interrater reliability of the Unified Parkinson's Disease Rating Scale motor examination. *Mov. Disord.* 9, 89–91. doi: 10.1002/mds.870090114

Roberts, J. E., Bailey D. B. Jr., Mankowski, J., Ford, A., Sideris, J., Weisenfeld, L. A., et al. (2009). Mood and anxiety disorders in females with the FMR1 premutation. *Am. J. Med. Genet. B Neuropsychiatr. Genet.* 150, 130–139. doi: 10.1002/ajmg.b.30786

Roberts, J. E., Tonnsen, B. L., McCary, L. M., Ford, A. L., Golden, R. N., and Bailey, D. B. Jr. (2016). Trajectory and predictors of depression and anxiety disorders in mothers with the FMR1 premutation. *Biol. Psychiatr.* 79, 850–857. doi: 10.1016/j.biopsych.2015.07.015

Robin, G., López, J. R., Espinal, G. M., Hulsizer, S., Hagerman, P. J., and Pessah, I. N. (2017). Calcium dysregulation and Cdk5-ATM pathway involved in a mouse model of fragile X-associated tremor/ataxia syndrome. *Hum. Mol. Genet.* 26, 2649–2666. doi: 10.1093/hmg/ddx148

Rodriguez-Revenga, L., Madrigal, I., Pagonabarraga, J., Xuncl,à, M., Badenas, C., Kulisevsky, J., et al. (2009). Penetrance of FMR1 premutation associated pathologies in fragile X syndrome families. *Eur. J. Hum. Genet.* 17, 1359–1362. doi: 10.1038/ejhg.2009.51

Schneider, A., Johnston, C., Tassone, F., Sansone, S., Hagerman, R. J., Ferrer, E., et al. (2016). Broad autism spectrum and obsessive-compulsive symptoms in adults with the fragile X premutation. *Clin. Neuropsychol.* 30, 929–943. doi: 10.1080/13854046.2016.1189536

Seltzer, M. M., Baker, M. W., Hong, J., Maenner, M., Greenberg, J., and Mandel, D. (2012). Prevalence of CGG expansions of the FMR1 gene in a US population-based sample. *Am. J. Med. Genet. B Neuropsychiatr. Genet.* 159, 589–597. doi: 10.1002/ajmg.b.32065

Shelton, A. L., Cornish, K. M., Kraan, C. M., Lozano, R., Bui, M., and Fielding, J. (2016). Executive dysfunction in female FMR1 premutation carriers. *Cerebellum* 15, 565–569. doi: 10.1007/s12311-016-0782-0

Soontarapornchai, K., Maselli, R., Fenton-Farrell, G., Tassone, F., Hagerman, P. J., Hessl, D., et al. (2008). Abnormal nerve conduction features in fragile X premutation carriers. *Arch. Neurol.* 65, 495–498. doi: 10.1001/archneur.65.4.495

Stacy, M. A., Elble, R. J., Ondo, W. G., Wu, S. C., Hulihan, J., and Group, T. S. (2007). Assessment of interrater and intrarater reliability of the Fahn–Tolosa–Marin Tremor Rating Scale in essential tremor. *Mov. Disord.* 22, 833–838. doi: 10.1002/mds.21412

Storey, E., Tuck, K., Hester, R., Hughes, A., and Churchyard, A. (2004). Inter-rater reliability of the International Cooperative Ataxia Rating scale (ICARS). *Mov. Disord.* 19, 190–192. doi: 10.1002/mds.10657

Tassone, F., Greco, C. M., Hunsaker, M. R., Seritan, A. L., Berman, R. F., Gane, L. W., et al. (2012). Neuropathological, clinical and molecular pathology in female fragile X premutation carriers with and without FXTAS. *Genes Brain Behav.* 11, 577–585. doi: 10.1111/j.1601-183X.2012.00779.x

Tassone, F., Hagerman, R. J., Garcia-Arocena, D., Khandjian, E., Greco, C., and Hagerman, P. J. (2004). Intranuclear inclusions in neural cells with premutation alleles in fragile X associated tremor/ataxia syndrome. *J. Med. Genet.* 41, e43–e43. doi: 10.1136/jmg.2003.012518

Tassone, F., Hagerman, R. J., Ikl,é, D. N., Dyer, P. N., Lampe, M., Willemsen, R., et al. (1999). FMRP expression as a potential prognostic indicator in fragile X syndrome. *Am. J. Med. Genet.* 84, 250–261.doi: 10.1002/(SICI)1096-8628(19990528)84:3<250::AID-AJMG17>3.0.CO;2-4

Tassone, F., Hagerman, R. J., Taylor, A. K., Gane, L. W., Godfrey, T. E., and Hagerman, P. J. (2000). Elevated levels of FMR1 mRNA in carrier males: a new mechanism of involvement in the fragile-X syndrome. *Am. J. Hum. Genet.* 66, 6–15. doi: 10.1086/302720

Tassone, F., Pan, R., Amiri, K., Taylor, A. K., and Hagerman, P. J. (2008). A rapid polymerase chain reaction-based screening method for identification of all expanded alleles of the fragile X (FMR1) gene in newborn and high-risk populations. *J Mol Diagn* 10, 43–49. doi: 10.2353/jmoldx.2008.070073

Todd, P. K., Oh, S. Y., Krans, A., He, F., Sellier, C., Frazer, M., et al. (2013). CGG repeat-associated translation mediates neurodegeneration in fragile X tremor ataxia syndrome. *Neuron* 78, 440–455. doi: 10.1016/j.neuron.2013.03.026

Trouillas, P., Takayanagi, T., Hallett, M., Currier, R. D., Subramony, S. H., Wessel, K., et al. (1997). International Cooperative Ataxia Rating Scale for pharmacological assessment of the cerebellar syndrome. The Ataxia Neuropharmacology Committee of the World Federation of Neurology. *J. Neurol. Sci.* 145, 205–211. doi: 10.1016/S0022-510X(96)00231-6

Wang, J. Y., Hessl, D., Hagerman, R. J., Simon, T. J., Tassone, F., Ferrer, E., et al. (2017). Abnormal trajectories in cerebellum and brainstem volumes in carriers of the fragile X premutation. *Neurobiol. Aging* 55, 11–19. doi: 10.1016/j.neurobiolaging.2017.03.018

Wang, J. Y., Hessl, D., Hagerman, R. J., Tassone, F., and Rivera, S. M. (2012). Age-dependent structural connectivity effects in fragile x premutation. *Arch. Neurol.* 69, 482–489. doi: 10.1001/archneurol.2011.2023

Wang, J. Y., Hessl, D., Schneider, A., Tassone, F., Hagerman, R. J., and Rivera, S. M. (2013). Fragile X-associated tremor/ataxia syndrome: influence of the FMR1 gene on motor fiber tracts in males with normal and premutation alleles fragile X-associated tremor/ataxia syndrome. *JAMA Neurology* 70, 1022–1029. doi: 10.1001/jamaneurol.2013.2934

Wechsler, D. (1997). *The Wechsler Adult Intelligence Scale (3rd Edn.) Administration and Scoring Manual*. Orlando, FL: The Psychological Corporation.

Wheeler, A. C., Bailey, D. B. Jr., Berry-Kravis, E., Greenberg, J., Losh, M., Mailick, M., et al. (2014). Associated features in females with an FMR1 premutation. *J. Neurodev. Disord.* 6, 30. doi: 10.1186/1866-1955-6-30

Winarni, T. I., Chonchaiya, W., Sumekar, T. A., Ashwood, P., Morales, G. M., Tassone, F., et al. (2012). Immune-mediated disorders among women carriers of fragile X premutation alleles. *Am. J. Med. Genet. A* 158, 2473–2481. doi: 10.1002/ajmg.a.35569

Zhao, X., Gazy, I., Hayward, B., Pintado, E., Hwang, Y. H., Tassone, F., et al. (2019). Repeat instability in the fragile X-related disorders: lessons from a mouse model. *Brain Sci* 9:52. doi: 10.3390/brainsci9030052

Conflict of Interest: The authors declare that the research was conducted in the absence of any commercial or financial relationships that could be construed as a potential conflict of interest.

frontiers in Molecular Biosciences

ORIGINAL RESEARCH
published: 29 January 2021
doi: 10.3389/fmolb.2020.600840

Human Cerebral Cortex Proteome of Fragile X-Associated Tremor/Ataxia Syndrome

Katharine Nichole Holm[1], Anthony W. Herren[2†], Sandra L. Taylor[3], Jamie L. Randol[1], Kyoungmi Kim[3,4], Glenda Espinal[1], Verónica Martínez-Cerdeño[4,5], Isaac N. Pessah[4,6], Randi J. Hagerman[4,7] and Paul J. Hagerman[1,4]*

[1] Department of Biochemistry and Molecular Medicine, University of California Davis School of Medicine, Davis, CA, United States, [2] Mass Spectrometry Research Core, University of California Davis, Davis, CA, United States, [3] Department of Public Health Sciences, Division of Biostatistics, University of California Davis School of Medicine, Davis, CA, United States, [4] Medical Investigation of Neurodevelopmental Disorders Institute, University of California Davis School of Medicine, Davis, CA, United States, [5] Department of Pathology and Laboratory Medicine, University of California Davis School of Medicine, Davis, CA, United States, [6] Department of Molecular Biosciences, University of California Davis School of Veterinary Medicine, Davis, CA, United States, [7] Department of Pediatrics, University of California Davis School of Medicine, Davis, CA, United States

OPEN ACCESS

Edited by:
Renate K. Hukema, Rotterdam University of Applied Sciences, Netherlands

Reviewed by:
Peng Jin, Emory University, United States
Ronald Buijsen, Leiden University Medical Center, Netherlands

***Correspondence:**
Paul J. Hagerman
pjhagerman@ucdavis.edu

†Present address:
Anthony W. Herren, Thermo Fisher Scientific, Waltham, MA, United States

Specialty section:
This article was submitted to Cellular Biochemistry, a section of the journal Frontiers in Molecular Biosciences

Received: *31 August 2020*
Accepted: *27 November 2020*
Published: *29 January 2021*

Citation:
Holm KN, Herren AW, Taylor SL, Randol JL, Kim K, Espinal G, Martínez-Cerdeño V, Pessah IN, Hagerman RJ and Hagerman PJ (2021) Human Cerebral Cortex Proteome of Fragile X-Associated Tremor/Ataxia Syndrome. Front. Mol. Biosci. 7:600840. doi: 10.3389/fmolb.2020.600840

Background: Fragile X-associated tremor/ataxia syndrome (FXTAS) is an adult-onset neurodegenerative disorder associated with premutation CGG-repeat expansions (55–200 repeats) in the 5′ non-coding portion of the *fragile X mental retardation 1* (*FMR1*) gene. Core features of FXTAS include progressive tremor/ataxia, cognitive decline, variable brain volume loss, and white matter disease. The principal histopathological feature of FXTAS is the presence of central nervous system (CNS) and non-CNS intranuclear inclusions.

Objective: To further elucidate the molecular underpinnings of FXTAS through the proteomic characterization of human FXTAS cortexes.

Results: Proteomic analysis of FXTAS brain cortical tissue ($n = 8$) identified minor differences in protein abundance compared to control brains ($n = 6$). Significant differences in FXTAS relative to control brain predominantly involved decreased abundance of proteins, with the greatest decreases observed for tenascin-C (TNC), cluster of differentiation 38 (CD38), and phosphoserine aminotransferase 1 (PSAT1); proteins typically increased in other neurodegenerative diseases. Proteins with the greatest increased abundance include potentially novel neurodegeneration-related proteins and small ubiquitin-like modifier 1/2 (SUMO1/2). The FMRpolyG peptide, proposed in models of FXTAS pathogenesis but only identified in trace amounts in the earlier study of FXTAS inclusions, was not identified in any of the FXTAS or control brains in the current study.

Discussion: The observed proteomic shifts, while generally relatively modest, do show a bias toward decreased protein abundance with FXTAS. Such shifts in protein abundance also suggest altered RNA binding as well as loss of cell–cell adhesion/structural integrity. Unlike other neurodegenerative diseases, the proteome of end-stage FXTAS does not suggest a strong inflammation-mediated degenerative response.

Keywords: FXTAS, DIA-MS, SUMO1/2, Tenascin-C, CD38, Fragile X Syndrome, FMRpolyG, FMR1

INTRODUCTION

Fragile X-associated tremor/ataxia-associated syndrome (FXTAS) is an adult-onset neurodegenerative disorder caused by premutation (PM) range expansion (50–200 repeats) of the trinucleotide (CGG) repeat element in the 5′ untranslated region of the *fragile X mental retardation 1* (*FMR1*) gene. Approximately 30–40% of male and 8–16% of female PM carriers will develop FXTAS, with onset of initial symptoms typically beginning in males in their early 60's (Leehey et al., 2007; Hagerman and Hagerman, 2016). Symptoms of FXTAS include intention tremor, gait ataxia, parkinsonism, neuropathy, white matter disease, and cognitive decline (Hall et al., 2014; Hagerman and Hagerman, 2016; Kong et al., 2017; Cabal-herrera et al., 2020). The principal neuropathological feature of FXTAS is the presence of generally solitary intranuclear inclusions in both neurons and astrocytes within the central nervous system (CNS) (Greco et al., 2002, 2006; Garcia-Arocena et al., 2009; Martínez Cerdeño et al., 2018), as well as in diverse non-CNS tissues (Greco et al., 2007; Hunsaker et al., 2011), mitochondrial dysfunction (Ross-Inta et al., 2010; Napoli et al., 2011; Kaplan et al., 2012; Cabal-herrera et al., 2020), microglia activation and senescence (Martínez Cerdeño et al., 2018), iron deposition (Ariza et al., 2018), and dysregulation of neuronal Ca^{2+} (Robin et al., 2017; Hagerman et al., 2018). While the correlation between repeat length and cellular dysfunction is well-characterized, the pathway of neuronal dysfunction, age-related disease progression, and incomplete penetrance of FXTAS within the PM population remains generally unresolved.

Several mechanisms of FXTAS pathogenesis have been proposed, many of which are based on increased *FMR1* mRNA expression and protein sequestration. In the RNA toxicity model, the expanded RNA CGG repeat is thought to be responsible for sequestration of proteins such as DiGeorge syndrome chromosomal (or critical) region 8 (DGCR8), thereby decreasing their cellular abundance and function (Norman et al., 2010; Hoem et al., 2011; Qurashi et al., 2011; Pretto et al., 2013; Hagerman and Hagerman, 2016; Sellier et al., 2017; Rodriguez and Todd, 2019). Another proposed, posttranscriptional model involves Repeat-Associated Non-AUG (RAN) translation that is initiated upstream of the AUG start codon, leading to translation through the CGG repeat and resulting in a polyglycine-containing peptide (FMRpolyG). Studies of the possible role of FMRpolyG in FXTAS pathogenesis, generally involving transgenic mouse models and/or *in vitro* cell models, have presented evidence of cellular toxicity of FMRpolyG and colocalization of the peptide with intranuclear inclusions (Todd et al., 2013; Buijsen et al., 2014; Oh et al., 2015; Sellier et al., 2017; Krans et al., 2019; Friedman-Gohas et al., 2020). However, to our knowledge, native FMRpolyG has not been quantified *in vivo* in patient-derived cells, except in trace amounts in the intranuclear inclusions of *postmortem* FXTAS cases (Ma et al., 2019).

Elucidation of differential protein translation and intranuclear protein abundance in PM subjects is essential to profiling the FXTAS proteomic landscape and may provide novel insights into disease pathology. To date, proteomic characterization of end-stage FXTAS in *postmortem* human brain tissue has not been performed. Our current findings suggest that abnormal or ineffective elimination of protein aggregates may underlie FXTAS pathogenesis; however, FMRpolyG, proposed as a driver in co-aggregation models of FXTAS (Todd et al., 2013; Oh et al., 2015; Krans et al., 2019), was not identified in either control or FXTAS *postmortem* brains.

MATERIALS AND METHODS

Study Design/Subjects

Samples of frozen brain tissue from frontoparietal cerebral cortex were obtained from our University of California (UC) Davis FXTAS/FXS Brain Repository and were utilized for the proteomic studies (**Table 1**). All samples were originally obtained under approved UC Davis Institutional Human Subjects guidelines. A total of eight PM/FXTAS and six control male samples were included in the mass spectrometry (MS) analysis. All PM/FXTAS subjects suffered from end-stage FXTAS, characterized by at least stage 4 and usually stage 6 FXTAS prior to death.

Sample Preparation

For proteomic analysis, tissue samples were extracted in 1 ml of sodium dodecyl sulfate (SDS) solubilization buffer [5% SDS, 50 mM triethylammonium bicarbonate (TEAB), 1× PhosSTOP phosphatase, and 1× cOmplete Mini Protease Inhibitor tabs (Roche)] and further disrupted by bead beating with a MagNA lyser (Roche) using three rounds of 20 s each at 7,000 rpm. Samples were clarified by centrifugation at 15,000×g for 10 min, and the resulting supernatant was taken for analysis. For each sample, protein concentration was determined by bicinchoninic acid (BCA) assay (Thermo-Pierce) and 100 μg of total protein was volume normalized, reduced and alkylated, and enzymatically digested with trypsin using S-Trap mini (Protifi) spin columns according to manufacturer instructions with the following modifications: samples were reduced with 20 mM dithiothreitol (DTT) (Sigma) for 20 min at 50°C, alkylated with 40 mM indole-3-acetic acid (IAA) (Sigma) for 30 min at room temperature, and digested with two rounds of trypsin (Worthington) addition each at a 1:25 (enzyme:protein) weight ratio. Samples were reacted with the first trypsin round for 2 h at 37°C, followed by a second addition and incubation overnight at 37°C. Samples were eluted, lyophilized (Labconco), and reconstituted in 100 mM TEAB. Peptide concentration was measured by fluorescent peptide assay (Pierce). Each sample was reconstituted in 2% acetonitrile/0.1% trifluoroacetic acid (TFA), and 1 μg was injected for analysis. Equal portions of all samples were mixed together to make a reference sample to be run multiple times for chromatogram library runs.

Liquid Chromatography Tandem Mass Spectrometry

Digested peptides were analyzed on a Thermo Scientific Fusion Lumos Orbitrap Mass Spectrometer in conjunction with an UltiMate 3000 RSLCnano ultra high-performance liquid chromatography (UHPLC) and EASY-Spray source operating in positive ionization mode. Peptides were loaded on a Thermo

TABLE 1 | Subject demographics (males)[a].

		Controls ($n = 6$, Male)	Premutation/FXTAS ($n = 8$, Male)
Age (years) at death		69 + 10.6	82 ± 4.6
PMI (h)		6.5 ± 3	11.5 ± 4.2
CGG repeat length		25 + 8.1	104.1 ± 13.1
Group	**CGG repeat size[b]**	**Age at death**	**Publication[c], case no.**
Control	29	53	
Control	13	69	
Control	25	79	
Control	26	66	
Control	37	N/A	
Control	33	69	
Premutation	93 ± 12	85	
Premutation	110 ± 13	87	a, case 11; b, case 4; c, case 2
Premutation	125	81	
Premutation	88 ± 1	82	c, case 12
Premutation	108 ± 10	78	c, case 16
Premutation	84 ± 13	79	
Premutation	110 ± 15	75	a, case 6; b, case 6; c, case 1
Premutation	93 ± 8	81	a, case 9; b, case 9; c, case 13

[a] *PMI data are available for three controls and three FXTAS cases only.*
[b] *For premutation repeats, "±" indicates range of detectable bands for multiple bands.*
[c] *a, (Greco et al., 2006); b, (Garcia-Arocena et al., 2009); c, (Pretto et al., 2013).*
FXTAS, fragile X-associated tremor/ataxia syndrome; PMI, postmortem interval.

Scientific Acclaim PepMap 100 C18 reversed-phase pre-column (100 μm × 20 mm, 100Å, 5U) before being separated using an EASY-Spray C18 reversed-phase analytical column (ES802, 75 μm × 250 mm, 100Å, 2U). Peptides were eluted with an increasing percentage of acetonitrile over the course of a 120-min gradient with a flow rate of 200 nl/min at 40°C.

Chromatogram Library Creation and Data-Independent Acquisition

Six gas-phase fractionated (GFP) chromatogram library injections were made using staggered 4-Da isolation windows across the mass range 400–1,000 m/z: GFP1 = 400–500 m/z, GFP2 = 500–600 m/z, GFP3 = 600–700 m/z, GFP4 = 700–800 m/z, GFP5 = 800–900 m/z, and GFP6 = 900–1,000 m/z. Targeted MS/MS were acquired in the orbitrap with a higher collisional dissociation energy of 30%, resolution of 30 K, maximum injection time of 60 ms, and an automatic gain control (AGC) target of 800%. Each individual sample was also similarly run in data-independent acquisition (DIA) mode (Hu et al., 2016; Zhang et al., 2020) using staggered isolation windows of 8 Da across the full mass range of 400–1,000 m/z with higher collisional dissociation energy of 30%, orbitrap resolution of 15 K, maximum injection time of 20 ms, and an AGC target of 800%.

Data Processing and Analysis

DIA data were analyzed using Scaffold DIA v.1.3.1 (Proteome Software, Portland, OR, USA). Raw data files were converted to mzML format using ProteoWizard v.3.0.11748. The Reference Spectral Library was created by EncyclopeDIA v.0.9.2. Chromatogram library samples were individually searched against Prosit predicted databases created using the Prosit online server (https://www.proteomicsdb.org/prosit/) and converted for ScaffoldDIA using the EncyclopeDIA tool. The input for the Prosit prediction consisted of the UniProt human reference proteome with a peptide mass tolerance of 10.0 ppm and a fragment mass tolerance of 10.0 ppm. Variable modification considered included oxidation of methionine, and static modification included carbamidomethyl of cysteine. The digestion enzyme was assumed to be trypsin with a maximum of one missed cleavage site allowed. Peptides identified in each search were filtered by a percolator to achieve a maximum false discovery rate (FDR) of 0.01. Individual search results were combined, and peptides were again filtered to an FDR threshold of 0.01 for inclusion in the reference library.

Peptide quantification was performed within Scaffold DIA. For each peptide, the five highest quality fragment ions were selected for quantitation. Proteins that contained similar peptides and could not be differentiated based on MS/MS analysis were grouped to satisfy the principles of parsimony. Only proteins with a minimum of two identified peptides were considered and filtered by a protein FDR threshold of 1.0%.

Statistical Analysis

Ion counts were obtained for 6,076 proteins. Protein quantities in each sample were total count normalized by scaling counts to the average sum of counts across all subjects. Proteins with more than two missing values in an experimental group were excluded from statistical analysis, leaving 5,863 proteins for analysis after correction. For each protein, individual values more than 2.5 standard deviations above the mean of $\log_2$ transformed counts were considered outliers and dropped from the analysis. This resulted in 121 values (0.15%) dropped, but did not result in any protein having more than two missing values per experimental group. Missing values were imputed as one half of the protein-specific observed minimum value. Protein counts were $\log_2$ transformed for statistical analysis to meet model assumptions. Age at death for one control subject was missing and imputed as the average age of control subjects.

Differential protein accumulation between FXTAS and control groups was first evaluated using two-sample *t*-tests with unequal variances. Second, to account for age difference, linear regression was used to identify differentially abundant proteins (DAPs) between groups with age included as a covariate in the model. For each analysis, Benjamini–Hochberg FDRs were calculated to account for multiple testing. A two-sample *t*-test with unequal variances was used to compare age at death and CGG repeat length between experimental groups. Statistical analyses were conducted in R Statistical Computing Software version 3.6.3. Complete list of proteins is available on Massive (ID: MSV000086400 https://massive.ucsd.edu/ProteoSAFe/dataset.

jsp?task=da97eab790e84cefbc13cc3769b0ba64) [activated upon acceptance].

RNA Extraction

Total RNA was isolated from each 100 mg lyophilized brain sample using Qiazol reagent (catalog # 79306, Qiagen) for tissue lysis and purified using the RNeasy mini kit (catalog # 74104, Qiagen) with column and DNAse treatment. Quality measurements of total RNA were performed using the Agilent Bioanalyzer RNA 6000 Nano kit (catalog # 5067-1511, Agilent Technologies).

RNA Sequencing

RNA sequencing (RNA-seq) libraries were prepared from the RNA of cortex sections (**Table 1**). Sequencing and library preparation were performed by the DNA technologies and Expression Analysis Core in the Genome Center of the University of California, Davis. RNA Integrity (RIN) scores were assessed for all samples, resulting in a mean of 6.4 ± 0.87 (range = 4.9–8.3). Gene expression profiling was carried out using a 3′-Tag-RNA-Seq protocol. Barcoded sequencing libraries were prepared using the QuantSeq FWD kit (Lexogen, Vienna, Austria) for multiplexed sequencing according to the recommendations of the manufacturer starting from 300 ng total RNA each. Both the unique dual index (UDI)-adapter and unique molecular identifier (UMI) Second Strand Synthesis modules were used (Lexogen). The fragment size distribution of the libraries was verified *via* microcapillary gel electrophoresis on a LabChip GX system (PerkinElmer, Waltham, MA). The libraries were quantified by fluorometry on a Qubit fluorometer (Life Technologies, Carlsbad, CA) and pooled in equimolar ratios. The library pool was quantified *via* quantitative PCR (qPCR) with a KAPA Library Quantification Kit (Kapa Biosystems/Roche, Basel, Switzerland) on a QuantStudio 5 system (Applied Biosystems, Foster City, CA). The libraries were sequenced on a HiSeq 4000 sequencer (Illumina, San Diego, CA) with single-end 100-bp reads.

Gene Ontology and Molecular Signatures Database Exploratory Analysis

The Molecular Signatures Database (Subramanian et al., 2005; Liberzon et al., 2016) (MsigDB, v7.1), Gene Set Enrichment Analysis (GSEA), and the Human Protein Atlas (proteinatlas.org, 2000; Thul et al., 2017) was used to evaluate the differences in protein accumulation between controls and FXTAS subjects. Pathway enrichment analysis was conducted to identify enriched groups of proteins that share common molecular functions defined by the C5: Gene Ontology (GO) gene sets, MF: molecular function from MSigDB (https://www.gsea-msigdb.org/gsea/msigdb/annotate.jsp). Only the proteins with a raw $p < 0.05$ ($n = 423$) were included in the enrichment analysis to select overrepresented protein sets. Resulting GO molecular functions were manually characterized into functional families.

RESULTS

Demographic Characteristics of Brain Samples Used in the Current Study

Subject characteristics are delineated in **Table 1**. Proteins used for MS were isolated from frontotemporal cortex of 14 male subjects (eight late-stage FXTAS/PM subjects and six controls without known neurological disease). The average age of FXTAS subjects was 82 ± 4 years (range: 75–87 years) and of control subjects was of 69 ± 10 years (range: 53–79 years). Female cases were not used for these studies to avoid confounding effects of variable activation ratio for the two X chromosomes. As expected, the difference in CGG repeat length between the control and FXTAS group was highly significant ($p < 0.001$), with an average CGG repeat length of 25 (±8.1) in the control group and an average length of 104.1 (±13.1) in the FXTAS group. However, FXTAS patients were also significantly older than the control group ($p = 0.027$). Therefore, age adjustment was performed in the analysis of all proteins for group comparison.

Identification of Differentially Abundant Proteins Associated With Fragile X-Associated Tremor/Ataxia Syndrome

DAPs were determined using two-sample *t*-tests and linear regression to adjust for age differences between FXTAS and control subjects. Without adjusting for age, analysis of the MS data identified 414 DAPs (**Table 2**) from the initial pool of 5,863 proteins after FDR correction (FDR < 0.2). However, adjusting for age differences reduced the number of DAPs to 16 proteins, of which four proteins demonstrated increased abundance and 12 proteins demonstrated decreased abundance (**Table 2**). Including age as a covariate did not change the direction of group differences for any of the DAPs but did decrease the magnitude of differences. Overall, the FXTAS cortex proteome does not demonstrate any significant bias toward overexpression or underexpression compared to controls; however, the majority of proteins with significant levels of differential expression are biased toward decreased abundance in FXTAS cortexes. Distribution of fold changes and FDR corrected *p*-values (*q*-values) for all proteins are represented in the volcano plot in **Figure 1**.

Fragile X-Associated Tremor/Ataxia Syndrome Proteome Pathway Enrichment

To elucidate cellular and biological significance of our DAPs, we used GSEA to perform GO analysis (Subramanian et al., 2005) and identify enriched GO terms associated with FXTAS DAPs (raw $p < 0.05$). Of the 303 proteins with decreased abundance, 232 proteins were associated with annotated functions/ontologies. The predominant functions of proteins with decreased abundance include protein binding (16%), hydrolysis (8%), RNA binding (6%), nucleotide binding (6%), cell adhesion (5%), gene regulation (5%), phosphate activity (5%), drug interaction (4%), structural integrity (4%), lipid binding (4%), and actin filament binding (3%) (**Figure 2A**). Of

the 122 proteins with increased abundance, 47 proteins were associated with ontologies/functions. The predominant functions of the proteins with increased abundance include RNA binding (32%), redox (22%), iron binding (14%), cofactor binding (13%), antioxidant activity (6%), and apoptosis (5%) (**Figure 2B**).

Fragile X Mental Retardation Protein-Associated mRNAs

To determine whether mRNA species known to associate with fragile X mental retardation protein (FMRP) (Pasciuto and Bagni, 2014b) are differentially expressed as proteins in FXTAS cortexes, the list of known FMRP-associated mRNAs was compared to the FXTAS proteome. Of the 54 mRNAs known to associate with FMRP, 37 (69%) were identified by MS in the FXTAS proteome (**Table 3**). Ras Homolog Family Member A (RHOA) protein was 11% decreased in FXTAS cortexes ($p = 0.001$, FDR = 0.21). Other nearly significant DAPs included potassium voltage-gated channel subfamily C member 1 (KCNC1) with 50% increased abundance and Ras-related C3 botulinum toxin substrate 1 (RAC1) and catenin beta-1 (CTNNB1), each with 12% decreased abundance ($p = 0.021$, FDR = 0.6). Distribution of fold change and FDR values of all 37 proteins are represented as volcano plots in **Figure 3**. While some of these proteins were differentially expressed at $p < 0.05$, none achieved significance of FDR < 0.2.

TABLE 2 | Differentially expressed proteins (FDR < 0.2).

Protein (gene symbol)	log2FC	Raw *p*-value	FDR
TNC	−2.858	0	0.056
CRYL1	−0.657	0	0.056
MTM1	−0.628	0	0.056
PSAT1	−0.564	0	0.056
RAB31	−0.296	0	0.056
SHISA4	−0.685	0	0.056
SUMO1P1	0.437	0	0.056
SUMO1	0.437	0	0.056
TMEM222	−0.449	0	0.073
RAB22A	−0.226	0	0.084
CD38	−2.626	0	0.107
PLCD3	−0.701	0	0.129
SEC23A	−0.82	0	0.129
RNF214	−0.707	0	0.134
GOT1	0.091	0	0.171
GNG3	0.155	0	0.171

FDR, false discovery rate; PSAT1, phosphoserine aminotransferase 1; RNF214, ring finger protein 214; TNC, tenascin-C.

Fragile X Mental Retardation Protein-Associated Proteins

We also analyzed proteins known to associate with FMRP (Pasciuto and Bagni, 2014a) to determine whether any are differentially expressed in FXTAS cortexes. Of the 53 proteins known to associate with FMRP, 25 were identified by MS in the FXTAS proteome (**Table 4**). None of the 25 FMRP-associated proteins were significantly differentially abundant in FXTAS cortexes at FDR < 0.2.

Calcium-Associated Proteins

Of the 716 proteins associated with calcium ion binding [GO:0005509 GO_Calcium_Ion_Binding] and calcium-associated proteins associated with FXTAS [*TPCN1*, *TPCN2*, *ORAI1*, *ORAI2*, *ORAI3*, *CACNA1D*, *CACNA1F*, *CACNA1A*, *CACNA1B*, *CACNA1E*, *CACNA1G*, *CACNA1H*, *CACNA1I*, and *P2RX1-7*] (Rovozzo et al., 2016), 262 (37%) were identified by MS in FXTAS cortexes. Although none of the proteins demonstrated significantly different abundance in FXTAS

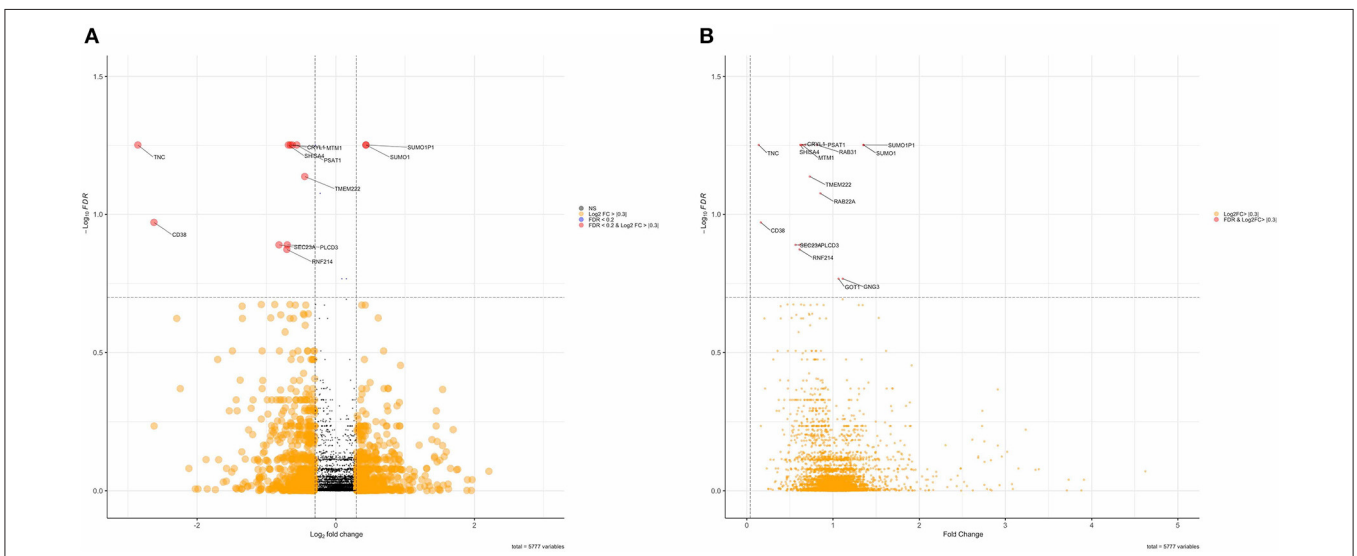

FIGURE 1 | (A) Volcano plot of Log2FC and false discovery rate (FDR) values of differentially abundant proteins. Red points are proteins with an FDR < 0.2. **(B)** Volcano plot of fold change values of differentially abundant proteins.

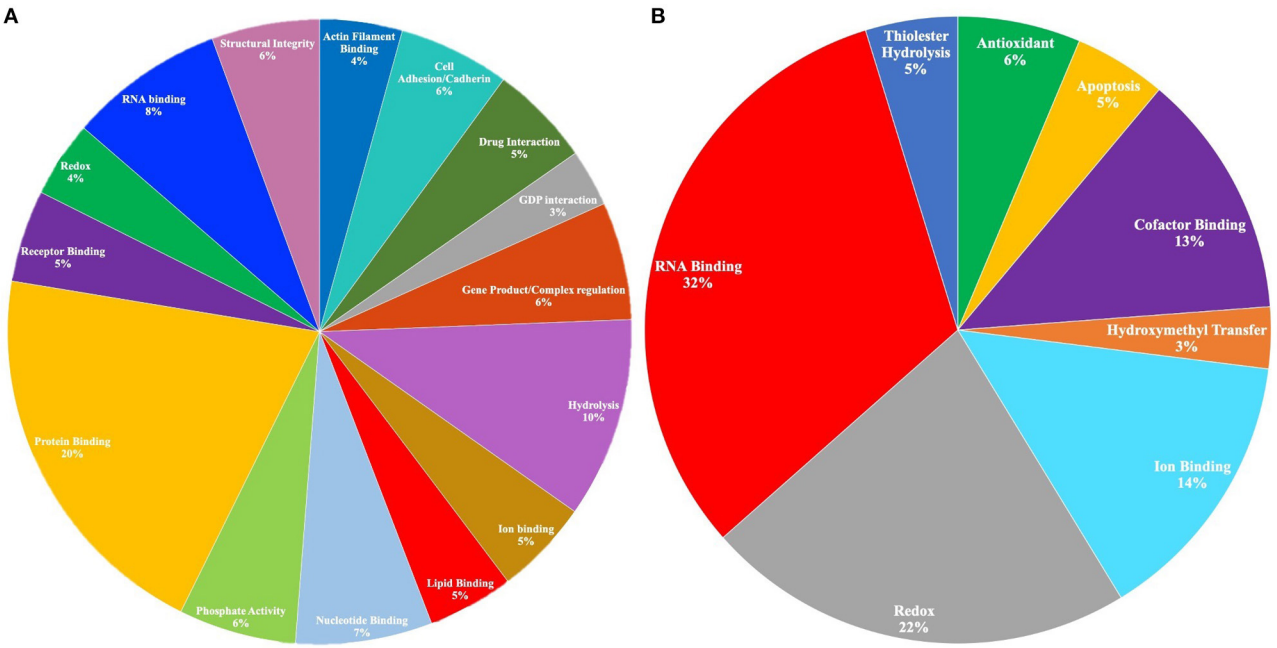

FIGURE 2 | (A) Gene Ontology (GO) molecular functions of proteins with decreased abundance in fragile X-associated tremor/ataxia syndrome (FXTAS) ($p < 0.05$). A total of 301 proteins were submitted in the original query, and 97 proteins were associated with GO molecular functions. Only the functions associated with >1% of the proteins in the query are depicted in the chart. **(B)** GO molecular functions of proteins with increased abundance in FXTAS ($p < 0.05$). A total of 121 proteins were submitted in the original query, and 10 proteins were associated with GO molecular functions.

cortexes at FDR < 0.2 (**Figure 4**), 28 proteins were significant before FDR correction (raw $p < 0.05$), including two proteins, versican proteoglycan (VCAN; FDR = 0.21) and desmoglein-1 (DSG1; FDR = 0.26), which demonstrated nearly significant decreased abundance (**Table 5**). Aside from calcium-ion binding, these proteins function as extracellular matrix (ECM) cell–cell adhesion, plasma membrane/cytosolic trafficking, and proliferative signaling.

Comparison to Alzheimer Disease and Parkinson Disease

Overlapping DAPs in FXTAS, Alzheimer disease (AD), and Parkinson disease (PD) were determined using the proteins described in previous proteomic analysis of PD (FDR < 0.2) reported by Dumitriu et al. (2016) and of AD reported by Hondius et al. (2016). For comparison, the FXTAS DAPs (determined by FDR < 0.2), PD DAPs (FDR < 0.2) listed in Dumitriu et al. (2016), and the AD DAPs (FDR < 0.05) listed in Hondius et al. (2016) were compared. The complete list of shared DAPs is described in **Table 6**. Of the shared proteins, phosphoserine aminotransferase 1 (PSAT1) and TNC (tenascin-C) were shared between AD and FXTAS, ring finger protein 214 (RNF214) was shared between PD and FXTAS, and only PSAT1 was shared between all three neurodegenerative diseases (**Figure 5**). Of these three proteins, all three proteins demonstrated decreased abundance in FXTAS.

DISCUSSION

Fragile X-Associated Tremor/Ataxia Syndrome Proteome

A striking feature of the current proteomic analysis is that the FXTAS proteome demonstrates differential abundance compared to the proteome of the control brains of only a small number of proteins compared to that of controls. Furthermore, the majority of these DAPs were biased toward decreased abundance, of transcriptional downregulation, and/or protein degradation in FXTAS. However, the absence of any substantial shift in protein abundance for the FXTAS proteome does not rule out more substantive shifts in the phosphoproteome and proteomes of other posttranslational modifications (PTMs), which are not identified in the current analysis.

Increased Small Ubiquitin-Like Modifier 1

Consistent with the studies of FXTAS inclusions by Ma et al. (2019), we observed modest, but significantly increased abundances of small ubiquitin-like modifier 1 (SUMO1)/SUMO1P1 and SUMO2 proteins in FXTAS cortex (50% increase in SUMO1 protein; 20% increase in SUMO2). SUMO1 is a member of the ubiquitin protein modifier superfamily and forms a posttranslational, reversible bond to lysine residues on target proteins (Wilson and Heaton, 2008; Matsuzaki et al., 2015). Unlike ubiquitin modifications, SUMO proteins

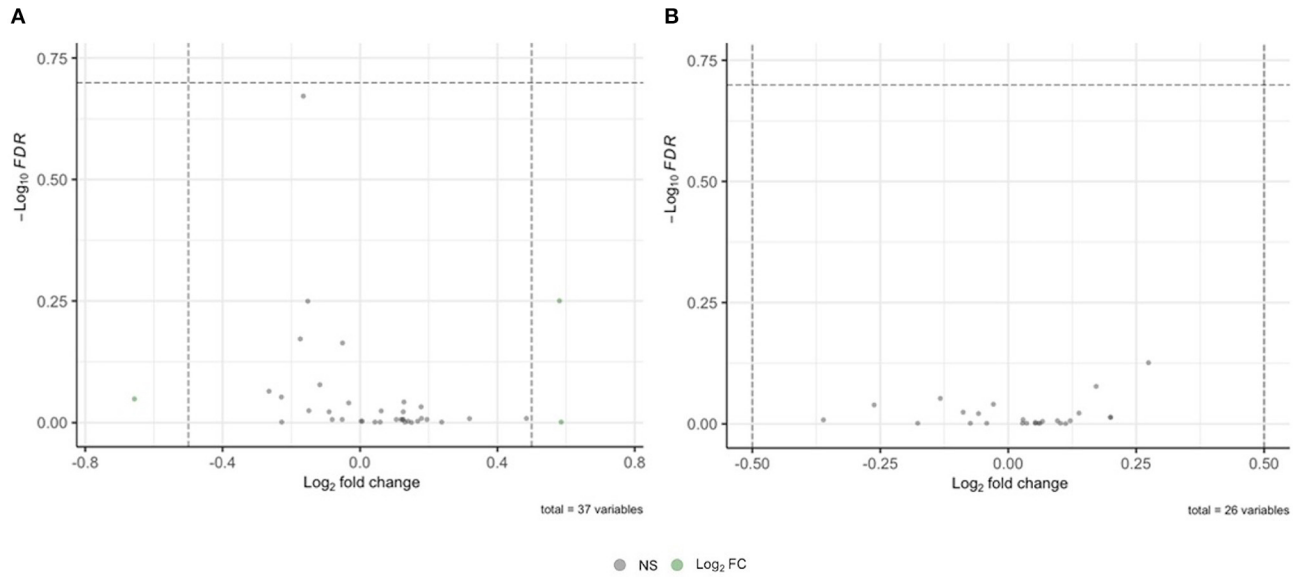

FIGURE 3 | Volcano plot of mRNA and proteins associated with fragile X mental retardation protein (FMRP) in fragile X-associated tremor/ataxia syndrome (FXTAS) cortexes. **(A)** No significant differences were found in proteins derived from FMRP-associated mRNA. **(B)** No significant differences were found in proteins derived from FMRP-associated proteins.

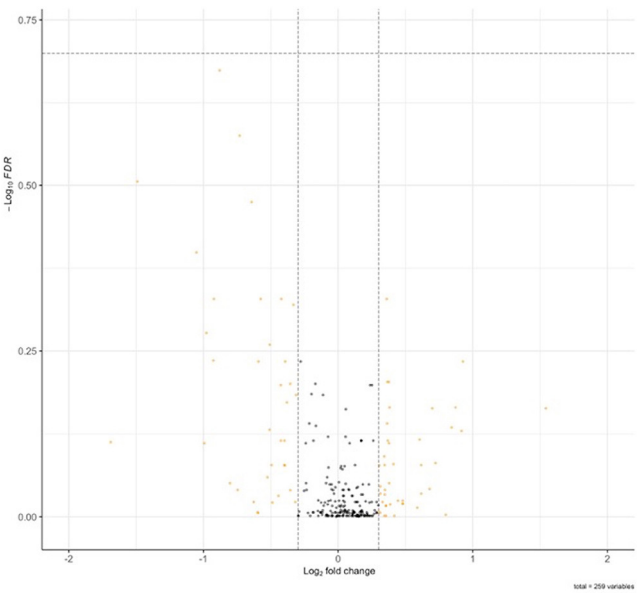

FIGURE 4 | Volcano plot of Ca^{2+} associated proteins in fragile X-associated tremor/ataxia syndrome (FXTAS) cortexes. No significant differences in Ca^{2+} associated proteins were identified in FXTAS cortexes.

are involved in the regulation of a variety of cellular processes such as nuclear transport, transcriptional regulation, apoptosis, and protein stability (Zhang et al., 2016). Growing evidence suggests that SUMOylation is a critical PTM in neuronal development and function, as well as in neurodegenerative disease and ischemic injury (Krumova and Weishaupt, 2013; Lee et al., 2013; Matsuzaki et al., 2015; Zhang et al., 2016). Recently, Khayachi et al. (2018) demonstrated that metabotropic glutamate receptor type 5 (mGluR5) activation induces SUMOylation of FMRP in neurons and subsequent dissociation of FMRP from dendritic RNA granules (Khayachi et al., 2018; Tang et al., 2018), indicating a critical role for SUMOylation in the regulation of mGluR5-mediated calcium signaling, spine density, and FMRP–RNA interactions. Furthermore, SUMOylated proteins were found to accumulate in insoluble inclusions in response to proteasomal inhibition, suggesting additional roles of SUMOs in protein aggregation and response to misfolded proteins (Tatham et al., 2011). An altered SUMO response possibly precedes the characteristic hallmarks of cellular dysfunction in PM carriers, which include downregulated signaling and impaired calcium signaling, as well as disturbed mitochondrial, endoplasmic reticulum (ER), and mGluR1/5 function. Reduced function of mGluR5 receptors in end-stage FXTAS (Pretto et al., 2014) and increased accumulation of SUMO-rich proteins in inclusions suggest a significant role of SUMO in protein processing and signaling in the progression of cellular dysregulation in FXTAS.

Recent studies provided evidence for the contribution of SUMOylation to misfolded protein granules/inclusions (Tatham et al., 2011) and regulation of synaptic function (Anderson et al., 2017). While increased SUMO abundance is consistent across both FXTAS inclusions and whole-cell cortex proteomes, further studies are needed to determine if the elevated neuronal cell SUMO abundance is the result of increased SUMO-conjugated proteins or free SUMO. As PTMs of FMRP are dependent on mGluR5 activation (Westmark and Malter, 2007), the reduction in mGluR5 receptors in FXTAS neurons may be responsible for altered FMRP-PTMs

TABLE 3 | Proteins translated from FMRP-associated mRNA in FXTAS cortex.

Protein (gene symbol)	Log2FC	Age-adjusted raw *p*-value	Age-adjusted FDR
RHOA	−0.165	0	0.213
KCNC1	0.581	0.004	0.562
CTNNB1	−0.152	0.124	0.563
RAC1	−0.174	0.008	0.673
DLGAP4	−0.051	0.744	0.686
AATK	−0.117	0.762	0.836
SPEN	−0.265	0.247	0.862
FMR1	−0.229	0.07	0.886
PLP1	−0.657	0.01	0.894
ARHGEF12	0.128	0.34	0.907
PPP2CA	−0.033	0.543	0.911
VDAC1	0.178	0.019	0.928
DAG1	−0.149	0.197	0.945
EEF2	0.062	0.428	0.946
PCDH10	0.126	0.523	0.95
PKP4	−0.09	0.135	0.95
APP	0.485	0.189	0.98
CAMK2A	0.179	0.053	0.98
KCND2	0.319	0.473	0.981
ARC	−0.052	0.872	0.985
DLG4	0.12	0.329	0.985
FUS	0.124	0.062	0.985
HNRNPA2B1	0.195	0.118	0.985
MAP1B	−0.081	0.373	0.985
OPHN1	0.126	0.466	0.985
PTPN5	0.106	0.613	0.985
AP2B1	0.14	0.109	0.993
MAP2	0.006	0.978	0.993
NLGN2	0.168	0.188	0.993
PIK3CB	0.003	0.975	0.993
ALDOA	0.044	0.28	0.997
APC	0.059	0.695	0.997
GABRB1	0.238	0.18	0.997
GABRD	0.586	0.11	0.997
MBP	−0.228	0.401	0.997
SOD1	0.131	0.085	0.997
PCLO	0.15	0.219	0.999

FMRP, fragile X mental retardation protein; FXTAS, fragile X-associated tremor/ataxia syndrome.

TABLE 4 | FMRP-associated proteins in FXTAS cortexes.

Protein (gene symbol)	Log2FC	Age-adjusted raw *p*-value	Age-adjusted FDR
TIA1	0.274	0.067	0.748
CAPRIN1	0.172	0.145	0.837
FXR2	−0.133	0.188	0.886
KIF1B	−0.029	0.248	0.911
STAU1	−0.262	0.262	0.914
HABP4	−0.088	0.347	0.946
DDX5	0.138	0.352	0.95
FXR1	−0.058	0.387	0.952
PURA	0.2	0.45	0.969
PURA	0.2	0.45	0.969
RPL5	0.029	0.503	0.98
YBX1	−0.361	0.525	0.981
MYO5A	0.121	0.595	0.985
RALY	0.096	0.562	0.985
AGO1	0.067	0.696	0.988
CYFIP2	0.053	0.76	0.993
APC	0.059	0.933	0.997
CYFIP1	0.028	0.877	0.997
EIF4E	0.062	0.972	0.997
EIF5	−0.074	0.861	0.997
KIF5A	−0.042	0.849	0.997
NUFIP2	−0.177	0.954	0.997
PAK1	0.053	0.861	0.997
RPL8	0.102	0.94	0.997
RPLP0	0.036	0.9	0.997

FMRP, fragile X mental retardation protein; FXTAS, fragile X-associated tremor/ataxia syndrome.

and consequentially reduced FMRP-mediated clearance of clearance of RNA granules, spine density and maturation, as well as increased excitotoxicity of the remaining mGluR5s. Altered downstream regulation of mGluR5-mediated Ca^{2+} signaling may explain the relationship between dysregulated intracellular Ca^{2+} signaling present in FXTAS neurons as well as the related loss of synaptic plasticity. Additional research is needed to explore the mGluR5 SUMO relationship and determine if mGluR5 inhibitors used for AD, such as memantine HCl (Namenda), 2-chloro-4-((2,5-dimethyl-1-(4-(trifluoromethoxy)phenyl)-1H-imidazol-4-yl)ethynyl)pyridine (CTEP), or basimglurant, may similarly ameliorate FXTAS-related cognitive decline and pathology. However, a preliminary trial of memantine HCl was not found to improve tremor, ataxia, or executive function (Seritan et al., 2014), although it did improve event-related potential (ERP) studies of language processing and attention (Yang et al., 2014, 2016).

Abnormal ubiquitin-proteasome system (UPS) function has been identified in many neurodegenerative diseases (Zheng et al., 2016), leading to toxic protein-rich inclusion indicators of disease. As SUMO proteins are responsible for both dynamic regulation of proteins as well as cross-communication with the UPS system (Wilson and Heaton, 2008), differential abundance of SUMOs may represent dysregulation of the UPS in FXTAS as well. Further research on the profile of SUMO proteins and related PTMs should be explored to determine if increased SUMOs in FXTAS patients are representative of proteasomal dysregulation as well.

Tenascin-C

Another observation of the current study is the significant decrease in abundance of TNC in the FXTAS cases. TNC is an ECM protein responsible for modulating several cellular functions, including cell adhesion, neurogenesis/axonal guidance, and mechanical stress (Midwood and Orend, 2009; Midwood et al., 2016; Wiemann et al., 2019). While TNC is highly expressed in neurons during development, the protein is indicative of growth and repair processes in adult tissue at sites of trauma, inflammation, and tumor development (Udalova

TABLE 5 | Calcium-binding associated DAPs ($p < 0.05$).

Protein (gene symbol)	Log2FC	Age-adjusted raw *p*-value	Age-adjusted FDR
VCAN	−0.881	0.001	0.212
DSG1	−0.732	0.002	0.266
EFEMP1	−1.491	0.003	0.312
CDH20	−0.644	0.003	0.335
CLEC3B	−1.053	0.005	0.399
CDH11	−0.423	0.011	0.469
EFHD2	0.36	0.01	0.469
EPS15	−0.576	0.01	0.469
S100A16	−0.923	0.009	0.469
SPARCL1	−0.333	0.012	0.479
S100A13	−0.979	0.017	0.528
NID1	−0.509	0.019	0.55
PCDHGC3	−0.927	0.023	0.581
C1R	0.927	0.028	0.583
HRNR	−0.28	0.026	0.583
PLS3	−0.394	0.027	0.583
PLSCR4	−0.593	0.028	0.583
EPDR1	0.365	0.036	0.626
SLC25A13	0.376	0.037	0.626
LCP1	−0.171	0.038	0.63
PLCD1	−0.357	0.037	0.63
PLS1	−0.427	0.04	0.633
SNCA	0.251	0.04	0.633
SNCB	0.237	0.04	0.633
TTYH1	−0.199	0.043	0.653
CDH2	−0.112	0.044	0.655
CDH8	−0.314	0.044	0.655
GSN	−0.382	0.049	0.672

DAP, differentially abundant protein.

TABLE 6 | Comparison of FXTAS, PD, and AD proteomes[a].

Protein (gene symbol)	FXTAS	AD	PD	FXTAS Log_2FC	FXTAS age-adjusted FDR
PSAT1	+	+	+	−0.564	0.056
RNF214	+	ND	+	−0.564	0.134
TNC	+	+	ND	−2.858	0.056

[a]*AD, Alzheimer disease; PD, Parkinson disease; FC, fold change; FXTAS, fragile X-associated tremor/ataxia syndrome; PSAT1, phosphoserine aminotransferase 1; RNF214, ring finger protein 214; TNC, tenascin-C.*

et al., 2011). We observed a significant, age-independent loss of both TNC protein and mRNA expression in FXTAS cortexes (**Figure 6**), as well as downregulation of a number of ECM and cell–cell adhesion-associated proteins. The observed decrease of TNC protein in FXTAS is unexpected and highlights a distinction between the FXTAS proteome and those of other neurodegenerative diseases, in which increased TNC protein abundance often correlates with an inflammatory response and initiation of other neurodegenerative diseases (Xie et al., 2013; Wiemann et al., 2019).

Increased *TNC* gene expression (increased mRNA abundance) has also been implicated in response to traumatic brain injury and subsequent activation of the inflammatory response pathway (Liu et al., 2018; Dai et al., 2019). However, *TNC* gene silencing after subarachnoid hemorrhage (SAH) was found to alleviate neuronal inflammation and apoptosis *via* phosphoinositide-3-kinase (PI3K)/Akt/nuclear factor (NF)-κB pathway activation and has been highlighted as a potential therapeutic target to prevent neuronal cell death after injury (Shiba et al., 2014; Liu et al., 2018). Thus, loss of TNC protein may be consistent with a compensatory cellular response in FXTAS, and elucidation of *TNC* gene expression may provide insight into how this response is regulated. *TNC* transcription is positively regulated primarily by transforming growth factor (TGF)-β and fibroblast growth factor 2 (FGF2) in astrocytes (Chiovaro et al., 2015). Although *TGF-β* mRNA was not significantly differentially expressed in FXTAS (unpublished), TGF-β protein trended upward [not significant (NS)] in our FXTAS cortexes. FGF2 protein was not identified in the MS dataset but found to be nearly significant in mRNA analysis (**Table 7**), with a 2-fold decrease in expression in FXTAS cortexes. *FGF-2* mRNA expression was also found to increase in degenerating neurons and correlate with microglial phagocytosis of debris (Noda et al., 2014); therefore, downregulated *FGF-2* in FXTAS may contribute to increased debris accumulation. Downregulation of this microglia-mediated phagocytosis, inflammatory, and apoptotic response suggests a distinct lack of response signaling present in most other neurodegenerative disorders. The nearly complete loss of *TNC* mRNA and TNC protein expression in FXTAS cortexes suggests a failure in cell injury response and survival pathways and is indicative of impaired pathway regulation.

Cluster of Differentiation 38

Cluster of differentiation 38 (CD38) protein, a pro-inflammatory enzyme responsible for degradation of nicotinic acid dinucleotide (NAD) and regulation of calcium-dependent myeloid-derived inflammatory cells (Blacher et al., 2019), was significantly less abundant in FXTAS cortexes. While CD38 protein abundance often increases with age and in other neurodegenerative diseases such as AD and PD (Dumitriu et al., 2016; Blacher et al., 2019; Guerreiro et al., 2020), the significant reduction of this pro-inflammatory protein is consistent with a non-inflammatory-mediated primary pathology in FXTAS. CD38 knockout models demonstrated altered microglial response and reduced pro-inflammatory cytokine secretion (Guerreiro et al., 2020). Due to the typical age-associated increase in CD38 expression, the lack of CD38 protein in FXTAS may not be due to direct downregulation but rather impaired initiation of this age-related response pathway or additional compensatory mechanisms.

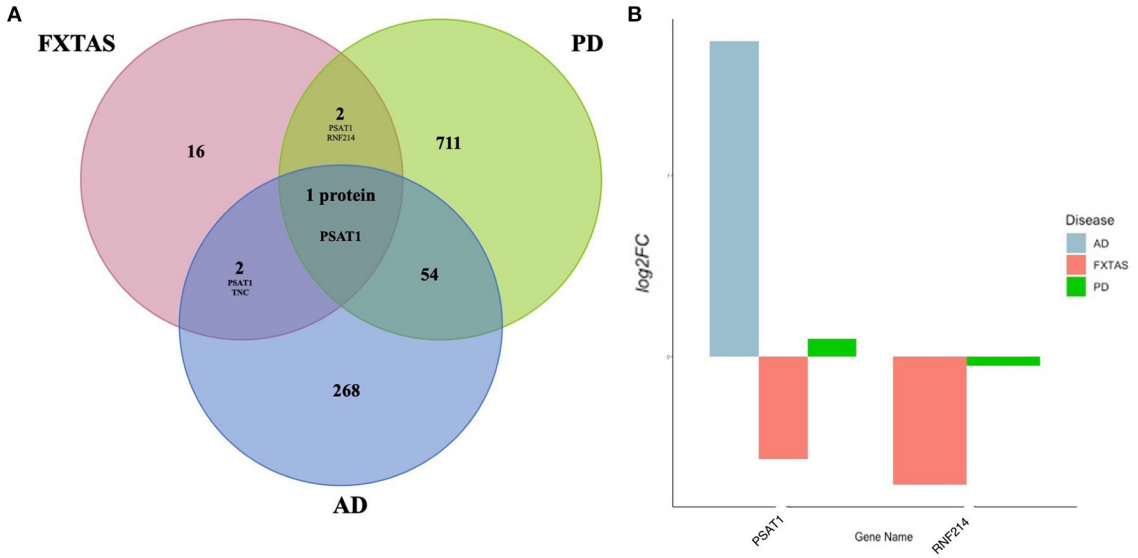

FIGURE 5 | Shared differentially abundant proteins (DAPs) between neurodegenerative disorders. **(A)** Venn diagram of significant [false discovery rate (FDR) < 0.2] DAPs in fragile X-associated tremor/ataxia syndrome (FXTAS), Alzheimer's Disease (AD), and Parkinson's Disease (PD). **(B)** Log2 fold change values of proteins shared between FXTAS, PD, and AD.

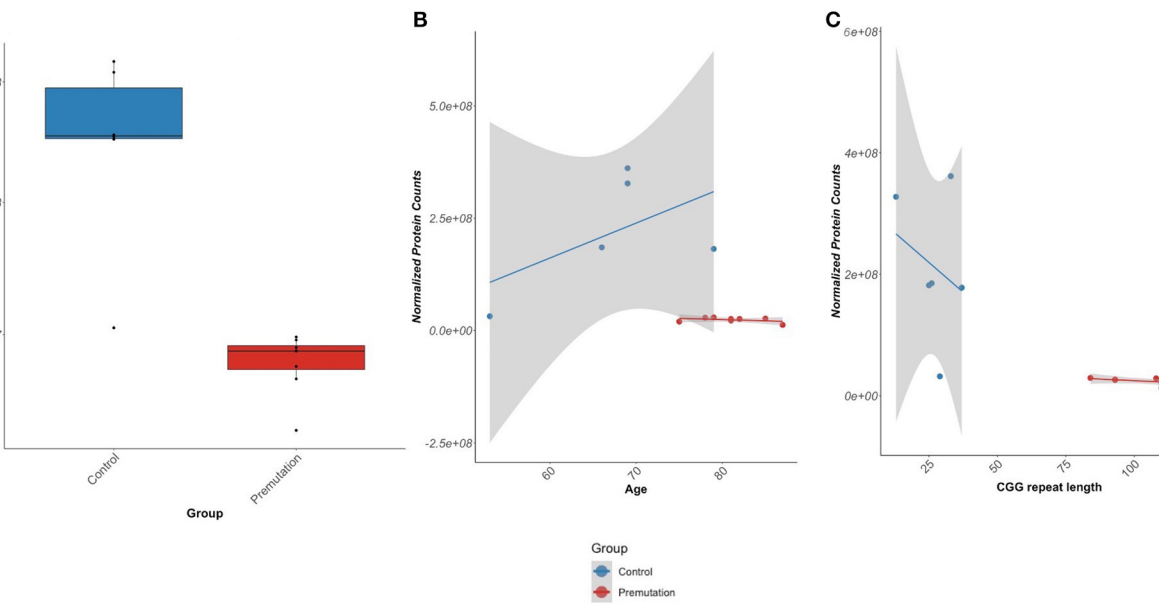

FIGURE 6 | Tenascin-C (TNC) protein expression. **(A)** TNC protein demonstrates significantly lower abundance in fragile X-associated tremor/ataxia syndrome (FXTAS) than unaffected control patients [false discovery rate (FDR) = 0.56]. **(B)** TNC protein abundance is significantly lower in FXTAS than unaffected controls, independent of age. **(C)** TNC protein abundance is lower in FXTAS than unaffected controls, with a slight dependence on CGG repeat length.

Cell Adhesion, Extracellular Matrix, and Actin Cytoskeleton

Many ECM, adhesion-interacting, and cytoskeletal proteins were among the most significant DAPs, including TNC, VCAN, CD44, and plectin (PLEC) (Li et al., 2019). While TNC, VCAN, CD44, and PLEC proteins were increased in AD patients in association with inflammation and synaptic plasticity (Hondius et al., 2016), these proteins were decreased in FXTAS cortexes, indicative of a unique and opposite regulation of this shared pathway.

TABLE 7 | mRNA expression of related proteins in FXTAS.

Gene name	Log2FC	Raw p Value	FDR
S100A13	−0.819661	2.51E-06	0.00824748
EFEMP1	−1.0957956	0.00786927	0.66824325
DEK	0.24087646	0.00867009	0.67817542
SPARC	−0.4185093	0.02028034	0.82975921
FGF2	−0.6323628	0.04052438	0.92959458
TGFB1	−0.1773479	0.82890012	0.99910395
TNC	−0.4960031	0.61936433	0.99910395
VCAN	−0.035502	0.86615008	0.99910395
EPS15	−0.1631534	0.10277535	0.99910395
S100A16	−0.3955453	0.25492682	0.99910395
PLSCR4	−0.5044934	0.12931283	0.99910395

FDR, false discovery rate; FXTAS, fragile X-associated tremor/ataxia syndrome; TNC, tenascin-C.

Ontology analysis of the proteins with decreased abundance demonstrated strong association with cell–cell adhesion pathways, suggesting that these intercellular junctions may be lost as potential precursors to apoptosis in FXTAS neuronal cells. Altered abundance of cell–cell adhesion-related proteins in PD and AD is indicative of a mechanistic role in neurodegenerative progression (Ramanan and Saykin, 2013). This pathway may contribute to the mechanisms preceding neuronal death through initial degradation of cell–cell junctions in the autophagic neurodegenerative response. Network analysis of AD at each stage of disease progression demonstrated dysregulation in actin-based cytoskeletal and cell–cell junction regulatory proteins in the initial stages, while the intermediate stages demonstrated impaired mitochondrial functions and redox signaling imbalance, and impaired pre-mRNA splicing and RNA stability in the advanced disease stages (Li et al., 2019). Identification of dysregulated cell–cell junctions may represent the cellular phenotype of neuronal cells initiating neurodegeneration, while dysregulation of mRNA splicing and stability may represent the population of cells in late-stage neurodegeneration. As our patient-derived samples were exclusively from late-stage FXTAS cortexes, the proteomic profile is representative of advanced disease progression. Additionally, the observed FXTAS proteomic shifts may only capture cells initiating or progressing toward neurodegeneration, while already degenerated cells would be unlikely to retain intact proteins for proteomic measurement.

Proteomic Profile of Calcium Dysfunction in Fragile X-Associated Tremor/Ataxia Syndrome

Calcium dysregulation has been observed in both hippocampal neurons from neonatal PM mice and PM patient-derived human dermal fibroblasts (Cao et al., 2013; Hagerman and Hagerman, 2015; Robin et al., 2017). PM neuronal cells demonstrate reduced expression of glutamate (Glu) transporters and the mGluR5 receptor, both of which are key mediators of calcium signaling (Cao et al., 2013; Pretto et al., 2014). Attenuated Glu signaling due to decreased mGluR5 availability is associated with increased excitotoxicity in many neurodegenerative disorders (Lewerenz and Maher, 2015; Crabbé et al., 2019) and may contribute to calcium dysfunction as well as downstream cdk5-ATM dysregulation in FXTAS.

We observed decreased abundance of the Ca^{2+} associated proteins VCAN, EGF containing fibulin extracellular matrix protein 1 (EFEMP1), epidermal growth factor receptor pathway substrate 15 (EPS15), S100 calcium binding protein A1 (S100A13), S100 Calcium Binding Protein A16 (S100A16), Cadherin 20 (CDH20), secreted protein acidic and cysteine rich (SPARC), Fibulin 1 (FBLN1), and phospholipid scramblase 4 (PLSCR4). Of these Ca^{2+}-associated proteins, VCAN, EFEMP1, EPS15, S100A16, S100A13, SPARC, and PLSCR4 were also downregulated as mRNA (**Table 7**). While Ca^{2+} dysregulation is a common hallmark of neurodegenerative diseases, Ca^{2+}-associated proteins commonly present with increased abundance in neurodegenerative diseases (Hondius et al., 2016; Bereczki et al., 2018). Furthermore, downregulation of these species as both mRNA and protein suggests transcriptional dysregulation of Ca^{2+}, and upstream regulation of Ca^{2+} homeostasis is a potential mechanism of pathology. These observations are consistent with the cytosolic Ca^{2+} dysregulation observed in the murine model (Robin et al., 2017).

Potential Biomarkers

DAPs, particularly those detected in cerebrospinal fluid (CSF) and serum at early stages of FXTAS, may serve as an early indicator of FXTAS progression and potential measurement of therapeutic efficacy. For example, TNC has been identified in CSF and serum after aneurysmal subarachnoid hemorrhage (Suzuki et al., 2010, 2011) and may serve as a potential biomarker for FXTAS. Further proteomic analysis of FXTAS CSF and/or serum in comparison to the cortex DAP biomarker candidates should be performed to determine if the FXTAS-associated loss of TNC expression is systemic throughout the nervous system and may serve as a potential biomarker for disease.

FMRpolyG

We did not detect FMRpolyG in any of the FXTAS or control brains used for the current study, despite our detection of the peptide in FMRpolyG peptide controls and our ability to detect expanded CGG-repeat FMRpolyG-GFP expressed in cultured human neural (SK) cells (**Supplementary Figure 1**). Our results are consistent with the observations of Ma et al. (2019) who observed only trace amounts of the peptide in FXTAS inclusions but no peptide in whole nuclear preps for the same cases. Moreover, we are unaware of any other study of CNS tissue that has identified/quantified FMRpolyG in human brain tissue other than by immunostaining of inclusions. This suggests that endogenous FMRpolyG is not abundantly expressed in CNS tissues and thus may not be present in sufficient quantities to initiate FXTAS neuropathology. Further studies aimed at quantifying FMRpolyG levels should therefore be

undertaken in the context of models proposed for its role in neurodegeneration.

Correlation Between Differentially Abundant Proteins and Fragile X-Associated Tremor/Ataxia Syndrome-Associated Dysfunction, mRNA, and Proteins

Surprisingly, we did not identify differential abundance of mitochondrial proteins or those associated with mitochondrial dysfunction in FXTAS cortexes. Despite the evidence demonstrating altered mitochondrial dysfunction and decreased mitochondrial protein expression in PM subjects (Ross-Inta et al., 2010; Napoli et al., 2016, 2018), dysfunction was not found in association with our DAPs in late-stage FXTAS. This may be the result of late-stage disease progression and the overall cellular abundance of proteins outweighing those specifically associated with mitochondria.

We also did not detect significant changes in the abundance of FMRP-associated mRNAs or proteins. The lack of significant differential abundance of this class of proteins may simply be due to the lack of significant variation in FMRP abundance within the FXTAS cortex samples.

CONCLUSIONS

MS analysis of male human cortex detected differential abundance of at least 16 proteins (FDR < 0.2) in late-stage FXTAS patients compared to controls. Several functional groups demonstrated decreased abundance, such as cell–cell adhesion/ECM, stress and cellular response, calcium signaling, and molecule metabolism systems. Increased abundance of proteins associated with transcriptional regulation, RNA binding, PI3K/Akt/mammalian target of rapamycin (mTOR) signaling, and SUMO regulation suggest dysregulation of pretranscriptional and posttranslational processes in FXTAS preceding neuronal death. Furthermore, many DAPs shared among other neurodegenerative disorders displayed opposite directional abundance in FXTAS when compared to the same proteins in AD and PD. This directional difference suggests potential shared degenerative pathways but differences in response mechanisms in late-stage FXTAS.

Further research on the upstream regulation of these proteins, presence of PTM modifications, subcellular localization, and correlation with mRNA levels should be addressed. Additional brain cell type-specific isolation and analysis would provide further insight into the differential function specialized to glia, astrocytes, oligodendrocytes, microglia, and neurons, as cell type-specific changes were identified in other neurodegenerative disorders (Cao et al., 2013; Pretto et al., 2014; Johnson et al., 2018; Wilson and Nairn, 2018; Dixit et al., 2019). Surprisingly, native FMRPolyG was not identified in FXTAS cortexes. Inflammatory-associated proteins were also significantly less abundant and may suggest an impaired inflammatory response or non-inflammatory pathway unique to FXTAS pathology when compared to other neurodegenerative diseases. These DAPs provide unique insight into mechanisms of FXTAS pathology, potential therapeutic targets, and candidate biomarkers for disease progression.

Limitations

Protein and RNA degradation are inherent to *postmortem* tissue, presenting a likely reduced number of transcript and protein abundance in our patient-derived cortex samples. As input proteins do not undergo amplification before detection, certain proteins may be present below the detection limit of non-targeted MS analysis. Lack of detection of proteins of interest is not confirmation of protein absence but may be the result of very low quantity/trace amounts. Targeted protein quantification is needed to determine if proteins of interest not identified in this study are in fact present at levels below the level of detection/quantification or if they were lacking altogether. In this regard, we were not successful in detecting TNC or CD38 using Western blot for either controls or FXTAS cases. This inability to detect these proteins by Western blot likely reflects their low concentrations in adult brain tissue. In our MS analysis, TNC represented about 14 ppm of total protein abundance and CD38, about 2.5 ppm. We note that in their study of CD38 in brain tissues, Mizuguchi et al. (1995) were unable to detect CD38 by Western blot unless they first enriched for CD38 by immunoprecipitation.

Access to human cortex samples was also limited, and the small sample size of eight FXTAS subjects and six control subjects likely resulted in lower statistical power while controlling for multiple testing by FDR for high-throughput proteomic data. To account for these limitations, proteins with a raw $p < 0.05$ but within the top 7% of differentially expressed proteins were considered for molecular function analysis. The nature of sample collection also resulted in *postmortem* interval (PMI) variation between subjects and groups. While all brain sections were obtained from the cerebral cortex, future studies are warranted to characterize differential protein abundance among additional brain regions.

DATA AVAILABILITY STATEMENT

The raw data supporting the conclusions of this article will be made available by the authors, without undue reservation.

ETHICS STATEMENT

All procedures were performed in compliance with the UCD Institutional Review Board and the 1964 Helsinki declaration, including subsequent amendments and ethical standards.

AUTHOR CONTRIBUTIONS

JR contributed additional data and edits upon reviewer-suggested revisions. All authors listed have made a substantial, direct and intellectual contribution to the work, and approved it for publication.

FUNDING

This research was funded by the NICHD grant HD036071, the R01 grant ES014901, the R01 grant 1NS107131, and the MIND Institute IDDRC grant P50 HD103526.

SUPPLEMENTARY MATERIAL

The Supplementary Material for this article can be found online at: https://www.frontiersin.org/articles/10.3389/fmolb.2020.600840/full#supplementary-material

Supplementary Figure 1 | FMRpolyG detected by western blot. SK-N-MC cells transfected with expression plasmid produced FMRpolyG with 63 glycines fused to GFP (**FpG-GFP**, 38.5kD) or **GFP** (26.9kD) alone as a control. For each sample, 80 micrograms total protein determined by BCA assay (Pierce 23255) were run on a Criterion™ TGX Any kD™ Precast Gel (Bio-Rad 567-1124) alongside 5 microliters of Chameleon Duo Pre-Stained Protein Ladder (LI-COR 928-60000) (**Marker**) for 45 minutes at 100 mA. Proteins were transferred to a nitrocellulose membrane at 30V overnight at 4°C. The membrane was blocked in 5% BSA in TBS for 1 h at room temperature. Rabbit anti-GFP (Invitrogen A-1122, 1:5,000) and mouse anti-FMRpolyG (gift from the lab of Nicholas Charlet #8MFM2F7, 1:100) primary antibodies in blocking buffer supplemented with 0.1% Tween-20 were applied to the membrane overnight at 4°C. LI-COR IRDye® 800CW anti-rabbit IgG and IRDye® 680LT anti-mouse IgG secondary antibodies in blocking buffer supplemented with 0.1% Tween-20 were applied at 1:20,000 for 1 h at room temperature. Membrane was visualized on the LI-COR Odyssey Near-Infrared (NIR) Fluorescent Imager in the **(A)** 700-nm and **(B)** 800-nm channel. A composite image **(C)** identifies FMRpolyG-GFP as overlapping GFP and FMRpolyG signals (see arrow).

REFERENCES

Anderson, D. B., Zanella, C. A., Henley, J. M., and Cimarosti, H. (2017). *Sumoylation: implications for neurodegenerative diseases. Adv. Exp. Med. Biol.* 963, 261–281.doi: 10.1007/978-3-319-50044-7_16

Ariza, J., Rogers, H., Hartvigsen, A., Snell, M., Judd, D., and Hagerman, P. (2018). Iron accumulation and dysregulation in the putamen in fragile X-associated tremor/ataxia syndrome. *Mov. Disord.* 32, 585–591. doi: 10.1002/mds.26902

Bereczki, E., Branca, R. M., Francis, P. T., Pereira, J. B., Baek, J. H., Hortobágyi, T., et al. (2018). Synaptic markers of cognitive decline in neurodegenerative diseases: a proteomic approach. *Brain* 141, 582–595. doi: 10.1093/brain/awx352

Blacher, E., Dadali, T., Bespalko, A., Haupenthal, V. J., Grimm, M. O. W., Hartmann, T., et al. (2019). Alzheimer's disease pathology is attenuated in a CD38-deficient mouse model. *Ann. J. Neurol.* 78, 88–103. doi: 10.1002/ana.24425

Buijsen, R. A. M., Sellier, C., Severijnen, L.-A. W. F. M., Oulad-Abdelghani, M., Verhagen, R. F. M., Berman, R. F., et al. (2014). FMRpolyG-positive inclusions in CNS and non-CNS organs of a fragile X premutation carrier with fragile X-associated tremor/ataxia syndrome. *Acta Neuropathol. Commun.* 2:162. doi: 10.1186/s40478-014-0162-2

Cabal-herrera, A. M., Tassanakijpanich, N., Salcedo-arellano, M. J., and Hagerman, R. J. (2020). Fragile X-associated tremor/ataxia syndrome (FXTAS): pathophysiology and clinical implications. *Int. J. Mol. Sci.* 21:4391. doi: 10.3390/ijms21124391

Cao, Z., Hulsizer, S., Cui, Y., Pretto, D. L., Kim, K. H., Hagerman, P. J., et al. (2013). Enhanced asynchronous Ca2+ oscillations associated with impaired glutamate transport in cortical astrocytes expressing Fmr1 gene premutation expansion. *J. Biol. Chem.* 288, 13831–13841. doi: 10.1074/jbc.M112.441055

Chiovaro, F., Chiquet-Ehrismann, R., and Chiquet, M. (2015). Transcriptional regulation of tenascin genes. *Cell Adhesion Migrat. 9*, 34–47. doi: 10.1080/19336918.2015.1008333

Crabbé, M., Dirkx, N., Casteels, C., and Laere, K., Van. (2019). Excitotoxic neurodegeneration is associated with a focal decrease in metabotropic glutamate receptor type 5 availability: an *in vivo* PET imaging study. *Sci. Rep.* 9:12916. doi: 10.1038/s41598-019-49356-x

Dai, Y., Sun, F., Zhu, H., Liu, Q., Xu, X., Gong, P., et al. (2019). Effects and mechanism of action of neonatal versus adult astrocytes on neural stem cell proliferation after traumatic brain injury. *Stem Cells* 37, 1344–1356. doi: 10.1002/stem.3060

Dixit, A., Mehta, R., and Singh, A. K. (2019). Proteomics in human Parkinson's disease: present scenario and future directions. *Cell. Mol. Neurobiol.* 39, 901–915. doi: 10.1007/s10571-019-00700-9

Dumitriu, A., Golji, J., Labadorf, A. T., Gao, B., Beach, T. G., Myers, R. H., et al. (2016). Integrative analyses of proteomics and RNA transcriptomics implicate mitochondrial processes, protein folding pathways and GWAS loci in Parkinson disease. *BMC Med. Genomics* 9:5. doi: 10.1186/s12920-016-0164-y

Friedman-Gohas, M., Elizur, S. E., Dratviman-Storobinsky, O., Aizer, A., Haas, J., Raanani, H., et al. (2020). FMRpolyG accumulates in FMR1 premutation granulosa cells. *J. Ovarian Res.* 13:22. doi: 10.1186/s13048-020-00623-w

Garcia-Arocena, D., Yang, J. E., Brouwer, J. R., Tassone, F., Iwahashi, C., Berry-Kravis, E. M., et al. (2009). Fibroblast phenotype in male carriers of FMR1 premutation alleles. *Hum. Mol. Genet.* 19, 299–312. doi: 10.1093/hmg/ddp497

Greco, C. M., Berman, R. F., Martin, R. M., Tassone, F., Schwartz, P. H., Chang, A., et al. (2006). *Neuropathology of fragile X-associated tremor/ataxia syndrome (FXTAS). Brain* 129, 243–255. doi: 10.1093/brain/awh683

Greco, C. M., Hagerman, R. J., Tassone, F., Chudley, A. E., Del Bigio, M. R., Jacquemont, S., et al. (2002). *Neuronal intranuclear inclusions in a new cerebellar tremor/ataxia syndrome among fragile X carriers. Brain* 125, 1760–1771. doi: 10.1093/brain/awf184

Greco, C. M., Soontrapornchai, K., Wirojanan, J., Gould, J. E., Hagerman, P. J., and Hagerman, R. J. (2007). *Testicular and pituitary inclusion formation in fragile X associated tremor/ataxia syndrome. J. Urol.* 177, 1434–1437. doi: 10.1016/j.juro.2006.11.097

Guerreiro, S., Privat, A.-L., Bressac, L., and Toulorge, D. (2020). CD38 in neurodegeneration and neuroinflammation. *Cells* 9:471. doi: 10.3390/cells9020471

Hagerman, P. J., and Hagerman, R. J. (2015). Fragile X-associated tremor/ataxia syndrome. *Ann. N. Y. Acad. Sci.*1338, 58–70. doi: 10.1111/nyas.12693

Hagerman, R. J., and Hagerman, P. (2016). Fragile X-associated tremor/ataxia syndrome-features, mechanisms and management. *Nat. Rev. Neurol.* 12, 403–412. doi: 10.1038/nrneurol.2016.82

Hagerman, R. J., Protic, D., Rajaratnam, A., Salcedo-Arellano, M. J., Aydin, E. Y., and Schneider, A. (2018). Fragile X-associated neuropsychiatric disorders (FXAND). *Front. Psychiatry*. 9:564. doi: 10.3389/fpsyt.2018.00564

Hall, D. A., Birch, R. C., Anheim, M., Jønch, A. E., Pintado, E., O'Keefe, J., et al. (2014). *Emerging topics in FXTAS. J. Neurodev. Disord.* 6:31. doi: 10.1186/1866-1955-6-31

Hoem, G., Raske, C. R., Garcia-Arocena, D., Tassone, F., Sanchez, E., Ludwig, A. L., et al. (2011). CGG-repeat length threshold for FMR1 RNA pathogenesis in a cellular model for FXTAS. *Hum. Mol. Genet.* 20, 2161–2170. doi: 10.1093/hmg/ddr101

Hondius, D. C., Van Nierop, P., Li, K. W., Hoozemans, J. J. M., Van Der Schors, R. C., Van Haastert, E. S., et al. (2016). Profiling the human hippocampal proteome at all pathologic stages of Alzheimer's disease. *Alzheimer's Dement.* 12, 654–668. doi: 10.1016/j.jalz.2015.11.002

Hu, A., Noble, W. S., and Wolf-Yadlin, A. (2016). Technical advances in proteomics: new developments in data-independent acquisition. *F1000Res.* 5:F1000 Faculty Rev-419. doi: 10.12688/f1000research.7042.1

Hunsaker, M. R., Greco, C. M., Spath, M. A., Smits, A. P. T., Navarro, C. S., Tassone, F., et al. (2011). *Widespread non-central nervous system organ pathology in fragile X premutation carriers with fragile X-associated tremor/ataxia syndrome and CGG knock-in mice. Acta Neuropathol.* 122, 467–479. doi: 10.1007/s00401-011-0860-9

Johnson, E. C. B., Dammer, E. B., Duong, D. M., Yin, L., Thambisetty, M., Troncoso, J. C., et al. (2018). *Deep proteomic network analysis*

of Alzheimer's disease brain reveals alterations in RNA binding proteins and RNA splicing associated with disease. Mol. Neurodegeneration 13:52. doi: 10.1186/s13024-018-0282-4

Kaplan, E. S., Cao, Z., Hulsizer, S., Tassone, F., Berman, R. F., Hagerman, P. J., et al. (2012). Early mitochondrial abnormalities in hippocampal neurons cultured from Fmr1 pre-mutation mouse model. *J. Neurochem*. 123, 613–621. doi: 10.1111/j.1471-4159.2012.07936.x

Khayachi, A., Gwizdek, C., Poupon, G., Alcor, D., Chafai, M., Cassé, F., et al. (2018). *Sumoylation regulates FMRP-mediated dendritic spine elimination and maturation. Nat. Commun*. 9:757. doi: 10.1038/s41467-018-03222-y

Kong, H. E., Zhao, J., Xu, S., Jin, P., and Jin, Y. (2017). Fragile X-associated tremor/ataxia syndrome: from molecular pathogenesis to development of therapeutics. *Front. Cell. Neurosci*. 11:128. doi: 10.3389/fncel.2017.00128

Krans, A., Skariah, G., Zhang, Y., Bayly, B., and Todd, P. K. (2019). Neuropathology of RAN translation proteins in fragile X-associated tremor/ataxia syndrome. *Acta Neuropathol. Commun.* 7:152. doi: 10.1186/s40478-019-0782-7

Krumova, P., and Weishaupt, J. H. (2013). Sumoylation in neurodegenerative diseases. *Cell Mol. Life Sci.* 70, 2123–2138. doi: 10.1007/s00018-012-1158-3

Lee, L., Sakurai, M., Matsuzaki, S., Arancio, O., and Fraser, P. (2013). *SUMO and Alzheimer's disease. NeuroMol Med.* 15, 720–736. doi: 10.1007/s12017-013-8257-7

Leehey, M. A., Berry-Kravis, E., Min, S.-J., Hall, D., Rice, C., Zhang, L., et al. (2007). Progression of tremor and ataxia in male carriers of the FMR1 premutation. *Movement Disord.* 22, 203–206. doi: 10.1002/mds.21252

Lewerenz, J., and Maher, P. (2015). Chronic glutamate toxicity in neurodegenerative diseases-what is the evidence? *Front. Neurosci.* 9:469. doi: 10.3389/fnins.2015.00469

Li, K. W., Ganz, A. B., and Smit, A. B. (2019). Proteomics of neurodegenerative diseases: analysis of human post-mortem brain. *J. Neurochem*. 151, 435–445. doi: 10.1111/jnc.14603

Liberzon, A., Birger, C., Ghandi, M., Jill, P., Tamayo, P., Jolla, L., et al. (2016). The molecular signatures database (MSigDB) hallmark gene set collection. *Cell Syst.* 1, 417–425. doi: 10.1016/j.cels.2015.12.004

Liu, L., Fujimoto, M., Nakano, F., Nishikawa, H., Okada, T., Kawakita, F., et al. (2018). *Deficiency of tenascin-c alleviates neuronal apoptosis and neuroinflammation after experimental subarachnoid hemorrhage in mice. Mol. Neurobiol.* 55, 8346–8354. doi: 10.1007/s12035-018-1006-z

Ma, L., Herren, A. W., Espinal, G., Randol, J., McLaughlin, B., Martinez-Cerdeño, V., et al. (2019). Composition of the intranuclear inclusions of fragile X-associated Tremor/Ataxia syndrome. *Acta Neuropathol. Commun.* 7, 1–26. doi: 10.1186/s40478-019-0796-1

Martínez Cerdeño, V., Hong, T., Amina, S., Lechpammer, M., Ariza, J., Tassone, F., et al. (2018). *Microglial cell activation and senescence are characteristic of the pathology FXTAS. Mov. Disord*. 33, 1887–1894. doi: 10.1002/mds.27553

Matsuzaki, S., Lee, L., Knock, E., Srikumar, T., Sakurai, M., Hazrati, L. N., et al. (2015). *SUMO1 affects synaptic* function, spine density and memory. *Sci. Rep.* 5:10730. doi: 10.1038/srep10730

Midwood, K. S., Chiquet, M., Tucker, R. P., and Orend, G. (2016). *Tenascin-C at a glance. J. Cell Sci.* 129, 4321–4327. doi: 10.1242/jcs.190546

Midwood, K. S., and Orend, G. (2009). *The role of tenascin-C in tissue injury and tumorigenesis. J. Cell Commun. Signal.* 3, 287–310. doi: 10.1007/s12079-009-0075-1

Mizuguchi, M., Otsuka, N., Sato, M., Ishii, Y., Kon, S., ichiro, Yamada, M., et al. (1995). *Neuronal localization of CD38 antigen in the human brain. Brain Res.* 697, 235–240. doi: 10.1016/0006-8993(95)00885-T

Napoli, E., Ross-Inta, C., Wong, S., Omanska-Klusek, A., Barrow, C., Iwahashi, C., et al. (2011). Altered zinc transport disrupts mitochondrial protein processing/import in fragile X-associated tremor/ataxia syndrome. *Hum. Mol. Genet*. 20, 3079–3092. doi: 10.1093/hmg/ddr211

Napoli, E., Schneider, A., Hagerman, R., Song, G., Wong, S., Tassone, F., et al. (2018). Impact of FMR1 premutation on neurobehavior and bioenergetics in young monozygotic twins. *Front. Genet*. 9:338. doi: 10.3389/fgene.2018.00338

Napoli, E., Song, G., Wong, S., Hagerman, R., and Giulivi, C. (2016). Altered bioenergetics in primary dermal fibroblasts from adult carriers of the FMR1 premutation before the onset of the neurodegenerative disease fragile X-associated tremor/ataxia syndrome. *Cerebellum* 15, 552–564. doi: 10.1007/s12311-016-0779-8

Noda, M., Takii, K., Parajuli, B., Kawanokuchi, J., Sonobe, Y., Takeuchi, H., et al. (2014). FGF-2 released from degenerating neurons exerts microglial-induced neuroprotection via FGFR3-ERK signaling pathway. *J. Neuroinflammation* 11, 1–11. doi: 10.1186/1742-2094-11-76

Norman, J. M., Cohen, G. M., and Bampton, E. T. W. (2010). The *in vitro* cleavage of the hAtg proteins by cell death proteases. *Autophagy* 6, 1042–1056. doi: 10.4161/auto.6.8.13337

Oh, S. Y., He, F., Krans, A., Frazer, M., Taylor Paul, J., Paulson, H. L., et al. (2015). RAN translation at CGG repeats induces ubiquitin proteasome system impairment in models of fragile X-associated tremor ataxia syndrome. *Hum. Mol. Genet*. 24, 4317–4326. doi: 10.1093/hmg/ddv165

Pasciuto, E., and Bagni, C. (2014a). SnapShot: FMRP interacting proteins. *Cell*. 159, 218–218.e1. doi: 10.1016/j.cell.2014.08.036

Pasciuto, E., and Bagni, C. (2014b). SnapShot: FMRP mRNA targets and diseases. *Cell 158,* 1446.e1–1446.e1. doi: 10.1016/j.cell.2014.08.035

Pretto, D. I., Hunsaker, M. R., Cunningham, C. L., Greco, C. M., Hagerman, R. J., Noctor, S. C., et al. (2013). *Intranuclear inclusions in a fragile X mosaic male. Transl. Neurodegener*. 2:10. doi: 10.1186/2047-9158-2-10

Pretto, D. I., Kumar, M., Cao, Z., Cunningham, C. L., Durbin-Johnson, B., Qi, L., et al. (2014). Reduced EAAT1 and mGluR5 expression in the cerebellum of FMR1 premutation carriers with FXTAS. *Neurobiol. Aging* 35, 1189–1197. doi: 10.1016/j.neurobiolaging.2013.11.009

proteinatlas.org. (2000). *The Human Protein Atlas.* Available online at: www.proteinatlas.org (accessed November 19, 2020).

Qurashi, A., Li, W., Zhou, J. Y., Peng, J., and Jin, P. (2011). *Nuclear accumulation of stress response mRNAs contributes to the neurodegeneration caused by fragile X premutation rCGG repeats. PLoS Genet.* 7:e1002102. doi: 10.1371/journal.pgen.1002102

Ramanan, V. K., and Saykin, A. J. (2013). Pathways to neurodegeneration: mechanistic insights from GWAS in Alzheimer's disease, Parkinson's disease, and related disorders. *Am. J. Neurodegener. Dis.* 2, 145–175.

Robin, G., López, J. R., Espinal, G. M., Hulsizer, S., Hagerman, P. J., and Pessah, I. N. (2017). *Calcium dysregulation and Cdk5-ATM pathway involved in a mouse model of fragile X-associated tremor/ataxia syndrome. Hum. Mol. Genet*. 26, 2649–2666. doi: 10.1093/hmg/ddx148

Rodriguez, C. M., and Todd, P. K. (2019). New pathologic mechanisms in nucleotide repeat expansion disorders. *Neurobiol. Dis.* 130:104515. doi: 10.1016/j.nbd.2019.104515

Ross-Inta, C., Omanska-Klusek, A., Wong, S., Barrow, C., Garcia-Arocena, D., Iwahashi, C., et al. (2010). Evidence of mitochondrial dysfunction in fragile X-associated tremor/ataxia syndrome. *Biochem. J.* 429, 545–552. doi: 10.1042/BJ20091960

Rovozzo, R., Korza, G., Baker, M. W., Li, M., Bhattacharyya, A., Barbarese, E., et al. (2016). *CGG repeats in the 5'UTR of FMR1 RNA regulate translation of other RNAs localized in the same RNA granules. PLoS ONE* 11:e0168204. doi: 10.1371/journal.pone.0168204

Sellier, C., Buijsen, R. A. M., He, F., Natla, S., Jung, L., Tropel, P., et al. (2017). Translation of expanded CGG repeats into FMRpolyG is pathogenic and may contribute to fragile X tremor ataxia syndrome. *Neuron* 93, 331–347. doi: 10.1016/j.neuron.2016.12.016

Seritan, A. L., Nguyen, D. V., Mu, Y., Tassone, F., Bourgeois, J. A., Schneider, A., et al. (2014). *Memantine for fragile x-associated tremor/ataxia syndrome: a randomized,* double-blind, placebo-controlled trial. *J. Clin Psychiatry*. 75, 264–271. doi: 10.4088/JCP.13m08546

Shiba, M., Fujimoto, M., Imanaka-Yoshida, K., Yoshida, T., Taki, W., and Suzuki, H. (2014). *Tenascin-C causes neuronal apoptosis after subarachnoid hemorrhage in rats. Transl. Stroke Res.* 5, 238–247. doi: 10.1007/s12975-014-0333-2

Subramanian, A., Tamayo, P., Mootha, V. K., Mukherjee, S., Ebert, B. L., Gillette, M. A., et al. (2005). Gene set enrichment analysis: a knowledge-based approach for interpreting genome-wide expression profiles. *Proc. Natl. Acad. Sci. U.S.A.* 102, 15545–15550. doi: 10.1073/pnas.0506580102

Suzuki, H., Kanamaru, K., Shiba, M., Fujimoto, M., Imanaka-Yoshida, K., Yoshida, T., et al. (2011). *Cerebrospinal fluid tenascin-C in cerebral vasospasm after aneurysmal subarachnoid hemorrhage. J. Neurosurg. Anesthesiol.* 23, 310–317. doi: 10.1097/ANA.0b013e31822aa1f2

Suzuki, H., Kanamaru, K., Suzuki, Y., Aimi, Y., Matsubara, N., Araki, T., et al. (2010). *Tenascin-C is induced in cerebral vasospasm after subarachnoid hemorrhage in rats and* humans: a pilot study. *Neurol. Res.* 32, 179–184. doi: 10.1179/174313208X355495

Tang, M., Lu, L., Xie, F., and Chen, L. (2018). SUMOylation of fragile X mental retardation protein: a critical mechanism of FMRP-mediated neuronal function. *Neurosci. Bull.* 34, 1100–1102. doi: 10.1007/s12264-018-0290-y

Tatham, M. H., Matic, I., Mann, M., and Hay, R. T. (2011). Comparative proteomic analysis identifies a role for SUMO in protein quality control. *Sci. Signal.* 4:rs4. doi: 10.1126/scisignal.2001484

Thul, P. J., Akesson, L., Wiking, M., Mahdessian, D., Geladaki, A., Ait Blal, H., et al. (2017). A subcellular map of the human proteome. *Science* 356:eaal3321. doi: 10.1126/science.aal3321

Todd, P. K., Oh, S., Krans, A., He, F., Sellier, C., Frazer, M., et al. (2013). CGG repeat-associated translation mediates neurodegeneration in fragile X tremor ataxia syndrome. *Neuron* 78, 440–455. doi: 10.1016/j.neuron.2013.03.026

Udalova, I. A., Ruhmann, M., Thomson, S. J. P., and Midwood, K. S. (2011). *Expression and immune function of tenascin-C. Crit. Rev. Immunol.* 31, 115–145. doi: 10.1615/CritRevImmunol.v31.i2.30

Westmark, C. J., and Malter, J. S. (2007). *FMRP mediates mGluR5-dependent translation of amyloid precursor protein. PLoS Biol.* 5:e52. doi: 10.1371/journal.pbio.0050052

Wiemann, S., Reinhard, J., and Faissner, A. (2019). *Immunomodulatory role of the extracellular matrix protein tenascin-C in neuroinflammation. Biochem. Soc. Trans.* 47, 1651–1660. doi: 10.1042/BST20190081

Wilson, R. S., and Nairn, A. C. (2018). *Cell-type-specific* proteomics: a neuroscience perspective. *Proteomes* 6:51. doi: 10.3390/proteomes6040051

Wilson, V. G., and Heaton, P. R. (2008). *Ubiquitin proteolytic* system: focus on SUMO. *Expert Rev. Proteomics* 5, 121–135. doi: 10.1586/14789450.5.1.121

Xie, K., Liu, Y., Hao, W., Walter, S., Penke, B., Hartmann, T., et al. (2013). *Tenascin-C deficiency ameliorates Alzheimer's disease-related pathology in mice. Neurobiol. Aging.* 34, 2389–2398. doi: 10.1016/j.neurobiolaging.2013.04.013

Yang, J. C., Niu, Y. Q., Simon, C., Seritan, A. L., Chen, L., Schneider, A., et al. (2014). Memantine effects on verbal memory in fragile X-associated tremor/ataxia syndrome (FXTAS): a double-blind brain potential study. *Neuropsychopharmacology* 39, 2760–2768. doi: 10.1038/npp.2014.122

Yang, J. C., Rodriguez, A., Royston, A., Niu, Y. Q., Avar, M., Brill, R., et al. (2016). Memantine improves attentional processes in fragile X-associated tremor/ataxia syndrome: electrophysiological evidence from a randomized controlled trial. *Sci. Rep.* 6:21719. doi: 10.1038/srep21719

Zhang, F., Ge, W., Ruan, G., Cai, X., and Guo, T. (2020). *Data-independent acquisition mass spectrometry-based proteomics and software tools: a glimpse in 2020. Proteomics* 20:e1900276. doi: 10.1002/pmic.201900276

Zhang, H., Wang, Y., Zhu, A., Huang, D., Deng, S., Cheng, J., et al. (2016). SUMO-specific protease 1 protects neurons from apoptotic death during transient brain ischemia/ reperfusion. *Cell Death Dis.* 7:e2484. doi: 10.1038/cddis.2016.290

Zheng, Q., Huang, T., Zhang, L., Zhou, Y., Luo, H., Xu, H., et al. (2016). *Dysregulation of ubiquitin-proteasome system in neurodegenerative diseases. Front. Aging Neurosci.* 8:303. doi: 10.3389/fnagi.2016.00303

Conflict of Interest: The authors declare that the research was conducted in the absence of any commercial or financial relationships that could be construed as a potential conflict of interest.

frontiers in Genetics

ORIGINAL RESEARCH
published: 09 February 2021
doi: 10.3389/fgene.2021.591211

A Unique Visual Attention Profile Associated With the *FMR1* Premutation

*Molly Winston[1], Kritika Nayar[1], Emily Landau[1], Nell Maltman[1], John Sideris[2], Lili Zhou[3], Kevin Sharp[3], Elizabeth Berry-Kravis[3] and Molly Losh[1]**

[1]Roxelyn and Richard Pepper Department of Communication Sciences and Disorders, Northwestern University, Evanston, IL, United States, [2]Chan Division of Occupational Science and Occupational Therapy, University of Southern California, Los Angeles, CA, United States, [3]Department of Pediatrics, Rush University Medical Center, Chicago, IL, United States

Atypical visual attention patterns have been observed among carriers of the fragile X mental retardation gene (*FMR1*) premutation (PM), with some similarities to visual attention patterns observed in autism spectrum disorder (ASD) and among clinically unaffected relatives of individuals with ASD. Patterns of visual attention could constitute biomarkers that can help to inform the neurocognitive profile of the PM, and that potentially span diagnostic boundaries. This study examined patterns of eye movement across an array of fixation measurements from three distinct eye-tracking tasks in order to investigate potentially overlapping profiles of visual attention among PM carriers, ASD parents, and parent controls. Logistic regression analyses were conducted to examine whether variables constituting a PM-specific looking profile were able to effectively predict group membership. Participants included 65 PM female carriers, 188 ASD parents, and 84 parent controls. Analyses of fixations across the eye-tracking tasks, and their corresponding areas of interest, revealed a distinct visual attention pattern in carriers of the *FMR1* PM, characterized by increased fixations on the mouth when viewing faces, more intense focus on bodies in socially complex scenes, and decreased fixations on salient characters and faces while narrating a wordless picture book. This set of variables was able to successfully differentiate individuals with the PM from controls (Sensitivity = 0.76, Specificity = 0.85, Accuracy = 0.77) as well as from ASD parents (Sensitivity = 0.70, Specificity = 0.80, Accuracy = 0.72), but did not show a strong distinction between ASD parents and controls (Accuracy = 0.62), indicating that this set of variables comprises a profile that is unique to PM carriers. Regarding predictive power, fixations toward the mouth when viewing faces was able to differentiate PM carriers from both ASD parents and controls, whereas fixations toward other social stimuli did not differentiate PM carriers from ASD parents, highlighting some overlap in visual attention patterns that could point toward shared neurobiological mechanisms. Results demonstrate a profile of visual attention that appears strongly associated with the *FMR1* PM in women, and may constitute a meaningful biomarker.

Keywords: autism spectrum disorder, social cognition, pragmatic language, eye tracking, fragile X mental retardation gene, fragile X syndrome

OPEN ACCESS

Edited by:
Laia Rodriguez-Revenga, Hospital Clínic de Barcelona, Spain

Reviewed by:
Maud de Dieuleveult, Assistance Publique Hopitaux De Paris, France
Randi Jenssen Hagerman, UC Davis, United States

***Correspondence:**
Molly Losh
m-losh@northwestern.edu

Specialty section:
This article was submitted to Genetics of Common and Rare Diseases, a section of the journal Frontiers in Genetics

Received: *04 August 2020*
Accepted: *11 January 2021*
Published: *09 February 2021*

Citation:
Winston M, Nayar K, Landau E, Maltman N, Sideris J, Zhou L, Sharp K, Berry-Kravis E and Losh M (2021) A Unique Visual Attention Profile Associated With the FMR1 Premutation. Front. Genet. 12:591211. doi: 10.3389/fgene.2021.591211

INTRODUCTION

A range of clinical and subclinical phenotypes result from mutations in the fragile X mental retardation gene (*FMR1*) on the X-chromosome involving a cytosine-guanine-guanine (CGG) repeat expansion in the promotor region of the gene (Bagni and Oostra, 2013). Specifically, a CGG repeat expansion of greater than 200 causes fragile X syndrome (FXS) and inhibits the production of the fragile X mental retardation protein (FMRP), a critical protein involved in synaptic pruning and neural maturation during development (Weiler and Greenough, 1999). FXS is characterized by developmental delays in language, intellectual ability, and social cognition, as well as increased anxiety, and is the leading single-gene disorder associated with autism spectrum disorder (ASD; Bailey et al., 2001; Hernandez et al., 2009). Whereas FXS has a prevalence of around 1 in 4,000 males and 1 in 7,000–10,000 females, the *FMR1* premutation (PM; *FMR1* expansion between 55 and 200 CGG repeats) is more prevalent and occurs in approximately 1 in 468 males and 1 in 151 females in the United States (Seltzer et al., 2012). The *FMR1* PM is also associated with a range of clinical phenotypes, including higher rates of psychiatric and medical comorbidities (Hagerman and Hagerman, 2002; Bourgeois et al., 2011; Besterman et al., 2014).

The PM has unique clinical risks, such as the potential presence of a Parkinson-like neurodegenerative disorder, fragile X-associated tremor and ataxia syndrome (FXTAS), which develops in a subset of carriers with the PM in advanced age (Hagerman et al., 2004). The PM is also associated with a higher risk of psychiatric disorders, including elevated rates of depression and anxiety (Hunter et al., 2008; Bourgeois et al., 2011). Differences in executive skills have also been reported, including working memory, inhibitory control, and processing speed (Wang et al., 2013; Shelton et al., 2014, 2015, 2016). Subclinical phenotypic differences have also been documented in social cognition (Cornish et al., 2005; Losh et al., 2008), language processing (Nayar et al., 2019), and social language use (Losh et al., 2012; Klusek et al., 2016) in women with the PM. Manifestation of the PM phenotype is thought to be in part related to molecular-genetic differences including levels of FMRP and CGG repeat length (Wheeler et al., 2014). Specifically, with respect to this study, some literature suggests that this variation is specifically related to social language (Klusek et al., 2018b) and fixation patterns (Nayar et al., 2019; Winston et al., 2020), although evidence is mixed (Cornish et al., 2005; Wheeler et al., 2014; Klusek et al., 2018a).

There is evidence to suggest that women with the PM may also display differences in patterns of visual fixation, which could reflect underlying differences in social processing and/or cognitive styles, potentially relating to observable clinical-behavioral features. For example, recent work has demonstrated less fluid and coordinated eye-voice control, wherein PM carriers displayed a greater number of repeat fixations during a task of concurrent eye tracking and language processing (Nayar et al., 2019). This less efficient eye-voice coordination not only related to reduced language automaticity and fluency, but also related to greater social language atypicalities and underlying molecular-genetic variation among PM carriers. In another study that examined looking patterns during a face processing task displaying face stimuli exhibiting either direct vs. averted gaze, Klusek et al. (2017) found that women with the PM did not show a preference for either gaze type; in contrast, controls demonstrated a clear attentional preference toward faces showing direct gaze. Importantly, increased dwell time (i.e., time spent fixating on a certain stimulus) on faces exhibiting direct gaze was associated with better social language use in controls but not in the PM, suggesting that PM carriers may not effectively capitalize on information from the eye region of the face. Relatedly, when women with the PM were asked to passively view a series of affective facial expressions, Winston et al. (2020) found that PM carriers displayed an atypical fixation pattern characterized by reduced attention to the eyes and increased attention to the mouth compared to control participants. Interestingly, this atypical fixation pattern was associated with better social language and social cognitive abilities in PM carriers, suggesting that the unique fixation pattern in PM carriers in this task may reflect different strategies for emotion processing than those employed by controls. Together, these results suggest that carriers of the PM demonstrate a different fixation style than controls which may be uniquely modulating social cognition and social language use.

Some studies have also demonstrated phenotypic similarities between carriers of the *FMR1* PM and first-degree relatives of individuals with ASD, who display subtle social cognitive and social language differences as well that are believed to reflect underlying genetic liability to ASD. Specifically, there is evidence that both PM carriers and parents of individuals with ASD show differences from controls on tasks tapping social cognition, such as when asked to infer emotions from the eye region of the face (Cornish et al., 2005; Losh et al., 2009). Moreover, a subgroup of parents of individuals with ASD as well as PM carriers demonstrate a constellation of subclinical traits that parallel the core features of ASD, referred to as the broad autism phenotype (BAP; Losh et al., 2012; Schneider et al., 2016). Indeed, results from Losh et al. (2012) suggest that PM carriers demonstrate elevated levels of personality traits (such as greater social aloofness and rigidity) and social language features consistent with that of the BAP. In addition, higher rates of clinical ASD have also been reported among PM carriers (Clifford et al., 2007).

Individuals with ASD as well as their parents show differences in gaze that complement the patterns observed in the PM. Many studies have shown that individuals with ASD tend to look less at the eyes when exploring faces and more at the mouth (Klin et al., 2002), spend less time looking at social features in scenes (Lee et al., 2019) and demonstrate decrease gaze-language coordination (Nayar et al., 2018) compared to controls. In parents of individuals with ASD, Lee et al. (2019) additionally demonstrated that parents of individuals with ASD who met criteria for the BAP showed distinct gaze profiles when viewing emotionally evocative scenes depicted in the thematic apperception test (TAT), allotting greater attention to faces in scenes in which the faces were featured most prominently, and more attention toward the setting in more

complex images with salient setting features. These differences in viewing patterns were associated with the quality of participants' narratives when telling stories about these scenes (particularly in the group which met criteria for the BAP), suggesting that atypical attentional patterns importantly relate to social communication. Furthermore, Nayar et al. (2018) observed that parents of individuals with ASD, particularly those who met criteria for the BAP, had reduced eye-voice coordination during rapid automatized naming, which was similarly linked with social language abilities, mirroring results reported among female carriers of the *FMR1* PM (Nayar et al., 2019). Together, results demonstrate that parents of individuals with ASD may demonstrate complementary looking patterns to PM carriers, potentially suggesting similar biological underpinnings of these shared phenotypic features.

Given the complex clinical and neurocognitive phenotypes associated with the *FMR1* PM, there is a need for research investigating endophenotypes, or intermediate phenotypes associated with a disorder or condition, but more proximally related to underlying genetics (Gottesman and Gould, 2003). Visual attention profiles may constitute a candidate endophenotype in the PM that overlaps with parents of individuals with ASD. Visual attention is easy to assay and holds strong connections to underlying biology, which may be relatable to downstream clinical-behavioral features that can be used to stratify biologically meaningful subgroups that may cross standard diagnostic boundaries (Frazier et al., 2016, 2018; Pierce et al., 2016). Studying how such potential endophenotypes may overlap in the *FMR1* PM and ASD relatives could offer insight into the potential role of the *FMR1* gene in ASD-related phenotypes. In this way, single-gene disorders such as FXS and others (e.g., 22q11.2 deletion syndrome and Angelman syndrome) have informed understanding of ASD-related phenotypes linked to known genetic variation (Peters et al., 2004; Fine et al., 2005).

A challenge to understanding whether visual attention profiles might constitute such endophenotypes, however, is that most studies of visual attention have focused on single tasks within a participant group, leaving unclear whether more pervasive visual attention profiles might exist across different contexts. It is possible that findings may be task dependent, as seen in other populations (Chawarska et al., 2012), and that important, broader attentional patterns might be revealed by examining performance over multiple tasks and contexts. Therefore, this study aimed to explore patterns of gaze across a series of different eye tracking tasks tapping social attention in complementary ways, including passive viewing of affective facial expressions, tasks requiring narration from a picture book, and a set of emotionally evocative scenes. This study makes use of existing fixation data previously analyzed independently only for group comparisons (Lee et al., 2019; Winston et al., 2020), as well as newly processed data from ASD parents and PM carriers, to build on prior work by applying a more powerful, statistically-driven, cross-contextual approach that combines such existing data within the same participants to characterize more comprehensive fixation profiles that may be characteristic of the PM phenotype, or potentially show overlap with ASD-related profiles. The primary goal of the study was to characterize fixation patterns across tasks that might best predict group membership, and in the case of carriers of the *FMR1* PM, potentially constitute specific gaze profiles associated with *FMR1* as well as identify areas of overlap among groups. We predicted that PM carriers would demonstrate a distinct fixation pattern that could be used to differentiate them from controls with high sensitivity and specificity, but not necessarily from parents of individuals with ASD, due to prior literature suggesting overlapping phenotypic features. Knowledge of such profiles could help to inform the phenotypic expression of the *FMR1* PM, and whether phenotypic overlap exists within related conditions. This information would be informative for stratifying groups based on shared phenotypes, for clinical and research purposes.

MATERIALS AND METHODS

Participants

Participants included 65 adult females with the *FMR1* PM (PM group), 188 parents of individuals with ASD (ASD parent group), and 84 parent controls (control group). As noted previously, a subset of participants was included in two previous reports examining the eye tracking tasks in isolation (Lee et al., 2019; Winston et al., 2020). New data are included as well, consisting of fixations to the facial stimuli task for ASD parents (whose fixation data to the narrative tasks were included in Lee et al., 2019) and fixation data from the two narrative tasks for PM carriers (whose face fixation data were reported previously in Winston et al., 2020). The aims, analyses, and results addressed in the present study are unique and have not been previously examined. The previously published research and rich existing dataset available for this study permitted a statistically-driven approach to investigate fixations across different social-emotional stimuli that might reveal visual fixation profiles that serve as endophenotypic markers. Control families were screened for personal or family history of ASD, FXS, or related neurodevelopmental disorders, including language-related delays. Carrier status was confirmed through analysis of CGG repeats either within the experimental protocol or confirmation from medical records. All participants were under the age of 66. Participants with the *FMR1* PM were additionally screened for FXTAS symptoms. Participants were also excluded if their Full Scale IQ was below 80 [obtained using the Wechsler Abbreviated Scale of Intelligence (WASI; Wechsler, 1999)]. The WASI was administered to all participants by a trained examiner and conducted in the laboratory, a quiet space in the participant's home, or another controlled environment that was convenient for participants if travel to the lab was not possible. The procedures for task administration were consistent across all tasks and groups, as described in Winston et al. (2020) and Lee et al. (2019). Significant differences between groups emerged for age (p = 0.006) and Full Scale IQ (p = 0.02); however, age was not associated with outcome variables (ps > 0.26), and IQ was only associated with one outcome variable (looking time toward faces; p = 0.02), and so were not included in

subsequent analyses (see **Table 1**). Additionally, because this study investigated the utility of eye tracking to classify groups, it was important to allow for full phenotypic variability, which may include differences in cognition. Sex differences within the control group and ASD parent group were assessed for the primary outcome variables using independent samples *t*-tests. No significant differences were observed (*ps* > 0.18), so the male and female groups were combined for data analyses. The study protocol was approved by Northwestern University's Institutional Review Board.

Eye-Tracking Stimuli

Wordless Picture Book

Participants viewed a 24-page wordless picture book, *Frog Where Are You?* (Mayer, 1969), about a boy and his dog searching for their lost pet frog. This picture book has been used frequently in studies of narrative across populations, and recently, to study visual attention during narration (Thurber and Tager-Flusberg, 1993; Tager-Flusberg, 1995; Losh and Capps, 2003; Norbury and Bishop, 2003; Reilly et al., 2004; Diehl et al., 2006; Colle et al., 2008; Sah and Torng, 2015). Participants narrated the story as they simultaneously viewed each page of the picture book on an eye-tracker. There was no time limit for completing the task. Administration methods were consistent with previous studies using this picture book task.

Thematic Apperception Test

Participants were shown a subset of six images varying in complexity from the TAT (Murray, 1943), a projective psychological test that uses ambiguous images. The TAT has been used in previous studies to elicit narratives, and the six images were selected to align with previous work (Lee et al., 2019). Participants viewed each image for 8 s and then were asked to tell a story about the image with a beginning, middle, and end and with details about the character's thoughts, feelings, and actions.

Affective Facial Expressions

Images from the NimStim Facial Stimulus Set (Farzin et al., 2009; Tottenham et al., 2009) were presented to participants and depicted happy, calm, and fearful faces. There were a total of 60 faces, comprised of 20 happy, 20 calm, and 20 fearful. In accordance with procedures outlined in Winston et al. (2020), participants first viewed a gray screen, then a scrambled face controlling for luminance for 1 s, and then a face depicting an emotion for 3 s.

TABLE 1 | Ratio of sex distribution, mean (M), and standard deviation (SD) for chronological age and IQ across groups.

	Control group *M (SD)*	ASD parent group *M (SD)*	PM group *M (SD)*
Males:Females	31:53	69:119	0:64
Chronological age	41.84 (10.11)	46.09 (7.86)	45.28 (10.17)
Full-scale IQ	116.85 (10.26)	111.67 (11.65)	111.84 (9.94)
CGG repeats	--	30.41 (4.23)	88.76 (16.64)
Quantitative FMRP	--	0.02 (0.008)	0.02 (0.008)
Activation ratio	--	--	0.47 (0.24)

M = mean; SD = standard deviation.

Data Processing

All tasks were presented to participants on a Tobii T60 eye tracker and gaze data were recorded from both eyes. For the picture book task, areas of interest (AOIs) were established including animate (i.e., all characters), protagonist (i.e., boy, dog, and frog), inanimate (i.e., setting), and the protagonist's focus of attention (i.e., where the protagonist is looking) regions. For the TAT task, AOIs included animate, face, body, and inanimate regions. AOIs from the TAT were generated for each image separately which corresponded to a category based on the predominant AOIs (setting, bodies, and faces). AOIs were expanded by 10% to account for loss of tracked fixations. For the TAT task, data for an image were excluded if there was less than 4 s of tracked fixations (out of a possible 8 s maximum). See (Lee et al., 2019) for a detailed explanation of eye tracking and quality control procedures for the picture book and TAT stimuli.

For the NimStim Facial Stimulus Set (AFE task), AOIs were established for the eyes, nose, and mouth regions of each face, and fixations to AOIs were analyzed by the proportion fixation duration to AOIs. Images were excluded if there were less than 50% of fixations for each image and if 50% of all trials were poor quality. See Winston et al. (2020) for an in-depth explanation of eye tracking and quality control procedures for pupil diameter and gaze fixation data.

Clinical-Behavioral Characteristics

Social Cognition

Participants completed the Reading the Mind from the Eyes Task (Baron-Cohen et al., 2001) where they were required to infer complex psychological expressions from a pair of eyes. There were 36 images of eyes. Scores were determined by the proportion of correct responses out of 36 (i.e., the maximum number of potential correct responses).

Social Language

The Pragmatic Rating Scale (PRS; Landa et al., 1992) was used to assess social language. Participants engaged in a semi-structured conversation about their life experiences, and the interactions were coded by raters blind to diagnosis status for pragmatic language violations (e.g., excessive detail and informal language).

Personality Features

Personality features related to the BAP (e.g., aloofness and rigidity) was assessed using the self-report version of the Broad Autism Phenotype Questionnaire (BAPQ; Hurley et al., 2007). The BAPQ consists of 36 items which were rated on a 6-point Likert scale ranging from "very rarely" to "very often."

FMR1 Molecular Characterization

Blood samples were collected from 49 PM carriers and processed to determine CGG repeat length, quantitative FMRP (pg/ug), and activation ratio (i.e., the percentage of cells which contain an X chromosome with an unaffected *FMR1* gene). FMRP was derived using the Luminex Technology immunoassay whereas *FMR1* genotyping was done with a highly sensitive PCR method (Asuragen; Filipovic-Sadic et al., 2010; LaFauci et al., 2013), and activation ratio was determined by a Southern blot protocol (Berry-Kravis et al., 2005; LaFauci et al., 2013). CGG repeat length and FMRP were also ascertained on 108 ASD parents using the aforementioned protocols.

Data Analysis Plan

Variable Selection

To determine the set variables across tasks which could be used as predictors of PM status, potentially constituting a PM-specific visual attention profile, group differences between individuals with the PM and controls were explored across the primary variables in each eye-tracking task using independent samples *t*-tests. One variable per task or per image if indicated for the TAT was then selected for subsequent profile analyses based on significance and effect size. Variability was also examined using normality statistics to assess for possible reasons for subsequent findings of measurement variance. Investigating across AOIs derived from the PB, PM carriers differed most from controls in their looking time toward the protagonist's focus of attention (PB-FOA; $t = 3.20$, $p = 0.002$, $d = 0.53$). Within the TAT, in the setting based slides, the PM carriers spent less time than controls looking at faces in one of two setting-dominated scenes depicting a surgical procedure (TAT Setting-Faces; $t = 2.15$, $p = 0.03$, $d = 0.35$) as well as in one of two body-dominant scenes (TAT Bodies-Faces; $t = 2.07$, $p = 0.04$, $d = 0.33$). Furthermore, within the TAT, PM carriers spent more time fixating on bodies in one of two face-dominant scenes (TAT Faces-Bodies; $t = -1.89$, $p = 0.03$, $d = 0.31$). As noted previously, findings related to differences between the ASD parent and control group in the context of the PB and TAT have been previously published (Lee et al., 2019). Finally, across all faces employed in the passive viewing task of affective facial expressions, PM carriers spent significantly more time fixating on the mouth compared to controls (AFE-Mouth; $t = -39.95$, $p < 0.001$, $d = -6.57$). Results related to this difference have been reported in greater detail in Winston et al. (2020).

Logistic Regression

Logistic regressions were conducted to assess the utility of a set of variables in which the PM carriers differed from controls as predictors of group membership. For logistic regressions, variables in which the PM group differed from controls were entered into the model (i.e., PB-FOA, TAT Setting-Faces, TAT Bodies-Faces, TAT Faces-Bodies, and AFE-Mouth), and predictive power was assessed. The mice package in *R Studio* was used for multiple imputation using chained equations with predictive mean matching to address missingness across tasks (van Buuren and Groothuis-Oudshoorn, 2011) using 70 imputed datasets using calculations based on missingness detailed in von Hippel (2020). Overall, 30% of the observations was imputed, 10% from the PB, 32% from TAT, and 70% from AFE. This imputation method takes into account all relevant fixation variables as well as group status to make predictions for missing values allowing for robust predictions despite great degrees of missingness (Vink et al., 2014). Pooled parameter results were obtained including pooled r^2, area under the curve (AUC; broadly denoting accuracy), and coefficients with the psfmi package. Variable selection was conducted using the backward stepwise selection and the pooling sampling variance method using a p-criterion of 0.10 to allow for a more exploratory approach.

Additional analyses of specificity and sensitivity were conducted on the stacked dataset, which has been shown to yield comparable results to more complex methodology (Thao and Geskus, 2019). A series of pairwise logistic regression analyses were conducted to assess the variables' predictive power and discriminability between the PM and control groups, PM and ASD parent group, and ASD parent and control group.

Correlations With *FMR1*-Related Variation

Pearson correlations were conducted to investigate relationships between key variables of interest and *FMR1* molecular-genetic variation in the PM group and ASD parent group.

Secondary Analysis of Group Classification Results

Using Mann-Whitney *U* tests to account for unequal sample sizes, we examined whether PM carriers who were misclassified in the logistic regression model as ASD parents might display higher rates of ASD-related features that comprise the BAP (e.g., pragmatic language differences), and may also show differences in *FMR1*-related molecular-genetic variability. Imputed values were averaged for these exploratory analyses due to constraints of the use of pooled imputed datasets. We also explored whether children with FXS of the misclassified PM parents may exhibit differences in ASD symptoms from children of correctly classified parents, by examining ASD symptom severity on the Autism Diagnostic Observation Schedule-2 (ADOS-2; Lord et al., 2001; Gotham et al., 2008).

RESULTS

Logistic Regression

PM Group vs. Control Group

Results indicate that PB-FOA and AFE-Mouth were all significant predictors of group status independently (*ps* < 0.05), with an overall pooled $r^2 = 0.30$ and AUC of 0.78 (maximum specificity = 0.71 and sensitivity = 0.68). The simplest model maintaining predictive power included only the PB-FOA and AFE-Mouth, with a pooled ROC of 0.77 (maximum specificity = 0.85 and sensitivity = 0.76). This model, conducted in the averaged imputed dataset, correctly classified 92% of the participants (77/84) from the control group and 68% PM carriers (44/65).

PM Group vs. ASD Parent Group

With each variable comprising the composite entered in the logistic regression model AFE-Mouth was the only independent significant predictor of group status ($p < 0.001$). Overall, the model incorporating all variables was able to predict group status with a pooled AUC of 0.74 (maximum specificity = 0.71, sensitivity = 0.68). The stepwise logistic regression model only maintained AFE-Mouth with a pooled AUC of 0.72 (maximum specificity = 0.80 and sensitivity = 0.70). This model, conducted in the average imputed dataset, correctly classified 98% of the ASD parents (183/188) and 62% of the PM carriers (40/65).

ASD Parent Group vs. Control Group

Of all the variables included in the model, only PB-FOA was a significant predictor of group status ($p = 0.05$). Together, the model with all variables had a pooled AUC of 0.62 ($r^2 = 0.05$; maximum specificity = 0.59 and sensitivity = 0.56). The stepwise regression model only maintained PB-FOA and comparable accuracy (0.60), specificity (0.52), and sensitivity (0.62). The final model correctly classified 98% of the ASD parents (185/188) and 4% of the control participants (3/84).

See **Figure 1** for all pairwise ROC curves. See **Table 2** for model parameters for each logistic regression model.

Correlations With *FMR1*-Related Variation

In the PM group, there were no significant correlations between CGG repeat length, FMRP, or activation ratio (*ps* > 0.13) and any of the eye-tracking variables [*note*: a significant correlation between CGG repeats and AFE-mouth was similarly not observed in Winston et al. (2020)]. In the ASD parent group, increased CGG repeats were associated with increased time spent looking at the mouth in the AFE task ($r = 0.45$, $p = 0.005$) as well as decreased time spent looking at the face in the TAT ($r = –0.22$, $p = 0.037$; see **Figure 2**). No associations were observed with FMRP in the ASD parent group (*ps* > 0.13).

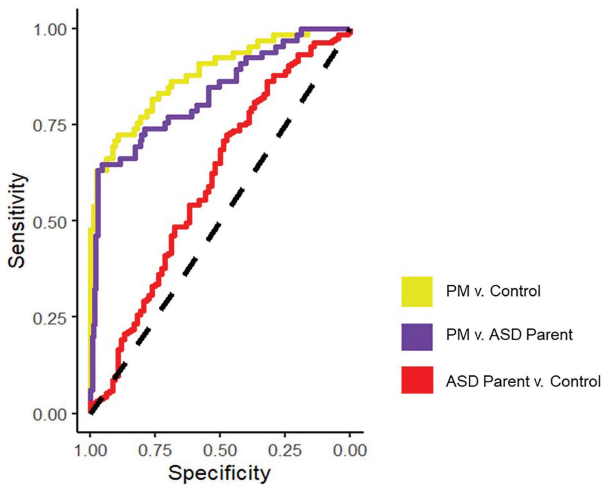

FIGURE 1 | ROC curves assessing discriminability across groups for the final logistic regression models on the averaged datasets.

Secondary Analyses of Misclassified PM Carriers

Exploratory analyses investigated whether those PM carriers who were misclassified as ASD parents ($n = 25$) might differ from correctly classified PM carriers along any clinical-behavioral characteristics. Results indicated that PM carriers who were incorrectly identified as ASD parents demonstrated greater pragmatic language violations as reflected by the dominating conversation factor (e.g., overly talkative and tangential; $U = 244.50$, $p = 0.006$) and marginally greater FMRP than the correctly classified carriers ($U = 155.00$, $p = 0.08$). They did not differ on any other features, including personality features of the BAP, social cognition, IQ or age (*ps* > 0.17). See **Figure 3** for all group comparisons.

There were 13 children included in analyses for the 25 PM carriers who were misclassified as ASD parents and 17 children included in analyses for the 40 correctly classified PM carriers. Results demonstrated that children of the misclassified PM carriers had marginally higher ASD symptom severity ($U = 67.00$, $p = 0.07$) and displayed more restrictive and repetitive behaviors ($U = 63.50$, $p = 0.05$; See **Figure 4**).

DISCUSSION

The present study examined patterns of looking across three separate eye tracking tasks in female carriers of the *FMR1* PM, parents of individuals with ASD, and controls, using a series *t*-tests and logistic regression analyses to investigate whether there may exist patterns of visual fixations across eye-tracking tasks, representing a PM-specific profile, that could effectively predict group membership. Results demonstrated that female carriers of the *FMR1* PM showed a distinct looking pattern in the affective facial expressions task, but across the other two tasks (i.e., a wordless picture book and images from the thematic apperception task), exhibited fixation patterns that were similar to ASD parents. Analysis of group classification revealed that this looking pattern may also be used to further differentiate a subgroup of PM carriers who display some degree of subclinical ASD-related features.

The PM Profile was comprised of variables across each of the three eye-tracking tasks in which PM carriers differed from controls with the highest effect size, including (1) time spent fixating on the protagonists' focus of attention in the wordless picture book (PB), (2) time spent fixating on faces and bodies in complex social scenes (TAT), and (3) time spent fixating on the mouth in the NimStim passive viewing task of affective facial expressions (AFE). Logistic regression analyses revealed differences in predictive power across these variables, highlighting the importance of fixations towards the mouth in particular in differentiating PM carriers from both ASD parents and controls. This finding is consistent with previous research suggesting that individuals with the *FMR1* PM attend to different features of the face (i.e., the mouth), whereas controls typically fixate on the eye region of the face (Bentin et al., 1996; Farroni et al., 2002; Henderson et al., 2005). Interestingly, in prior work, parents of individuals with ASD showed greater reliance on the mouth than other areas of the

TABLE 2 | Model parameters for each logistic regression model.

	Predictor	Original model			Final model		
		Estimate	Confidence interval	*p*	Estimate	Confidence interval	*p*
PM vs. TD							
TAT	Setting: Faces[3]	−0.01	−0.05, 0.03	0.56	--	--	--
	Bodies: Faces[1]	−0.002	−0.03, 0.03	0.89	--	--	--
	Faces: Bodies[2]	0.004	−0.04, 0.04	0.85	--	--	--
Picture book	Focus of attention	−0.13	−0.26, −0.003	0.05	−0.15	−0.27, −0.04	0.008
Affective facial expressions	Mouth	0.03	0.01, 0.05	0.001	0.03	0.01, 0.05	<0.001
PM vs. ASD parents							
TAT	Setting: Faces[4]	−0.02	−0.04, 0.01	0.20	--	--	--
	Bodies: Faces[2]	0.01	−0.01, 0.03	0.49	--	--	--
	Faces: Bodies[1]	0.005	−0.02, 0.03	0.67	--	--	--
Picture book	Focus of attention[3]	−0.06	−0.17, 0.05	0.29	--	--	--
Affective facial expressions	Mouth	0.03	0.01, 0.05	<0.001	0.03	0.01, 0.04	<0.001
ASD parents vs. TD							
TAT	Setting: Faces[3]	0.002	−0.02, 0.02	0.83	--	--	--
	Bodies: Faces[1]	−0.01	−0.03, 0.01	0.36	--	--	--
	Faces: Bodies[4]	0.0002	−0.02, 0.02	0.99	--	--	--
Picture book	Focus of attention	−0.09	−0.18, −0.01	0.04	−0.11	−0.19, −0.02	0.02
Affective facial expressions	Mouth[2]	0.0006	−0.01, 0.01	0.91	--	--	--

Superscript denotes when the variable was excluded in the stepwise logistic regression procedure.

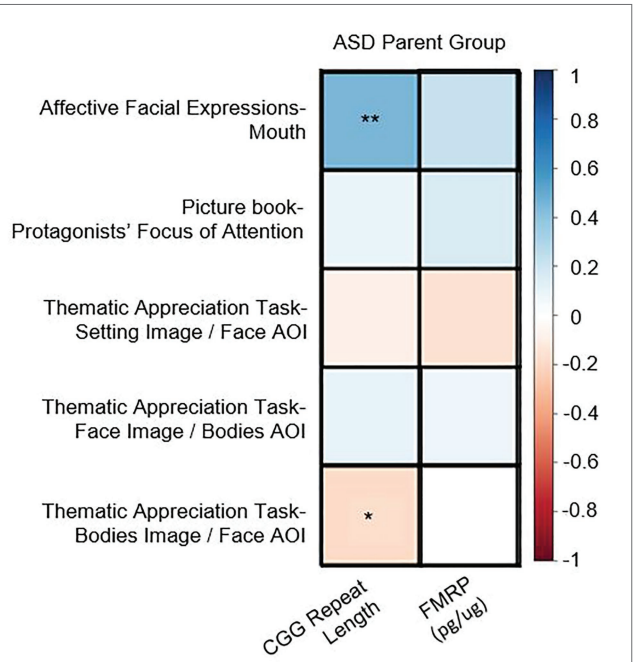

FIGURE 2 | Correlation matrix for genetics associations observed in the autism spectrum disorder (ASD) parent group across key areas of interest (AOI; $^{*}p < 0.05$, $^{**}p < 0.01$).

face when making affective judgments (Adolphs et al., 2008), and differences in facial processing have also been noted (Losh et al., 2009), and linked to underlying neural correlates such as amygdala activation (Yucel et al., 2015), similar to findings from studies of PM males (Hessl et al., 2007). However, results from the present study highlight looking towards the mouth as a more specific predictor of PM status, despite some differences present in ASD parents as well. A prior study including a subset of the present sample demonstrated that increased time spent fixating on the mouth was associated with better social cognitive abilities and fewer pragmatic (i.e., social) language violations (Winston et al., 2020). Likewise, Klusek et al. (2017) showed that PM carriers did not demonstrate a preference towards direct gaze compared to averted gaze, and there was no relationship between time spent fixating on the eyes and better pragmatic language abilities, in contrast to results observed in the control group. Taken together with prior work, these findings might suggest that PM carriers use different visual processing strategies which may affect social engagement.

The other variables which comprise the PM Profile were not statistically selected in analyses using backward selection for the PM and ASD parent groups and are particularly noteworthy given prior evidence of phenotypic similarities between these groups, including pragmatic language, social cognition, and personality features consistent with the BAP (Losh et al., 2012; Klusek et al., 2017). When examining social scenes, parents of individuals with ASD included in the present study, particularly those exhibiting features of the BAP, spent more time fixating on the background of complex social scenes in the TAT (Lee et al., 2019), which is consistent with patterns observed in the PM in which they spent less time fixating on emotionally salient aspects of scenes (e.g., faces). This similarity in looking patterns may account for the results here indicating that individual fixations within scenes in the TAT and PB were unable to differentiate group the PM group from the ASD parent group with sufficient sensitivity and specificity. Therefore, while these particular AOIs may not be informative in differentiating the PM group from the ASD parent group, they may be useful in tapping similarities in neurobiology or genetics underlying attention

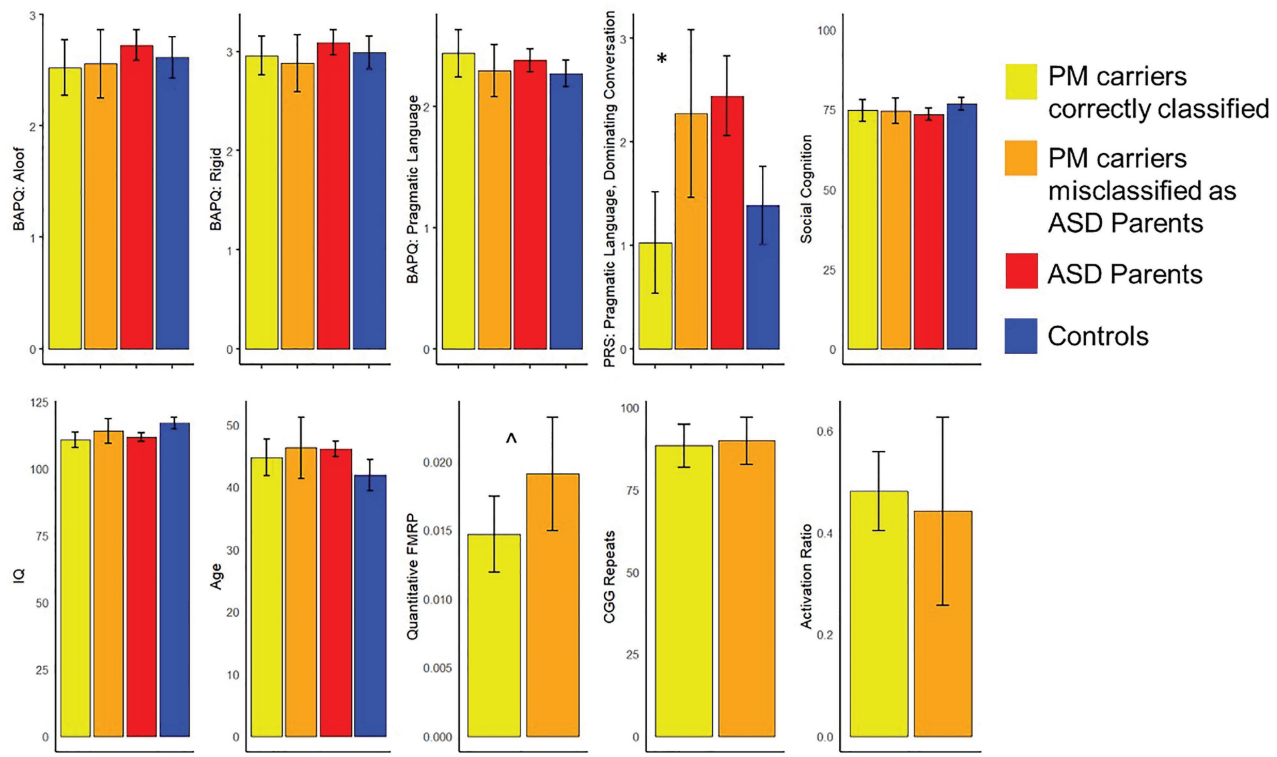

FIGURE 3 | Comparisons of clinical-behavioral and *FMR1*-related variables between the premutation (PM) carriers who were misclassified as ASD parents and those who were correctly classified (*$p < 0.05$, ^$p < 0.10$). Of note, controls are not included in comparisons related to broad autism phenotype (BAP) features, and ASD parents and controls were not included in comparisons related to *FMR1* molecular-genetic variation.

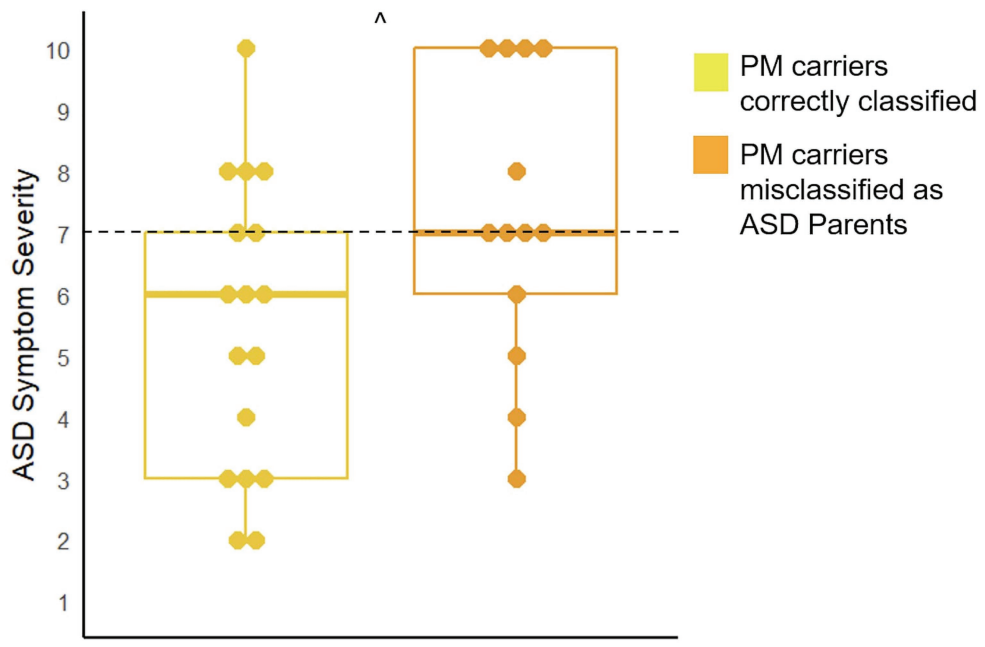

FIGURE 4 | Comparison of ASD symptom severity as measured by the ADOS-2 in the children of PM carriers who were misclassified as ASD parents and those who were correctly classified (^$p < 0.10$). The cut-off for meeting criteria for ASD is seven (range: 1–10).

allocation in complex social scenes. In contrast, exhibiting increased fixations toward the mouth during face processing tasks might reflect a more specific characteristic of the PM group.

Interestingly, secondary analyses examining phenotypic differences in PM carriers who were incorrectly classified as ASD parents showed that this group demonstrated increased pragmatic language violations (at rates similar to the ASD parent group), and higher levels of FMRP, but did not differ in IQ, age, social cognition, or other BAP features. Furthermore, children of the group of PM carriers who were misclassified as ASD parent's demonstrated overall greater ASD symptom severity, and more severe repetitive behaviors than children from the group of correctly classified as PM carriers. Evidence that higher rates of ASD-related characteristics were present in the misclassified PM carriers and in their children with FXS could suggest the presence of additional etiologic factors in this subgroup of families, such as differences in genetic background, including variation in ASD risk genes known to interact with *FMR1* (Belmonte and Bourgeron, 2006; Darnell et al., 2011; Hagerman et al., 2011; Steinberg and Webber, 2013). As such, these findings may warrant further investigation into the specific phenotypes (and aspects of pragmatic language in particular) that might distinguish a cluster of PM carriers who share features with ASD relatives. Such overlapping phenotypes could help to guide investigations into etiologic factors related to ASD features in *FMR1* mutation conditions (e.g., potential involvement of ASD risk genes that are known interactors with *FMR1*).

Correlational analyses revealed an association between higher CGG repeats and time spent looking at the mouth on the affective facial expressions task specifically in the ASD parent group. This association highlights that *FMR1* CGG repeats within the normal range may be related to PM-specific traits. Higher CGG repeats within the PM range have been associated with a range of PM phenotypic characteristics (Wheeler et al., 2014), and this finding adds to some literature suggesting that variation within the gray zone or at the upper/lower end of the normal range may confer risk for medical problems and cognitive differences (Bretherick et al., 2005; Mailick et al., 2014). Findings reported here suggest that visual processing strategies may be an additional such phenotype, influenced by even subtle *FMR1* variation.

Taken together, results of this study highlight the utility of eye tracking in the context of a face processing task as a tool for prediction of PM status and specific endophenotypic marker. Findings also provide evidence of overlap in visual fixation patterns with parents of individuals with ASD, suggesting potentially shared neurobiological mechanisms underlying phenotypes observed across these populations. Results may therefore help to elucidate etiology for ASD traits that may express across different diagnostic boundaries. Likewise, these indices reflecting shared clinical-behavioral features may be used to further stratify the PM group into more clinically, and potentially etiologically homogenous subgroups for use in clinical and biological studies. Furthermore, results support the utility of eye-tracking data to characterize endophenotypic markers in female carriers of the *FMR1* PM, and illustrate the unique predictive power of specific variables derived using eye-tracking data in differentiating group membership.

Several strengths and limitations of the study should be considered in the interpretation of results. A strength of this study includes the data-driven investigation of visual attention profiles across contexts and multiple groups of relatively substantial sample size. Importantly, by moving beyond investigation of fixation data within single tasks, analyses aimed to characterize broader visual attention profiles that may characterize specific groups, potentially show group overlap, and help to target studies connecting these phenotypes to underlying biology. Studying visual attention across tasks that varied in complexity and social demands permitted a relatively comprehensive assessment of attentional patterns that might contribute to understanding of the *FMR1* PM phenotype (Klin et al., 2002; Shic et al., 2011; Chawarska et al., 2012). Additionally, the inclusion of parents of individuals with ASD as an additional comparison group with carriers of the *FMR1* PM is important, given the strong overlap between ASD and *FMR1*-related conditions (Cornish et al., 2005; Clifford et al., 2007; Losh et al., 2008; Klusek et al., 2017; Nayar et al., 2018, 2019), and presence of a relatively large number of high confidence ASD risk genes that are known interactors with *FMR1* (Belmonte and Bourgeron, 2006; Darnell et al., 2011; Hagerman et al., 2011; Ascano et al., 2012; Steinberg and Webber, 2013; De Rubeis et al., 2014). Phenotypic comparisons across these groups may help to identify shared endophenotypes that can elucidate common etiologic factors across conditions. A limitation, noted previously, is that not all participants contributed data for each task. However, mitigating this concern is that analyses applied multiple imputation using chained equations (MICE) with predictive mean matching, and auxiliary variables to inform imputation and avoid biases present in other single imputation techniques (Schafer, 1999; Stuart et al., 2009; Azur et al., 2011). Future work with larger samples would benefit from split datasets, to permit training and testing, and may also fruitfully consider machine learning approaches and cross-validation measures. Finally, it will be important to investigate whether the PM visual attention profile identified here might extend to males with the PM, and constitute a *FMR1*-related endophenotype that could help to characterize the profile of the *FMR1* PM in males and females, and guide future investigations of gene-brain-behavior connections in PM carriers.

DATA AVAILABILITY STATEMENT

The datasets presented in this study can be found in online repositories. The names of the repository/repositories and accession number(s) can be found at: https://nda.nih.gov/edit_collection.html?id=1958.

ETHICS STATEMENT

The studies involving human participants were reviewed and approved by Northwestern University Institutional Review Board. The patients/participants provided their written informed consent to participate in this study.

AUTHOR CONTRIBUTIONS

MW conceptualized project questions, analyzed the data, and drafted the initial manuscript. KN, EL, and NM assisted in preparing the dataset and provided valuable feedback on manuscript drafts. KN and EL further assisted in completing verifications of published results as well as contributed to manuscript preparation. JS provided further consultation and verification of statistical methods and results. LZ, KS, and EB-K provided resources for genetic analysis of the *FMR1* gene, helped to draft the Materials and Methods section pertaining to genetic analyses, and provided essential expertise in the interpretation of results. ML secured funding for the projects from which these data were drawn, helped to conceptualize the project, interpret data, and develop the manuscript. All authors contributed to the article and approved the submitted version.

FUNDING

This work was funded through the National Institutes of Health (R01DC010191, R01MH091131, P30HD03110) and the National Science Foundation (BCS-0820394).

ACKNOWLEDGMENTS

We are grateful to the many individuals who participated in this study. We would like to acknowledge Michelle Lee, Abigail L. Hogan, and Daniel Hamburger for their initial efforts related to the management and processing of the data. We would also like to thank Faraz Farzin for sharing of her eye tracking stimuli and assistance in creation of the protocol for collection of data pertaining to the NimStim task.

REFERENCES

Adolphs, R., Spezio, M. L., Parlier, M., and Piven, J. (2008). Distinct face-processing strategies in parents of autistic children. *Curr. Biol.* 18, 1090–1093. doi: 10.1016/j.cub.2008.06.073

Ascano, M. J., Mukherjee, N., Bandaru, P., Miller, J. B., Nusbaum, J. D., Corcoran, D. L., et al. (2012). FMRP targets distinct mRNA sequence elements to regulate protein expression. *Nature* 492, 382–386. doi: 10.1038/nature11737

Azur, M. J., Stuart, E. A., Frangakis, C., and Leaf, P. J. (2011). Multiple imputation by chained equations: what is it and how does it work? *Int. J. Methods Psychiatr. Res.* 20, 40–49. doi: 10.1002/mpr.329

Bagni, C., and Oostra, B. A. (2013). Fragile X syndrome: from protein function to therapy. *Am. J. Med. Genet. A* 161A, 2809–2821. doi: 10.1002/ajmg.a.36241

Bailey, D. B.,. J., Hatton, D. D., Skinner, M., and Mesibov, G. (2001). Autistic behavior, FMR1 protein, and developmental trajectories in young males with fragile X syndrome. *J. Autism Dev. Disord.* 31, 165–174. doi: 10.1023/a:1010747131386

Baron-Cohen, S., Wheelwright, S., Hill, J., Raste, Y., and Plumb, I. (2001). The "Reading the Mind in the eyes" test revised version: a study with normal adults, and adults with Asperger syndrome or high-functioning autism. *J. Child Psychol. Psychiatry* 42, 241–251. doi: 10.1111/1469-7610.00715

Belmonte, M. K., and Bourgeron, T. (2006). Fragile X syndrome and autism at the intersection of genetic and neural networks. *Nat. Neurosci.* 9, 1221–1225. doi: 10.1038/nn1765

Bentin, S., Allison, T., Puce, A., Perez, E., and McCarthy, G. (1996). Electrophysiological studies of face perception in humans. *J. Cogn. Neurosci.* 8, 551–565. doi: 10.1162/jocn.1996.8.6.551

Berry-Kravis, E., Potanos, K., Weinberg, D., Zhou, L., and Goetz, C. G. (2005). Fragile X-associated tremor/ataxia syndrome in sisters related to X-inactivation. *Ann. Neurol.* 57, 144–147. doi: 10.1002/ana.20360

Besterman, A. D., Wilke, S. A., Mulligan, T. E., Allison, S. C., Hagerman, R., Seritan, A. L., et al. (2014). Towards an understanding of neuropsychiatric manifestations in fragile X premutation carriers. *Future Neurol.* 9, 227–239. doi: 10.2217/fnl.14.11.

Bourgeois, J. A., Seritan, A. L., Casillas, E. M., Hessl, D., Schneider, A., Yang, Y., et al. (2011). Lifetime prevalence of mood and anxiety disorders in fragile X premutation carriers. *J. Clin. Psychiatry* 72, 175–182. doi: 10.4088/JCP.09m05407blu.

Bretherick, K. L., Fluker, M. R., and Robinson, W. P. (2005). FMR1 repeat sizes in the gray zone and high end of the normal range are associated with premature ovarian failure. *Hum. Genet.* 117, 376–382. doi: 10.1007/s00439-005-1326-8

Chawarska, K., Macari, S., and Shic, F. (2012). Context modulates attention to social scenes in toddlers with autism. *J. Child Psychol. Psychiatry* 53, 903–913. doi: 10.1111/j.1469-7610.2012.02538.x

Clifford, S., Dissanayake, C., Bui, Q. M., Huggins, R., Taylor, A. K., and Loesch, D. Z. (2007). Autism spectrum phenotype in males and females with fragile X full mutation and premutation. *J. Autism Dev. Disord.* 37, 738–747. doi: 10.1007/s10803-006-0205-z

Colle, L., Baron-Cohen, S., Wheelwright, S., and van der Lely, H. K. (2008). Narrative discourse in adults with high-functioning autism or Asperger syndrome. *J. Autism Dev. Disord.* 38, 28–40. doi: 10.1007/s10803-007-0357-5

Cornish, K., Kogan, C., Turk, J., Manly, T., James, N., Mills, A., et al. (2005). The emerging fragile X premutation phenotype: evidence from the domain of social cognition. *Brain Cogn.* 57, 53–60. doi: 10.1016/j.bandc.2004.08.020

Darnell, J. C., Van Driesche, S. J., Zhang, C., Hung, K. Y., Mele, A., Fraser, C. E., et al. (2011). FMRP stalls ribosomal translocation on mRNAs linked to synaptic function and autism. *Cell* 146, 247–261. doi: 10.1016/j.cell.2011.06.013

De Rubeis, S., He, X., Goldberg, A. P., Poultney, C. S., Samocha, K., Cicek, A. E., et al. (2014). Synaptic, transcriptional and chromatin genes disrupted in autism. *Nature* 515, 209–215. doi: 10.1038/nature13772

Diehl, J. J., Bennetto, L., and Young, E. C. (2006). Story recall and narrative coherence of high-functioning children with autism spectrum disorders. *J. Abnorm. Child Psychol.* 34, 87–102. doi: 10.1007/s10802-005-9003-x

Farroni, T., Csibra, G., Simion, F., and Johnson, M. H. (2002). Eye contact detection in humans from birth. *Proc. Natl. Acad. Sci. U. S. A.* 99, 9602–9605. doi: 10.1073/pnas.152159999

Farzin, F., Rivera, S. M., and Hessl, D. (2009). Brief report: visual processing of faces in individuals with fragile X syndrome: an eye tracking study. *J. Autism Dev. Disord.* 39, 946–952. doi: 10.1007/s10803-009-0744-1

Filipovic-Sadic, S., Sah, S., Chen, L., Krosting, J., Sekinger, E., Zhang, W., et al. (2010). A novel FMR1 PCR method for the routine detection of low abundance expanded alleles and full mutations in fragile X syndrome. *Clin. Chem.* 56, 399–408. doi: 10.1373/clinchem.2009.136101

Fine, S. E., Weissman, A., Gerdes, M., Pinto-Martin, J., Zackai, E. H., McDonald-McGinn, D. M., et al. (2005). Autism spectrum disorders and symptoms in children with molecularly confirmed 22q11. 2 deletion syndrome. *J. Autism Dev. Disord.* 35, 461–470. doi: 10.1007/s10803-005-5036-9

Frazier, T. W., Klingemier, E. W., Beukemann, M., Speer, L., Markowitz, L., Parikh, S., et al. (2016). Development of an objective autism risk index using remote eye tracking. *J. Am. Acad. Child. Adolesc. Psychiatry* 55, 301–309. doi: 10.1016/j.jaac.2016.01.011

Frazier, T. W., Klingemier, E. W., Parikh, S., Speer, L., Strauss, M. S., Eng, C., et al. (2018). Development and validation of objective and quantitative eye tracking-based measures of autism risk and symptom levels. *J. Am. Acad. Child. Adolesc. Psychiatry* 57, 858–866. doi: 10.1016/j.jaac.2018.06.023

Gotham, K., Risi, S., Dawson, G., Tager-Flusberg, H., Joseph, R., Carter, A., et al. (2008). A replication of the autism diagnostic observation schedule (ADOS) revised algorithms. *J. Am. Acad. Child Adolesc. Psychiatry* 47, 642–651. doi: 10.1097/CHI.0b013e31816bffb7

Gottesman, I. I., and Gould, T. D. (2003). The endophenotype concept in psychiatry: etymology and strategic intentions. *Am. J. Psychiatry* 160, 636–645. doi: 10.1176/appi.ajp.160.4.636

Hagerman, R., Au, J., and Hagerman, P. (2011). FMR1 premutation and full mutation molecular mechanisms related to autism. *J. Neurodev. Disord.* 3, 211–224. doi: 10.1007/s11689-011-9084-5

Hagerman, R. J., and Hagerman, P. J. (2002). The fragile X premutation: into the phenotypic fold. *Curr. Opin. Genet. Dev.* 12, 278–283. doi: 10.1016/S0959-437X(02)00299-X

Hagerman, R. J., Leavitt, B. R., Farzin, F., Jacquemont, S., Greco, C. M., Brunberg, J. A., et al. (2004). Fragile-X-associated tremor/ataxia syndrome (FXTAS) in females with the FMR1 premutation. *Am. J. Hum. Genet.* 74, 1051–1056. doi: 10.1086/420700

Henderson, J. M., Williams, C. C., and Falk, R. J. (2005). Eye movements are functional during face learning. *Mem. Cogn.* 33, 98–106. doi: 10.3758/BF03195300

Hernandez, R. N., Feinberg, R. L., Vaurio, R., Passanante, N. M., Thompson, R. E., and Kaufmann, W. E. (2009). Autism spectrum disorder in fragile X syndrome: a longitudinal evaluation. *Am. J. Med. Genet. A* 149A, 1125–1137. doi: 10.1002/ajmg.a.32848

Hessl, D., Rivera, S., Koldewyn, K., Cordeiro, L., Adams, J., Tassone, F., et al. (2007). Amygdala dysfunction in men with the fragile X premutation. *Brain* 130, 404–416. doi: 10.1093/brain/awl338

Hunter, J. E., Allen, E. G., Abramowitz, A., Rusin, M., Leslie, M., Novak, G., et al. (2008). Investigation of phenotypes associated with mood and anxiety among male and female fragile X premutation carriers. *Behav. Genet.* 38, 493–502. doi: 10.1007/s10519-008-9214-3.

Hurley, R. S., Losh, M., Parlier, M., Reznick, J. S., and Piven, J. (2007). The broad autism phenotype questionnaire. *J. Autism Dev. Disord.* 37, 1679–1690. doi: 10.1007/s10803-006-0299-3

Klin, A., Jones, W., Schultz, R., Volkmar, F., and Cohen, D. (2002). Visual fixation patterns during viewing of naturalistic social situations as predictors of social competence in individuals with autism. *Arch. Gen. Psychiatry* 59, 809–816. doi: 10.1001/archpsyc.59.9.809

Klusek, J., Fairchild, A. J., and Roberts, J. E. (2018a). Vagal tone as a putative mechanism for pragmatic competence: an investigation of carriers of the FMR1 Premutation. *J. Autism Dev. Disord.* 49, 197–208. doi: 10.1007/s10803-018-3714-7

Klusek, J., McGrath, S. E., Abbeduto, L., and Roberts, J. E. (2016). Pragmatic language features of mothers with the FMR1 premutation are associated with the language outcomes of adolescents and young adults with fragile X syndrome. *J. Speech Lang. Hear. Res.* 59, 49–61. doi: 10.1044/2015_JSLHR-L-15-0102

Klusek, J., Porter, A., Abbeduto, L., Adayev, T., Tassone, F., Mailick, M., et al. (2018b). Curvilinear association between language disfluency and FMR1 CGG reapt size across the normal, intermediate, and premutation range. *Front. Genet.* 9:344. doi: 10.3389/fgene.2018.00344

Klusek, J., Schmidt, J., Fairchild, A. J., Porter, A., and Roberts, J. E. (2017). Altered sensitivity to social gaze in the *FMR1* premutation and pragmatic language competence. *J. Neurodev. Disord.* 9:31. doi: 10.1186/s11689-017-9211-z

LaFauci, G., Adayev, T., Kascsak, R., Kascsak, R., Nolin, S., Mehta, P., et al. (2013). Fragile X screening by quantification of FMRP in dried blood spots by a luminex immunoassay. *J. Mol. Diagn.* 15, 508–517. doi: 10.1016/j.jmoldx.2013.02.006.

Landa, R., Piven, J., Wzorek, M. M., Gayle, J. O., Chase, G. A., and Folstein, S. E. (1992). Social language use in parents of autistic individuals. *Psychol. Med.* 22, 245–254.

Lee, M., Nayar, K., Maltman, N., Hamburger, D., Martin, G. E., Gordon, P. C., et al. (2019). Understanding social communication differences in autism spectrum disorder and first-degree relatives: a study of looking and speaking. *J. Autism Dev. Disord.* 50, 2128–2141. doi: 10.1007/s10803-019-03969-3

Lord, C., Rutter, M., DeLavore, P. C., and Risi, S. (2001). *Autism diagnostic observation schedule*. Los Angeles, CA: Western Psychological Services.

Losh, M., Adolphs, R., Poe, M. D., Couture, S., Penn, D., Baranek, G. T., et al. (2009). Neuropsychological profile of autism and the broad autism phenotype. *Arch. Gen. Psychiatry* 66, 518–526. doi: 10.1001/archgenpsychiatry.2009.34

Losh, M., and Capps, L. (2003). Narrative ability in high-functioning children with autism or Asperger's syndrome. *J. Autism Dev. Disord.* 33, 239–251. doi: 10.1023/a:1024446215446

Losh, M., Childress, D., Lam, K., and Piven, J. (2008). Defining key features of the broad autism phenotype: a comparison across parents of multiple- and single-incidence autism families. *Am. J. Med. Genet. B Neuropsychiatr. Genet.* 147B, 424–433. doi: 10.1002/ajmg.b.30612

Losh, M., Klusek, J., Martin, G. E., Sideris, J., Parlier, M., and Piven, J. (2012). Defining genetically meaningful language and personality traits in relatives of individuals with fragile X syndrome and relatives of individuals with autism. *Am. J. Med. Genet. B Neuropsychiatr. Genet.* 159B, 660–668. doi: 10.1002/ajmg.b.32070

Mailick, M. R., Hong, J., Rathouz, P., Baker, M. W., Greenberg, J. S., Smith, L., et al. (2014). Low-normal FMR1 CGG repeat length: phenotypic associations. *Front. Genet.* 5:309. doi: 10.3389/fgene.2014.00309

Mayer, M. (1969). *Frog, where are you?* New York: Dial Press.

Murray, H. A. (1943). *Thematic apperception test*. Cambridge, Massachusetts: Harvard University Press.

Nayar, K., Gordon, P. C., Martin, G. E., Hogan, A. L., La Valle, C., McKinney, W., et al. (2018). Links between looking and speaking in autism and first-degree relatives: insights into the expression of genetic liability to autism. *Mol. Autism.* 9:51. doi: 10.1186/s13229-018-0233-5

Nayar, K., McKinney, W., Hogan, A. L., Martin, G. E., La Valle, C., and Sharp, K., et al. (2019). Language processing skills linked to FMR1 variation: a study of gaze-language coordination during rapid automatized naming among women with the FMR1 premutation. *PLoS One* 14:e0219924. doi: 10.1371/journal.pone.0219924

Norbury, C. F., and Bishop, D. V. (2003). Narrative skills of children with communication impairments. *Int. J. Lang. Commun. Disord.* 38, 287–313. doi: 10.1080/136820310000108133

Peters, S. U., Beaudet, A. L., Madduri, N., and Bacino, C. A. (2004). Autism in Angelman syndrome: implications for autism research. *Clin. Genet.* 66, 530–536. doi: 10.1111/j.1399-0004.2004.00362.x

Pierce, K., Marinero, S., Hazin, R., McKenna, B., Barnes, C. C., and Malige, A. (2016). Eye tracking reveals abnormal visual preference for geometric images as an early biomarker of an autism spectrum disorder subtype associated with increased symptom severity. *Biol. Psychiatry* 79, 657–666. doi: 10.1016/j.biopsych.2015.03.032

Reilly, J., Losh, M., Bellugi, U., and Wulfeck, B. (2004). "Frog, where are you?" narratives in children with specific language impairment, early focal brain injury, and Williams syndrome. *Brain Lang.* 88, 229–247. doi: 10.1016/S0093-934X(03)00101-9

Sah, W. -h., and Torng, P. -c. (2015). Narrative coherence of mandarin-speaking children with high-functioning autism spectrum disorder: an investigation into causal relations. *First Lang.* 35, 189–212. doi: 10.1177/0142723715584227

Schafer, J. L. (1999). Multiple imputation: a primer. *Stat. Methods Med. Res.* 8, 3–15. doi: 10.1177/096228029900800102

Schneider, A., Johnston, C., Tassone, F., Sansone, S., Hagerman, R. J., Ferrer, E., et al. (2016). Broad autism spectrum and obsessive-compulsive symptoms in adults with the fragile X premutation. *Clin. Neuropsychol.* 30, 929–943. doi: 10.1080/13854046.2016.1189536.

Seltzer, M. M., Baker, M. W., Hong, J., Maenner, M., Greenberg, J., and Mandel, D. (2012). Prevalence of CGG expansions of the FMR1 gene in a US population-based sample. *Am. J. Med. Genet. B Neuropsychiatr. Genet.* 159B, 589–597. doi: 10.1002/ajmg.b.32065

Shelton, A. L., Cornish, K. M., Godler, D. E., Clough, M., Kraan, C., Bui, M., et al. (2015). Delineation of the working memory profile in female FMR1 premutation carriers: the effect of cognitive load on ocular motor responses. *Behav. Brain Res.* 282, 194–200. doi: 10.1016/j.bbr.2015.01.011.

Shelton, A. L., Cornish, K., Kraan, C., Georgiou-Karistianis, N., Metcalfe, S. A., Bradshaw, J. L., et al. (2014). Exploring inhibitory deficits in female premutation carriers of fragile X syndrome: through eye movements. *Brain Cogn.* 85, 201–208. doi: 10.1016/j.bandc.2013.12.006

Shelton, A. L., Cornish, K. M., Kraan, C. M., Lozano, R., Bui, M., and Fielding, J. (2016). Executive dysfunction in female FMR1 Premutation carriers. *Cerebellum* 15, 565–569. doi: 10.1007/s12311-016-0782-0

Shic, F., Bradshaw, J., Klin, A., Scassellati, B., and Chawarska, K. (2011). Limited activity monitoring in toddlers with autism spectrum disorder. *Brain Res.* 1380, 246–254. doi: 10.1016/j.brainres.2010.11.074

Steinberg, J., and Webber, C. (2013). The roles of FMRP-regulated genes in autism spectrum disorder: single- and multiple-hit genetic etiologies. *Am. J. Hum. Genet.* 93, 825–839. doi: 10.1016/j.ajhg.2013.09.013

Stuart, E. A., Azur, M., Frangakis, C., and Leaf, P. (2009). Multiple imputation with large data sets: a case study of the children's mental health initiative. *Am. J. Epidemiol.* 169, 1133–1139. doi: 10.1093/aje/kwp026

Tager-Flusberg, H. (1995). 'Once upon a ribbit': stories narrated by autistic children. *Br. J. Dev. Psychol.* 13, 45–59. doi: 10.1111/j.2044-835X.1995.tb00663.x

Thao, L. T. P., and Geskus, R. (2019). A comparison of model selection methods for prediction in the presence of multiply imputed data. *Biom. J.* 61, 343–356. doi: 10.1002/bimj.201700232

Thurber, C., and Tager-Flusberg, H. (1993). Pauses in the narratives produced by autistic, mentally retarded, and normal children as an index of cognitive demand. *J. Autism Dev. Disord.* 23, 309–322.

Tottenham, N., Tanaka, J. W., Leon, A. C., McCarry, T., Nurse, M., Hare, T. A., et al. (2009). The NimStim set of facial expressions: judgments from untrained research participants. *Psychiatry Res.* 168, 242–249. doi: 10.1016/j.psychres.2008.05.006.

van Buuren, S., and Groothuis-Oudshoorn, K. (2011). Mice: multivariate imputation by chained equations in R. *J. Stat. Softw.* 45, 1–67. doi: 10.18637/jss.v045.i03

Vink, G., Frank, L. E., Pannekoek, J., and Van Buuren, S. (2014). Predictive mean matching imputation of semicontinuous variables. *Statistica Neerlandica* 68, 61–90. doi: 10.1111/stan.12023

von Hippel, P. T. (2020). How many imputations do you need? A two-stage calculation using a quadratic rule. *Sociol. Methods Res.* 49, 699–718. doi: 10.1177/0049124117747303

Wang, J. Y., Hessl, D., Iwahashi, C., Cheung, K., Schneider, A., Hagerman, R. J., et al. (2013). Influence of the fragile X mental retardation (FMR1) gene on the brain and working memory in men with normal FMR1 alleles. *NeuroImage* 65, 288–298. doi: 10.1016/j.neuroimage.2012.09.075.

Wechsler, D. (1999). *WASI: Wechsler abbreviated scale of intelligence*. San Antonio, TX: Psychological Corporation.

Weiler, I. J., and Greenough, W. T. (1999). Synaptic synthesis of the fragile X protein: possible involvement in synapse maturation and elimination. *Am. J. Med. Genet.* 83, 248–252.

Wheeler, A. C., Bailey, D. B. Jr., Berry-Kravis, E., Greenberg, J., Losh, M., Mailick, M., et al. (2014). Associated features in females with an FMR1 premutation. *J. Neurodev. Disord.* 6:30. doi: 10.1186/1866-1955-6-30.

Winston, M., Nayar, K., Hogan, A. L., Barstein, J., La Valle, C., Sharp, K., et al. (2020). Physiological regulation and social-emotional processing in female carriers of the FMR1 premutation. *Physiol. Behav.* 214:112746. doi: 10.1016/j.physbeh.2019.112746

Yucel, G. H., Belger, A., Bizzell, J., Parlier, M., Adolphs, R., and Piven, J. (2015). Abnormal neural activation to faces in the parents of children with autism. *Cereb. Cortex* 25, 4653–4666. doi: 10.1093/cercor/bhu147

Conflict of Interest: The authors declare that the research was conducted in the absence of any commercial or financial relationships that could be construed as a potential conflict of interest.

Advantages of publishing in Frontiers

OPEN ACCESS
Articles are free to read for greatest visibility and readership

FAST PUBLICATION
Around 90 days from submission to decision

HIGH QUALITY PEER-REVIEW
Rigorous, collaborative, and constructive peer-review

TRANSPARENT PEER-REVIEW
Editors and reviewers acknowledged by name on published articles

Frontiers
Avenue du Tribunal-Fédéral 34
1005 Lausanne | Switzerland

Visit us: www.frontiersin.org
Contact us: frontiersin.org/about/contact

REPRODUCIBILITY OF RESEARCH
Support open data and methods to enhance research reproducibility

DIGITAL PUBLISHING
Articles designed for optimal readership across devices

FOLLOW US
@frontiersin

IMPACT METRICS
Advanced article metrics track visibility across digital media

EXTENSIVE PROMOTION
Marketing and promotion of impactful research

LOOP RESEARCH NETWORK
Our network increases your article's readership